THE IMPACT OF IRRIGATION CONDITIONS ON THE SPATIAL DEVELOPMENT OF MICROBIAL COLONIES IN BIOHEAPS

By Research Candidate:
REBECCA ANGELA CHIUME

Student No: CHMREB002

Supervisors:
Prof. S.T.L. Harrison Dr. S. Minnaar

Thesis submitted in partial accomplishment of the requirements of the

Master of Science in Engineering degree,

Centre for Bioprocess Engineering Research,

Department of Chemical Engineering,

University of Cape Town

February 2011

DECLARATION

I know the meaning of plagiarism and declare that all the work in the document, save for that which is properly acknowledged, is my own.

This has not been submitted for any degree or examination in any other university.

Signed: _____ **Date**: February 2011

Rebecca Angela Chiume

DEDICATION

"I dedicate in the 1st instance this thesis to GOD without whom I could not have successfully attained my current disposition through times of uncertainty and much challenges. I live to give HIM praise.

**Jeremiah 29:11* "For I know the plans I have for you," declares the LORD, "plans to prosper you and not to harm you, plans to give you hope and a future." – The Holy Bible*

I thank HIM also for my family; Dad, Mum, Dumile, Dumisani and Amanda, who together with HIS mercies have been the driving force behind my life's successes. All these sources have been the pillars upon which I am able to stand. Helping Words and Words of Wisdom have encouraged and assisted greatly in facing the challenges that I met. Such words I share below:

"A family that prays together stays together." – Al Scalpone

"He who always strives to carry out everything he does as well as possible will be able to master what otherwise is far removed from his accustomed work." – HELPING WORDS

Words cannot express my grateful thanks to those above who have made me who I am.

SYNOPSIS

Heap bioleaching is a microbially-assisted metal extraction process in which metals are recovered from low grade ore by ferric iron and acid leach agents. Heap bioleaching provides several advantages over conventional technologies, such as simple and safe operation; short commission times; low capital and operation cost; and acceptable recoveries. The challenge with heap bioleaching systems is ensuring leach durations are minimised and metal recovery optimised, by understanding and controlling the key parameters that influence the sub-processes.

There is limited understanding of microbially operated bioheaps. To date, literature that deals with microbial colonisation has focused mainly on the degree of attachment of microorganisms to the mineral concentrates, the mechanisms behind microbial attachment, extracellular polymeric substance (EPS) formation, and more recently the location and specificity of microbial attachment to mineral. Extensive studies on microbial attachment to mineral surfaces have been reported (Gehrke *et al*., 1998; Sampson *et al*., 2000; Kinzler *et al*., 2003; Rodriguez *et al*., 2003; Sand and Gehrke, 2006; Ghauri *et al*., 2007; Africa *et al*., 2010; Bromfield *et al*., 2010). These observations have limited applications because most experimental findings were derived from systems with conditions which were not analogous to actual heap bioleaching environments. Additionally, there is still a need to be informed of the effect of heap leaching flow dynamics on the fate of micro-organisms accumulating within the heap environment and the transportation of micro-organisms through the heap to active surface sites.

This thesis contributes to the bioleaching knowledge base by improved understanding of the relationships between hydrodynamics and micro-organism-ore contacting and colonisation through an integrated study of microbiological and hydrological aspects of heap bioleaching within systems that mimic actual bio-heap environments. Particularly, the impact of the irrigation application rate on microbial colonisation and the influence of discrete solution flow paths on the propagation and spatial distribution of micro-organisms were investigated within simulated laboratory scale heap bioleaching systems containing low grade copper-bearing mineral ore.

The study intends to address these specific key factors:

- The initial development of microbial propagation, attachment, growth and colonisation with respect to time, location within the ore bed, and irrigant source.
- The quantification of the relative proportions of planktonic to interstitial to attached cells and assessment of the influence of irrigation rate and time on the accumulation of cells within these different locations.
- The influence of high irrigation rates on cell detachment from the mineral surface.
- The change in bed saturation as a function of irrigation rate and solution flow from a single point source of irrigation.

A 4 kg column reactor was packed with ore containing 0.69% copper and inoculated with a mixed mesophilic culture containing *Acidithiobacillus caldus, Acidithiobacillus ferrooxidans, Acidithiobacillus thiooxidans* and predominantly *Leptospirillum ferriphilum*, whilst operating as a continuous flow through system. The effect of irrigation rates of 2, 6 and 18 $L/m^2.h$ on microbial attachment, growth and subsequent colonisation was assessed in this system. A novel in-bed sampling procedure was utilised to obtain ore samples at intervals during the bioleaching experimental runs, from which the cells were mechanically detached and an analysis of cell densities within the

planktonic and attached phases was conducted. For the first time, the microbial population was assessed across location i.e. free flowing liquid, interstitial and ore attached.

The in-bed sampling technique commissioned was shown to facilitate non-destructive sampling of the ore bed in the column bioleach system. This allowed monitoring of the ore-associated microbial population over the course of the leach runs. Findings showed increasing cell numbers in the ore bed over time. More cells were observed in the stagnant fluid in the interstitial regions than attached firmly to the ore or planktonically. Higher degrees of attachment and accumulation of micro-organisms in the ore bed were attained at low flow rates owing to the longer residence time of micro-organisms in the system. Detachment and consequently greater cell exportation from the column was observed in the higher flow regimes, postulated to be attributed to the higher shear stress induced. The average growth rates on the ore based on a combination of the interstitial and attached microbial communities were 0.0053, 0.0052 and 0.0043 h^{-1} for 2, 6 and 18 $L/m^2.h$ respectively. These growth rates were lower than those obtain in previous investigations on both low grade ore in column reactors and batch and continuous culture work. The differences were attributed to the operating temperature of approximately 23 °C within this investigation.

A packed box reactor was operated under continuous flow conditions, using a mixed mesophilic consortium (as above) to inoculate the low grade copper-containing ore bed. The box was sectioned into 9 zones in a 3x3 formation, whilst having 13 ports at the bottom of the system for collection of the pregnant leach solution (PLS). Ore samples were removed from the ports at intervals during the leaching process and assessments of these samples included moisture content and cell densities, allowing for the post-inoculation propagation and spatial distribution of the micro-organisms to be monitored in relation to the solution distribution from a single point source of irrigation. A low concentration of micro-organisms ($1.4x10^{10}$cells/kg ore at 22 days post inoculation) was retained in the ore bed initially. Increased cell numbers and retention within the system was observed, showing the ability of the micro-organisms to colonise the ore bed from very low cell numbers. Higher degrees of microbial colonisation were observed within the zones closer to and vertically below the irrigation point source, shown by the increasing cell densities. A reasonable correlation between the moisture contents, fluid flow and the cell densities was attained. The trends showed limited lateral fluid flow and cell migration. Preferential flow paths were shown to exists, which influenced the dispersion of microbial communities across the heap and caused regions with limited solution-ore contacting to remain partially-colonised.

Some recommendations have been made for future studies, namely:

- The use of the in-bed sampling apparatus to assess colonisation at different heights within the bed of a particular leaching system and fully characterise the microbial species present in the ore samples extracted.
- The investigation of the influence of ferrous iron concentration on the attachment and retention of cells within heap systems.
- The analysis of the changing physico-chemical conditions in the box reactor leach run.
- The use of tracer studies in the box reactor to quantify the fluid flow distribution across the bed and the residence time of solution, solutes and cells within the system.
- The assessment of microbial colonisation via irrigation inoculation from multiple drip points.

ACKNOWLEDGEMENTS

I am sincerely grateful to all those who contributed to fulfilment of my thesis:

- Firstly, I will honour the Lord for keeping me strong and helping me to persevere.
- Thank you to my supervisor, Prof S.T.L. Harrison, and co-supervisor, Dr. S. Minnaar, for their input and guidance along the way. It was greatly appreciated.
- A heartfelt thank you to the Centre for Bioprocess Engineering Research (CeBER) staff. Frances Pocock and Emmanuel Ngoma, for their ability to manage the labs effectively and for their technical assistance, as well as Sue Jobson for managing administrative issues.
- A big thank you goes out to the rest of the CeBER members for their support and friendship. Seun, Chris, Olga, Elaine, Alex, and Yousef, your input has been of great value.
- For their financial support in my scholastic development, I would like to thank the Centre for Bioprocess Engineering Research and the Chemical Engineering department, at UCT, the National Research Foundation (NRF), and Cape Biotech Trust.
- Thank you to my friends for keeping me motivated, whilst balancing out the academic life with less stressful activities. Thanks, Amanda, Ingrid, Porogo, Gracia, Simba, Selaelo, Asanda, Doreen, Sabatha, Allison, Natasha, Tapiwa, Kutlwano, Takundwa, Lesego and Lusanda.
- To Mo for helping me to figure out how to use the pixplot application on MATLAB®.
- Last but definitely not least, to my family for your prayers, love and encouragement; all of which will forever be reciprocated. I am blessed to have you.

TABLE OF CONTENTS

Page

DECLARATION ..... **ii**

DEDICATION ..... **iii**

SYNOPSIS ..... **iv**

ACKNOWLEDGEMENTS ..... **vi**

TABLE OF CONTENTS ..... **vii**

LIST OF FIGURES ..... **xi**

LIST OF TABLES ..... **xvi**

NOMENCLATURE ..... **xviii**

GLOSSARY ..... **xx**

1 CHAPTER 1: INTRODUCTION **1**

1.1 Background **1**

1.2 Problem Statement and Research Objectives **1**

1.3 Scope and Limitations **2**

1.4 Plan of Development/Thesis structure **2**

2 CHAPTER 2: LITERATURE REVIEW **4**

2.1 Overview of Heap Bioleaching **4**

2.1.1 *Description of Heap Bioleaching Operations* *4*

2.1.2 *Factors Affecting Heap Bioleaching* *6*

2.1.3 *Leaching Chemistry* *6*

2.1.4 *Bioleaching Mechanisms* *8*

2.2 Function of Microbes in the Leaching Process **8**

2.2.1 *Microbial Characteristics and Diversity* *8*

2.2.2 *Microbial Consortium* *9*

2.3 Microbial Colonisation **10**

2.3.1 *Transport of Microbes to Mineral Surface* *10*

2.3.2 *Initial Microbial Adherence to Ore* *11*

2.3.3 *Attachment Bonds and Sites* *11*

2.3.4 *Microbial Growth Dynamics and Heap Colonisation* *14*
2.3.5 *Detachment of Microbes from Ore* *17*
2.3.6 *Attachment and Colonisation Studies Conducted in CeBER* *18*
2.4 Solution Flow and Microbial Distribution Characteristics 18
2.4.1 *Characteristics of Solution Flow* *18*
2.4.2 *Influence of Irrigation Rate on Microbial Transport and Colonisation* *20*
2.4.3 *Microbial Retention in Porous Systems* *22*
2.4.4 *Solution-Microbe Interaction Studies Conducted in Related Fields* *24*
2.4.4.1 *Bioaccumulation* *24*
2.4.4.2 *Methods Employed to Investigate Bioclogging* *24*
2.4.4.3 *Observations* *25*
2.4.5 *Review of Investigation Conducted* *26*
2.5 Conclusions and Research Motivation 27
2.6 Research Hypotheses and Key Questions 28
3 CHAPTER 3: MATERIALS AND EXPERIMENTAL METHODOLOGY .29
3.1 Mineral Analysis 29
3.2 Microbial Cultures 30
3.3 Feed Media 30
3.4 Equipment 31
3.4.1 *Column Reactor* *31*
3.4.1 *In-bed Sampler* *32*
3.4.2 *Box Reactor* *34*
3.5 Analysis 35
3.5.1 *Determination of Bacterial Concentration* *35*
3.5.2 *Spectrophotometric Ferrous Iron Assay* *36*
3.5.3 *Total Iron Assay on Spectrophotometer* *36*
3.5.4 *Determination of Total Copper and Iron Concentration via AAS* *37*
3.6 Experiments 37
3.6.1 *Column Heap Operation* *37*
3.6.2 *Perspex Box Heap Operation* *37*
3.7 Data Handling 38
3.8 Sample Collection and Storage 39
3.9 Assumptions and Limitations 39

3.10 Research Strategy 40

4 CHAPTER 4: EFFECT OF IRRIGATION APPLICATION RATES ON MICROBIAL COLONISATION 41

4.1 Introduction 41

4.2 Experimental Approach 41

4.2.1 *Experimental procedure 41*

4.3 Preliminary study 42

4.3.1 *Flow Rates and Moisture Content 42*

4.3.2 *Copper Extraction 44*

4.3.3 *Solution Chemistry of Leachate 45*

4.3.4 *Microbial Analysis 45*

4.4 Responses to Varied Irrigation Application Rates 48

4.4.1 *Flow Rates and Moisture Content 48*

4.4.2 *Copper Liberation 50*

4.4.3 *pH, Redox Potential, Ferrous and Total Iron Profiles 52*

4.4.4 *Microbial Colonisation 56*

4.4.5 *Reproducibility of Experiment 64*

4.5 Discussion and Conclusions 66

5 CHAPTER 5: PROPAGATION OF MICRO-ORGANISMS FROM A POINT SOURCE 69

5.1 Introduction 69

5.2 Experimental Approach 69

5.2.1 *Experimental procedure 69*

5.3 Results and Discussion of Microbial Propagation 70

5.3.1 *Solution Flow and Moisture Content 70*

5.3.2 *Bioleaching Performance 74*

5.3.1 *Solution Chemistry of Leachate 75*

5.3.2 *Microbial Propagation and Colonisation 80*

5.4 Discussion and conclusions 85

6 CHAPTER 6: CONCLUSIONS AND RECOMMENDATIONS.....86

6.1 Introduction 86

6.2 Irrigation Rate and Colonisation 86

6.3 Fluid Flow from Discrete Irrigation Points 88

6.4 Recommendations 88

REFERENCES 90

APPENDICES 96

Appendix A – Feed Solution and Culture Preparation 96

Acid Solution for Agglomeration 96

Acid-wash Feed Solution 96

Feed Solution 96

Microbial Cultures 96

Appendix B – Analytical methods 97

Microscopic Cell Counting Method 97

Ferrous and Total Iron Concentration via Spectrophotometry 97

Appendix C – Raw Data Calculations 100

Appendix D – Supporting Data 102

Appendix E – MATLAB® Code 105

Appendix F – Raw Data 106

Preliminary Run Data 106

Run 2 Column Data 114

Run 3 Column Data 115

Box Data 116

LIST OF FIGURES

Figure 2-1: Typical heap leaching circuit, showing solution flow through the ore bed, aeration to promote bioleaching of sulphide minerals, recovery of copper metal and recycling of barren solution to minimise water use (Adapted from Watling, 2006). 5

Figure 2-2: Illustration of heap leaching reactions catalysed by microbes (adapted from Schippers *et al.*, 1996; Rohwerder and Sand, 2007). 7

Figure 2-3: Microbial transport to the ore surface (adapted from van Loosdrecht *et al*., 1990) 11

Figure 2-4: Reversible and irreversible adhesion to ore surfaces (adapted from van Loosdrecht *et al*., 1990)..... 11

Figure 2-5: Firm attachment via EPS formation (adapted from van Loosdrecht *et al.*, 1990)..... 13

Figure 2-6: Bioaccumulation on surfaces within the packed bed system (adapted from van Loosdrecht *et al*., 1990)..... 14

Figure 2-7: A typical microbial growth curve (adapted from Bailey and Ollis, 1986) 15

Figure 2-8: Detachment of micro-organisms from biofilms and surfaces..... 18

Figure 2-9: Demonstration of preferential flow conditions within unsaturated porous media (adapted from O'Kane *et al*. (2000). 20

Figure 2-10: Cross-sectional sketch of three different degrees of saturation of porous media (extracted and adapted from Wan *et al*., 1994). 23

Figure 2-11: Illustration of the development of colonisation and water content distribution (Extracted from Yarwood et al., 2006). 25

Figure 2-12: Bucket reactor set up with 3 concentric layers: dots represent solution collection points from 9 different zones (Van Hille *et al*. (2010) experimental setup) 26

Figure 3-1: Cumulative particle size distribution of the low grade copper-bearing ore..... 29

Figure 3-2: Schematic of heap leach column (adapted from van Hille *et al.*, 2010)..... 31

Figure 3-3: Mini-scale column heap leaching circuit: the experimental set-up 32

Figure 3-4: In-bed sampling procedure 33

Figure 3-5: Schematic of box reactor experimental set-up..... 34

Figure 3-6: Illustration of box zone separations used for the in-bed sampling 38

Figure 3-7: Outline of research approach 40

Figure 4-1: Illustration of column experimental set-up..... 42

Figure 4-2: Effluent flow rate profile as a function of time during the bioleaching of low grade copper bearing ore, given for different irrigation rates 2, 6 and 18 L/m^2.h, during the preliminary run. 43

Figure 4-3: Moisture content of the ore bed pre-leaching and post-leaching (50 days), given for different irrigation rates 2, 6 and 18 L/m^2.h, during the preliminary run. 43

Figure 4-4: Cumulative copper liberation as a function of time during the bioleaching of low grade copper bearing ore, given for different irrigation rates 2, 6 and 18 L/m^2.h, during the preliminary run. 44

Figure 4-5: Ferrous iron concentration in the eluted solution passing through the column heap as a function of time, given for different irrigation rates 2, 6 and 18 L/m^2.h, during the preliminary run... 45

Figure 4-6: Trend in (a) the pH and (b) the redox potential, of the eluted solution passing through the column heap given for different irrigation rates 2, 6 and 18 L/m^2.h, during the preliminary run. 47

Figure 4-7: Trend in (a) the cell concentration and (b) the cumulative number of cells, exported in the leachate passing through the heap, given for different irrigation rates 2, 6 and 18 L/m^2.h, during the preliminary run. 47

Figure 4-8: Moisture content of the ore bed pre-, during and post-leaching, determined from the ore samples periodically removed from the heap systems using the in-bed sampling technique, given for different irrigation rates 2, 6 and 18 L/m^2.h, during experimental (a) run 2 and (b) run 3..... 50

Figure 4-9: Cumulative copper liberation during the bioleaching of low grade copper bearing ore, given for experimental (a) run 2 at irrigation rates ◊ - 2 L/m^2.h, □ - 6 L/m^2.h and Δ - 18 L/m^2.h, and (b) run 3 at irrigation rates ♦ - 2 L/m^2.h, ■ - 6 L/m^2.h – A, x - 6 L/m^2.h – B and ▲ - 18 L/m^2.h. Arrow are indicative of in-bed sampling days. 51

Figure 4-10: Visual evidence of jarosite/iron hydroxide precipitation, obtained from the ore extracted using the in-bed sampling technique, on day 18 of leaching at an irrigation rate of 6 l/m^2/h, during experimental run 2. 52

Figure 4-11: Trend in the pH of the eluted solution passing through the column heap during the bioleaching of low grade copper bearing ore, given for experimental (a) run 2 at irrigation rates ◊ - 2 L/m^2.h, □ - 6 L/m^2.h and Δ - 18 L/m^2.h, and (b) run 3 at irrigation rates ♦ - 2 L/m^2.h, ■ - 6 L/m^2.h – A, x - 6 L/m^2.h – B and ▲ - 18 L/m^2.h. Arrows are indicative of in-bed sampling days. 53

Figure 4-12: Trend in the redox potential of the eluted solution passing through the column heap during the bioleaching of low grade copper bearing ore, given for experimental (a) run 2 at irrigation rates ◊ - 2 L/m^2.h, □ - 6 L/m^2.h and Δ - 18 L/m^2.h, and (b) run 3 at irrigation rates ♦ - 2 L/m^2.h, ■ - 6 L/m^2.h – A, x - 6 L/m^2.h – B and ▲ - 18 l/m^2/h. Arrow are indicative of in-bed sampling days. 54

Figure 4-13: Total and ferrous iron concentration profile of the eluted solution passing through the column heap during the bioleaching of low grade copper bearing ore, given for experimental (a) run 2 at irrigation rates ◊ - 2 L/m^2.h, □ - 6 L/m^2.h and Δ - 18 L/m^2.h, and (b) run 3 at irrigation rates ♦ - 2 L/m^2.h, ■ - 6 L/m^2.h – A, x - 6 L/m^2.h – B and ▲ - 18 L/m^2.h. Arrows indicative of in-bed sampling days..... 55

Figure 4-14: Schematic of the inside of the heap, showing planktonic cells in the flowing mobile liquid phase, microorganisms weakly and strongly associated with the ore surfaces, and microorganisms accumulating within the stagnant regions of the porous rocks..... 56

Figure 4-15: Cumulative removal of microbial cells in column effluent during the bioleaching of low grade copper bearing ore, given for experimental (a) run 2 at irrigation rates ◊ - 2 L/m^2.h, □ - 6 L/m^2.h and Δ - 18 L/m^2.h, and (b) run 3 at irrigation rates ♦ - 2 L/m^2.h, ■ - 6 L/m^2.h – A, x - 6 L/m^2.h – B and ▲ - 18 L/m^2.h. Error bars represent the propagated error determined from the standard deviation of the mean cell count within each experimental run. Arrows are indicative of in-bed sampling days. 58

Figure 4-16: Microbial growth curve obtained by combining the interstitial and attached cells accumulated in the ore bodies, determined from the mechanical detachment of cells from the ore samples periodically removed from the heap systems using the in-bed sampling technique, given for experimental (a) run 2 at irrigation rates ◊ - 2 L/m^2.h, □ - 6 L/m^2.h and Δ - 18 L/m^2.h, and (b) run 3 at irrigation rates ♦ - 2 L/m^2.h, ■ - 6 L/m^2.h – A, x - 6 L/m^2.h – B and ▲ - 18 L/m^2.h. Error bars represent the standard deviation of the ore-associated cell counts. The 'poly.' lines were generated in excel using the trendline option for polynomials of order 2..... 60

Figure 4-17: Comparison of planktonic cells (removed within each time period), interstitial, and attached microorganisms present in the column reactors, determined from the mechanical detachment of cells from the ore samples periodically removed from the heap systems using the in-bed sampling technique, given for replicate runs (a) Run 2 (b) Run 3A and (c) Run 3B, at an irrigation rate of 6 L/m^2.h. 62

Figure 4-18: Microbial attachment to the low grade copper bearing ore body in the column reactors, determined from the mechanical detachment of cells from the ore samples periodically removed from the heap systems using the in-bed sampling technique, given for different irrigation rates 2, 6 and L/m^2.h for run 2. 63

Figure 4-19: Microbial growth curve obtained by combining the interstitial and attached cells accumulated in the ore bodies, determined from the mechanical detachment of cells from the ore samples periodically removed from the heap systems using the in-bed sampling technique, obtained from duplicate experimental runs at 2 L/m^2.h. Error bars represent the standard deviation of the ore-

associated cell counts. The 'poly.' lines were generated in excel using the trendline option for polynomials of order 2. 64

Figure 4-20: Microbial growth curve obtained by combining the interstitial and attached cells accumulated in the ore bodies, determined from the mechanical detachment of cells from the ore samples periodically removed from the heap systems using the in-bed sampling technique, obtained from triplicate experimental runs at 6 L/m^2.h. Error bars represent the standard deviation of the ore-associated cell counts. The 'poly.' lines were generated in excel using the trendline option for polynomials of order 2. 65

Figure 4-21: Microbial growth curve obtained by combining the interstitial and attached cells accumulated in the ore bodies, determined from the mechanical detachment of cells from the ore samples periodically removed from the heap systems using the in-bed sampling technique, obtained from duplicate experimental runs at 18 L/m^2.h. Error bars represent the standard deviation of the ore-associated cell counts. The 'poly.' lines were generated in excel using the trendline option for polynomials of order 2. 65

Figure 5-1: Total effluent flow rate profile as a function of time during the bioleaching of low grade copper-bearing ore in a box reactor, at an irrigation rate of 6 l/m^2/h, corresponding to 360 ml/h. The arrows are indicative of the in-bed sampling points..... 70

Figure 5-2: Profile of fluctuating effluent flow rates during the bioleaching of low grade copper bearing ore in a box reactor, given for each of the 13 outlet ports. The arrows are indicative of in-bed sampling points. 71

Figure 5-3: Moisture content of the ore bed during leaching, determined from the ore samples periodically removed from the heap systems, given for sampling times (a) day 24 and (b) day 49. 72

Figure 5-4: Moisture content of the ore bed during leaching, determined from the ore samples periodically removed from the heap systems, given for sampling times (a) day 63 and (b) day 83. 73

Figure 5-5: Copper analysis showing (a) the concentration profile and (b) the cumulative copper removal as a function of time during the bioleaching of low grade copper bearing ore, given for each of the 13 effluent collection ports, determined from atomic absorption spectroscopy. 76

Figure 5-6: Total cumulative copper liberation as a function of time during the bioleaching of low grade copper bearing ore, determined from atomic absorption spectroscopy. 77

Figure 5-7: Trend in (a) the pH and (b) the redox potential, of the eluted solution passing through the box heap, given for each of the 13 effluent collection ports. The arrow is indicative of the inoculation point..... 78

Figure 5-8: Iron analysis showing (a) the ferrous iron concentration and (b) the total iron concentration as a function of time, determined spectrophotometrically using the colorimetric 1-10 phenanthroline method, given for ports 1, 2, 3, 4, 5, 6, 8 and 12. 79

Figure 5-9: Trend in (a) the cell concentration and (b) the cumulative number of cells, exported in the leachate passing through the heap, given for outlet ports 1, 2, 3, 4, 5, 6, 8, and 12. 81

Figure 5-10: Cell densities of the 9 zones in the ore bed, determined from mechanical detachment and microscopic analysis of the ore samples periodically removed from the heap systems, given for day 49 (22 days post inoculation). 82

Figure 5-11: Cell densities of the 9 zones in the ore bed, determined from mechanical detachment and microscopic analysis of the ore samples periodically removed from the heap systems, given for day 63 (36 days after inoculation). 83

Figure 5-12: Cell densities of the 9 zones in the ore bed, determined from mechanical detachment and microscopic analysis of the ore samples periodically removed from the heap systems, given for day 83 of the leaching duration (56 days post inoculation). 83

LIST OF TABLES

Table 2-1: Heap bioleaching parameters (adapted from Pradhan *et al.*, 2008) 6

Table 2-2: Operating ranges for important bioleaching bacteria operating in the mesophilic or early thermophilic temperature range (Information extracted from Rossi (1990), Watling (2006) and Schippers (2007)). 12

Table 2-3: Growth rates of mesophilic micro-organisms in various systems 16

Table 2-4: Forms of preferential flow (O'Kane *et al.*, 2000) 19

Table 2-5: Influence of irrigation to height ratio over bioleaching in columns or heaps (extracted from Lizama *et al.*, 2005) 21

Table 2-6: Typical phase region in porous media (adapted from Bartlett, 1992) 23

Table 3-1: Mineral contributions to the available copper, in the low grade copper-bearing ore sample 29

Table 3-2: Sensitivity analysis to determine inoculum concentration 30

Table 3-3: Column specifications 31

Table 3-4: Box reactor geometry 35

Table 4-1: Copper analysis over the 3 flow systems during leaching run 1 after 45 days 44

Table 4-2: Analysis of the micro-organisms present in the inoculum and in the ore bed at the end of the experiment determined from the mechanical detachment of cells from the ore samples periodically removed from the heap systems using the in-bed sampling technique, given for a single sample of the interstitial phase under the different irrigation rates 2, 6 and 18 $l/m^2/h$, during the preliminary run. ... 48

Table 4-3: Copper analysis over the 3 flow systems during leaching run 2 after 32 days 50

Table 4-4: Copper analysis over the 3 flow systems during leaching run 3 after 32 days 50

Table 4-5: Total cumulative exported cells after 32 days leaching for runs 2 and 3, and the preliminary run 1 57

Table 4-6: Growth rates (μ^{max} = bacterial specific growth rate [h^{-1}]) calculated based on the ore-associated microbial population within the columns 59

Table 4-7: Cell balance over the 3 flow systems during leaching run 2 at day 32 61

Table 4-8: Cell balance over the 3 flow systems during leaching run 3 at day 32 64

Table 5-1: The relative proportions of ore-associated micro-organisms present in each of the 9 zones in the ore bed, determined from the mechanical detachment and microscopic analysis of cells obtained

from the ore samples periodically removed from the box, given for intervals during the leaching run on days 49, 63 and 83 corresponding to 22, 36 and 56 days post-inoculation (n.d = not detectable)... 84

NOMENCLATURE

Abbreviations

AMD	- Acid mine drainage
ARD	- Acid rock drainage
CeBER	- Centre for Bioprocess Engineering Research
DNA	- Deoxyribonucleic acid
EOM	- Extracellular organic material
EPS	- Extracellular polymeric substances
IX	- Ion Exchange
MRI	- Magnetic resonance imaging
PCR	- Polymer chain reaction
PLS	- Pregnant leach solution
PSD	- Particle size distribution
SEM	- Scanning electron microscopy
SX	- Solvent extraction

Chemical Formulae

CO_2	- Carbon dioxide
Cu	- Copper
CuO	- Copper (II) oxide
Cu_2S	- Chalcocite
$CuFeS_2$	- Chalcopyrite
Fe	- Iron
Fe^{3+}	- Ferric iron
Fe^{2+}	- Ferrous iron
FeS_2	- Pyrite
$FeSO_4.7H_2O$	- Ferrous sulphate
H_2O	- Water
H_2S	- Hydrogen sulphide

H_2SO_4	- Sulphuric acid
K_2SO_4	- Potassium sulphate
$(NH_4)_2SO_4$	- Ammonium sulphate
$NH_4H_2PO_4$	- Ammonium di-hydrogen orthophosphate
O_2	- Oxygen
S	- Elemental sulphur

Symbols	**Description**	**Units**
A	- Cross-sectional area	m^2
A_o	- Arrhenius constant	h^{-1}
d	- Particle diameter	m
E_a	- Activation energy	kJ mol^{-1}
K	- Permeability coefficient	
K_s	- Half saturation constant	g L^{-1}
I/H	- Irrigation to height ratio	L m^{-3} min^{-1}
p	- Fluid head	m
ρ	- Fluid density	kg m^{-3}
q_x	- Flow rate	m^3 s^{-1}
R	- Universal gas constant	
Re	- Reynolds number	dimensionless
r_x	- Rate of multiplication of micro-organisms	g L^{-1} h^{-1}
S	- Limiting substrate concentration	g L^{-1}
T	- Growth temperature	K
t	- Time	h
μ	- Specific growth rate	h^{-1}
μ_{max}	- Maximum specific growth rate	h^{-1}
μ_L	- Fluid velocity	m/s
X	- Concentration of micro-organisms	g L^{-1}

GLOSSARY

Acidophile	Microorganism which grows optimally at low pHs, typically between 1.0 and 4
Archaea	Grouping of microorganisms based on the genetic make-up and metabolic functions
Autotroph	Microorganisms that utilise carbon dioxide (CO_2) as their only carbon source
Chemotaxis	Active orientation of bacterium in a chemical
Extreme thermophile	Microorganism that can grow at elevated temperatures i.e. above 65°C
Heterogeneous	Different in nature
Heterotroph	Microorganism that utilises organic materials as their only carbon source
Homogeneous	Uniform; consistent
Inhibition	Prevention of microbial functions such as biooxidation of ferrous iron in the case of bioleaching microorganisms
Inoculum	Initial microbial cells added to the heap system from which microbial growth proceeds to provide a sufficient culture to facilitate the leaching process
Leachate	Effluent leach solution
Mesophile	Microorganism that can grow in the temperature range 20-40°C
Metabolism	The system of chemical reactions occurring within the microbial cells, including both the breakdown of compounds via catabolism and the synthesis of compounds through anabolism
Moderate thermophile	Microorganism that can grow in the temperature range 40-60°C
Ore-associated micro-organisms	Combination of interstitial and attached cells
Planktonic	Freely suspended
Raffinate	Acidified leach solution used to irrigate ore bed

1 CHAPTER 1: INTRODUCTION

1.1 Background

Pyrometallurgical and hydrometallurgical processes are used in the extraction and refining of metals, such as copper, from ore. The conventional pyrometallurgical methods employed are smelting following crushing, milling and concentration by flotation, whilst typical hydrometallurgical approaches use acid-leaching in tanks or heaps and pressure oxidation.

Copper-mining and subsequent acid leaching has been applicable since the 1960's (Petersen and Dixon, 2007a). Copper was easily recovered from the available high grade ores via smelting. More recently, the copper reserves available contain low grade, complex and refractory ores (Watling, 2006). This makes the use of conventional extraction methods *e.g.* crushing and milling for liberation, concentration by flotation followed by smelting, a less viable option due to the economic feasibility associated with these energy intensive and environmentally harmful processes (Viera *et al.*, 2007). The development of heap bioleaching as an alternative efficient technology provides high metal recoveries within a reasonable timeframe, at a low cost and with low processing energies. Heap bioleaching provides several advantages over other technologies, such as the use of simple equipment and operation; short construction times; low investment and operational costs; an environmentally friendly process and acceptable yields (Watling, 2006; Pradhan *et al.*, 2008). A key challenge is in ensuring leach times required are minimised.

Heap bioleaching is a hydrometallurgical process which involves the microbially-assisted leaching of sulphide minerals. It is commonly employed when dealing with low grade and run-of-mine ores as it allows processing without energy intensive milling (Rawlings and Johnson, 2007). Bioleaching technology attracts global attention. Bioleaching operations have been employed in Australia, Brazil, Chile, China and Peru (Petersen and Dixon, 2007a).

Efforts to optimise the bioleaching process are key to adding value to industrial applications. With the abundance of mineral reserves on the African continent in general, maintaining a leading position in this field will likely place South Africa in a strategic position. Industry players and science councils active in South Africa such as 'Mintek', 'Goldfields', 'Anglo American Corporation' and 'BHP Billiton' have already contributed substantially to bioleaching research and development {R&D} over the years. Furthermore, extensive research on bioleaching technology has been conducted by Universities, making the bioleaching process a considerably developed technology. There are still limitations to this technology, particularly in heap bioleaching, as only partial process control can be exerted due to the numerous parameters which influence the process (Petersen and Dixon, 2007b).

1.2 Problem Statement and Research Objectives

Harnessing the available mineral reserves plays a major role in socio-economic development (Ndlovu, 2008). Downturn of minerals prices on the world market, and the economic recession led to decreased mining activity and closure of mines culminating in the loss of employment (Ndlovu, 2008). Although copper prices have increased again, it is imperative to develop technologies that are less susceptible to fluctuations in the mineral price, cost effective, simple to apply and improve resource productivity (Ndlovu, 2008; Watling, 2006; Afewu and Dixon, 2006; Pradhan *et al.*, 2008).

Acid Rock/Mine Drainage (ARD/AMD) is a major environmental problem in many regions, caused by mineral exploitation (Rohwerder and Sand, 2007). ARD causes the acidification, high salts loading

(particularly SO_4^{2-}) with concomitant metal deportment and heavy metal contamination of ground water systems. The formation of ARD occurs through the same set of reactions as in bioleaching environments. The leaching of waste rocks and tailings is undesired. Therefore it is useful to use understanding of bioleaching sub-processes, to provide solutions for reducing ARD. This demands a comprehensive awareness of the processes and sub-processes which contribute to heap leaching competency. Optimisation of bioleaching processes reduces leaching times and enhances the extent of extraction, thereby decreasing the amount of ARD generated subsequently. Heaps that are well colonised by leaching microorganisms are expected to have high copper recoveries within a shorter timeframe than un-colonised heaps. However, there is dearth of understanding of the phenomena involved in microbially operated bioheaps (Pradhan *et al.* 2008). Watling (2006) highlighted the cause of lack of in-depth understanding of bioleaching to the separated and independent focus of investigations on different aspects such as chemistry, microbiology and hydrodynamics. Effective bioleaching necessitated focus on interactions between these aspects.

Microbial attachment to mineral surfaces has been studied extensively (Gehrke *et al*., 1998; Sampson *et al*., 2000; Kinzler *et al*., 2003; Rodriguez *et al*., 2003; Sand and Gehrke, 2006; Ghauri *et al*., 2007; Africa *et al.*, 2010; Bromfield *et al*., 2010). The ability of micro-organisms to propagate through the heap to favourable sites and locations for growth and biooxidation is unaccounted for, as is the role heap hydrodynamics plays in the microbial attachment and detachment processes. Further, literature lacks knowledge of detachment mechanisms, only making plausible reference to detachment attributed to hydrodynamic shear stress (Rossi, 1990; van Loosdrecht *et al*., 1990; Pintelon *et al*., 2009; van Hille *et al.*, 2010). Although this phenomenon has been reported by Rockhold *et al*. (2002), the microbial system under investigation differed from typical bioleaching systems. Therefore, research focussed on the impact of irrigation rates (hence fluid shear) and solution flow through the heap on the spatial distribution of microbial cells is required. This thesis addresses this in part, focusing specifically on:

- The effect of irrigation inoculation at different rates on the initial microbial attachment and subsequent colonisation of the ore, studied using a heap leach column system.
- The effect of increased irrigation rates on the detachment of micro-organisms from heaps.
- Microbial propagation from a single point source and its relation to fluid flow.
- Microbial colonisation of the ore body relative to the single irrigation point through the measurement of the changes in population density of microbial species with time and location through a simulated box heap.

1.3 Scope and Limitations

The aim of this study is to add to the bioleaching knowledge base by providing inter-disciplinary research through integration of microbiological and hydrological aspects of heap bioleaching. This investigation focuses on the impact of solution flow patterns and velocity on the propagation and subsequent colonisation of heaps in a system that mimics the real life heap situation as opposed to colonisation studies conducted in batch or stirred tank reactor processes.

1.4 Plan of Development/Thesis structure

This thesis begins with an extensive review of the available literature relevant to the current study, presented in Chapter 2. This provides an overview of the heap bioleaching technology, the past and current advancements and key research areas pertinent to the improvement of this technology and its

application. The review identifies some gaps and inconsistencies in the heap leaching knowledge base. The two key foci for this investigation are to review microbial attachment and colonisation, and heap hydrology in conjunction with colonisation. Studies conducted in systems related to heap leaching systems were also reviewed, owing to the limited studies within heap bioleaching. The research objectives and hypotheses developed from the literature evaluation are presented.

The experimental programme adopted to test the hypotheses, is presented in Chapter 3. In this chapter, the reactor systems used are described. Novel sampling approaches are fully described. Further, the methodologies used and the experimental approach is detailed.

Column reactor studies were used to interrogate the effect of differing irrigation rates on microbial colonisation. Irrigation rates of 2 to 18 $l/m^2/h$ were selected to span the range used industrially. These results are presented and discussed in Chapter 4. The box reactor was used to investigate the propagation of micro-organisms through the ore bed from a single point source of irrigation. These results are presented and discussed in Chapter 5.

Chapter 6 highlights the link between solution flow and microbial colonisation providing a discussion of the experimental findings and their implications, drawing conclusions from these finding and providing recommendations for further investigations within this research field.

2 CHAPTER 2: LITERATURE REVIEW

The literature review herein provides a detailed analysis of the background knowledge of heap bioleaching processes (Section 2.1) and previous work conducted with emphasis on microbiological and hydrological aspects of heap bioleaching. The review introduces the role of micro-organisms in the leaching process in Section 2.2. It highlights the current understanding of microbial colonisation and cell attachment in batch systems in Section 2.3. In Section 2.4, microbial propagation in unsaturated flow systems is considered. Some hydrology models are discussed with emphasis on the lack of accountability of the interactions between microbial growth and solution flow. Microbial colonisation of particulate systems from other scientific and engineering fields have contributed to identification of the possible effects of solution flow on microbial transport and colonisation, and the counteractive effect of microbial growth on solution flow patterns. Some experimental methodologies employed in previous studies render them inapplicable to the heap leaching system. In Sections 2.5 and 2.6, the integration of the knowledge reviewed leads to presentation of the research objectives and hypotheses.

2.1 Overview of Heap Bioleaching

2.1.1 *Description of Heap Bioleaching Operations*

Heap bioleaching is a microbially-mediated process in which metals are extracted from low grade ore. Most typically the bioleaching of base metal sulphides by ferric iron and acid leach agents, re-generated microbially, is considered. However, other bioleach systems are also relevant. Figure 2-1 depicts a typical heap bioleaching operation for low grade sulphidic minerals. The heaps are constructed by first blending the ore for grade control, then crushing it to particle sizes to provide suitable mineral liberation for significant extraction within a suitable leaching time (Bartlett, 1992) while ensuring ore bed permeability, typically < 25 mm (Petersen and Dixon, 2007a). The ore is agglomerated with acidified solution prior to stacking (Petersen and Dixon, 2007a). Agglomeration is a process in which fine-grained particles and clays (~1 mm) within the ore are attached to larger particles (10 to 20 mm) (O'Kane *et al.*, 2000). Bouffard (2008) reported particle size distribution showing a substantial decrease in the free fines fraction post-agglomeration. Flow conditions improve by eliminating the ability of the fines and clays to restrict flow, thereby providing good permeability (Bartlett, 1992; O'Kane *et al.*, 2000). Furthermore, agglomeration promotes the formation of a more homogeneous heap (O'Kane *et al.*, 2000) for uniform percolation, thus efficient metal extraction (Bartlett, 1992; Petersen and Dixon, 2007b).). The heap is stacked on an impermeable layer connected to a drainage system (Petersen and Dixon, 2007a). An aeration system is inserted at the base of the heap. Typically during stacking, layers of coarse and fine textured material develop naturally within heap piles causing segregation (Bartlett, 1992; O'Kane *et al.*, 2000) and preferential flow develops under these conditions, leaving areas within the heap unleached (Decker and Tyler, 1999; O'Kane *et al.*, 2000). In some operations chemical wetting agents are added to the leach solution to reduce the surface tension of liquids, resulting in increased flow and thorough wetting of the heap (O'Kane *et al.*, 2000).

After construction, the heap is aerated from the bottom via a pipeline network system (Petersen and Dixon, 2007a). Aeration rates range from 0.08 to 2 $m^3/m^2/h$ (Petersen and Dixon, 2007a). The heap is irrigated from above using raffinate, an acidic leach solution containing nutrients such as ferrous iron, which is applied over the heap surface employing irrigation rates ranging from 5 to 20 $L/m^2.h$ and

using drippers typically spaced 30 to 100 cm apart (Petersen and Dixon, 2007a). Optimal dripper spacing should be determined for efficient wetting and colonisation of all heap zones. Solution distribution through the heap is governed by the combined effects of gravity and capillary action (Petersen and Dixon, 2003). As solution percolates through the ore bed, the minerals dissolve into solution whilst influencing solution-ore and microbe-ore contact. The solution flow also plays an important role in facilitating the transfer of heat within the heap (Petersen and Dixon, 2007a).

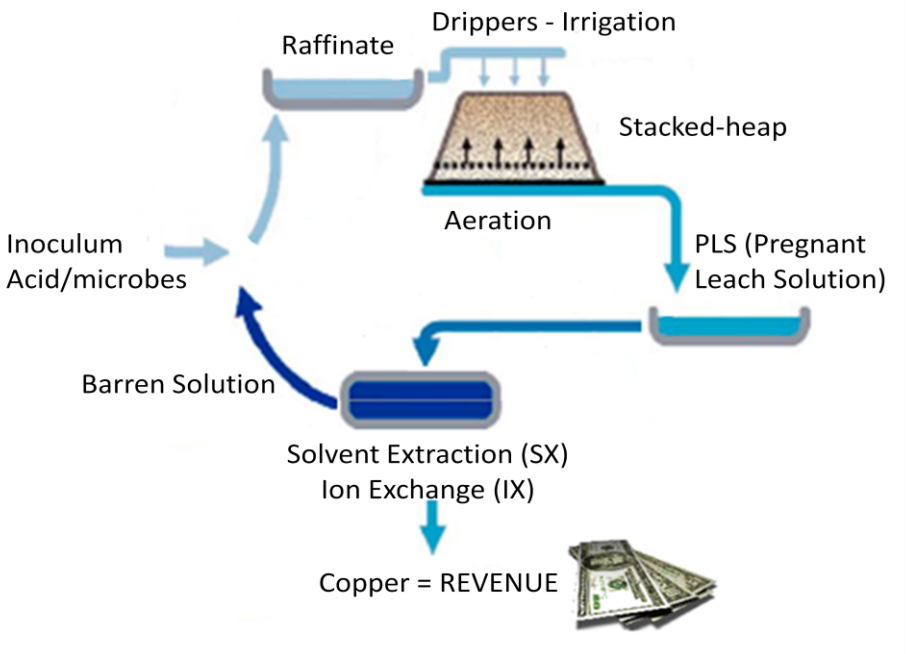

Figure 2-1: Typical heap leaching circuit, showing solution flow through the ore bed, aeration to promote bioleaching of sulphide minerals, recovery of copper metal and recycling of barren solution to minimise water use (Adapted from Watling, 2006).

The heap is inoculated with a variety of micro-organisms (Brierley, 2001), reviewed in Section 2.2, which catalyse the iron and sulphur oxidation reactions that occur during the bioleaching process. Efficient irrigation is necessary for transport of micro-organisms, reactant solutes and leaching products into and out of the heap, and maintenance of temperatures within the limits of activity of the micro-organisms (Petersen and Dixon, 2007a). There is a lag time before the micro-organisms grow and begin to contribute to sulphide oxidation. This lag time can be reduced by utilising leach solutions containing active microbial populations already acclimatised to leaching environments (Watling, 2006). The drainage system collects the pregnant leach solution (PLS) (Petersen and Dixon, 2007a). This undergoes further processing to recover the metal via solvent extraction and electro-winning or ion exchange using a resin bed. The effluent, i.e. barren solution, is recycled for re-irrigating the heap. Organic matter remaining in the recycled effluent can cause microbial inhibition (Brierley, 2001; Rawlings *et al.*, 2003; Pradhan *et al.*, 2008). Pradhan *et al.* (2008) reported that metal oxidation mediated by micro-organisms can be inhibited by accumulation of heavy metals such as copper, zinc, arsenic and iron. High metal concentrations become toxic to the micro-organisms lowering bio-oxidation rates (Pradhan *et al.*, 2008). Escobar and Lazo (2003) suggested dilution of irrigation solution to avoid the build up of constituents inhibiting microbial growth and activity. Alternatively, flushing out the heap from time to time could be considered. However, this may not be practical on a large industrial heap scale. In both cases, impact on the water balance must be considered.

2.1.2 *Factors Affecting Heap Bioleaching*

Several environmental, biological and physicochemical factors have significant effects on the yield achieved by heap bioleaching processes. Pradhan *et al*. (2008) have identified the important factors summarised in Table 2-1.

Table 2-1: Heap bioleaching parameters (adapted from Pradhan *et al.*, 2008)

Parameter	
Ore mineralogy:	The ore must contain sulphide minerals susceptible to ferric and acidic leaching and access to the mineral must be assured by suitable particle sizes or porosity. The gangue material influences acid consumption and may liberate additional ions into solution *e.g.* Al^{3+}, Mg^{2+}. Chalcopyrite-containing ores require higher temperatures for effective leaching (Watling, 2006), suggesting that ore mineralogy has an effect on the temperature that would be required to attain maximum metal extraction.
Aeration:	The supply of O_2 and CO_2 to the leaching system provides components required for microbial growth and ferrous iron oxidation.
Irrigation:	The irrigant supplies reactant solutes *e.g.* H_2SO_4, controls precipitation of salts that might block the percolation channels, controls pH and, to an extent, temperature via heat transfer within the heap. Note that acid consumption is a major contributor to processing costs (Watling, 2006).
Temperature:	The temperature of the heap determines which microbes govern the heap during the course of the bioleaching process. Microbial populations are dynamic, adapting to the changing heap leaching environment.
Biology:	The microbial diversity and adaptation abilities of micro-organisms, population density and spatial distribution of micro-organisms, location with respect to mineral grains, and microbial activity play significant roles in the leaching process.
pH:	Control of the leaching environment for optimal microbial activity.
Redox potential:	The rate of mineral dissolution is a function of the ferric to ferrous iron ratio (Fe^{3+}/Fe^{2+}). High redox potentials tend to inhibit the bioleaching of chalcopyrite (Córdoba *et al*., 2008)

Rossi (1990) reported that metal recovery is dependent on the following: (i) contact of leach solutions with the highest proportion of accessible mineral surface area (exposure and percolation); and (ii) access of gases (*i.e.* O_2 and CO_2) required for micro-organisms' metabolism and oxidation process to the highest portion of wetted mineral surface (oxygenation). Efficient exposure, percolation and oxygenation of the heap is associated with properly designed and constructed heaps as is operating with all controllable leaching parameters at their optimum.

2.1.3 *Leaching Chemistry*

This study is focused on the leaching of copper bearing ores that typically are comprised of copper oxides *e.g.* CuO, and copper sulphides *e.g.* Cu_2S. The most abundant copper sulphide mineral is chalcopyrite, $CuFeS_2$, which is very refractory. Further passivation of the mineral surface is caused by

jarosite precipitation (Watling, 2006). Typical leaching reactions occurring in the heap are described by Watling (2006) and illustrated in Figure 2-2.

The reaction pathways are complex and have been outlined by Sand and Gehrke (2006) and Rohwerder and Sand (2007). The leaching process involves mineral oxidation by ferric ions (Fe^{3+}) releasing the copper ions (Cu^{2+}) into solution (Equation 1). The non-oxidative dissolution of the mineral by sulphuric acid (H_2SO_4) occurs simultaneously (Equation 2).

$$CuFeS_2 + 4Fe^{3+} \rightarrow 5Fe^{2+} + Cu^{2+} + 2S^0 \quad [1]$$

$$CuFeS_2 + 4H^+ \rightarrow Fe^{2+} + Cu^{2+} + 2H_2S \quad [2]$$

$$2Fe^{2+} + 2H^+ + 0.5O_2 \rightarrow 2Fe^{3+} + H_2O \quad [3]$$

$$2S + 3O_2 + 2H_2O \rightarrow 2H_2SO_4 \quad [4]$$

$$4FeS_2 + 15O_2 + 2H_2O \rightarrow 4Fe^{3+} + 8SO_4^{2-} + 4H^+ \quad [5]$$

Microbial ferrous iron oxidation reactions also occur (Equation 3). The oxidation of ferrous ion to ferric ion regenerates the Fe^{3+} ions required in the metal dissolution reaction. This reaction may induce high redox potentials (0.65-0.70 V SHE) which are less conducive to chalcopyrite oxidation because any ferric precipitates formed hinder the bioleaching process (Watling, 2006).

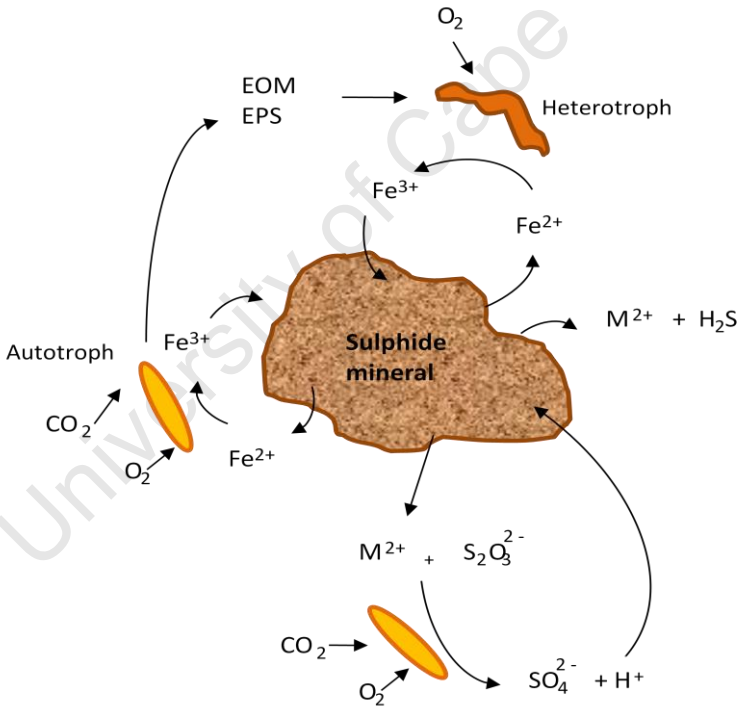

Figure 2-2: Illustration of heap leaching reactions catalysed by microbes (adapted from Schippers *et al.*, 1996; Rohwerder and Sand, 2007).

During the mineral dissolution, the sulphur component of the sulphide mineral undergoes two different oxidation mechanisms (Schippers *et al.*, 1996; Schippers, 2007; Rohwerder and Sand, 2007). Acid-insoluble metal sulphides, *e.g.* pyrite (FeS_2), proceed via the thiosulphate pathway in which thiosulphate is oxidised to sulphate and elemental sulphur (Schippers *et al.*, 1996; Schippers, 2007; Rohwerder and Sand, 2007). Acid-soluble sulphide minerals, *e.g.* chalcopyrite ($CuFeS_2$), are transformed into elemental sulphur in the absence of sulphur reducing micro-organisms through the polysulphide pathway (Schippers *et al.*, 1996; Schippers, 2007; Rohwerder and Sand, 2007). The

oxidation of sulphur to sulphate (Equation 4) generates acid required to leach the mineral and maintain a low pH environment. Maintenance of preferred pH range of 1 to 2 is important for both microbial iron and sulphur oxidation, leading to ferric iron and acid regeneration by microbial populations (Watling, 2006). Low pH is also important to maximise the solubility of iron as it is a key leach agent and precipitates may passivate the mineral surface and influence bed permeability.

2.1.4 *Bioleaching Mechanisms*

The involvement of micro-organisms in the leaching reactions has been the subject of much debate. Direct leaching was one of the main mechanisms proposed (Devasia *et al*., 1993). In this mechanism it was proposed that micro-organisms attached to mineral surface to oxidise the sulphide phase by enzymatic attack, without any requirement for ferric or ferrous ions. Tributsch (2001) reported that observations from electron microscopy images contradicted this mechanism. To date, the key leaching mechanisms postulated to contribute to bioleaching of mineral sulphides and highlighted in previous studies (Devasia *et al*. 1993; Tributsch, 2001; Sand *et al*. 2001; Rawlings, 2002; Sand and Gehrke, 2006; and Watling, 2006) are:

- *Indirect non-contact mechanism:* Micro-organisms oxidise ferrous ions to ferric ions in bulk solution, and sulphides or intermediates to sulphate and acid. The sulphide mineral is either oxidised by ferric ions or dissolved in the acidic solution (Tributsch, 2001). No adhesion of micro-organisms to the mineral surface is required *i.e.* oxidation may occur by planktonic bacteria (Devasia *et al*., 1993; Tributsch, 2001; Sand and Gehrke, 2006).
- *Indirect contact mechanism:* Micro-organisms attached to the mineral surface oxidise ferrous ions to ferric ions within a biofilm comprised of micro-organisms and extracellular polymeric substances (EPS). The EPS acts as a reaction medium in which the ferric ions and protons generated induce thiosulphate and sulphate formation (Tributsch, 2001).
- *Cooperative leaching mechanism:* This is the result of symbiotic activity between the freely suspended micro-organisms and the attached cells (Tributsch, 2001). The waste ferrous and sulphur species released during the sulphide mineral leaching are used as an energy source by the suspended cells (Tributsch, 2001).

These mechanisms indicate the importance of both microbial retention within the leaching environment and attachment to mineral surfaces. Further, quantitative studies on the ability of attached communities to enhance biooxidation over unattached cells could inform the mechanisms proposed.

2.2 Function of Microbes in the Leaching Process

2.2.1 *Microbial Characteristics and Diversity*

The role of micro-organisms in the heap is analogous to a catalyst (Pradhan *et al*., 2008) as portrayed in Section 2.1.3. Both bacteria and archaea are found in the natural leaching environment and grow in inorganic, aerobic and low pH environments (Rawlings and Johnson, 2007). Generally all micro-organisms require nutrients such as carbon, oxygen, nitrogen, sulphur, and phosphorus for growth, cell maintenance and metabolic activities (Bailey and Ollis, 1986). The carbon source used by the micro-organisms implicated to play the dominant role in bioleaching is carbon dioxide (CO_2) obtained from air, which renders them autotrophic (Rawlings and Johnson, 2007; Pradhan *et al.*, 2008). Bioleaching micro-organisms typically oxidise iron and/or sulphur to provide a metabolic energy *i.e*. they are chemolithotrophs (Rodriguez *et al*., 2003). Autotrophic micro-organisms may produce extracellular organic material (EOM) and EPS providing a carbon source for the heterotrophic micro-organisms

present in the heaps (Pradhan *et al*., 2008). Metabolising waste organic products is important to maintain a suitable leaching environment and avoid inhibition of microbial growth and biooxidation (Rawlings and Johnson, 2007).

The bioleaching micro-organisms are subjected to further classification because they function at different temperatures. The temperature regimes for effective microbial activity are: 20 to 40 °C for mesophilic microbes (predominantly bacteria); 40 to 60 °C for moderately thermophilic microbes (bacteria and archaea); and greater than 65 °C for extreme thermophilic microbes (predominantly archaea) (Bailey and Ollis, 1986; Rawlings and Johnson, 2007). By increasing the heap temperature, typically through exothermic oxidation reactions, the microbial community present is modified to favour the development of thermophilic micro-organisms (Pradhan *et al*., 2008). These higher temperatures of 60 °C and above are recognised to enhance chalcopyrite leaching and to be necessary to achieve desired copper recoveries.

The main mesophilic micro-organisms reported in bioleaching systems are *Acidithiobacillus caldus, Acidithiobacillus ferrooxidans, Acidithiobacillus thiooxidans, Leptospirillum ferriphilum*, and *Leptospirillum ferrooxidans* (Table 2-2). Extensive studies have been conducted on *Acidithiobacillus ferrooxidans* (Schippers, 2007; Watling, 2006). This micro-organism is Gram negative, rod shaped, chemolithotrophic acidophile which derives energy from both iron and sulphur oxidation (Devasia *et al.*, 1993; Karavaiko *et al*., 2006; Watling, 2006; Schippers, 2007). It is characterised by the optimal pH of 2.5 and temperature range of 30 to 35 °C. The growth range of *Acidithiobacillus ferrooxidans* is from pH 1.3 to 4.5 and 10 to 37 °C (Schippers, 2007). Its growth can be inhibited by high ferric ion (Fe^{3+}) concentrations (Watling, 2006). Recently *At. ferrooxidans* has been reported to include four subspecies (Schippers, 2007). *Acidithiobacillus thiooxidans* is a sulphur oxidising acidophile which functions optimally at pH 2 to 3.0 and 28 to 30 °C, with a wide growth range from pH 0.5 to 5.5 and 10 to 37 °C (Schippers, 2007). *Acidithiobacillus caldus* is also a sulphur oxidising autotroph which functions optimally at pH 2.0 to 2.25 and 45 °C, with an operational growth range from pH 1.0 to 3.5 and 32 to 52 °C (Schippers, 2007). *Leptospirillum ferriphilum* and *Leptospirillum ferrooxidans* are more tolerant to high temperatures (Table 2-2), have low optimum pH ranges of 1.3 to 1.8 and 1.5 to 3.0 respectively and documented ranges for growth of pH 1.3 to 4.0 (Schippers, 2007). These micro-organisms are also excellent scavengers of Fe^{2+}, functioning well at high redox potentials. *L. ferrooxidans* were found to be the dominant population in copper ore bioleaching tanks using low ferrous iron concentrations (Pradhan *et al.*, 2008). *L. ferriphilum* is typically reported as the dominant bacterium in mesophilic tank systems for pyrite or arsenopyrite leaching (Coram and Rawlings, 2002). This micro-organism has a spiral shape (Karavaiko *et al*., 2006). To maintain an active population of micro-organisms, it is important to understand how they are affected by the inherent changing heap environment.

2.2.2 ***Microbial Consortium***

Rawlings and Johnson (2007) have reviewed some of the microbial aspects of bioleaching indicating that current focus is on the selection of microbial communities which provide enough biodiversity for optimal heap leaching performance. Johnson's research group is conducting work on designing combinations of microbial consortia to endorse effective microbial activity and adaptability to the changing leaching environment. Identification of all micro-organisms present in leaching environments and extensive research on their specific contributions to the biooxidation process enables separation of microbes with significant effects from those with a lesser impact. This will contribute to the design of appropriate inoculum compositions specific to the different bioleaching

environments (*e.g*. extremely low to extremely high temperature leaching conditions). The utilisation of only the relevant microbial populations could potentially reduce operational cost associated with aeration and nutrient supply that would otherwise be incurred when undesired microbial communities are present in the heap (Rawlings and Johnson, 2007).

So far, Johnson's work has shown that mixed cultures are more efficient in the bioleaching process than pure cultures. Further, it is well known that mixed cultures enhance process robustness and resilience to perturbations (Roychoudhury, 2004; Miura *et al*., 2007; Oyekola, 2008). This also corresponds to typical industrial practice, leading to the choice of a mixed culture of mesophilic microorganisms to inoculate the systems utilised in this investigation.

2.3 Microbial Colonisation

Many studies have looked at the contribution of microbial communities in bioheaps with the main focus currently centred on identifying key micro-organisms and their colonisation of heaps. Colonisation studies (Gehrke *et al*., 1998; Sampson *et al*., 2000; Kinzler *et al*., 2003; Rodriguez *et al*., 2003; Sand and Gehrke, 2006; Ghauri *et al*., 2007) focused on the attachment step, dealing with the mechanisms behind initial microbial attachment and EPS formation and its role in biofilm formation. More recently focus has turned to the location and specificity of microbial attachment to minerals (Africa *et al.*, 2009, 2010; Bromfield *et al*., 2010).

Microbial colonisation of the mineral surface occurs through the following steps:

(i) The transport of microbial cells through the heap to the mineral surface (Rossi, 1990; van Loosdrecht *et al*., 1990). The micro-organisms can either be eluted in the leachate, or accumulated within the heap in the stagnant zones or attached to the ore surface.

(ii) The selective reversible and irreversible attachment to the mineral surface (Rossi, 1990; van Loosdrecht *et al*., 1990, Rockhold *et al*., 2002). Reversible attachment accounts for the micro-organisms loosely associated with the ore surface, whilst the irreversible attachment accounts for the micro-organisms strongly associated. The micro-organisms can be detached from the ore surfaces by repulsive electrostatic forces (Ghauri *et al.*, 2007; Rodriguez *et al.* 2003) and shear forces (Rossi, 1990; van Loosdrecht *et al*., 1990; Rockhold *et al*., 2002; Pintelon *et al*., 2009; van Hille *et al*., 2010). The potential for detachment of microbial cells from the ore also creates an exchange between planktonic cells and the sessile micro-organisms (van Loosdrecht *et al*., 1990).

(iii) Growth and multiplication of micro-organisms resulting in the formation of microbial colonies which contribute to bioleaching (Rossi, 1990; van Loosdrecht *et al*., 1990, Rockhold *et al*., 2002).

The aforementioned steps are elaborated in the following sections.

2.3.1 *Transport of Microbes to Mineral Surface*

The first step in the colonisation process is for the micro-organisms to contact the ore (Lizama *et al.*, 2005). This is achieved by the transportation of the micro-organisms through the heap to the vicinity of exposed sites on the mineral surface (Rossi, 1990). Solutes and micro-organisms permeate porous media by various transport mechanisms governed by the hydraulic and geochemical properties of the heap (Decker and Tyler, 1999). Van Loosdrecht *et al*. (1990) stated that transport occurs via three different modes, shown in Figure 2-3:

(i) Diffusive transport as a result of Brownian motion (Rossi, 1990; van Loosdrecht *et al*., 1990).

(ii) Convective transport due to fluid flow (van Loosdrecht *et al*., 1990).

(iii) Active movement by chemotaxis in which the micro-organisms move in response to a chemical concentration gradient (van Loosdrecht *et al*., 1990).

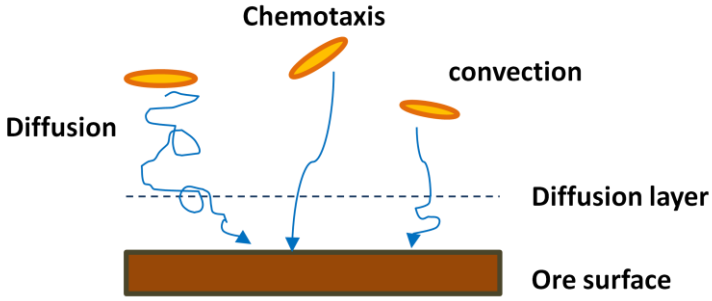

Figure 2-3: Microbial transport to the ore surface (adapted from van Loosdrecht *et al*., 1990)

2.3.2 *Initial Microbial Adherence to Ore*

Once the micro-organisms are within the vicinity of the solid-liquid interface, they adhere to the mineral surfaces, as shown in Figure 2-4, by two approaches:

(i) Selective reversible adhesion where the micro-organisms attach instantaneously, exhibiting Brownian motion (Rossi, 1990; van Loosdrecht *et al*., 1990). These micro-organisms are easily detached from the surface by moderate fluid shear (Rossi, 1990; van Loosdrecht *et al*., 1990).

(ii) Irreversible attachment where the micro-organisms form a permanent bond with the mineral surface (Rossi, 1990). These cells may be removed by a strong shear force (van Loosdrecht *et al*., 1990), although complete removal has not yet been confirmed.

Figure 2-4: Reversible and irreversible adhesion to ore surfaces (adapted from van Loosdrecht *et al*., 1990)

The rate of attachment is directly proportional to the cell concentration and physicochemical properties of fluid media system (Rockhold *et al*., 2002). Reversible and irreversible adhesion both plays an important role in controlling microbial retention. Increasing bacterial retention with decreasing saturation and increasing air-water interface is expected (Wan *et al.*, 1994; Chen, 2008) as reviewed in Section 2.4.3.

2.3.1 *Attachment Bonds and Sites*

Previous studies (Ghauri *et al.*, 2007; Rodriguez *et al.* 2003) have shown that microbial attachment to mineral sulphides is also attributed to the electrostatic interaction between positively charged cell surfaces and negatively charged mineral. Cell attachment is associated with variable physiological changes in micro-organisms (Lehman *et al.* 2001; Watling, 2006). After the initial adhesion to the ore surface, many micro-organisms excrete extracellular polymeric substances (EPS) which mediate their attachment to the ore (van Loosdrecht *et al*., 1990; Gehrke *et al*., 1998; Kinzler *et al*., 2003; Watling, 2006; Sand and Gehrke, 2006; Rohwerder and Sand, 2007; Pradhan *et al*., 2008) (Figure 2-5).

Table 2-2: Operating ranges for important bioleaching bacteria operating in the mesophilic or early thermophilic temperature range (Information extracted from Rossi (1990), Watling (2006) and Schippers (2007)).

Microbial Species	Carbon source	Energy Oxidiser source	pH optimum	pH operational growth range	Temperature optimum (°C)	Temperature operational growth range (°C)
Acidithiobacillus ferrooxidans	Autotrophic	Iron and sulphur	2.5	1.3 to 4.5	30 to 35	10 to 37
Acidithiobacillus thiooxidans	Autotrophic	Sulphur	2.0 to 3.0	0.5 to 5.5	28 to 30	10 to 37
Acidithiobacillus acidophilus	Autotrophic	Sulphur	~ 3	~ 3	25 to 30	25 to 30
Acidithiobacillus caldus	Autotrophic	Sulphur	2.0 to 2.5	1.0 to 3.5	45	32 to 52
Leptospirillum ferrooxidans	Autotrophic	Iron	1.5 to 3.0	1.3 to 4.0	28 to 30	~ 30
Leptospirillum ferriphilum	Autotrophic	Iron	1.3 to 1.8	-	30 to 37	-
Ferrimicrobium acidiphilum	Heterotrophic	Iron	2 to 2.5	1.3 to 4.8	37	< 10 to 45
Ferroplasma acidiphilum	Autotrophic Heterotrophic	Iron	1.7	1.3 to 2.2	35	15 to 45
Sulfobacillus thermosulfidooxidans	Autotrophic Heterotrophic	Iron and sulphur	~ 2	1.5 to 5.5	45 to 48	20 to 60

Extracellular polymeric substances have been shown to contain sugars, uronic acids, lipids and, in some cases, proteins (Kinzler *et al*., 2003; Rohwerder and Sand, 2007; Michel *et al*., 2009). The exact compositions were found to be micro-organism and substrate dependent (Sand and Gehrke, 2006; Rohwerder and Sand, 2007). The EPS biofilm provides a better leaching environment by providing proximity to source of electron donor and more stable physiological environment (Rohwerder and Sand, 2007).

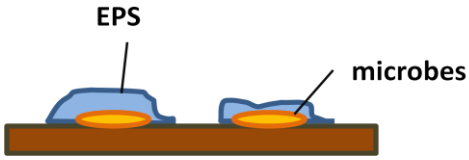

Figure 2-5: Firm attachment via EPS formation (adapted from van Loosdrecht *et al.*, 1990)

Attachment of micro-organisms to ore is dependent on the mineral surface area availability, particle size distribution (PSD), compaction and permeability of the heap. Microbial association with mineral favours dislocation and grain boundaries present on the mineral surfaces (Gehrke *et al*., 1998). Micro-organisms are assumed to be captured at the solid-liquid interface (by physicochemical deposition) and the air-water interface (Wan *et al.*, 1994; Chen, 2008). While in some microbial systems, the cells tend to grow to form large aggregates in interstitial spaces (Rockhold *et al*., 2002), in mineral bioleaching systems it is postulated that the cells form a monolayer on the ore surface and limited or no multi-layer structures of the chemolithoautotrophs are seen. Van Hille *et al.* (2010) reported both planktonic and mineral associated micro-organisms in the low grade ore bed and suggested that both contribute to bioleaching of sulphide minerals, as the cells oxidise ferrous ions present within the minerals, mobile and stagnant liquid phases. However, limited research has been conducted to quantify the relative impact of attached and planktonic microbial communities.

Escobar *et al*. (2004) concluded that sulphur oxidation by *S. metallicus* grown on chalcopyrite (70°C, pH 1.8) was only initiated by attached micro-organisms after a significant lag period. The estimated attached cell population was 68% and attachment occurred within 4 days of inoculation. A correlation between the proportion of attached micro-organisms, bioleaching rates and recovery should exist but has not been reported to date. Sampson *et al*. (2000), Rodriguez *et al*. (2003) and Ghauri *et al*. (2007) have shown that microbial attachment to the mineral phase varies with different microbial species (different strains, mesophilic or thermophilic) and the mineral content (types and concentrations). *Acidithiobacillus ferrooxidans* attaches selectively to iron containing sulphides confirming microbial attachment is mineral and site specific (Watling, 2006). Rodriguez *et al*. (2003) investigated the degree of attachment of mesophilic and thermophilic micro-organisms on three different sulphide minerals (chalcopyrite, pyrite, and sphalerite). The results indicated that attachment is a rapid process. Furthermore, in the pyrite experiment, greater attachment of mesophiles than thermophiles was found. However, lower attachment was observed for the other minerals. Sampson *et al*. (2000) showed attachment of micro-organisms to the mineral sulphides to be dependent on the growth substrates used. All these studies (Sampson *et al*., 2000; Rodriguez *et al*., 2003; Ghauri *et al.*, 2007) focused on attachment to pure minerals and mineral concentrates in shake flask experiments and are restricted to a limited set of microbial species, in particular *Acidithiobacillus ferrooxidans*. These previous studies on attachment are extremely important in understanding the microbial activity occurring within the leaching environment although the observations have limited applications because the experimental conditions are unrepresentative of the heap bioleaching environment.

Africa *et al.* (2009, 2010) developed a novel biofilm reactor, in which *At. ferrooxidans* and *L. ferriphilum* were inoculated onto low grade chalcopyrite-containing ore. The micro-organisms attached and colonised the mineral surface. Thin sections of ore (60 to 100 µm) were sampled for analysis under an epifluorescent microscope to allow for the visualisation of the spatial distribution of the microbial species as a function of ore composition (Africa *et al.*, 2009, 2010). The study confirmed that the bioleaching micro-organisms colonised the mineral surface with a mono-layer biofilm. Further, preferential attachment of the micro-organisms to the ore surface was observed. Africa *et al.* (2009, 2010) noted that preferential attachment was not limited to areas with a dominant sulphide mineral content. This correlates with the attachment studies conducted by Bromfield *et al.* (2010) were *Metallosphaera hakonensis* was first cultivated in different growth media (elemental sulphur, ferrous iron, chalcopyrite and pyrite) and then attached to varying substrates (pyrite concentrate, chalcopyrite concentrate and low grade ore) in glass columns (2.5 cm diameter, 19 cm length) filled with ore-coated glass beads. Bromfield *et al.* (2010) reported rapid attachment to all mineral types. Higher attachment to the low grade ore was attained by the pyrite grown culture over cultures grown in the other media. The microbial attachment was also monitored as a function of temperature *i.e.* experiments conducted at 25, 45 and 65 °C. A faster rate of attachment was observed for higher temperatures, with greater attachment attained at higher temperatures for all mineral substrates. Attachment of *Metallosphaera hakonensis* to the minerals at 25 °C was low, ranging from 20 to 40 %.

2.3.2 *Microbial Growth Dynamics and Heap Colonisation*

After attachment to the ore surface, the overall accumulation of microbial cells within the porous matrix environment is controlled by the multiplication of the microbes (van Loosdrecht *et al*., 1990; Rockhold *et al*., 2002; Lizama *et al.*, 2005). During microbial growth, the cells may attach to the solid support to form a monolayer or attach to one another within the EPS layer forming micro-colonies and biofilms (van Loosdrecht *et al*., 1990). Biofilms found in the bioleaching environment are thought only to form mono-layers, which lead to the eventual colonisation of the whole heap (Figure 2-6). Rockhold *et al*. (2002) suggested EPS could have potential for a water-holding capacity. Therefore, biofilm formation could increase the retention of leach solution, increasing the residence and contact time of solution and micro-organisms with the mineral phase to enhance metal recovery. Alternatively, higher solution hold-up within the system could stimulate further oxygen transfer limitations. EPS has been suggested to provide a location concentration of ferric irons, enhancing mineral leaching (Gehrke *et al*., 1998).

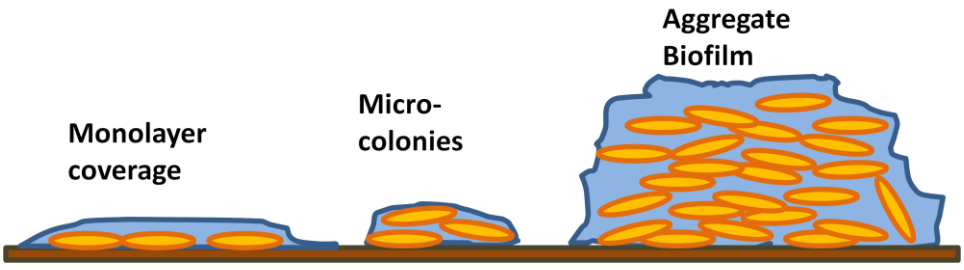

Figure 2-6: Bioaccumulation on surfaces within the packed bed system (adapted from van Loosdrecht *et al*., 1990)

A typical microbial growth curve is illustrated in Figure 2-7. Once the micro-organisms are introduced into the heap leaching systems via inoculation, they may experience a lag phase in which their growth is restricted due to their slow adaptation from the conditions in the previous environment to the new leaching environment (Shuler and Kargi, 1992). To minimise the lag phase, a highly active and

concentrated microbial population is used in the inoculum (Bailey and Ollis, 1986; Shuler and Kargi, 1992). Further, the conditions for inoculums development should be match with those present in the heap to minimise adaptation required.

Once the cells have adapted to the leaching environment, the micro-organisms use the nutrients available for assimilation and energy provision to enable multiplication under balanced growth conditions during the exponential phase (Shuler and Kargi, 1992). Bioleaching micro-organisms gain energy for growth through the oxidation of ferrous iron and inorganic sulphur compounds (Devasia *et al*., 1993) to regenerate ferric iron and sulphuric acid.

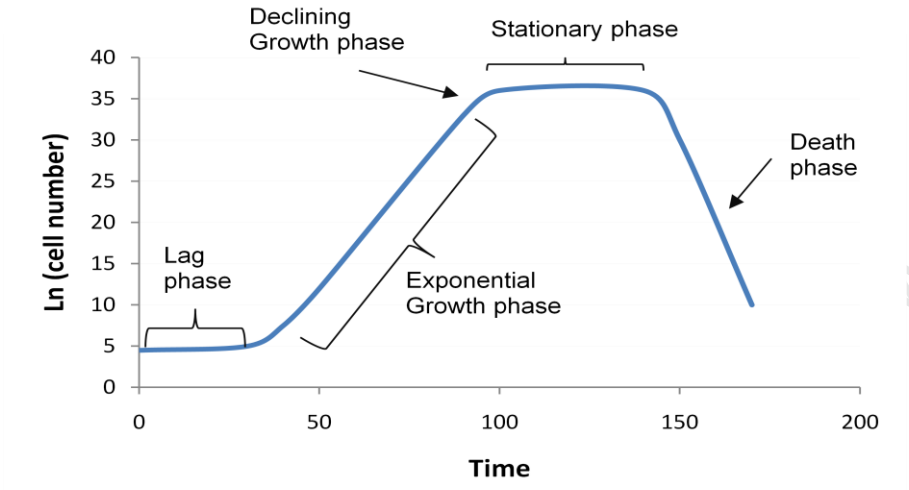

Figure 2-7: A typical microbial growth curve (adapted from Bailey and Ollis, 1986)

The rate at which the micro-organisms multiply, r_X, is a first order function of the microbial species concentration, X, where:

$$r_x = \frac{dX}{dt} = \mu X \qquad \text{(Equation 2.1, Pirt, 1975)}$$

μ is the specific growth rate [h^{-1}]. Substrate-limited growth during the exponential phase can be described by Monod kinetics (Monod, 1949), in which the specific growth rate is given by equation 2.2.

$$\mu = \frac{\mu_{max}\, S}{K_s + S} = \frac{\mu_{max}\, Fe^{2+}}{K_s + Fe^{2+}} \qquad \text{(Equation 2.2)}$$

S is the substrate concentration. For bioleaching the limiting substrates that the micro-organisms rely on are typically the reduced ferrous and sulphur compounds. Equation 2.2 above is shown for ferrous iron as limiting substrate. Here K_s is the ferrous iron concentration corresponding to the specific growth rate at half its maximum value (Bailey and Ollis, 1986). Additional limiting substrates *e.g.* CO_2 or O_2 can be included using a multiplicative term expressed in Equation 2.3. The Monod kinetics approach is simple and effective when determining growth rates for continuous culture.

$$\mu = \mu_{max}\left(\frac{S_1}{K_{S1} + S_1}\right)\left(\frac{S_2}{K_{S2} + S_2}\right) \qquad \text{(Equation 2.3)}$$

$$\mu = A_o e^{-\frac{E_a}{RT}} \qquad \text{(Equation 2.4)}$$

Table 2-3: Growth rates of mesophilic micro-organisms in various systems

Micro-organism	Substrate	System	Temperature (°C)	pH	Growth rate (μ, h^{-1})	Reference
At. ferrooxidans	Low grade chalcopyrite containing ore	Glass column (0.4 m height, 160 mm inner diameter)	RT ± 23	1.7	0.0364 from day 16 to 22, 0.0005 from day 23 to 50	Minnaar *et al.*, 2010
At. ferrooxidans	Ferrous iron	Batch shake flask	Optimal	Optimal	0.19	Karavaiko *et al.*, 2006
At. ferrooxidans	Sulphur	″	″	″	0.069	″
At. ferrooxidans	Chalcopyrite	″	″	″	0.05	″
At. thiooxidans	Sulphur	″	″	″	0.046	″
At. thiooxidans	Low grade chalcopyrite containing ore	Glass column (0.4 m height, 160 mm inner diameter)	RT ± 23	1.7	0.083 from day 16 to 22, 0.0008 from day 23 to 50	Minnaar *et al.*, 2010
At.caldus	″	″	″	″	0.0045, 0.0038	″
L. ferriphilum	″	″	″	″	0.0343, 0.0051	″
Predominantly *L. ferrooxidans*	Ferrous iron media	Continuous flow bioreactor (Height: Diameter ratio of 1.32, working volume of 1 L)	30	1.7	0.079	Dempers *et al.*, 2003
″	″	″	35	1.7	0.119	″
″	″	″	40	1.7	0.038	″
″	″	″	″	1.5	0.077	″
″	″	″	″	1.3	0.087	″
″	″	″	″	1.1	0.089	″
L. ferrooxidans	″	″	40	1.1	0.1024	Breed and Hansford, 1999
″	″	″	″	1.3	0.1043	″
″	″	″	″	1.5	0.1227	″
″	″	″	″	1.7	0.0952	″
L. ferrooxidans	Ferrous iron	Batch shake flask	Optimal	Optimal	0.069	Karavaiko *et al.*, 2006
Mixed culture	Low grade chalcocite ore	Shake flask			0.109	Petersen and Dixon, 2007a

Aside from microbial growth being a function of the growth substrate available, bacterial growth is also known be pH dependent and has an Arrhenius dependence on temperature (equation 2.4, where E_a is the activation energy, R is the Universal gas constant, A_o is the Arrhenius constant and T is the growth temperature). Typically the growth rate increases with increasing temperature and pH until optimum growth condition are reached. Some growth rates determined in previous studies (Breed and Hansford, 1999; Dempers *et al.*, 2003) have been presented Table 2-3.

Investigations into the growth kinetics of bioleaching micro-organisms have been conducted mostly in continuous culture systems (Breed and Hansford, 1999; Dempers *et al.*, 2003; Karavaiko *et al*., 2006; Petersen and Dixon, 2007a; Minnaar *et al*., 2010). Dempers *et al.* (2003) reported growth rates of a mixed mesophilic consortium under conditions typical of a *Leptospirillum* dominated culture, based on their ferrous iron bioenergetics. These are displayed in Table 2-3 for a range of mesophilic temperatures (30 to 40 °C) and low pH values (pH 1.1 to 1.7). Recent studies of growth rates on whole ore suggest low values in the absence of high Fe^{2+} concentrations, giving maximum specific growth rates of the mesophiles in the range 0.01 to 0.08 h^{-1} with rates decreasing below 0.01 h^{-1} under conditions of mass transfer limitation (Minnaar *et al*., 2010) (Table 2-3). The growth rate experiment was performed in glass columns (0.4 m, 160 mm diameter) at pH 1.7 and room temperature (±23°C) using low grade chalcopyrite containing ore inoculated with a mixed consortium containing *At. caldus, At. ferrooxidans, At. thiooxidans*, and *L. ferriphilum*. Growth rates of *At. ferrooxidans* on various substrates, in batch shake flask under optimal growth conditions, has also been documented by Karavaiko *et al*. (2006). Further, growth rates of mixed mesophilic populations (*At. ferrooxidans*, *At. thiooxidans, and L. ferrooxidans*) on low grade copper containing ore (1.45 % copper) have been reported by Petersen and Dixon (2007a). Increasing cell concentration with increased depth in the column was observed over time. Petersen and Dixon (2007a) postulated that the slow propagation of micro-organisms through the ore bed can be linked to low copper liberation rates. The growth rate reported for the culture was 0.109 h^{-1}. Plumb *et al*. (2008) monitored the growth of pure and mixed bioleaching strains, on low grade chalcopyrite ore, in batch shake flask experiments. All strains showed an increase in cell number with time. Further, a slower increase in cell number was observed with decreasing temperature.

After the exponential growth phase, a decline in growth rate is experienced when key nutrients in the heap environment become depleted (Shuler and Kargi, 1992), conditions become inhibitory for the micro-organisms due to the accumulation of dissolved salts, metals and hydroxyl-iron precipitates, or as heap temperatures exceed the operation window in which mesophilic micro-organisms function, creating changing community dynamics as moderately thermophilic and thermophilic species start to grow. In the stationary phase, the growth rate and death rate are balanced while metabolism continues (Bailey and Ollis, 1986; Shuler and Kargi, 1992). Thereafter, an increasing death rate results in the declining cell numbers (Bailey and Ollis, 1986). To maintain a healthy and active microbial population within the heaps, one has to understand the nature of the bioleaching micro-organisms and factors controlling their growth and metabolism.

2.3.1 *Detachment of Microbes from Ore*

A study by Rockhold *et al*. (2002) showed that the rate of detachment of micro-organisms from solid surfaces is a function of the attached cell population size, the nature of attachment and the hydrodynamic shear stress present in the system supported by Rossi (1990), van Loosdrecht *et al*. (1990) and Pintelon *et al*. (2009). Figure 2-8 illustrates detachment of micro-organisms from the mineral surface. Additionally the growth of the micro-organisms results in the release of new micro-

organisms from the micro-colonies and biofilms into the flowing fluid phase (van Loosdrecht *et al*., 1990). The potential for detachment of microbial cells from the ore creates an exchange between the planktonic cells and the sessile micro-organisms (van Loosdrecht *et al*., 1990).

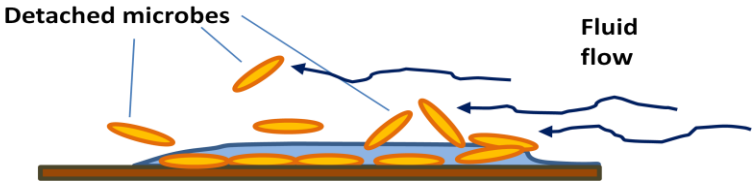

Figure 2-8: Detachment of micro-organisms from biofilms and surfaces

2.3.2 *Attachment and Colonisation Studies Conducted in CeBER*

One of the main sub-processes within heap bioleaching on which the Centre of Bioprocess Engineering Research (CeBER), at the University of Cape Town, focuses is microbial colonisation. Research within this space has previously and is currently focused on the surface sites and mineral species to which the micro-organisms attach preferentially (Africa *et al.*, 2009, 2010; Bromfield *et al*. 2010), the effect of temperature and pH on microbial growth kinetics on low grade ore (Minnaar *et al*., 2010, Tupikina *et al*., 2010), EPS formation and attachment (work unpublished). These studies are positioned to lead to a more thorough understanding of the behaviour of micro-organisms within heap systems. Understanding factors that affect colonisation will lead to effective utilisation of the microbial communities present during the leaching process.

2.4 Solution Flow and Microbial Distribution Characteristics

Rossi (1990) noted that the physicochemical and biological attraction mechanisms such as chemotaxis, Brownian motion, electrostatic attraction, and cell surface hydrophobicity are only effective at short range. These mechanisms only become effective when micro-organisms are sufficiently close to sites within the vicinity of the mineral surfaces (Rossi, 1990). Therefore, to promote attachment of the micro-organisms to the ore, enhanced transport, propagation and subsequent dispersion of the micro-organisms through the heap, via efficient solution flow, in search of preferential conditions and active sites on the mineral surfaces biooxidation of ferrous iron is required. Initial rates of bioleaching can be improved by effective heap inoculation (Pradhan *et al.*, 2008). However, initial microbial distribution is expected to be uneven due to the different adsorption isotherms of various bioleaching micro-organisms (Rawlings *et al.*, 2003) and variation in fluid flow. Irrigation systems and schedules should seek to provide adequate mobility of micro-organisms to maximise the uniformity and distribution within the ore bed.

2.4.1 *Characteristics of Solution Flow*

Adequate and uniform flow is critical for effective leaching of heaps (O'Kane *et al*. 2000), yet difficult to attain on non-ideal porous systems. Petersen and Dixon (2007) stated that efficient percolation is dependent on distribution of solution flow channels and relative size of stagnant zones. The rate at which fluid flows through an ideal saturated bed is defined by Darcy's Law:

$$q_x = \frac{K}{\mu_L} \times \frac{dp}{dt} \times A \qquad \text{(Equation 2.5, Rossi, 1990)}$$

q_x is the flow rate [m^3/s], μ_L is the fluid viscosity [Ns/m^2], p is the fluid head (pressure), A is the cross-sectional area [m^2] and K is the permeability coefficient. Heap systems operating under low flow form unsaturated ore beds, in which the available void spaces are filled with a combination or air, water

vapour and water. In unsaturated flow systems, the degree of bed wetness and hydraulic conductivity vary constantly, rendering unsaturated fluid flow complex and difficult to model.

Three flow regimes in the unsaturated bed described by Bartlett (1992; 1997), include: (i) capillary drainage with no solution flow, (ii) percolation and (iii) solution flooding (no air flow). The downward percolation of leach solution through unsaturated heaps is driven by gravity, and influenced by upward air flow driven by the buoyancy gradient induced by changes in air temperature and composition (Bartlett, 1992). Forces resist fluid movement through the heap; these forces are gravity, surface tension and atmospheric pressure (Bartlett, 1992). These forces combined with fluid forces could contribute to the detachment of microbes from the mineral surface and cause the washout of planktonic cells.

Decker and Tyler (1999) reported the existence of preferential pathways which permit much of the leach solution to migrate rapidly to the heap pad while contacting only a small fraction of the solid material (Rossi, 1990). Preferential flow exists in three forms: funnelling, short-circuiting and fingering (O'Kane *et al.*, 2000), detailed in Table 2-4.

Table 2-4: Forms of preferential flow (O'Kane *et al.*, 2000)

Type of flow	
Funnelling:	Solution flows preferentially through the layers easily permeated according to the texture of the material in the porous bed.
Short circuiting:	Flow occurs through the larger pores. High application rates cause high water-saturation leading to a significant amount of short-circuiting.
Fingering:	The development of an interface when the fluid infiltration of the porous bed displaces another fluid of different density or viscosity.

O'Kane *et al.* (2000) undertook a laboratory column study to characterise the nature of preferential flow within heap leach piles and its impact on mineral leaching. Preferential flow paths were dependent on the physical properties of layers, stress state, and degree of saturation i.e. solution application rate (O'Kane *et al.* 2000). The study demonstrated the application of unsaturated zone hydrology to aspects of heap and dump leach hydraulic dynamics. The reported results suggested that where solution application rates were greater than the saturated hydraulic conductivity of the finer material, preferential flow in the coarser layer resulted. However, when the application rates were less than the saturated hydraulic conductivity of the fine material, the preferred path became the finer material (Figure 2-9).

Wu *et al*. (2007; 2009), conducted research analysing the effect of preferential flow on copper recovery. Solution channelling and non-uniform flow was reported as a consequence of the heterogeneity of the material within the packed bed. The penetration of solution through the porous bed was attributed to the capillary action of micropores and crannies. The study reported that solution tends to move rapidly through a heap that is finely packed, whereas the solution seeps through heap containing coarse particle, corresponding to observations in the study by O'Kane *et al.* (2000) for low flow.

Despite the known existence of preferential flow phenomenon, comprehension on the extent of its impact on heap leaching is lacking. An understanding of leach solution flow paths through the heap from a point source is required. Analysis of the significance of preferential flow on the distribution of microbial communities within heap systems, will allow for the identification of 'dry zones' to which solutes and micro-organisms have not been transferred, implying low microbial attachment and biooxidation in these regions.

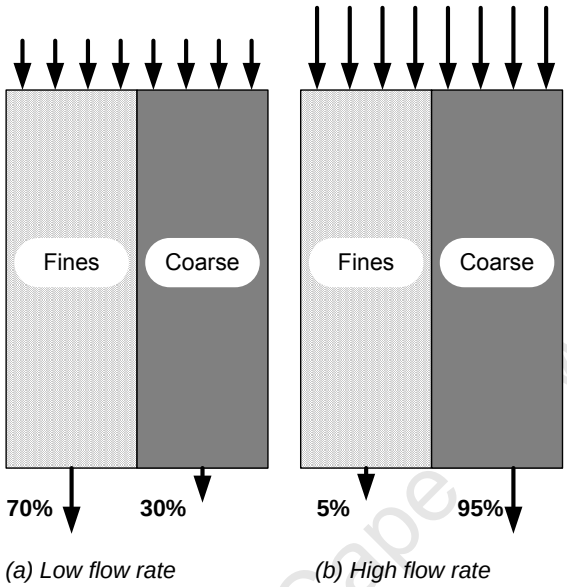

Figure 2-9: Demonstration of preferential flow conditions within unsaturated porous media (adapted from O'Kane *et al*. (2000).

2.4.2 *Influence of Irrigation Rate on Microbial Transport and Colonisation*

Rossi (1990) reported that the solution flow distribution through the heap is unpredictable when operating at flow rates lower than $3x10^{-4}$ $m^3/m^2/s$ (i.e. <1080 $L/m^2/h$). At higher flow rates the flow distribution pattern is not a function of the flow rate, as it is more stable (Rossi, 1990). Bioheaps are typically irrigated at an application rate which does not cause saturation (Brierley, 2001); oxygen and carbon dioxide gas-liquid mass transfer to solution and the micro-organisms is enhanced under unsaturated conditions. Industrial irrigation rates are usually low in the range 5 to 10 $L/m^2/h$ (Petersen and Dixon, 2007a). The use of low irrigation rates on ores with low inherent permeability provides the best control of PLS grade for easier solution processing (O'Kane *et al.*, 2000). Low irrigation rates have direct or indirect beneficial effects on microbial activity through heat conservation (Du Plessis *et al*., 2007). Reduced irrigation rates cause increased gradient effects and can result in the accumulation of soluble salts and the development of high osmotic potential which both have a detrimental impact on microbial activity (Du Plessis *et al*., 2007).

Most discussion on the effect of irrigation rate on heap leaching is informed by the interpretation of results simulated by heap leaching models rather than actual experiments. Researchers have simulated the effects of irrigation rate on temperature in the heap, sulphide oxidation rates and metal recovery (Cooper and Dixon, 2006; Bouffard and Dixon, 2009). Bouffard and Dixon (2009) predicted that microbial activity was inhibited at low irrigation rates because of jarosite precipitation attributed to the increased ferric iron concentration within the heap. Few researchers have assessed the ability of the bioleaching micro-organisms to colonise the ore and thrive under the different solution flow rates employed during heap leaching operations experimentally.

Magnetic Resonance Imaging (MRI) techniques were used by Graf von der Schulenburg *et al*. (2007) to assess fluid velocities through porous media. MRI was also adopted in investigations related to biofilm growth to verify various model simulations (Graf von der Schulenburg *et al*., 2007; Graf von der Schulenburg *et al*., 2008; Pintelon *et al*., 2009).

Sen *et al*. (2005) modelled the effect of solution velocity on microbial transport proposing significant effects which can be correlated to rates of colonisation and biooxidation. The model simulation showed faster bacterial transport rates with increasing flow velocity. Lizama *et al*. (2005) focused on leaching of pyrite and sphalerite at different heights and irrigation rates. Growth rates of moderate thermophiles, *Acidithiobacillus caldus* and *Sulfobacillus thermosulfidooxidans*, were reported as a function of the irrigation to height ratio, *I/H* (L/m^3.min). The relationship between this ratio and the specific bacterial growth rate was given by equations 2.6 and 2.7, for sphalerite and pyrite respectively.

$$\mu_{sphalrite}\left(d^{-1}\right) = 0.62 \times \left(\frac{I}{H}\right) + 0.018 \qquad \text{(Equation 2.6)}$$

$$\mu_{pyrite}\left(d^{-1}\right) = 0.089 \times \left(\frac{I}{H}\right) + 0.025 \qquad \text{(Equation 2.7)}$$

The experimental results showed an increase in growth rate with increase in the irrigation to height ratio. Lower attachment to the mineral surface was noted at high *I/H* ratios and colonisation of sphalerite was more rapid than that of pyrite. However, Lizama's study concluded that increased irrigation rates had no effect on the time period for the initial colonisation of the mineral surface. Refer to Table 2-5 for a summary of the reported results.

Table 2-5: Influence of irrigation to height ratio over bioleaching in columns or heaps (extracted from Lizama *et al.*, 2005)

Condition	Effect	Limiting Conditions
Increase in *I/H*	- Faster bioleach rate	- Flooding
	- Faster mineral colonisation	- Decomposition of agglomerate
	- Faster pH breakthrough	- Migration/washout of fines
	- More sulphur oxidation/acid generation	
	- Faster net ferric generation	
Decrease in *I/H*	- Less sulphur oxidation/acid generation	- Acid limitations
	- Slower net ferric generation	- Excessive ferric precipitation
	- Slower pH breakthrough	
	- Slower mineral colonisation	
	- Slower bioleach rate	

The work conducted by Lizama *et al.* (2005) is limited, requiring further and more rigorous studies on other systems in order to understand whether the initial colonisation is in fact influenced by the

irrigation rate. Therefore, it may be beneficial to reassess the effect of irrigation rates on microbial transport, attachment and colonisation rates with a more rigorous approach i.e. tracking the development of the microbial colonies by monitoring the increasing cell numbers in the heap systems as the leaching process progresses. Thus far, researchers have not been able to achieve this as there were no methods available to extract ore samples from the column testwork systems. The Centre of Bioprocess Engineering Research (CeBER, at UCT) has developed an in-bed sampling technique from which representative ore samples can be obtained at intervals during the leaching process. The investigation herein has adopted this technique to attain a better understanding of the occurrences in heap systems with regards to microbial attachment at different irrigation rates.

Increased irrigation rates could result in differing hydrodynamic conditions i.e. saturation of heap, and fluid flow shear stress within the heap system. Microbial growth rates and metabolic activity could be hindered in response to this potential phenomenon. As previously mentioned, microbes and solute species in the leach solution are transported through the heap by gravity and other means (Rossi, 1990). The fluid motion can be laminar or turbulent. The fluid motion is a function of the dimensionless Reynolds number (Re), defined as:

$$\mathrm{Re} = \frac{v \times d \times \rho_{LEACHATE}}{\mu_{LEACHATE}} \qquad \text{(Equation 2.8, adapted from Rossi, 1990)}$$

Where, v is the fluid velocity [m/s], d_p is the ore particle diameter [m], $\rho_{LEACHATE}$ is the density [kg/m^3], and $\mu_{LEACHATE}$ is the fluid viscosity [Ns/m^2]. For a value of Re < 0.9, the flow regime can be defined as laminar (Rossi, 1990). Calculations can be done to determine the type of flow regime present in the heap leaching systems.

As previously mentioned, even a mild shear fluid force can cause detachment of microbes from the mineral surface, hence allowing them to be washed out of the heap. In continuous culture systems using planktonic cells, growth of bacteria under conditions of increasing solution flow rate result in the enrichment of fast growing bacteria while slow growing bacteria are washed out (Watling, 2006; Rawlings and Johnson, 2007). Micro-organisms attached firmly to the mineral surface are retained in the system. It has also been suggested that the microbial cells populate the solution within the stagnant pore network (Petersen and Dixon, 2007b). However, the magnitude of this population has not been reported experimentally through accounting for the interstitial population within colonised heap systems.

2.4.3 *Microbial Retention in Porous Systems*

Effectively managed solution flow and aeration ensures sufficient retention of cells and oxygenation of porous systems. Typically, the different phases present in unsaturated porous media are described by Bartlett (1992; 1997) (Table 2-6) with emphasis on the: (i) *mobile phase:* leach liquid and gas filled voids (inter-rock void spaces) and (ii) *immobile phase:* solution filled ore pores (intra-rock porosity). This is further illustrated by Figure 2-10.

Wan *et al*. (1994) employed visualisation with quantification to determine the effect of cell surface hydrophobicity and gas saturation on microbial transport using two different bacterial strains, one hydrophilic and the other hydrophobic. The experiments were conducted in glass micro-models packed with quartz sand which simulated the complexities of natural porous media (Wan *et al*., 1994). The cells were injected and the initial cell breakthrough was determined. Figure 2-10 illustrates the three different degrees of gas saturation used to test the effect of the gas-water interface on microbial retention. There was good reproducibility within and across experimental runs. Wan *et al*. (1994)

reported that the retention rate of bacteria was proportional to the gas saturation in porous media. They attributed this to the observed preferential sorption of bacteria onto the gas-water interface over the solid-water interface. While this is an expected observation for the system used, it is not expected to be extrapolated to sulphidic mineral systems as sulphide minerals are recognised to have a much greater affinity for bacteria over quartz (Africa *et al*., 2009, 2010; Bromfield *et al*., 2010). Therefore, the gas-liquid and solid-liquid interfaces play a role in microbial transport and retention (Wan *et al*., 1994). Rockhold *et al*. (2002) suggested that oxygen limitations could also propel the preferential growth of aerobic bacteria at the air-water interface, and oxygen gradients favour the migration of motile aerobic micro-organisms to this interface via chemotaxis (Rockhold *et al*., 2002). The study (Wan *et al*., 1994) showed that hydrophobic cells have a greater affinity for the gas-liquid and the solid-liquid interface than the hydrophilic cells. Therefore, the hydrophobic bioleaching micro-organisms could have longer retention times within the heap, contributing to more bio-oxidation. The experiments also showed that under slow-flow conditions a static gas-water interface developed, consequently inhibiting microbial transport. Wan *et al*. (1994) noted that high solution velocities induced shear stress which could mobilise the gas-water interface, potentially enhancing bacterial transport. However, the hydrodynamic stress caused by high solution velocities could have a negative effect on the leaching process caused by the detachment of active micro-organisms from the mineral surface. Wan *et al*. (1994) established that the cell mass recovery in the effluent was inversely proportional to the gas saturation, confirming that water-saturated conditions are unfavourable for cell attachment to the solid phase and oxygen transport.

Table 2-6: Typical phase region in porous media (adapted from Bartlett, 1992)

Phase		**Stagnant/mobile**	**Typical volume (%)**
Solid rocks (includes closed pores)	- V_s	Stagnant (dead space)	59%
Open porosity within rocks	- ε	Stagnant (dead space)	2.40%
Solution void space between rocks	- V_l	Mobile (water flow)	19 to 21.5%
Air void space between rocks	- V_g	Mobile (airflow) + trapped air pockets	18.1 to19.6%

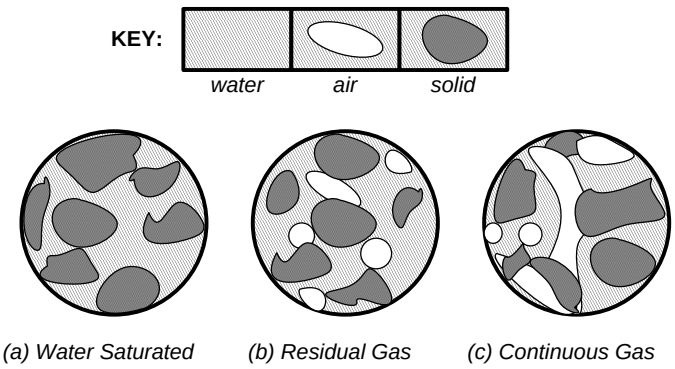

Figure 2-10: Cross-sectional sketch of three different degrees of saturation of porous media (extracted and adapted from Wan *et al*., 1994).

2.4.4 *Solution-Microbe Interaction Studies Conducted in Related Fields*

2.4.4.1 *Bioaccumulation*

Thullner (2010) and Pintelon *et al*. (2009) described the 'bioclogging' effect as the accumulation of microbial cells leading to reduction in permeability due to plugging of pore space, with associated decreases in hydraulic conductivity of the porous medium. Multiple factors control the bioclogging effect, including the following: fluid shear, porous media particle size, substrate and nutrient supply, and EPS producing capacity (Vandevivere and Baveye, 1992; Thullner, 2010; Pintelon *et al*., 2009).

Yarwood *et al.* (2006) reviewed several studies on the transport of soil bacteria through both saturated and unsaturated porous media, noting the lack of definition on the impact of microbial growth on hydrological properties. Several investigators in other fields such as soil-groundwater engineering, agricultural engineering and contaminant hydrology have assessed this bioclogging phenomenon through laboratory and theoretical studies (Vandevivere and Baveye, 1992; Thullner *et al*., 2002; 2004; Rockhold *et al*., 2002; Yarwood *et al.*, 2006; Rockhold *et al*., 2007; Seitert and Engesgaard, 2007; Thullner, 2010). The studies have focused on the dynamic interaction between microbial growth, fluid flow, solute transport and gas exchange through porous media. Extrapolation of their findings to the heap bioleaching space has not been implemented.

2.4.4.2 *Methods Employed to Investigate Bioclogging*

Most studies investigated the bioclogging effects using columns packed with either sand or glass beads. These systems differ from typical heap structures which have more random packing due to the variations in ore particle sizes, the pore network created during stacking, and the shrinking particle effect as a consequence of mineral leaching. Water containing nutrients for microbial growth is percolated through the system allowing investigators to assess 1-D or 2-D unsaturated flow. Column experiments operated as 1-D systems are under the assumption of evenly distributed flow (Thullner, 2010).

Pintelon *et al*. (2009) used a Lattice-Boltzmann simulation to illustrate the temporal distribution of microbial communities over time, verified by magnetic resonance imaging (MRI) data. The studies (Thullner *et al*., 2002; Yarwood *et al.*, 2006; Seitert and Engesgaard, 2007) used tracer tests to investigate changes in flow and transport properties due to bioclogging of porous media. The columns were packed with porous media, such as sand or glass beads, operated under continuous flow conditions and fully saturated. Monitoring of the flow rate and changes in the hydraulic head, measured using pressure transducers located at different depths in the column, enabled changes in hydraulic conductivity to be determined from Darcy's law (Seitert and Engesgaard, 2007).

Yarwood *et al.* (2006) and Rockhold *et al*. (2007) combined light transmission and bioluminescence for non-invasive monitoring of the interactions and evolving patterns of microbial growth, water flow and solute transport in unsaturated porous media. HK44 bacterium was genetically modified with a *lux* gene that resulted in bioluminescence on exposure to salicylate (Yarwood *et al.*, 2006). Therefore, bioluminescence was used to quantify the sequential and spatial development of colonisation by relating it to cell population density measured by dilution plating. Hydraulic flow paths were determined by pulsing bromophenol blue dye (indicator) through the bed and water-saturation was measured by light transmission and gravimetric analysis.

2.4.4.3 *Observations*

Bioclogging of the pores by soil bacteria growing on organic compounds as the main carbon source was observed, typically occurring within 2 to 4 weeks of inoculation (Thullner, 2010). This led to preferential flow paths (Yarwood *et al.,* 2006; Thullner, 2010). Previous studies have shown that during microbial growth and colonisation, there are biomass-induced changes in pressure heads, water contents and permeability reduction (Rockhold *et al*., 2002; Yarwood *et al.,* 2006; Seitert and Engesgaard, 2007).

The study by Seitert and Engesgaard (2007) reported decreased hydraulic conductivity of 2 to 4 orders of magnitude in their systems as a consequence of bioclogging. The hydraulic conductivity decreased by 4 orders of magnitude at the top of the column and 2 orders of magnitude throughout the whole column. This indicated that the initial microbial growth occurred near the point source of irrigation, consuming the majority of the substrate, depleting the supply to micro-organisms located at increasing depths causing them to either decay or migrate upstream by chemotaxis (Seitert and Engesgaard, 2007; Thullner, 2010). Seitert and Engesgaard (2007) also suggested that further changes in hydraulic conductivity could be attributed to detachment and migration of micro-organisms downstream. A regression analysis showed that solution velocity through colonised regions was significantly reduced during the initial days of the experiments (Yarwood *et al.,* 2006).

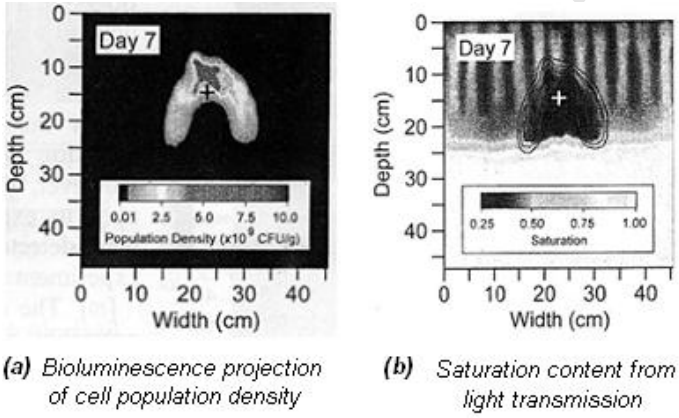

Figure 2-11: Illustration of the development of colonisation and water content distribution (Extracted from Yarwood et al., 2006).

Some studies indicated that the bioclogging effect was localised such that the hydraulic properties of the whole system remained constant (Thullner *et al*., 2002; Yarwood *et al.,* 2006). This suggested that microbial growth and accumulation can manifest greater heterogeneity within porous structure or homogenise the effect (Rockhold *et al*., 2002), resulting in preferential flow paths and/or stabilised flow patterns (Thullner *et al*., 2002). Yarwood *et al. (*2006) noted that the expansion of microbial colonies was mainly lateral and downward, but upward expansion also occurred (Figure 2-11(a)). Hence cells can migrate upward against solution flow. Yarwood *et al.* (2006) attributed these observations to the physical clogging of ore pores due to accumulation of cells and microbially induced changes in the chemical properties of liquid and solid phases (Yarwood *et al.,* 2006).

Yarwood *et al.* (2006) also implicated EPS formation in the bioclogging of localised pore networks. However, their study did not quantify or account for the presence of EPS. Vandevivere and Baveye (1992) compared an EPS-producing strain with a non-EPS producing mutant strain. They only observed the bioclogging effect in the system containing the heterotrophic EPS producing bacterial strain. Bioclogging induced by EPS formation was suggested to be stimulated by high nutrient loading

(Thullner, 2010). Protocol for isolation and quantification of EPS in batch (Gehrke *et al*., 1998; Kinzler *et al*., 2003) and continuous culture systems (Michel *et al*. 2009) have been developed.

The observations from the aforementioned studies have resulted in the modelling of the interactions between fluid flow and bioclogging attributed to microbial growth. These models only consider 1-D flow and ignore the multi-dimensional flow paths that would be accessible to percolating leach solution (Thullner, 2010). Further, the knowledge gained from the studies conducted in agricultural and soil engineering fields (Ginn *et al*., 2002; Rockhold, 2002; Sen *et al*., 2005; Yarwood *et al*., 2001; 2006; Chen, 2008; Thullner, 2010), has not been applied to the heap leaching systems. However, its application is limited because heap leaching systems are more complex structures than the porous media evaluated in the other studies (in terms of ore mineralogy, particles size distributions, microbial diversity and operating conditions).

Several investigators have reported on their attempts to model heap hydrology (Decker and Tyler, 1999; Bouffard and Dixon, 2001; Cariaga *et al*., 2005; Lin *et al*., 2005; Dixon and Afewu, 2006; Dixon and Petersen, 2007). Most heap leach models incorporate liquid dynamics, mass transport, heat transfer, and mineral leaching reactions. However, different approaches are used to account for the factors above in terms of the equations developed. In general, microbial propagation has not been considered explicitly. Therefore, current bioleaching models need to be extended. The models should be designed on a better understanding of the behaviour of micro-organisms within the heap in order to predict the rate and extent of microbial transport, colonisation and activity. However, development of the modelling aspect is beyond the scope of this thesis.

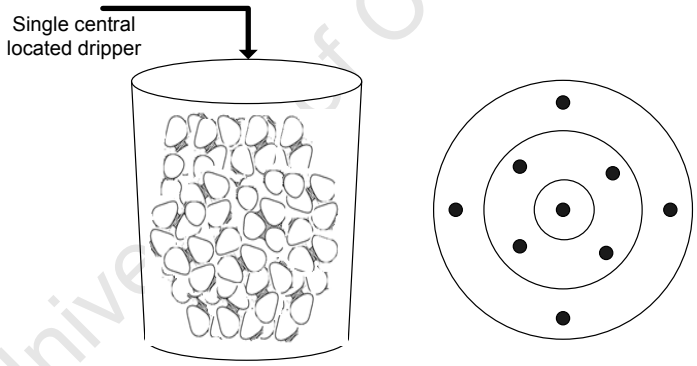

Figure 2-12: Bucket reactor set up with 3 concentric layers: dots represent solution collection points from 9 different zones (Van Hille *et al*. (2010) experimental setup)

2.4.5 ***Review of Investigation Conducted***

Preliminary research on microbial propagation and colonisation has been conducted in the Centre of Bioprocess Engineering Research group (CeBER), at the University of Cape Town. Van Hille *et al.* (2010) used a bucket reactor (320 mm diameter, 400 mm high) to observe the radial distribution of leach solution and microbial populations (Figure 2-12). The bucket was packed with agglomerated ore divided into 3 concentric annuli and two layers separated by stitched shade cloth made from high density polyethylene. The system was irrigated from a single central point and solution was collected from 9 outlets, corresponding to the annuli. Van Hille *et al.* (2010) found that high feed rates resulted in preferential flow paths. In an attempt to rectify the preferential flow effects, reduced flow velocities were employed in latter experiments; however reduced liquid feed rates did not result in greater radial diffusion of microbes. The study concluded that liquid flow affected the distribution of attached micro-organisms. It showed that leaching efficiency was a function of liquid flow and microbial

colonisation. It was recommended that more detailed investigations of fluid flow in conjunction with microbial colonisation would contribute to increased understanding of microbially operated heaps.

2.5 Conclusions and Research Motivation

The literature review has highlighted the gap in the understanding of the fluid-micro-organism interactions in the unsaturated ore bed used in heap bioleaching. Few researchers have paid attention to this area, leaving the knowledge of these interactions to be derived from other scientific fields. Understanding the transport of solutes in heap leaching is important to optimise microbial propagation, contacting of mineral and leach agents and transport of dissolved metals out of the heap. This highlights the need to gain a better understanding of (i) the irrigation system, (ii) transport and dispersion of reactants, products and micro-organisms through the heap, and (iii) the effect of irrigation rates on microbial attachment, detachment and colonisation rates. This knowledge is required to optimise irrigation conditions, and promote microbial transport and activity to enhance microbial colonisation of the heap.

To date, the literature has shown:

- The adsorption and selective attachment of micro-organisms onto the solid mineral surface (van Loosdrecht *et al*., 1990; Gehrke *et al*., 1998; Sampson *et al*., 2000; Kinzler *et al*., 2003; Rodriguez *et al*., 2003; Sand and Gehrke, 2006; Ghauri *et al*., 2007; Africa *et al*., 2009, 2010; Bromfield *et al*. 2010).
- The growth rates of bioleaching micro-organisms on different substrates under varied leaching conditions (Breed and Hansford, 1999; Dempers *et al*., 2003; Karavaiko *et al*., 2006; Minnaar *et al*., 2010).
- The existence of preferential flow paths which cause inefficient heap leaching (Rossi, 1990; Decker and Tyler, 1999; O'Kane *et al*., 2000; Wu *et al*., 2007; 2009).
- The radial distribution of micro-organisms as a function of fluid flow (Van Hille *et al.,* 2010). Van Hille *et al.* (2010) reported that lower feed flow rates had a greater tendency to induce solution channelling which affected the microbial distribution.
- The impact of irrigation rates on initial microbial transport and colonisation in porous medium lacks quantification. The study by Lizama *et al*. (2005) concluded that irrigation to height ratios influenced the microbial growth and attachment rates whilst the model (Sen *et al*., 2005) inferred that increased flow velocity increases microbial breakthrough rates. Although the results were from different systems, i.e. heap vs. soil-groundwater, good reasoning alludes to higher irrigation rates having a significant impact on microbial transport and initial rates of colonisation.
- The potential for the occurrence of interactions between micro-organisms and fluid flow (Vandevivere and Baveye, 1992; Thullner *et al*., 2002; 2004; Rockhold *et al*., 2002; Yarwood *et al.,* 2006; Rockhold *et al*., 2007; Seitert and Engesgaard, 2007; Thullner, 2010). Additionally, a bioclogging effect was observed in these soil and ground water environments, but has not been suggested in bioheaps. The absence of the bioclogging effect in heap systems could be due to the autotrophic nature of the bioleaching micro-organisms.

2.6 Research Hypotheses and Key Questions

The review of several studies in the preceding section has indicated key gaps in the understanding of interaction between solution flow and the microbial phase in the heap leaching environment. More specifically, there is a need to relate microbial mobility, degree of attachment and growth of the micro-organisms to the irrigation conditions employed and the heterogeneity of the heap structure which induces preferential flow through certain zones. Quantitative studies on attached and unattached microbial populations under continuous flow heap conditions rather than closed batch agitated systems need to be conducted. Further, knowledge of the spatial and temporal development of colonisation in the heap bed will allow the heap hydrology modellers to account for the interactive effects of solution flow and microbial growth.

Two hypotheses were formulated and the key questions derived from them are highlighted as follows:

Employing low irrigation application rates will facilitate good microbe-mineral contacting enhancing colonisation rates while preventing detachment of microbes due to fluid shear.

- How does the initial microbial colonisation develop, *i.e.* how does the microbial population density change, with time during the heap leaching process?
- How is the relative location of cells within the ore bed (i.e. planktonic, interstitial and attached) influenced by the irrigation rate and time?
- Will decreased irrigation rates facilitate increased attachment and colonisation of the minerals surface?
- Do higher flow velocities mediate the detachment of cells from the mineral surface?

The microbial colonisation and moisture content vary in relation to their location relative to a point source of irrigation. Further the extent of microbial colonisation in a section of the bed is a function of its moisture content.

- How does the microbial population density change with time and location during the heap leaching process, relative to the irrigant source?
- How does moisture content and solution flow path change with time and location with respect to irrigation from a single point source?
- Do moisture contents and flow paths correlate with the propagation and distribution of microbial communities through the heap?

3 CHAPTER 3: MATERIALS AND EXPERIMENTAL METHODOLOGY

In this chapter, the detailed experimental approach adopted in order to achieve the study's objectives and elucidate the hypotheses is presented. The aim of the study herein was to assess the effect of irrigation application rate on microbial attachment and growth during the initial colonisation phase, as well as to monitor the progression of microbes from a single point source of irrigation in a simulated box heap. This section provides information on the ore composition (Section 3.1), microbial cultures utilised (Section 3.2) and feed solution (Section 3.3). The irrigation rate investigated in laboratory column reactors while propagation from a single point irrigation source was studied in a two dimensional box reactor. These are presented in Sections 3.4 and 3.5 respectively in terms of reactor design, operating protocols and experimental approach. In Section 3.6 the analytical techniques employed are detailed, and some of the assumptions and limitations taken into consideration (Section 3.8).

3.1 Mineral Analysis

Low grade copper-bearing ore, characterised by 0.69%, 2.95% and 2.02% copper, iron and sulphur content respectively was utilised. The composition of minerals from which the copper present in the ore is sourced is displayed in Table 3-1. The crushed ore with 80% passing 6000 µm, was characterised by the cumulative particle size distribution displayed in Figure 3-1.

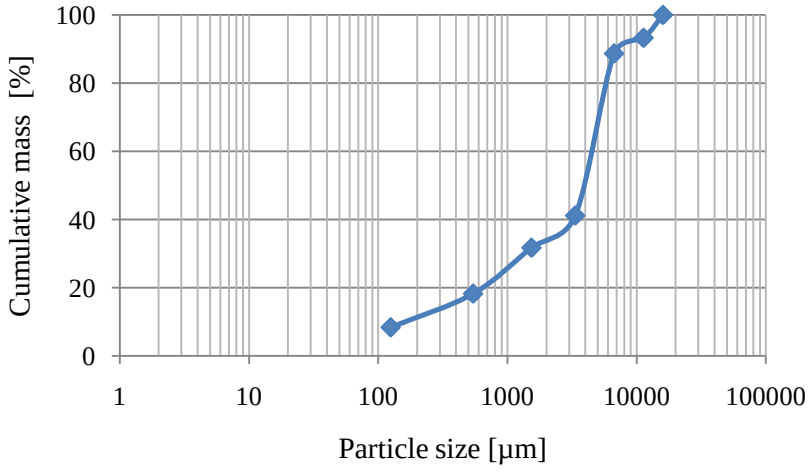

Figure 3-1: Cumulative particle size distribution of the low grade copper-bearing ore.

Table 3-1: Mineral contributions to the available copper, in the low grade copper-bearing ore sample

Copper Source	% Contributed to Cu content	% in Ore
Chalcopyrite	28.4	0.196
Chalcocite	41.8	0.288
Covellite	6.7	0.046
Bornite	15.1	0.104
Bronchantite	1.7	0.012
Chrysocolla	0.38	0.003
Tenorite	0.4	0.003

3.2 Microbial Cultures

Mesophilic microbes were employed in the investigations because the experiments were setup under the ambient temperature regime (±23 °C), to relate to and compare with other investigations conducted in CeBER used to mimic the start-up condition of the heap. The mixed mesophiles used were obtained from a stock culture containing these microorganisms: *At. ferrooxidans, At. thiooxidans, At. caldus,* and predominantly *L. ferriphilum,* confirmed by qPCR. The DNA extraction and qPCR methods used were reported in Bryan *et al*. (2011). The micro-organisms were grown on pyrite concentrate in a batch stirred tank reactor at 30°C. The stock was sub-cultured on a weekly basis to allow the microbes to remain active. This was achieved by the removal of approximately 300 ml liquid and re-filling the volume up to the litre mark with fresh media.

A sensitivity analysis was conducted to determine which inoculum concentration should be employed in order for cell concentration to be within the detection limit (Table 3-2). Cell counts were performed on samples taken from the stock culture using Thoma counting chamber. The industry standard concentration is 10^{10} cells/ton of ore. Inoculation concentrations ranging from 10^{8} to 10^{13} cells/ton of ore were considered. The calculation assumed that 4 kg of ore was inoculated with the considered amount, and only 50% of cells remained attached within the column over the first day, whilst the rest was eluted under varying irrigation rates (2 to 18 l/m^2/h). Given that the detection limit of the cell counting method was 3x10^5cells/ml, the inoculum concentration of 10^{12} cells/ton of ore was utilised in this investigation. The cells were added to a small volume of feed solution and fed to the heap systems via irrigation rather than agglomeration inoculation.

Table 3-2: Sensitivity analysis to determine inoculum concentration

Inoculation concentration (cells/ton)	**1.0E+08**	**1.0E+09**	**1.0E+10**	**1.0E+11**	**1.0E+12**	**1.0E+13**
Cells inoculated (cells)	4.0E+05	4.0E+06	4.0E+07	4.0E+08	4.0E+09	4.0E+10
Cell eluted assuming only 50% cells attach (cells)	2.0E+05	2.0E+06	2.0E+07	2.0E+08	2.0E+09	2.0E+10
Min cell concentration eluted (cells/ml)	5.9E+01	5.9E+02	5.9E+03	5.9E+04	5.9E+05	5.9E+06
Max cell concentration eluted (cells/ml)	5.3E+02	5.3E+03	5.3E+04	5.3E+05	5.3E+06	5.3E+07

3.3 Feed Media

For sources of ferrous iron and other nutrients required for microbial growth the feed was prepared in 20 L batches with the following composition; 0.5 g/L ferrous sulphate ($FeSO_4.7H_2O$), 183.3mg/L $(NH_4)_2SO_4$, 60.5 mg/L $NH_4H_2PO_4$, and 111.2 mg/L K_2SO_4 in deionised water. The pH was adjusted to pH 1.15 using 96-98% concentrated sulphuric acid (H_2SO_4) as per the conditions used in other investigations in the CeBER department. All reagents were of analytical grade. Non-sterile feed was employed with the heap systems being fed from the same feed reservoir to maintain consistency. Each batch of newly prepared feed underwent solution analysis i.e. pH and redox potential.

3.4 Equipment

3.4.1 *Column Reactor*

Representations of the heap leach column and experimental set-up used are shown in Figure 3-2 and Figure 3-3. Identical small scale heap leach columns of 100 mm diameter and 360 mm height were utilised (Table 3-3). 4kg of crushed acid-agglomerated ore was loaded into each column, with the ore bed resting upon a layer of marbles supported by a perforated sieve plate. Layers of marbles were placed onto the top of the ore beds to ensure uniform distribution of solution (Bouffard and Dixon, 2001).

Table 3-3: Column specifications

Parameter	Specification
Height	360 mm
Diameter	100 mm
Weight	Packed with ~ 4 kg of ore

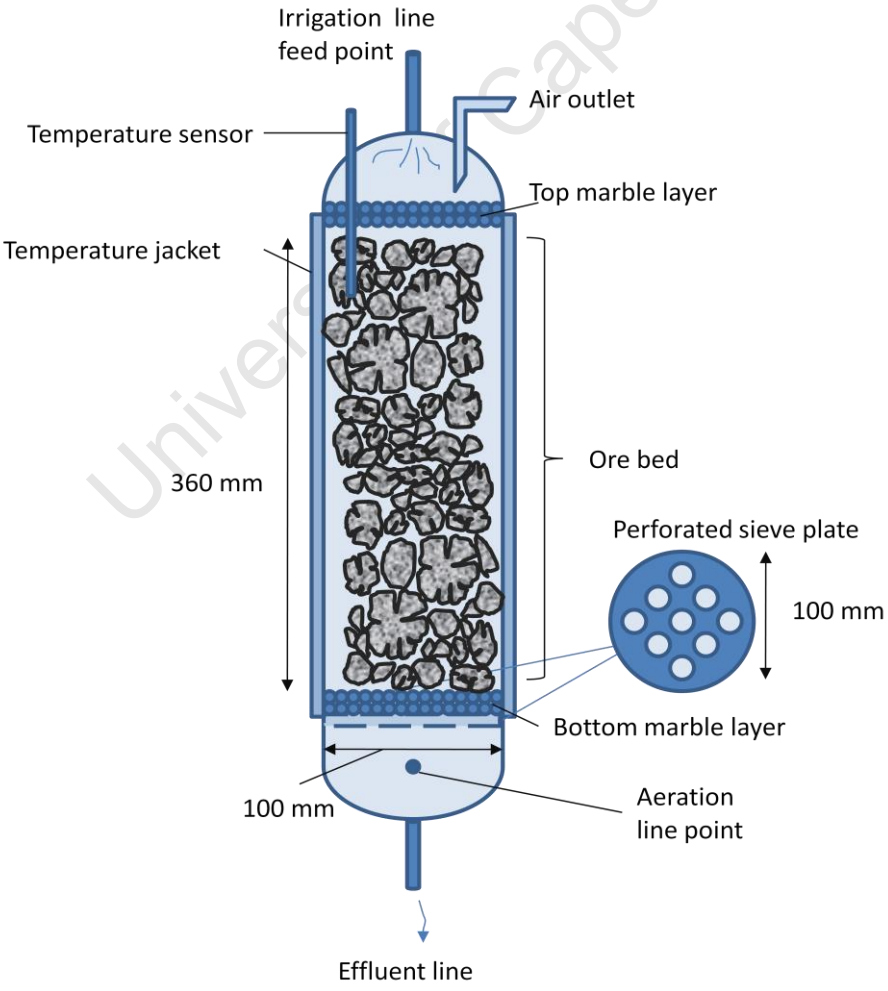

Figure 3-2: Schematic of heap leach column (adapted from van Hille *et al.*, 2010)

3.4.1 *In-bed Sampler*

The in-bed sampling procedure used in the current study was developed within the Centre for Bioprocess Engineering Research at the University of Cape Town. The in-bed sampling technique was used for the characterisation and quantification of the microbial community associated with the mineral ore bed as a function of time, following inoculation and subsequent colonisation (Chiume *et al.*, 2010). The investigation conducted herein was utilised to assess the technique, providing a novel approach to the attainment of time progression data at the laboratory scale, not reported previously. The procedure followed is displayed in Figure 3-4. Step 1: The leaching column was opened from the bottom. A similar sized column was constructed and attached to the bottom of the leaching column. Step 2: The ore bed was slowly lowered into the attached column without disturbance of the ore bed. Step 3: A sheet of metal was placed through the slit to cut through the bed. The bottom section was then removed, from which an ore sample was taken (~ 200 g). Step 4: The ore bed was replaced and column operation proceeded.

KEY:

A – Air Outlet

B – Column

C – PLS Collection vessel

D – Temperature sensor

E – Rotameter

F – Inlet feed point

G – Air inlet

H – Pump

Figure 3-3: Mini-scale column heap leaching circuit: the experimental set-up

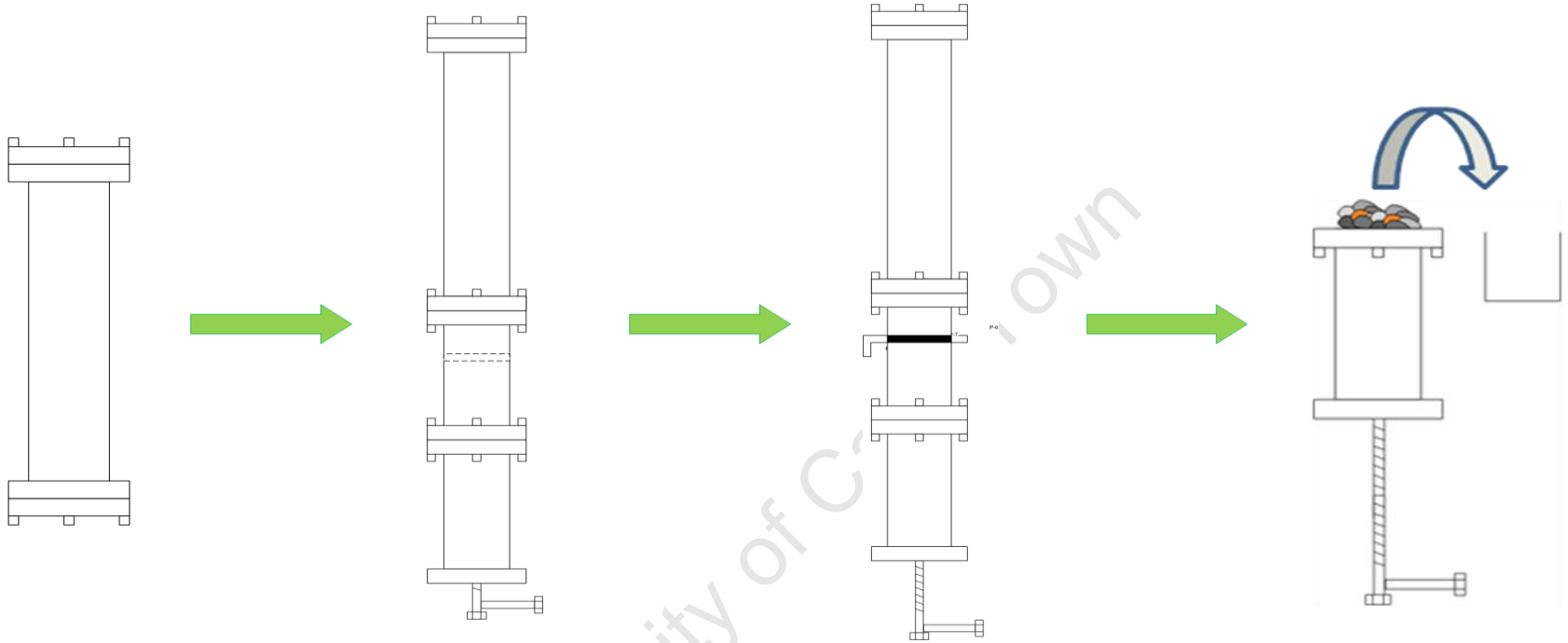

Step 1 **Step 2** **Step 3**

Figure 3-4: In-bed sampling procedure

3.4.2 *Box Reactor*

A perspex box heap was used in the current study to allow for some visualisation of the leaching process. A representation of the box set-up used is shown in Figure 3-5. The box specifications are given in Table 3-4.

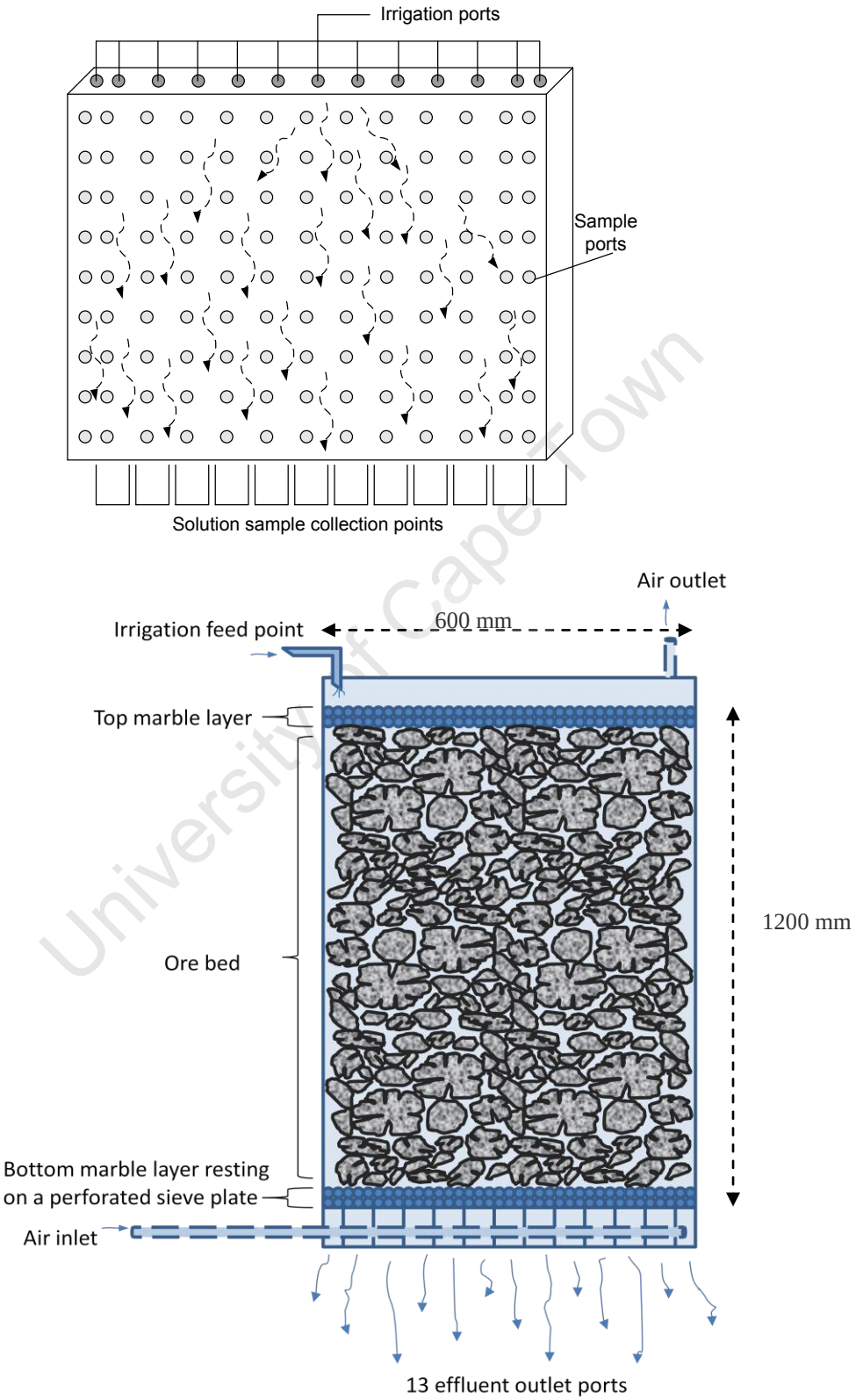

Figure 3-5: Schematic of box reactor experimental set-up

The ore was packed on top of a marble layer, supported by a perforated plate which ensured even gas distribution from the bottom aeration point. The box contained 13 irrigation ports and 13 collection ports situated at the bottom of the system, illustrated in Figure 3-5. There were samples ports in a 9x13 configuration for the top two sections and 8x13 at the bottom section.

Table 3-4: Box reactor geometry

Parameter	Specification
Height	400 - 1200 mm (adjustable)
Width	600 mm
Breadth	100 mm
Weight	Packed with ~ 132 kg of ore

3.5 Analysis

The collected effluent volumes were measured for mass balancing purposes. Samples of the PLS underwent analysis. The pH was measured using a Metrohm 691 pH meter to ensure that an acid environment was maintained for efficient biooxidation. The probe was calibrated for the pH range 1 to 4, error < 1 %. Redox potential was measured with a calibrated Crison GLP 21 Redox meter, and the accuracy of the probe reading was tested against a standard redox buffer solution (potential of 468 mV at 25 °C), error < 1 %. Total iron and ferrous iron concentration were measured using spectrophotometry (Section 3.5.2 and 3.5.3). Total iron and copper concentrations were also obtained from Atomic absorption assays (Section 3.5.4)

Samples of ore collected were analysed for moisture content and cell counts (Section 3.5.1) to help quantify solution retention and microbial attachment and population densities in the simulated heap systems.

3.5.1 *Determination of Bacterial Concentration*

Cell counts were done on the effluent and detachment samples using a Thoma Counting Chamber under an Olympus BX40 Microscope at x1500 magnification (oil phase, phase contrast optics) The detection limit of direct counting method using this counting chamber is $3x10^5$cells/ml, with < 25 % error. Note that where dilutions are needed, it is optimal to count between 30 and 300 cells to reduce the error.

The cell concentration was determined using the following equations:

$$Volume\ \_of\ \_1\_small\ \_square\ \_[mm^3] = depth \times area$$

$$Cell\ \_concentrat\ ion\ \_[cells\ /ml\ ] = \frac{cells\ \_counted\ \times \frac{total\ \_no\ \_of\ \_big\ \_squares\ \_(16)}{no\ \_of\ \_squares\ \_counted\ \_(4)}}{volume\ \_of\ \_1\_small\ \_square \times total\ \_no.\_of\ \_small\ \_squares}$$

Isolation of cells from the ore prior to cell counting was done using the detachment protocol developed in the Centre for Bioprocess Engineering Research, at UCT, and reported by Bryan *et al.* (2011). The detachment protocol was developed to be able to distinguish between the planktonic, interstitial,

weakly-associated and strongly attached microorganisms present within heap systems. A representative quantity of ore was taken from each system (Approximately 200g per column at each sampling interval and 20g per zone during the box reactor experimental run). The first stage involved the addition of non-ferrous media (2 g ore: 1 mL liquid), gently washing the ore by swirling the flask. The solution decanted was analysed for interstitial cell counts. In the second stage, media was added to the ore in the ratio of 1 mL liquid to 2 g ore and vortexed for 2 min. The decanted solution was centrifuged (800g, 1 min at room temperature, Beckman Centrifuge JA 10). The supernatant was collected and the media-vortex-centrifuge step was repeated twice. All the solution recovered from this stage was combined to quantify the weakly-attached cell phase detached by the media. In the third stage, a detergent Tween-20 (0.4% v/v) was added to the ore. The sample was vortexed (2 min) and the decanted solution was centrifuged (800g, 1 min at room temperature). The supernatant was collected and the Tween-vortex-centrifuge step was repeated. The solution recovered from this stage was combined to quantify the firmly-attached cell phase detached by Tween-20.

The cell counts were determined on the day that the samples were collected because the samples cannot be kept for an extended period (APHA, 1985). From this data the concentration of planktonic, interstitial and attached cells were generated. The effluent sample was used for the planktonic cell count in cells/mL and the ore samples was used to determine the interstitial (weakly associated) attached and strongly attached cells counts as cells per kg ore.

3.5.2 *Spectrophotometric Ferrous Iron Assay*

The ferrous iron concentration was quantified spectrophotometrically using the colorimetric 1-10 phenanthroline method described by Komadel and Stucki (1988), detailed protocol in Appendix B2. The spectrophotometry assay works through the detection of the light intensity prior to absorption of a light beam being passed through the sample.

Ammonium acetate buffer solution (2 mL) and 1-10 phenanthroline indicator solution (2 mL) were added to 1 mL of the sample (diluted appropriately). The reaction mixtures were vortexed to ensure good mixing. An orange-red complex formed when ferrous ions were present. The absorbance was read at a wavelength of 510nm with a Thermo Scientific Heλios α UV Visible Spectrophotometer. The absorbance was correlated with ferrous concentration using a ferrous standard curve generated between 0 to 50 ppm for the relationship between the two parameters (Standard curve and reagent preparation found in Appendix B). The correlation curve breaks down at an absorbance greater than 2.

Additionally, low concentrated samples introduce more relative uncertainty. For reproducibility and to reduce the error, triplicate analyses were performed with error < 10 % within the higher concentrated samples. Over dilution of samples resulted in larger errors.

Due to the conversion of ferrous to ferric iron by both biotic and abiotic reactions, the analysis was conducted immediately after sample collection (APHA, 1985). Note that the presence of copper ions can interfere with the ferrous iron assays, but the concentration of copper in the samples analysed was low enough to evade this effect.

3.5.3 *Total Iron Assay on Spectrophotometer*

A procedure similar to the ferrous ion assay was employed to determine the total iron concentration daily. After the ferrous absorbances were read, an excess amount of hydroxylamine was added to the samples to convert all the iron present to the ferrous form. Following conversion of the iron the spectrophotometric method was used; absorbance values were measured and compared to the ferrous standard curve to obtain the concentrations.

3.5.4 *Determination of Total Copper and Iron Concentration via AAS*

Weekly bulk samples were collected to quantify the total iron (Fe) and copper (Cu) concentration. Effluent solution concentrations were determined from light transmission characteristics of the samples (APHA, 1985). Atomic absorption spectroscopy (Varian Spectra AA 110) assays were conducted and the data provided evidence of pyrite oxidation and allowed the copper recovery to be determined. Due to the tendency of ion adsorption onto the surface of sample collection containers, the samples were analysed as close to the collection time as possible (APHA, 1985).

3.6 Experiments

3.6.1 *Column Heap Operation*

The experiment presented herein was formulated to provide a comparison of microbial attachment and growth at low and high flows with that of the industrial standard. This was achieved by monitoring development of microbial colonisation through the measurement of the changes in population density as a function of time, using a new in-bed sampling extraction technique.

The experiments were conducted in small scale heap leach columns. The irrigation application rates employed were 2, 6 and 18 L/m^2.h, were the standard rate is 6 L/m^2.h. These conditions chosen were based on typical industrial irrigation rates, 5 to 20 L/m^2.h (Petersen and Dixon, 2007a), and the range used by Lizama *et al*. (2005) in their study (1.8 to 21.6 L/m^2.h).

The ore was agglomerated using 50 ml deionised H_2O/ kg ore with 3.7 ml conc. H_2SO_4 / kg ore to secure the fines fraction. Prior to inoculation, the ore beds were acid-washed at the same rate (6 L/m^2.h) for 2 days to remove readily leachable materials and stabilise the pH of the system at the specified design condition i.e. pH 1.15. Reagent preparation is outlined in Appendix A. The columns operated under ambient temperature conditions, with the pH of the feed solution being maintained at pH 1.15. Columns were irrigated from above with acidic raffinate solution and air supplied from the bottom at 200 ml/min (in excess to prevent oxygen limitations), which resulted in counter-current flow systems. The feed solution was delivered into the columns using a Masterflex® consol drive, with L/S™ 7014/20 standard pump heads and L/S™ 14 Norprene® tubing.

In industry solution is typically recycled due to solution management schemes. However, the current study assessed systems which operated with once through continuous solution flow. The leachate eluted was collected from the drainage systems at the bottom of the columns. Effluent samples were collected daily for analysis outlined in Section 3.5. Microbial growth rates were obtained from the cell count data collected from assessments of the ore samples obtained via the in-bed sampling techniques described in Section 3.4.2.

3.6.2 *Perspex Box Heap Operation*

The objective of this experiment was to assess the lateral flow of leach solution from a single point source of irrigation by monitoring the moisture content through a grid of nine zones and solution flow through the 13 effluent ports. Zones A, D and G form Region I, zones B, E, H form Region II, whilst zones C, F and I make up Region III. The microbial propagation from a single point source and the subsequent colonisation of the heap were also evaluated.

The ore (132 kg) was agglomerated with 50 ml deionised H_2O/ kg ore and 3.7 mL conc. H_2SO_4 / kg ore, prior to loading into the box. The heap bed was initially wetted from the top via multiple irrigation points. Thereafter the bed was acid-washed with acidified distilled water at pH 1.15 for 26 days prior

to inoculation. This was done to wash out soluble copper oxides, inhibitory precipitates, and lower the pH of the leaching environment to the design specification of pH 1.15.

The bed was then inoculated with a mixed mesophilic culture (10^{12} cells/ton ore) on day 27, done via irrigation at a rate of 6 L/m^2.h from a single point source and aerated at 1.75 L/min (supplied in excess). In-bed sampling of the heap was conducted using ore samples collected through the face ports, allowing the microbial distribution to be analysed in relation to moisture content across 9 different zones (Figure 3-6) in the ore bed over an 83 day leaching period. There were 13 drainage ports at the bottom in which the percolating solution from each of the different sections was collected daily. Sample analysis is detailed in Section 3.5.

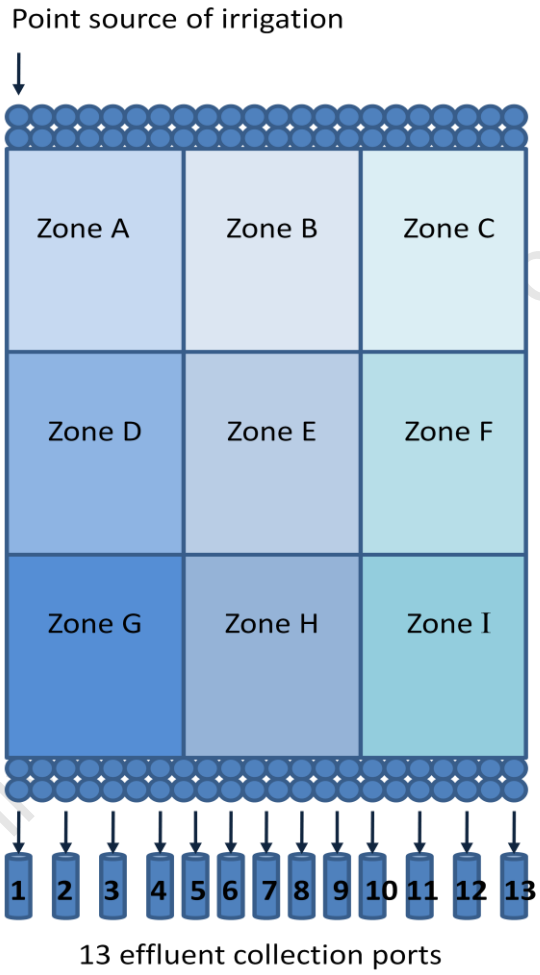

Figure 3-6: Illustration of box zone separations used for the in-bed sampling

3.7 Data Handling

Moisture content calculations:

$$Moisture\ \_content\ \_[\%] = \frac{(Wet\ \_mass) - (Dry\ \_mass)}{Wet\ \_mass} \times 100\ \%$$

Copper recovery calculations:

$$Copper\ \_recovery\ \_[\%] = \frac{(Copper\ \_concentration\ \_[g/l]) \times (Effluent\ \_volume\ \_[l])}{Total\ \_mass\ \_copper\ \_in\ \_ore} \times 100\ \%$$

The rate at which the bacteria multiplied, r_x, is a function of the available microbial population, X, at a particular time, t.

$$r_x = \frac{dX}{dt} = \mu X$$

The growth rates, μ, were calculated using the concentration, X, represented by the sum of the interstitial and attached cells, whilst neglecting the planktonic cells which were removed from the column.

3.8 Sample Collection and Storage

Clean sample containers were utilised in the study presented herein. The storage time of the AAS samples was limited (maximum 1 week). The deterioration of sample was minimised by storage at 4°C.

3.9 Assumptions and Limitations

The following assumptions and limitations were taken into consideration during the course of the experiments:

- The systems used were agglomerated and uniformly packed.
- Micro-organisms used to inoculate the system were in an active growth state prior to transfer.
- The effluent cell concentration values obtained were assumed to be the planktonic/detached cell population. For days on which the cell counts could not be performed, averages of the previous and succeeding days' values were used.
- Negligible cell attachment to column walls.
- Negligible attachment of the micro-organisms to the box reactor walls.
- The ferrous, total iron and ferric iron data was attained from the spectrophotometer. The ferric iron expelled in the effluent was determined from $Fe^{Total}{}_{out} - Fe^{2+}{}_{out} = Fe^{3+}{}_{out}$.

It was difficult to simulate ideal heap conditions. Once the ore was packed into the systems, the beds slumped during the initial irrigation period. Therefore, the beds were allowed to settle before conducting experiments, rendering them stable. The box was considered to be packed uniformly *i.e.* uniform porosity with space and time. Flow through the box heap was expected to occur in both vertical and horizontal planes.

3.10 Research Strategy

The experimental work was structured such that the hypotheses presented in Section 2.6 were interrogated. The schematic in Figure 3-7 outlines how each of the key questions coincides with an aspect of the experimental data attained.

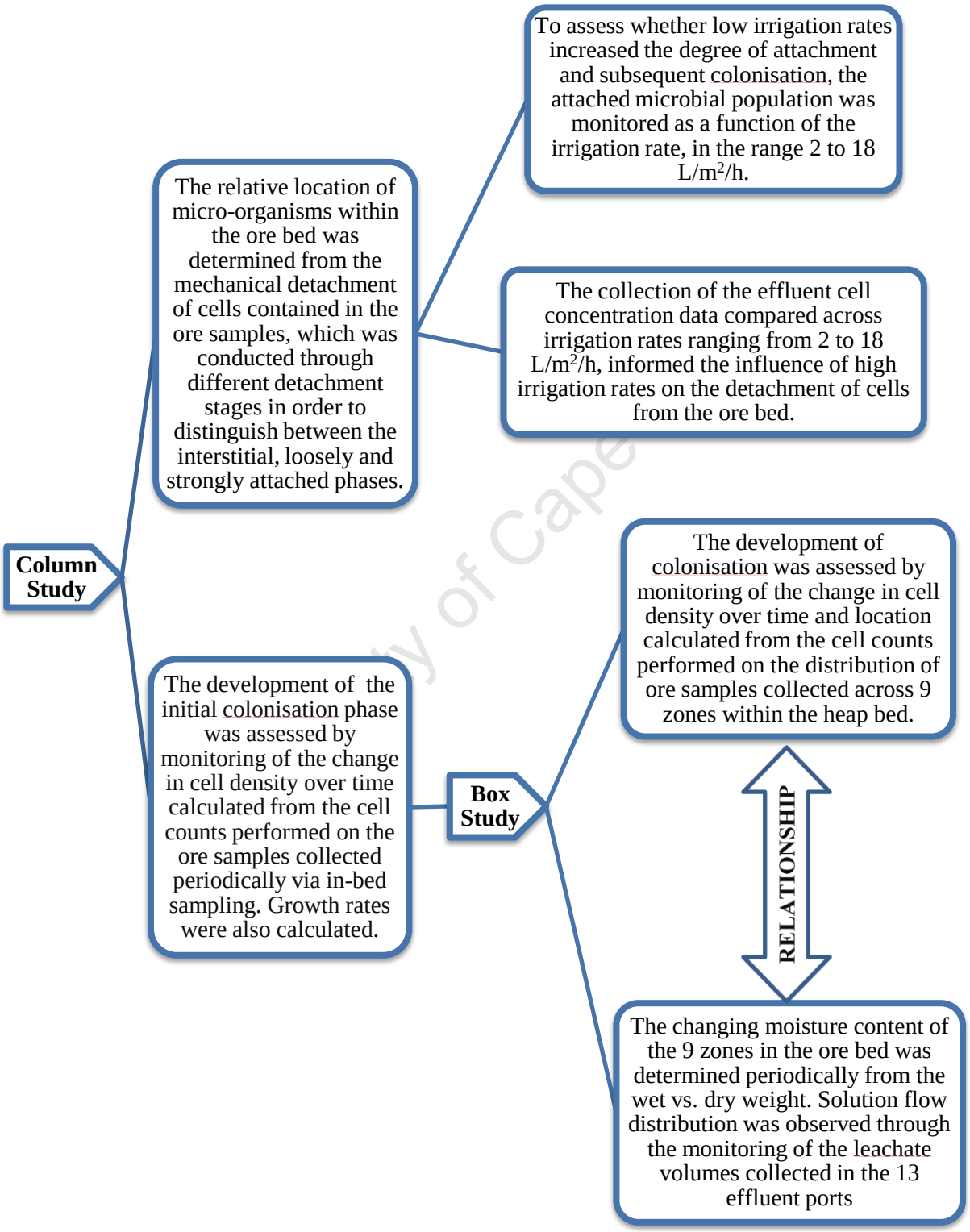

Figure 3-7: Outline of research approach

4 CHAPTER 4: EFFECT OF IRRIGATION APPLICATION RATES ON MICROBIAL COLONISATION

4.1 Introduction

Efficient microbial colonisation of the heap is essential for optimal levels of microbial activity, mineral recovery and sustainable bioleaching. Microbial colonisation occurs through the following steps; (i) the transport of microbes throughout the heap within the vicinity of exposed sites on the mineral surface, (ii) the selective reversible and irreversible attachment to the mineral surface (Rossi, 1990; van Loosdrecht *et al*., 1990) and (iii) growth and retention of microbes resulting in the formation of microbial colonies which contribute to biooxidation (Rossi, 1990; van Loosdrecht *et al*., 1990; Rockhold *et al*., 2002; Pintelon *et al*., 2009). Mueller (1996) suggested that transport of microbial organisms through the heap to the mineral surfaces could be a rate limiting step in the colonisation process. Loosely attached microorganisms may detach from the ore surfaces by repulsive electrostatic forces (Ghauri *et al.*, 2007; Rodriguez *et al.* 2003) and mild shear forces (Rossi, 1990; van Loosdrecht *et al*., 1990; Rockhold *et al*., 2002; Pintelon *et al*., 2009). Rockhold *et al*. (2002) claimed that the detachment of microbes during the various colonisation phases and the inevitable cell death are also controlling factors in the overall accumulation of cells in porous systems. Therefore, a thorough understanding of the parameters affecting microbial colonisation will lead to a more in-depth comprehension of the heap bioleaching environment.

Adequate flow is necessary for the heap to be leached in an economical time, while uniform flow is needed to allow all the ore to be thoroughly leached (O'Kane *et al*. 2000). However, the flow regime can also influence hydrodynamic conditions within the heap system which may affect the microbial growth rates, cause metabolic inhibition and detachment of active microbial populations during the leaching process. Therefore, understanding the impact of fluid dynamics on microbial migration and colonisation is important.

The aim of this study is to add to the bioleaching knowledge base through integrated study of microbiological and hydrological aspects of heap bioleaching, through a comparative study on the effect of irrigation application rates on microbial colonisation in simulated heap structures.

4.2 Experimental Approach

Heap leach column test work was conducted to determine the effect of irrigation inoculation at different solution application rates on the microbial attachment and subsequent colonisation of the ore.

4.2.1 *Experimental procedure*

The more detailed materials and methods are provided in Sections 3.4, 3.5 and 3.6. The experiments were conducted in small scale leach columns, illustrated by Figure 4-1, using varying flow rates based on the range of industrial irrigation rates (5 to 20 L/m^2.h - Petersen and Dixon, 2007a), and the range (1.8 to 21.6 L/m^2.h) used by Lizama *et al*. (2005) in their study. The flow conditions tested in the three systems were 2, 6 and 18 L/m^2.h, which covers part of the range of operating conditions used in bioleaching heaps. The columns were aerated at 200 ml/min and inoculated with 10^{12} cells/ton of ore using a mesophilic stock culture containing *At.caldus, At.ferrooxidans, At.thiooxidans* and *L.ferriphilum*. The columns were inoculated with a high cell density to ensure rapid colonisation and thus eliminating this parameter from being a limiting factor. The columns were monitored regularly and daily analyses were conducted.

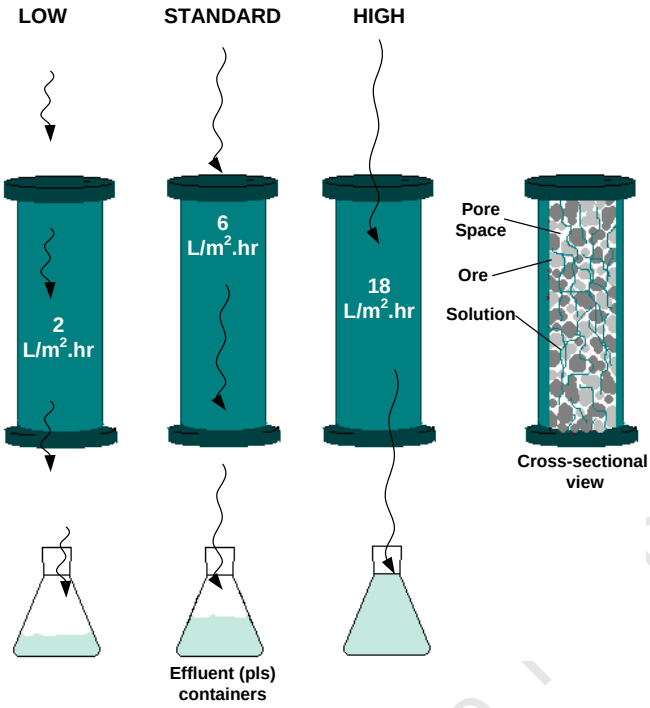

Figure 4-1: Illustration of column experimental set-up

In the preliminary experimental run, the columns were acid washed for 1 day at 6 L/m^2.h to remove inhibitory substances and create an environment conducive to microbial attachment to the ore surface. Thereafter experimental feed rates were established. The preliminary experiments ran for 48 days and the columns were taken down. During the column unloading, the ore from each column was separated into 3 sections to allow analyses to be conducted on the top, middle and bottom zones of the column. Cell densities were determined by detaching the microbes from the ore (viz. detachment protocol in Section 3.5). The water content was determined by drying samples in the 80°C oven over a 24 hr period

During further experimental runs, in-bed sampling was used to extract ore from the middle section of the heap beds at certain intervals during the leaching process. This novel in-bed sampling technique (Section 3.4) was used to gain novel insight into the microbial growth and the interstitial, weakly and strongly attached microbial population. Consequently, the preliminary run provides a comparative indication of the process sensitivity to the in-bed sampling technique. The leaching time allowed was reduced to a period of 32 days as the information pertinent to this study could be obtained within this period. Similar analyses were performed on the ore. Real time PCR analyses were conducted to determine the microbial species associated the ore at the end of the initial colonisation period.

4.3 Preliminary study

4.3.1 *Flow Rates and Moisture Content*

The leachate flow rates as a function of time are presented in Figure 4-2. The outlet flow rates fluctuated slightly during the course of the experimental run. The evaporation rates, calculated as the difference between flow rate entering and leaving, were 2.61, 2.06 and 21.38 ml/h for 2, 6 and 18 L/m^2/h respectively. These accounted for less than 0.2% of the volume entering.

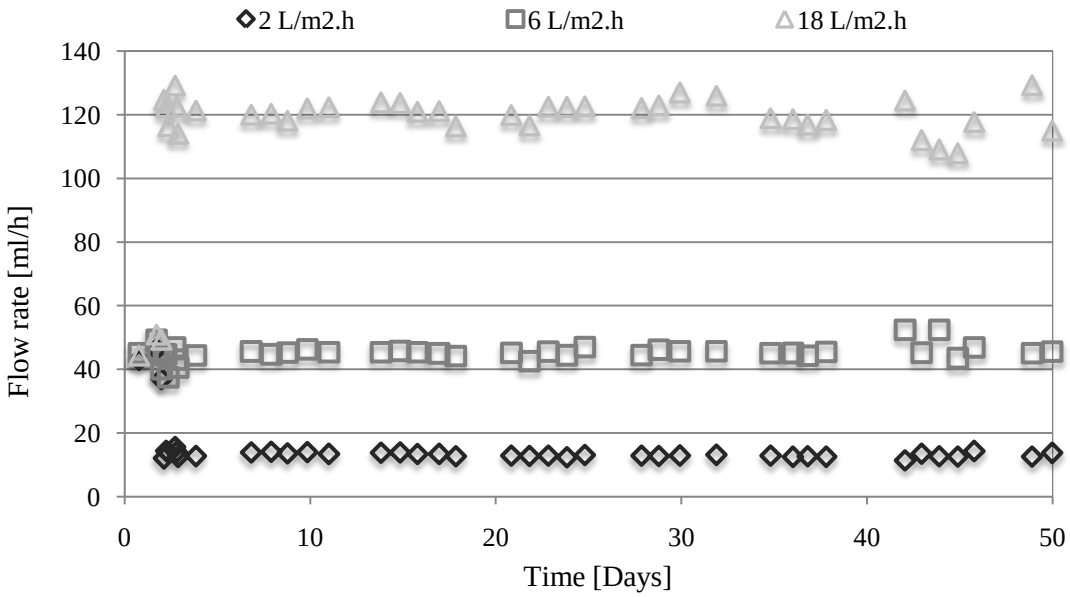

Figure 4-2: Effluent flow rate profile as a function of time during the bioleaching of low grade copper bearing ore, given for different irrigation rates 2, 6 and 18 L/m^2.h, during the preliminary run.

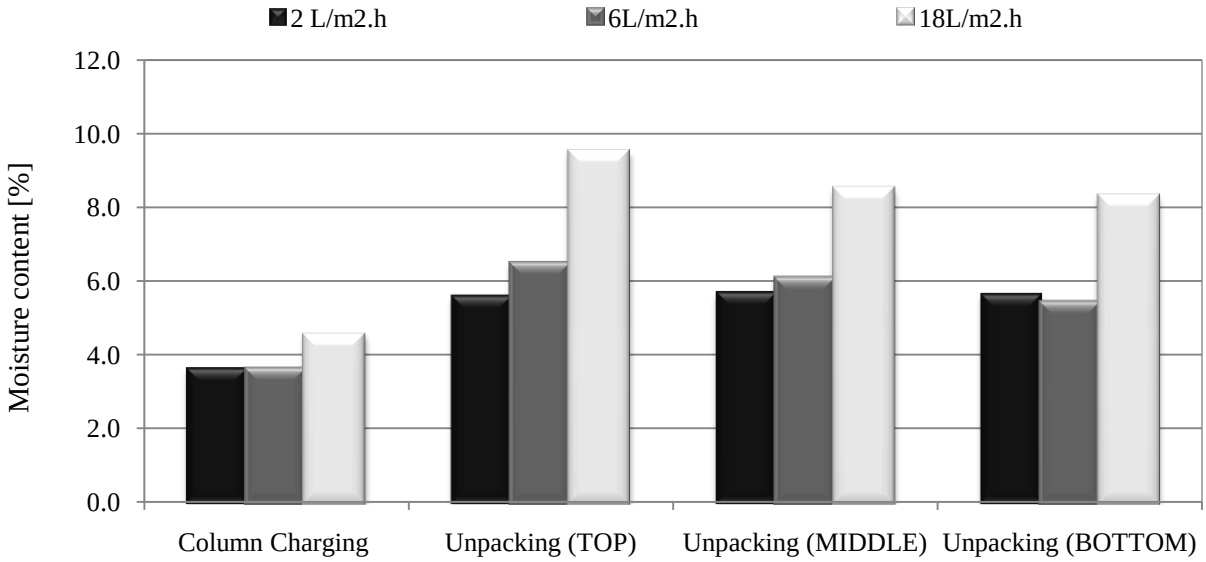

Figure 4-3: Moisture content of the ore bed pre-leaching and post-leaching (50 days), given for different irrigation rates 2, 6 and 18 L/m^2.h, during the preliminary run.

The moisture content of the ore bed taken before and after the preliminary bioleaching run is displayed in Figure 4-3. The initial moisture contents were 3.6, 3.6 and 4.5% for 2, 6 and 18 L/m^2.h respectively. The final moisture content was determined for the top, middle and bottom sections of the ore bed. Within the top section of the bed the moisture contents were 5.6, 6.5 and 9.5% for 2, 6 and 18 L/m^2.h respectively. The middle zone of the bed yielded moisture contents of 5.7, 6.1 and 8.5% for 2, 6 and 18 L/m^2.h respectively, whilst moisture contents at the bottom were 5.6, 5.4 and 8.3% for 2, 6 and 18 L/m^2.h respectively. The moisture contents show that the solution distribution was fairly uniform at low flow (5.63± 0.05 % at 2 L/m^2.h). The moisture contents were much higher (8.3 to 9.5 %) at 18

L/m^2.h indicating that the bed saturation increased at high irrigation rates. In the more saturated bed, a trend of increased moisture content at the top of the bed was observed.

4.3.2 *Copper Extraction*

The mineralogy of the low grade copper bearing ore used in the leaching experiment contained 0.69% copper (Cu) and 2.95% iron, i.e. 27 g and 115 g respectively for 4 kgs. Figure 4-4 shows the cumulative copper liberation as a function of time at the various irrigation rates, during the preliminary run. Of the available copper, the amounts extracted over the first 45 day period were 12, 11 and 21 % for 2, 6 and 18 L/m^2.h respectively, owing to the short leach duration as column leach systems typically run for +300 days. Post the acid wash period, the copper liberated via bioleaching occurred at a similar rate under low flow conditions, 0.073 and 0.068 g/day for 2 and 6 L/m^2.h respectively. At 18 L/m^2.h the copper was extracted at a higher rate of 0.115 g/day. The highest Cu recovery was observed for 18 L/m^2.h as a consequence of a higher proportion of acid-soluble copper being extracted in the initial acid-wash stage even though all systems were operating at the standard rate of 6 L/m^2.h during this period (Table 4-1). This difference could be attributed to the heterogeneity of the ore originally loaded into the different systems.

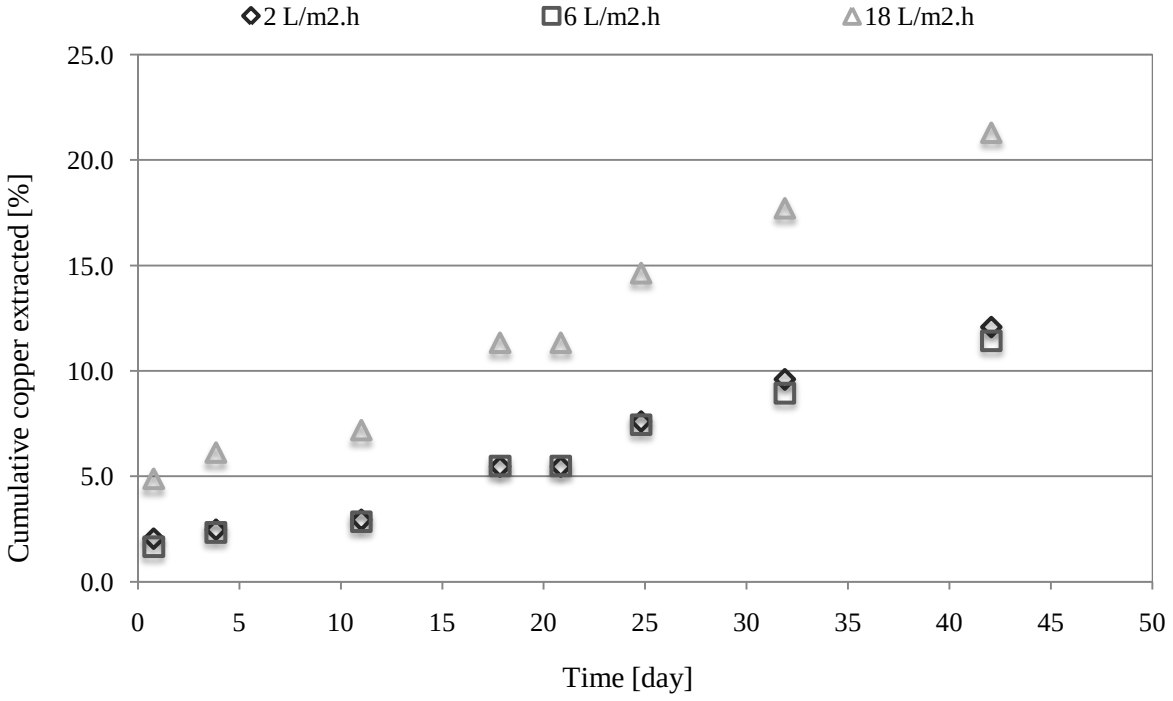

Figure 4-4: Cumulative copper liberation as a function of time during the bioleaching of low grade copper bearing ore, given for different irrigation rates 2, 6 and 18 L/m^2.h, during the preliminary run.

Table 4-1: Copper analysis over the 3 flow systems during leaching run 1 after 45 days

	Irrigation rate [L/m^2.h]		
	2	6	18
Cu in ore loaded [g]	28.64	28.64	28.91
Cu removed in leachate [g]	3.47	3.26	6.16
Total Cu recovered [%]	**12.1**	**11.4**	**21.3**
Cu recovered after acid wash [%]	**2.3**	**2.3**	**6.1**
Average Cu concentration in leachate [g/l]	**0.30**	**0.09**	**0.06**

4.3.3 *Solution Chemistry of Leachate*

Figure 4-5 shows the ferrous iron concentration in the eluted leachate as a function of time at different irrigation rates, during the preliminary run. The initial ferrous iron concentration supplied through the feed solution was 0.5 g/l. The concentration of ferrous iron first eluted was higher (0.62 g/l) at 18 L/m^2.h than the other flow rates, 0.34, and 0.3g/l for 2 and 6 L/m^2.h respectively. Post inoculation on day 2, the ferrous iron concentration decreased rapidly over the next 5 days due to the microbial oxidation of ferrous to ferric iron, corresponding to the changing redox potential during that period. After 8 days the ferrous iron concentration of the effluent was very low reaching depletion.

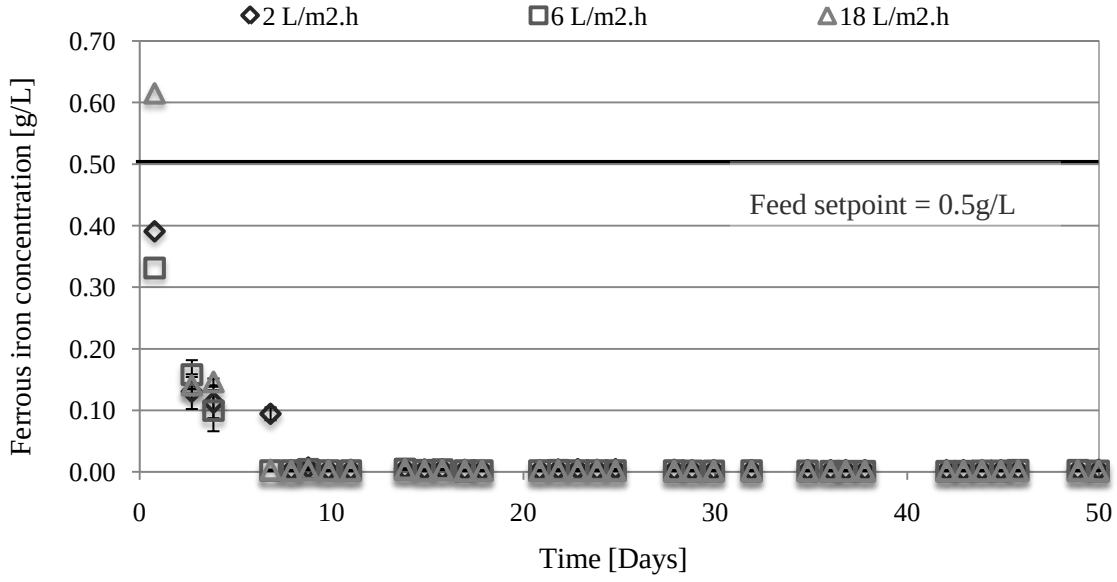

Figure 4-5: Ferrous iron concentration in the eluted solution passing through the column heap as a function of time, given for different irrigation rates 2, 6 and 18 L/m^2.h, during the preliminary run.

Figure 4-6 (a) and (b) show the redox and pH profiles of the eluted leachate as a function of leach time at different irrigation rates. The redox potential of the feed solution was ~370 mV. The redox potential of the leachate increased slowly from 350 to 450 mV during the first 5 day phase. The redox potential increased rapidly from 450 to 650 mV between days 5 and 12, due to enhanced microbial growth and biooxidation of ferrous to ferric iron. Thereafter, the redox potential fluctuated between 630 and 670 mV. At 2 L/m^2.h, the redox potential of the system took longer to increase, stabilising at 650 mV. The feed solution was at a pH of 1.15. The pH of the eluted solution fluctuated around pH 1.2 for 6 and 18 L/m^2.h. The profile indicated that the pH was higher, pH 1.35, at 2 L/m^2.h than for the other irrigation conditions.

4.3.4 *Microbial Analysis*

Figure 4-7 (a) and (b) shows the leachate cell concentration and the cumulative number of planktonic cells leaving the ore bed in the PLS as a function of time, at irrigation rates of 2, 6 and 18 L/m^2.h, during the preliminary run. The systems had been inoculated with micro-organisms in an active growth stage, rendering cells detectable under the microscope at this stage. The relative uncertainty in the cell counts was high (> 30 %) within the first 10 days. This was due to the low cell concentration being detected. The cell concentration within the effluent solution increased up to ~3x10^{6}cells/ml over the days 3 to 10, indicating significant microbial growth and subsequent detachment occurring within

all systems and corresponding to the increasing redox potentials. Thereafter a decrease in cell number exported from the columns observed. After 48 days of leaching, the cumulative cell exportation from the column was observed as approximately $2.8x10^{11}$, $8.0x10^{10}$, and $1.87x10^{10}$ cells respectively, for 18, 6 and 2 L/m^2.h with the propagated cumulative error being < 30 %. The PLS cell concentrations ranged from $7.3x10^5$ to $1.5x10^6$cells/ml. The larger cell removal at the higher flow conditions could be attributed to the detachment of cells as a consequence of the greater shear stress induced by the tangential fluid flow across the mineral surface as suggested by Bartlett (1992).

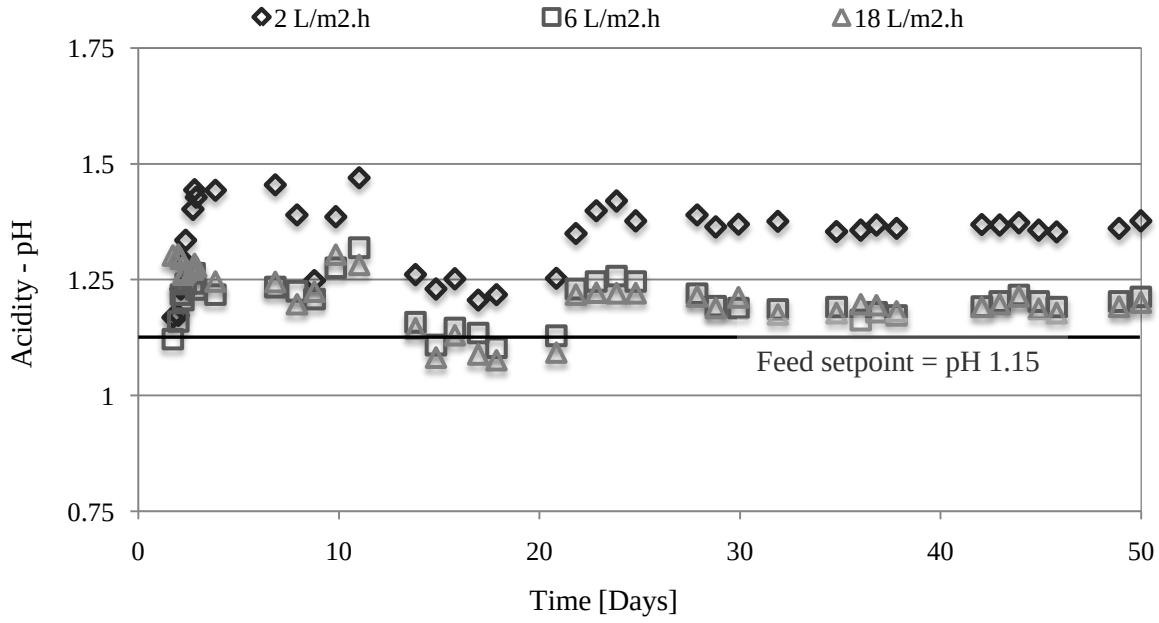

(a) pH

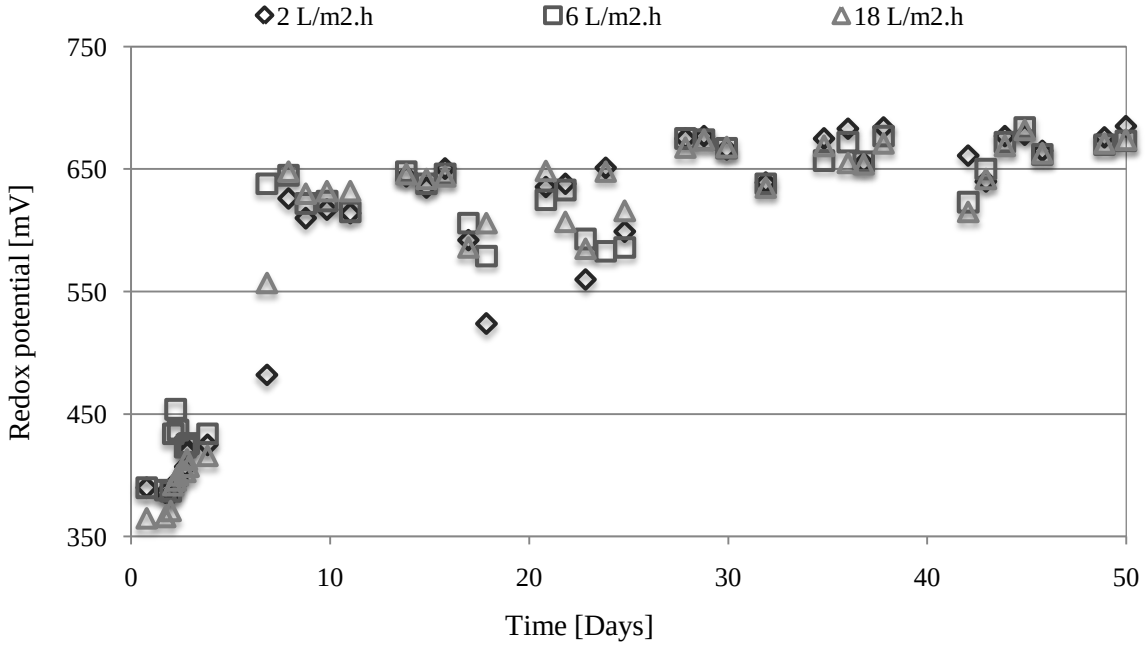

(b) Redox potential

Figure 4-6: Trend in (a) the pH and (b) the redox potential, of the eluted solution passing through the column heap given for different irrigation rates 2, 6 and 18 L/m^2.h, during the preliminary run.

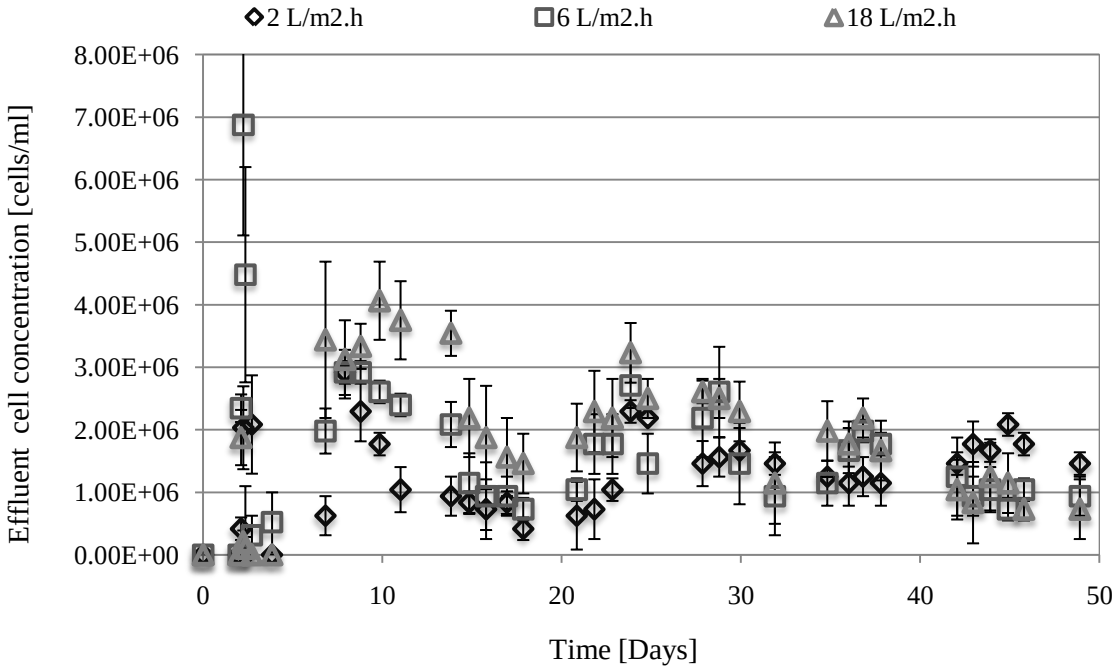

(a) Effluent cell concentration

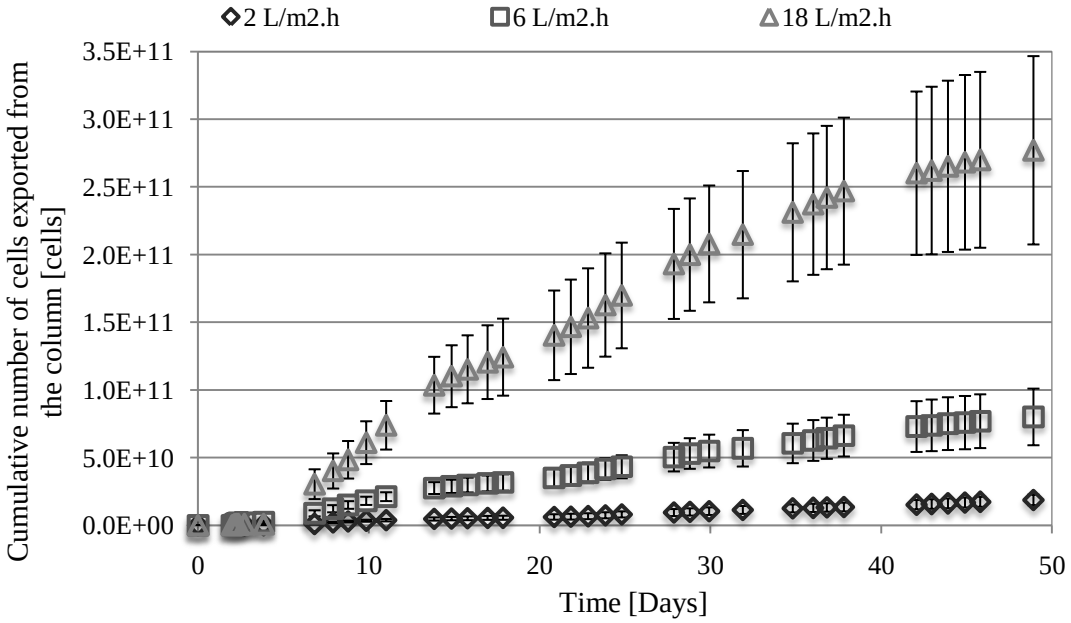

(b) Cumulative cell count

Figure 4-7: Trend in (a) the cell concentration and (b) the cumulative number of cells, exported in the leachate passing through the heap, given for different irrigation rates 2, 6 and 18 L/m^2.h, during the preliminary run.

A species analysis on the mesophilic culture present at the start and end of the bioleaching experimental run is shown in Table 4-2. The analysis conducted post leaching was only performed on samples obtained for the interstitial phase as cell counts in this phase were high enough to be quantified. Note: the analysis was not reproduced. *L. ferriphilum* was identified as the dominant

micro-organism via qPCR (> 89 % dominance) followed by *At. caldus*. This also corresponded to the observed dominance of spiral shaped bacteria over rod shaped under the microscope for all microbial phases (planktonic, interstitial and attached). This could be due to the bioleaching conditions used which created a low pH (1.15) environment known to favour *L. ferriphilum* over the other species present (Rossi, 1990; Watling, 2006; Schippers, 2007).

Table 4-2: Analysis of the micro-organisms present in the inoculum and in the ore bed at the end of the experiment determined from the mechanical detachment of cells from the ore samples periodically removed from the heap systems using the in-bed sampling technique, given for a single sample of the interstitial phase under the different irrigation rates 2, 6 and 18 l/m^2/h, during the preliminary run.

Sample	*At. ferrooxidans*	*L. ferriphilum*	*At. thiooxidans*	*At. caldus*	*At. ferrooxidans D2*
Stock	0.00%	99.88%	0.00%	0.12%	0.00%
2 L/m^2.h	0.00%	94.84%	0.00%	5.01%	0.14%
6 L/m^2.h -A	0.00%	97.74%	0.00%	2.26%	0.01%
6 L/m^2.h - B	0.00%	97.21%	0.00%	2.78%	0.01%
18 L/m^2.h	0.00%	89.19%	0.00%	10.78%	0.03%

4.4 Responses to Varied Irrigation Application Rates

This section presents the results and discussion of the microbial colonisation of the heap leaching system in response to irrigation inoculation application rates. A brief outline of the experiment was provided in Section 4.2. There are differences between the preliminary experiment (run 1) and runs 2 and 3. These differences are attributed to the slight disturbance of the systems during in-bed sampling, which was not performed previously within the preliminary run.

4.4.1 *Flow Rates and Moisture Content*

Three columns were operated simultaneously at irrigation rates of 2, 6 and 18 L/m^2.h respectively, over replicate runs 2 and 3. The leachate flow rates as a function of time fluctuated slightly during the course of the experimental runs (see Appendix. The volumetric flow rates out of the system were constant within (10%) for the duration of the leach run (data not shown), indicating low influence of the in-bed sampling technique, described in Section 3, on the heap systems. The in-bed sampling was conducted on days 14, 18, 24 and 32 for run 2, and days 7, 19, 28 and 32 for run 3.

The moisture content of the ore bed taken before, during and after the bioleaching experimental runs is displayed in Figure 4-8. The initial moisture content ranged from 5.0 to 5.2 % for all flow rates across replicate runs. During run 2, the moisture contents increased gradually over time. The moisture content increased to 8.8±1.2 % after 14 days, further increasing to 10.7±0.3 % on day 24, for 2 L/m^2.h. Similarly, at 6 L/m^2.h, the moisture content increased to 8.2±1.2 % on day 14, reaching a plateau at 9.6±0.3 % on day 24. In the system operating at 18 L/m^2.h, the moisture content was higher than that observed for the lower irrigation rates, reaching a plateau of 12.1± after 24 days of irrigation. During run 3, the moisture contents showed a similar trend to that observed in both run 2 and the preliminary run. For 2 L/m^2.h, the moisture content increased to 6.7±0.8 % after 7 days, further increasing to

7.89±0.4 % on day 19, reaching as high as 9.2±0.5 % on day 32. At 6 L/m^2.h, the moisture content differed slightly between replicate columns, ranging from 6.5 – 8.0 ±0.8 % on day 7, and increasing to 9.9- 10.4±0.5 % on day 32. Again, the moisture content was higher at 18 L/m^2.h, increasing from 8.7±0.8 % on day 7 to 10.4±0.4 % on day 19 and reaching 13.5± 0.5 % after 32 days of irrigation. In all runs, the higher moisture contents observed for 18 l/m^2/h indicated a more water saturated ore bed.

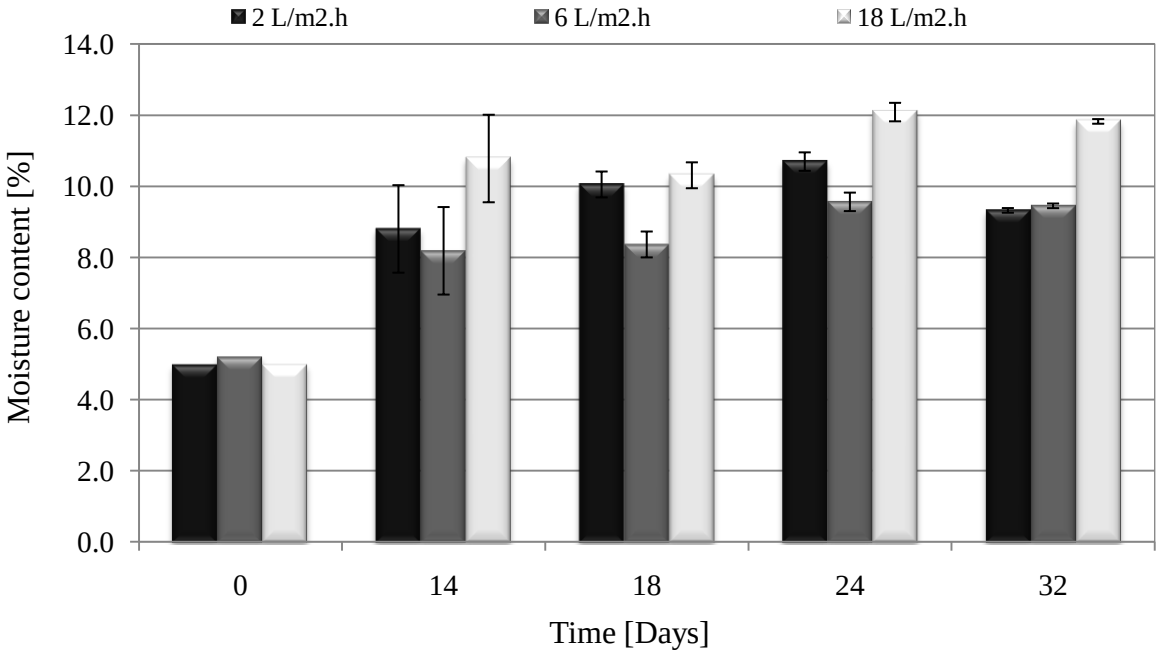

(a) Run 2

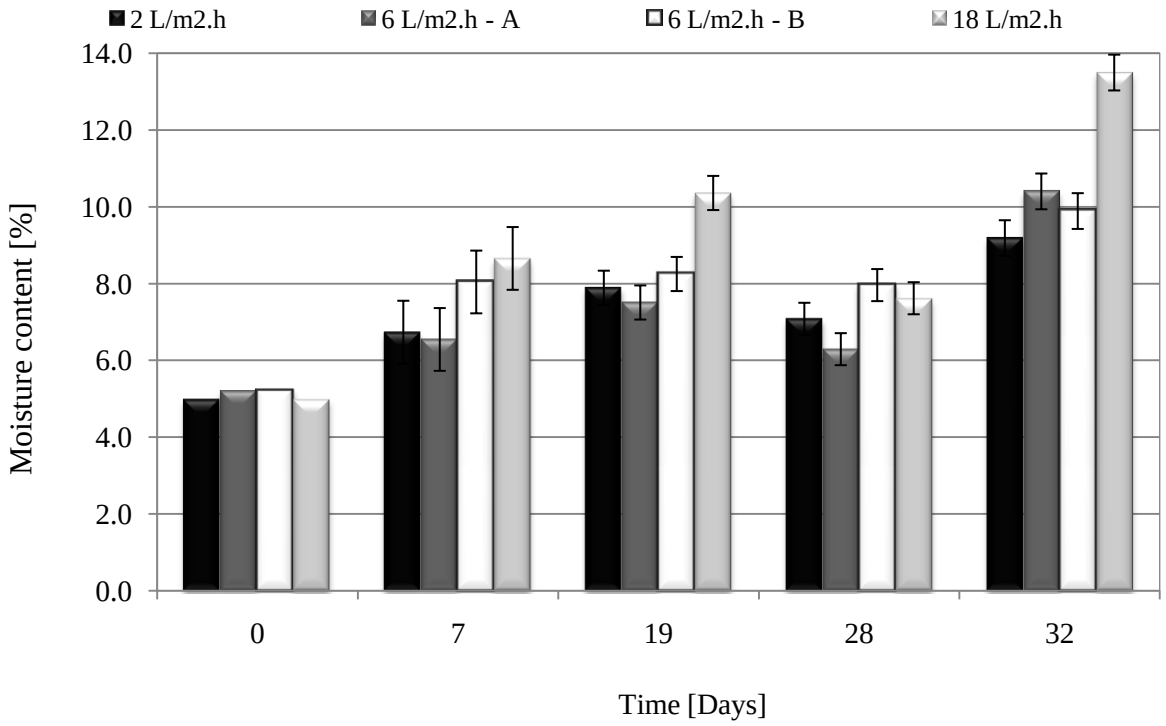

(b) Run 3

Figure 4-8: Moisture content of the ore bed pre-, during and post-leaching, determined from the ore samples periodically removed from the heap systems using the in-bed sampling technique, given for different irrigation rates 2, 6 and 18 L/m^2.h, during experimental (a) run 2 and (b) run 3.

4.4.2 *Copper Liberation*

Figure 4-9 shows the cumulative copper liberation as a function of time at the various irrigation rates, during replicate runs, giving an indication of the leaching performance at different irrigation rates. Additionally, Table 4-3 and Table 4-4 show the copper recovery at the end of the leaching period and the average copper concentration in the eluted leachate, for runs 2 and 3. These values can be compared to those presented for the preliminary run in Table 4-1.

Table 4-3: Copper analysis over the 3 flow systems during leaching run 2 after 32 days

	Irrigation rate [L/m^2.h]		
	2	6	18
Cu in ore loaded [g]	27.32	26.77	26.98
Cu removed in leachate [g]	6.52	7.09	7.74
Total Cu recovered [%]	**23.9**	**26.5**	**28.7**
Cu recovered after acid wash [%]	**10.2**	**11.4**	**10.9**
Average Cu concentration in leachate [g/l]	**0.31**	**0.16**	**0.15**

Table 4-4: Copper analysis over the 3 flow systems during leaching run 3 after 32 days

	Irrigation rate [L/m^2.h]			
	2	6	6 rpt	18
Cu in ore loaded [g]	24.50	27.53	28.01	26.22
Cu removed in leachate [g]	3.94	5.47	5.77	7.81
Total Cu recovered [%]	**16.1**	**19.9**	**20.6**	**29.8**
Cu recovered after acid wash [%]	**7.8**	**8.1**	**8.2**	**10.5**
Average Cu concentration in leachate [g/l]	**0.33**	**0.24**	**0.24**	**0.24**

In all runs, the copper was leached rapidly during the first 3 days of leaching recovering the vast majority of the acid-soluble copper during the acid wash stage. Thereafter, the rate of copper liberation decreased gradually and remained almost constant for the duration of the leaching process. This was also shown by the initial bright blue colour of the effluent that was observed, after which the leachate became a pale blueish green colour which was more prominent at low flow due to the higher copper concentrations in the effluent. The copper extraction over the 32 day leaching period was 23.9, 26.5 and 28.7 % for 2, 6 and 18 L/m^2.h respectively during run 2, and 16.1, 19.9, 20.6 and 29.8 % for 2, 6-A, 6-B and 18 L/m^2.h respectively, during run 3. The highest copper recovery was observed for 18 L/m^2.h across all runs. Note: during run 3 the in-bed sampling caused the column operating at 18 L/m^2.h to block by day 25. This was due to compression of the ore bed from the gravity pull, causing the copper eluted to be more concentrated as the solution infiltrated the ore bed at a slower rate. Lower Cu extraction at low flow could be attributed to mass transfer limitations due to the slow delivery of reactants, e.g. acid, to the active leaching sites and the removal of reaction products from this vicinity. These results suggest that to reduce mass transfer limitations associated with leaching, an irrigation rate > 6 L/m^2.h should be employed. The copper concentration in the eluted solution was higher for 2 L/m^2.h, at 0.30, 0.31 and 0.33 g/l for runs 1, 2 and 3 respectively.

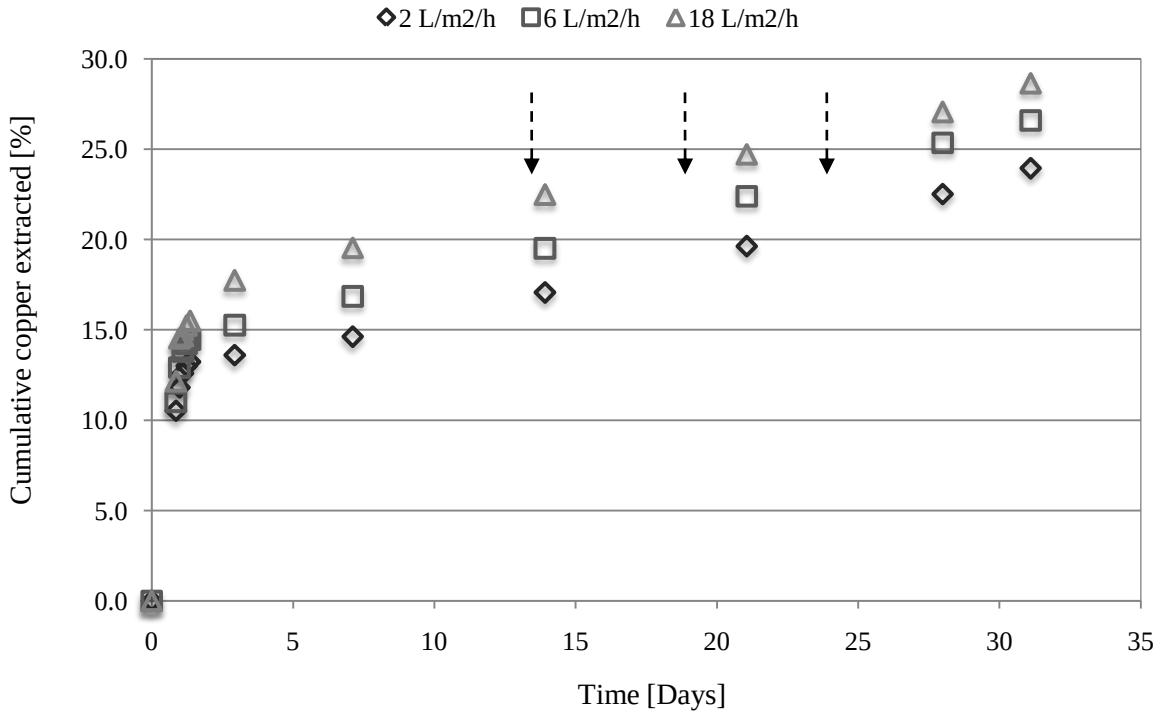

(a) Run 2

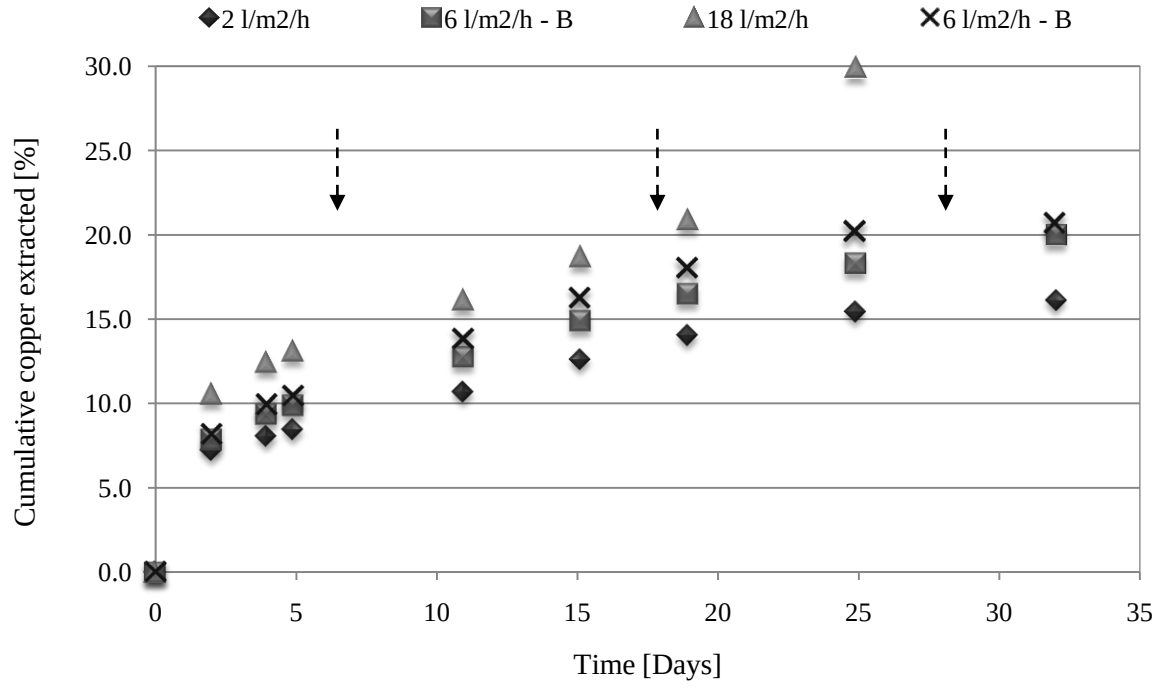

(b) Run 3

Figure 4-9: Cumulative copper liberation during the bioleaching of low grade copper bearing ore, given for experimental (a) run 2 at irrigation rates ◊ - 2 L/m^2.h, □ - 6 L/m^2.h and Δ - 18 L/m^2.h, and (b) run 3 at irrigation rates ♦ - 2 L/m^2.h, ■ - 6 L/m^2.h – A, x - 6 L/m^2.h – B and ▲ - 18 L/m^2.h. Arrow are indicative of in-bed sampling days.

4.4.3 *pH, Redox Potential, Ferrous and Total Iron Profiles*

Figure 4-11 (a) and (b) show pH of the leachate as a function of time, for different irrigation rates during replicate runs. The feed solution supplied to the columns had a specification of pH 1.15. The pH of all the systems was initially high (> pH 1.2) during days 4 to 8. Thereafter the pH decreased to fluctuate within the range of the feed pH. There was no significant difference between the pH at the different flow rates 6 and 18 L/m^2.h. During run 2, at low flow (2 L/m^2.h) the pH remained higher (~ pH 1.35) than for the other irrigation conditions. However, during run 3, the pH of the leachate was initial high at 2 L/m^2/h i.e. pH 1.6 between days 4 to 10. Thereafter, the pH decreased to within the range of the other systems, fluctuating between pH 1 and 1.5. The fluctuations observed for run 3 were unexpected, and could possibly be attributed to the in-bed sampling points. A higher pH environment that develops under low flow conditions could cause precipitation and jarosite formation (Lizama *et al*., 2005). Maintaining a low pH in the columns ensures that the iron does not precipitate out of solution, hence, avoids inhibition of microbial activity and promotes optimal leaching. Precipitation was minimised by keeping the pH below 1.8, therefore precipitation was not expected to be a big factor within these systems. Figure 4-10 shows the precipitation observed during in-bed sampling.

Figure 4-10: Visual evidence of jarosite/iron hydroxide precipitation, obtained from the ore extracted using the in-bed sampling technique, on day 18 of leaching at an irrigation rate of 6 l/m^2/h, during experimental run 2.

Figure 4-12 (a) and (b) show the redox potential as a function of time, given for various irrigation rates during replicate runs. The arrows indicate the days on which in-bed sampling was conducted. The fluctuations in the redox potential at 18 L/m^2.h correspond to the days immediately after each in-bed sampling point, indicating greater susceptibility of the high flow system to changes in the leaching environment caused by the in-bed sampling procedure technique. However, in run 3 less fluctuation was observed. The use of a low ferrous iron concentration in feed solution, i.e. 0.5 g/l, could have affected the Fe^{3+}/Fe^{2+} couple from being the most dominant redox couple and thus adding to the fluctuation observed. The initial redox potential was 380 mV. The redox potential of the leachate increased slowly from 400 to 470 mV during the initial 10 day phase at irrigation rates 6 and 18 l/m^2/h. The low redox phase was longer than that observed during the preliminary experiment. The length of this phase was attributable to the high rate of mineral leaching in comparison to ferrous iron oxidation. At the higher irrigation rates (6 and 18 L/m^2.h) from day 10 to 12, there was a significant increase in redox potential from about 450 to 650 mV, indicating the rate of microbial oxidation of ferrous iron was greater than ferric leaching of the sulphide minerals present. Thereafter, the redox potential fluctuated between 600 and 650 mV. Under low flow conditions (2 L/m^2.h), the redox

potential took longer to climb to 600 mV (17 days) than the other flow conditions, before stabilising at 650 mV.

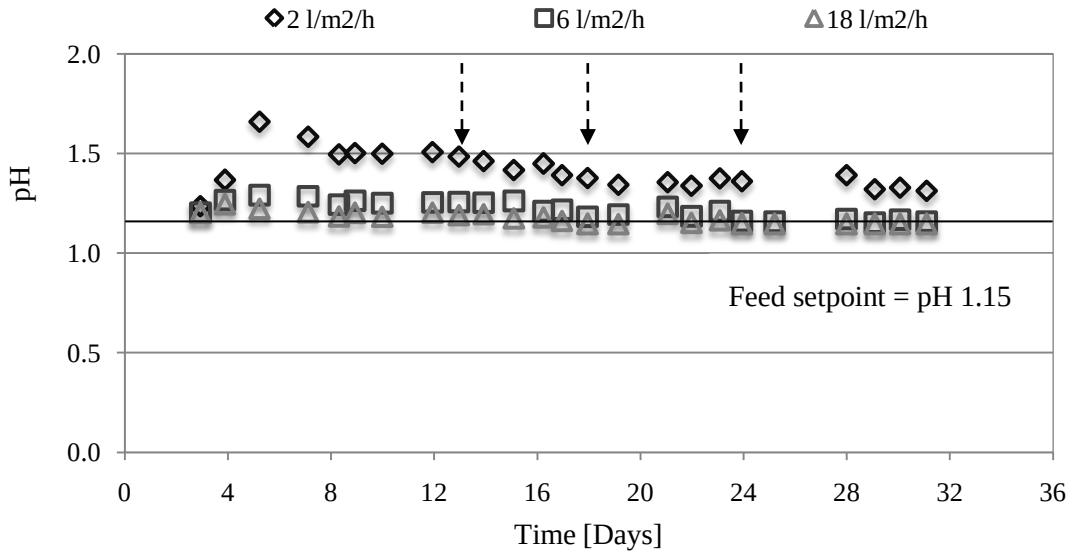

(a) Run 2

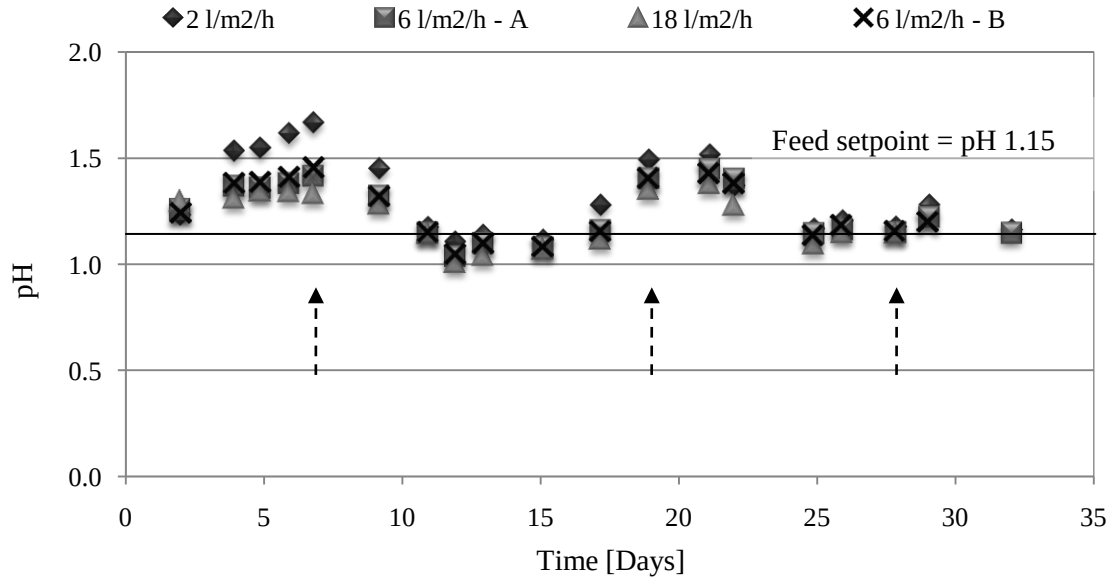

(b) Run 3

Figure 4-11: Trend in the pH of the eluted solution passing through the column heap during the bioleaching of low grade copper bearing ore, given for experimental (a) run 2 at irrigation rates ◊ - 2 L/m^2.h, □ - 6 L/m^2.h and Δ - 18 L/m^2.h, and (b) run 3 at irrigation rates ♦ - 2 L/m^2.h, ■ - 6 L/m^2.h – A, x - 6 L/m^2.h – B and ▲ - 18 L/m^2.h. Arrows are indicative of in-bed sampling days.

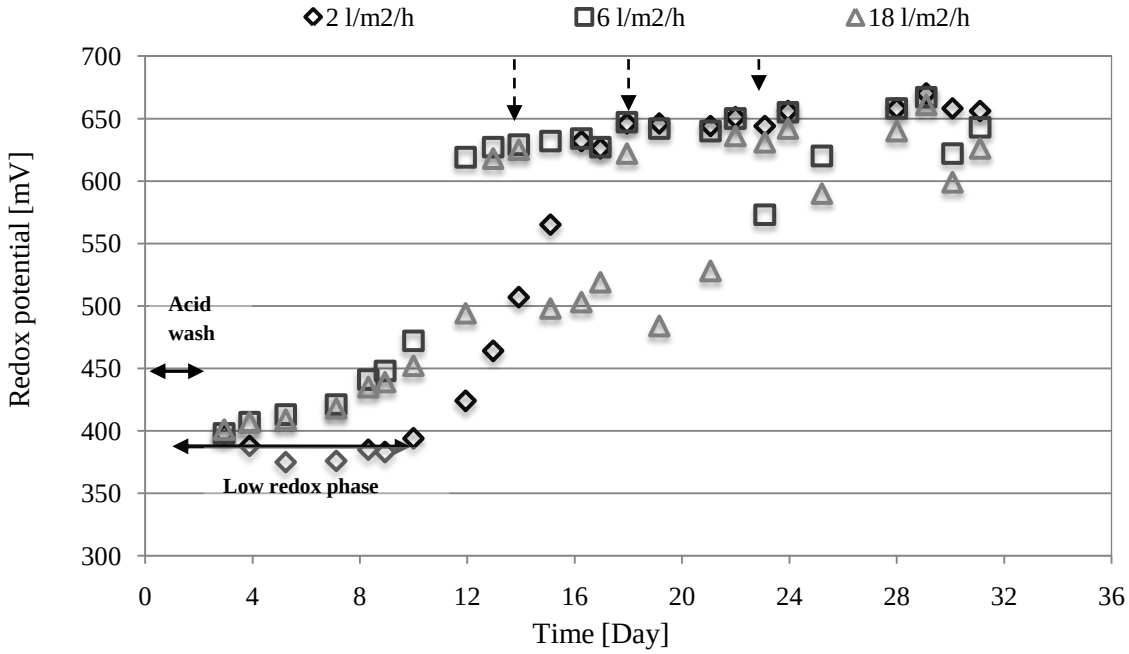

(a) Run 2

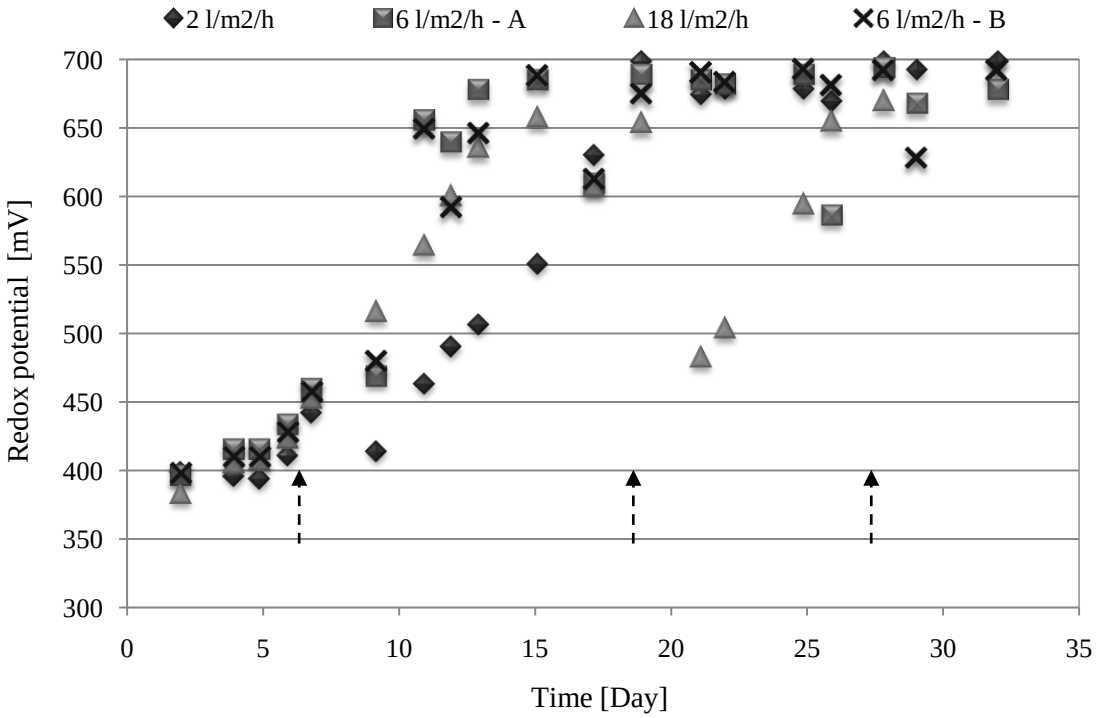

(b) Run 3

Figure 4-12: Trend in the redox potential of the eluted solution passing through the column heap during the bioleaching of low grade copper bearing ore, given for experimental (a) run 2 at irrigation rates ◊ - 2 L/m^2.h, □ - 6 L/m^2.h and Δ - 18 L/m^2.h, and (b) run 3 at irrigation rates ♦ - 2 L/m^2.h, ■ - 6 L/m^2.h – A, x - 6 L/m^2.h – B and ▲ - 18 l/m^2/h. Arrow are indicative of in-bed sampling days.

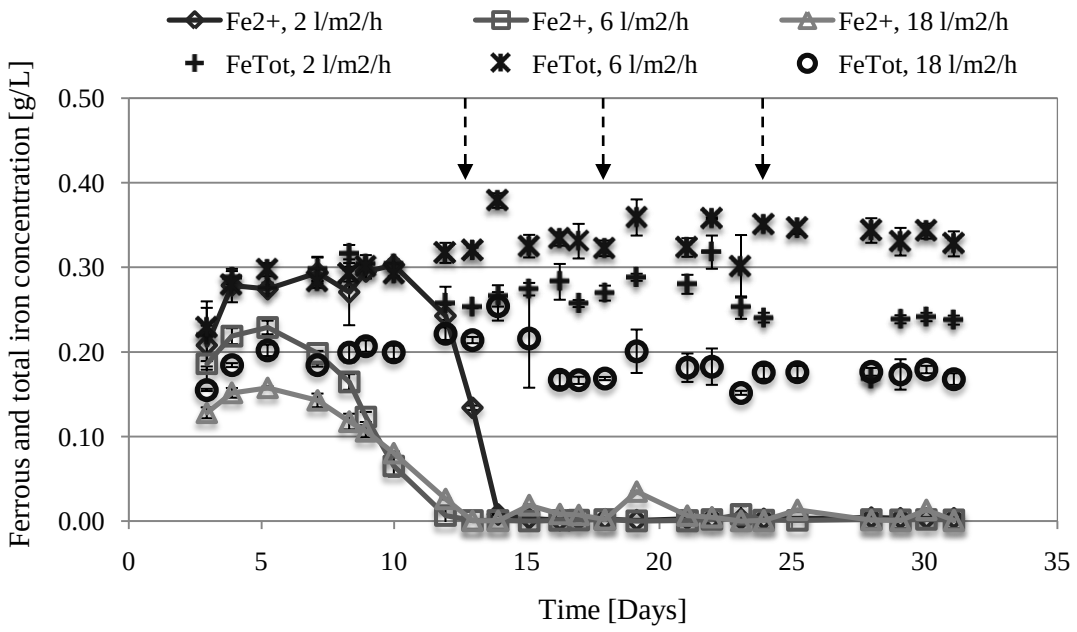

(a) Run 2

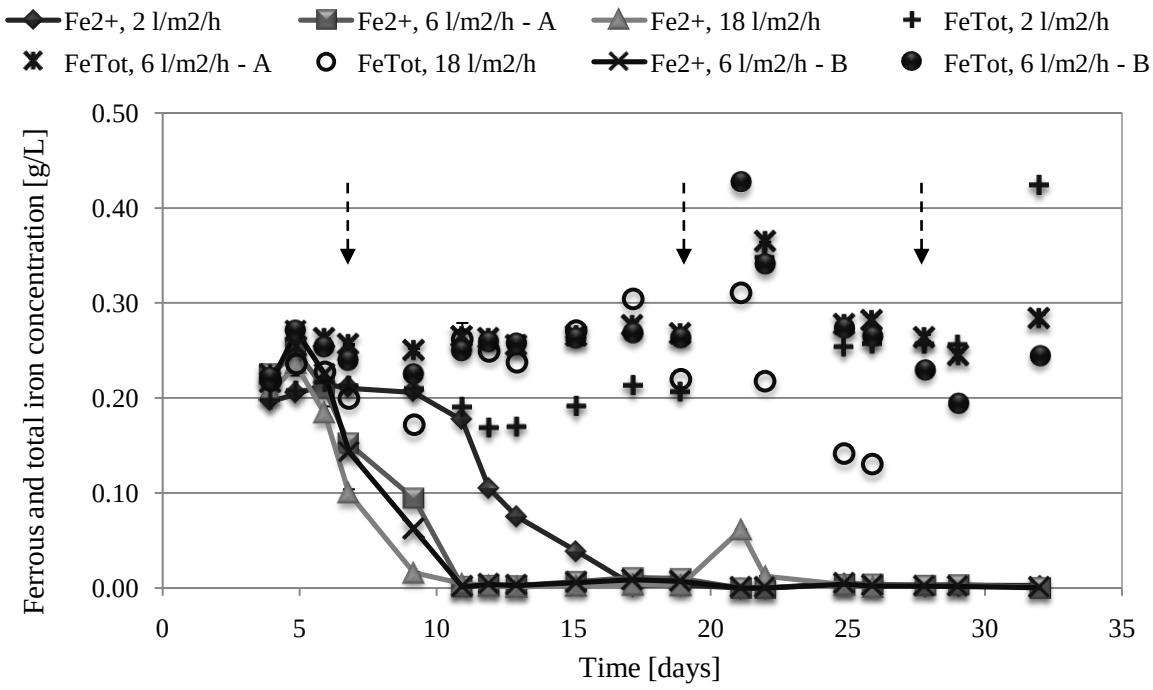

(b) Run 3

Figure 4-13: Total and ferrous iron concentration profile of the eluted solution passing through the column heap during the bioleaching of low grade copper bearing ore, given for experimental (a) run 2 at irrigation rates ◊ - 2 L/m^2.h, □ - 6 L/m^2.h and Δ - 18 L/m^2.h, and (b) run 3 at irrigation rates ♦ - 2 L/m^2.h, ■ - 6 L/m^2.h – A, x - 6 L/m^2.h – B and ▲ - 18 L/m^2.h. Arrows indicative of in-bed sampling days.

Figures 4-13 (a) and (b) show the total and ferrous iron concentrations of the leachate as a function of time at the various irrigation rates, during replicate runs. During run 2 the ferrous iron concentration increased slightly during the initial stage of leaching, between days 3 to 6, then decreased rapidly to low values (< 0.05 g/L) after 12 days. The initial increase was probably due to leaching of iron-

containing minerals within the ore bed. The onset of ferric iron generation was slower at 2 L/m^2.h, commencing at 10 days, corresponding to the lag in the redox potential. The peak ferrous iron concentration was higher (~0.3g/L) at 2 L/m^2.h than for the other flow conditions (0.24 and 0.15 g/L for 6 and 18 L/m^2.h respectively). The total iron concentration was higher (~0.35 g/L) at 6 L/m^2.h, whilst the concentration at 2 and 18 L/m^2.h fluctuated around 0.25 and 0.17 g/L respectively. The trends in run 3 were similar. However, they were not as obvious due to the fluctuations in the data. The increased fluctuation could be attributed to the fluctuating pH as a result of acid consumption which could have caused the precipitation of iron. The total iron concentration values are lower than the feed concentration of 0.5 g/L, which further suggests the occurrence of iron accumulation and precipitation within the systems. Slight increases in the ferrous iron concentration were observed after in-bed sampling of the high flow system (18 L/m^2.h), indicative of the slight sensitivity of the system to the in-bed sampling procedure at high irrigation rates. The presence of ferric iron, shown by the difference between the total and ferrous iron concentrations, verified the presence of microbial activity within the heap systems.

4.4.4 *Microbial Colonisation*

The development of the microbial species during the initial period of colonisation is presented in this section. The in-bed sampling technique used allowed for the quantification of the microbial community associated with the mineral ore bed as a function of time, following inoculation and subsequent colonisation. The differentiation of the microbial phase present within the heap is first discussed, followed by the results of the microbial analysis of the leachate and then the results of the in-bed ore sampling analysis.

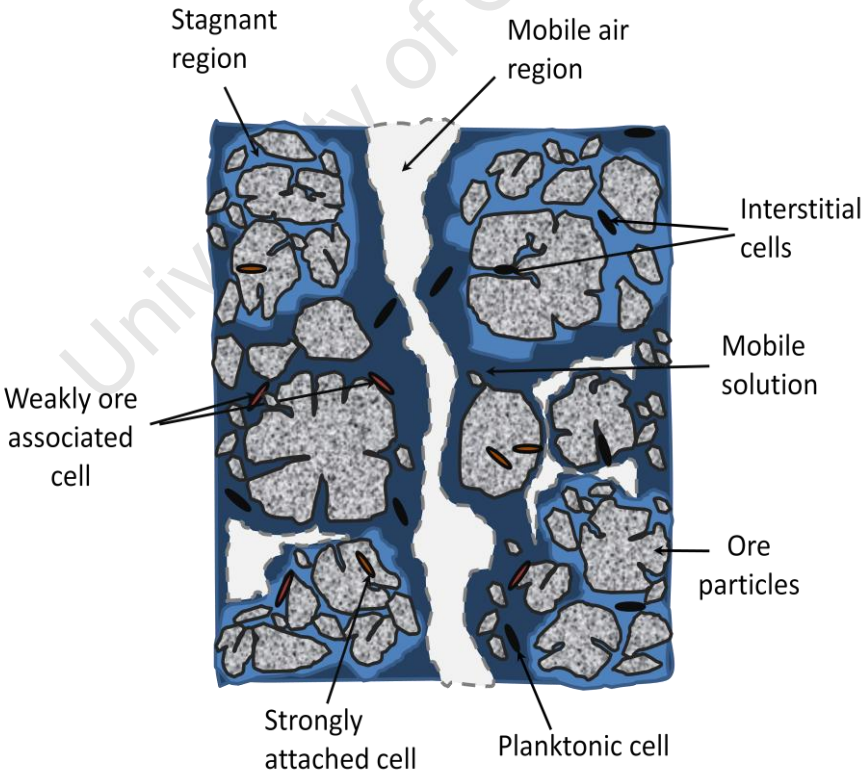

Figure 4-14: Schematic of the inside of the heap, showing planktonic cells in the flowing mobile liquid phase, microorganisms weakly and strongly associated with the ore surfaces, and microorganisms accumulating within the stagnant regions of the porous rocks.

The microbes present within the heap system can be differentiated into three categories, illustrated in Figure 4-14. The first category is the attached population, which contains micro-organisms which are either loosely attached to the mineral surfaces in response to surface interactions or micro-organisms which are strongly attached after initial adhesion to the surface by electrostatic forces followed by the formation of an EPS biofilm which mediates and strengthens the bond to the mineral surface (van Loosdrecht *et al*., 1990; Ghauri *et al.*, 2007; Rodriguez *et al.* 2003). The microbial phase, known as the planktonic phase, comprises micro-organisms in the flowing liquid phase that are readily recovered to the effluent stream (PLS). A third category of micro-organisms accumulate within the stagnant fluid zones and pore spaces and are referred to as interstitial cells. Colonisation studies have not yet distinguished these categories effectively, dealing with only the combined ore-associated population and the planktonic cells. Interstitial cells may be expected to be divided between these conventional categories, with the majority being quantified with the ore-associated fraction and labelled as "attached".

Table 4-5: Total cumulative exported cells after 32 days leaching for runs 2 and 3, and the preliminary run 1.

	Cells ($x10^{10}$)		
Irrigation rate ($L/m^2.h$)	2	6	18
Run 1	1.1	5.7	22
Run 2	2.2	6.5	7.0
Run 3	1.2	4.2	5.9

The planktonic cells present in the free-flowing liquid are exported from the heap systems via pregnant leach solution. Figure 4-15 (a) and (b) shows the cumulative planktonic cells leaving the ore bed in the PLS over time, at irrigation rates of 2, 6 and 18 $L/m^2.h$, during replicate runs. Due to the low detection limit of the microscopic cell counting technique ($3x10^5$ cells/ml), no cells were detectable in the eluted solution during the first 8 days of leaching. This could also be attributed to the cell attachment to the ore followed by a period of low growth in which the microorganisms adapted to the new heap leaching environment. Microbial cells were detected in the eluted leachate on day 8 at an average concentration of ~$1.0x10^6$cells/ml in both runs (see cell concentration data in Appendix D). Thereafter an increase in cell number exported from the columns was observed, corresponding to the increased redox potential showing microbial growth within the systems. The microbial cell concentrations in the PLS from all three columns fluctuated, with maximum cell concentrations reaching $6.0x10^6$ cells/ml (2 $L/m^2.h$), $3.8x10^6$ cells/ml (6 $L/m^2.h$) and $3x10^6$ cells/ml (18 $L/m^2.h$) during run 2, and $5.4x10^6$ cells/ml (2 $L/m^2.h$), $3.5x10^6$ cells/ml (6 $L/m^2.h$) and $2.5x10^6$ cells/ml (18 $L/m^2.h$) during run 3 (data shown in Appendix D). After 32 days of leaching during run 2, high cell exportation from the column was observed for 6 and 18 $L/m^2.h$ removing approximately $6.5x10^{10}$ and $7.0x10^{10}$ cells respectively, compared to $2.2x10^{10}$ cells at 2 $L/m^2.h$, with the propagated cumulative error being < 25 %. The larger cell removal at the higher flow conditions could be attributed to the detachment of cells as a consequence of the greater shear stress induced, suggesting a lower colonisation of the heap at higher irrigation rates. In this data, there was little variation between the planktonic cell data for irrigation rates of 6 and 18 $L/m^2.h$. However, the preliminary and replicate runs showed higher cell removal from the column for high flow (18 $L/m^2.h$) with run 3 showing a total of $2.2x10^{11}$ cells exported after 32 days leaching, compared to $1.1x10^{10}$ and $5.7x10^{10}$ cells for 2 and 6 $L/m^2.h$ respectively (Table 4-5).

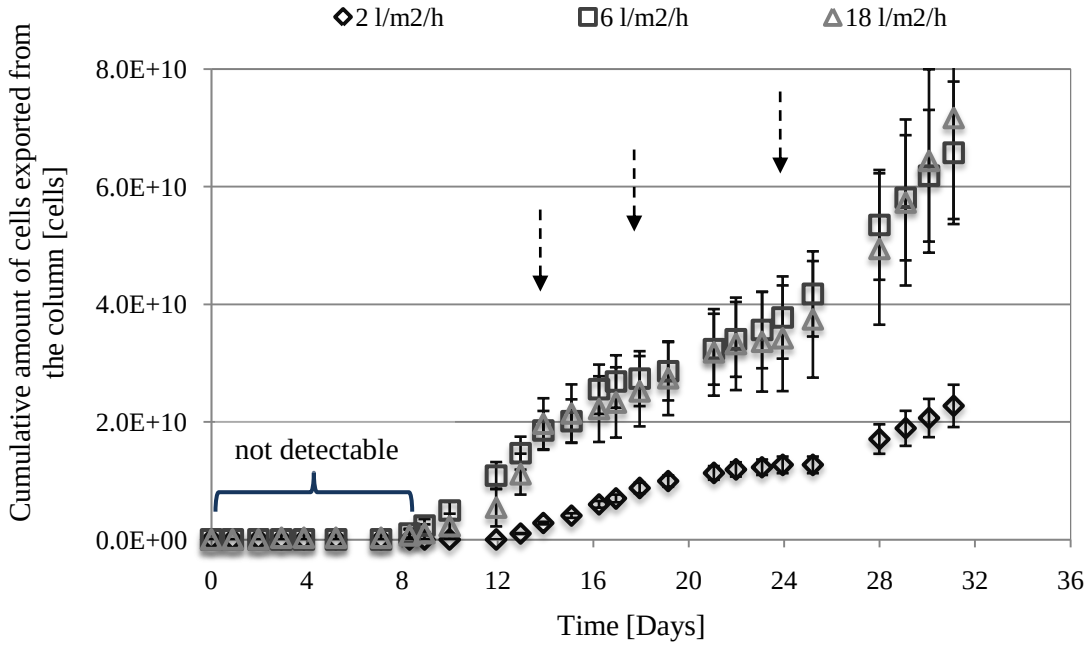

(a) Run 2

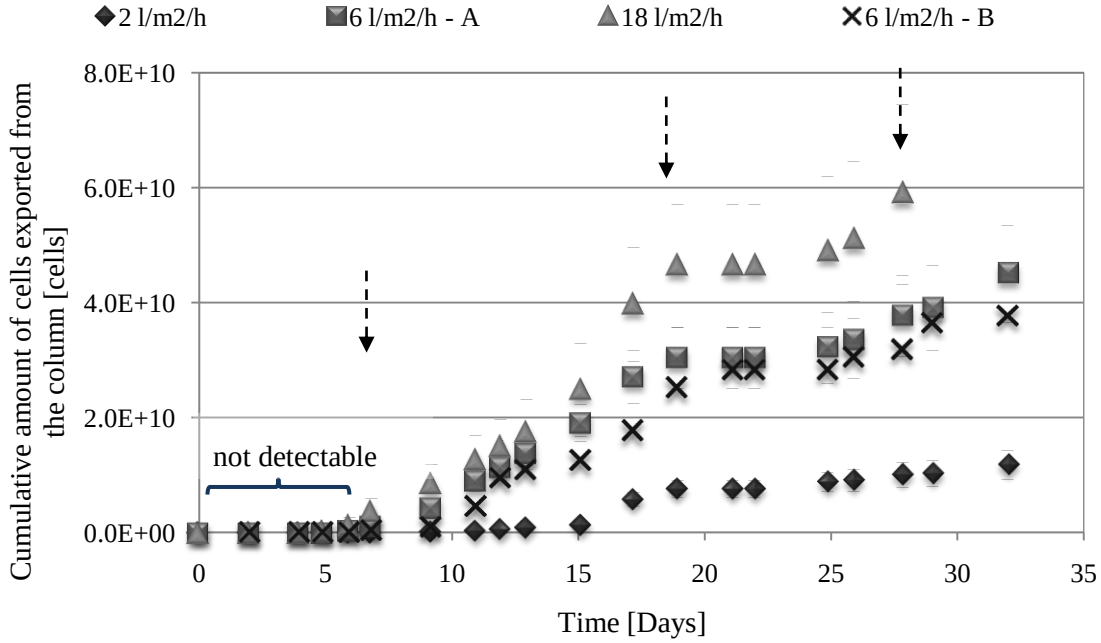

(b) Run 3

Figure 4-15: Cumulative removal of microbial cells in column effluent during the bioleaching of low grade copper bearing ore, given for experimental (a) run 2 at irrigation rates ◊ - 2 L/m^2.h, □ - 6 L/m^2.h and Δ - 18 L/m^2.h, and (b) run 3 at irrigation rates ♦ - 2 L/m^2.h, ■ - 6 L/m^2.h – A, x - 6 L/m^2.h – B and ▲ - 18 L/m^2.h. Error bars represent the propagated error determined from the standard deviation of the mean cell count within each experimental run. Arrows are indicative of in-bed sampling days.

Figure 4-16 (a) and (b) show the growth curve of the ore-associated cells determined by in-bed sampling and detachment during the leach runs, at irrigation rates of 2, 6 and 18 L/m^2.h, during replicate runs. The error bars for each experimental run present the standard deviation across triplicate cell counts as a percentage of the mean.

Increased accumulation of microbes within the systems was observed over the leaching period, under all flow conditions resulting in final concentrations of ore associated cells of $4.3x10^{13}$ (2 L/m^2.h), $3.0x10^{13}$ (6 L/m^2.h) and $2.0x10^{13}$ (18 L/m^2.h) cells/ton ore remaining in the columns after 32 leaching days during run 2 and $4.3x10^{13}$ (2 L/m^2.h), $4.7x10^{13}$ (6 L/m^2.h) and $2.4x10^{13}$ (18 L/m^2.h) cells/ton ore during run 3. The final cell concentration at 2 L/m^2.h was the same across run 2 and 3. The final concentration at 6 L/m^2.h was higher during run 3 than run 2. Both runs showed lower cell counts at 18 L/m^2.h. Inversely, a greater number of ore associated bacteria accumulated in the systems under low flow conditions (2 and 6 L/m^2.h). The preliminary run was longer than runs 2 and 3 (50 days) therefore the final cell concentrations observed were higher.

The specific growth rates for the ore-associated cells, obtained from the gradient of ln(X) as a function of time are shown in Table 4-6. The microbial growth rates determined for 2 and 6 L/m^2.h are equal, with average rates of 0.0053 and 0.0052 h^{-1} respectively. The growth rate at 18 L/m^2.h was lower (0.0043 h^{-1}) by 18%. No in-bed sampling was conducted in run 1; therefore the growth rates obtained cannot be related to the preliminary run.

Table 4-6: Growth rates (μ^{max} = bacterial specific growth rate [h^{-1}]) calculated based on the ore-associated microbial population within the columns

Condition [L/m^2.h]	μ^{max} [h^{-1}] determined based on ore-associated ore population		
	Run 2	Run 3A/B	Average
2	0.0055	0.0051	0.0053
6	0.0052	0.0054/51	0.0052
18	0.0043	0.0043	0.0043

Comparison of the growth rate data to previously published literature, presented in Table 2-3, showed microbial growth in the column study to be low. Growth kinetics investigations carried out in continuous culture reported growth rates ranging from 0.038 to 0.119 h^{-1} for experiments conducted with temperatures varying from 30 to 40°C and pH from 1.1 to 1.7, using a mixed culture of mesophilic bacteria under conditions typical of a *Leptospirillum* dominated culture (Breed and Hansford, 1999; Dempers *et al.,* 2003). Further growth kinetics studies conducted under optimal batch shake flask conditions indicated growth rates ranging from 0.046 to 0.19 h^{-1} (Karavaiko *et al.,* 2006). Further unpublished growth rates on whole ore suggest specific growth rates of the mesophiles in the range 0.01 to 0.08 h^{-1} (Minnaar *et al*. 2010). The growth rates determined in this study are less than 15% of those reported by Breed and Hansford (1999), Dempers *et al.* (2003) and Karavaiko *et al.* (2006). Additionally, the growth rates are approximately 50% of the lower rates demonstrated on whole ore using qPCR to quantify cell growth (Minnaar *et al*. 2010), showing a clear difference in microbial growth within the various leaching environments. Further it is recognised that by neglecting the planktonic cells the growth rate may be underestimated. However, the relative proportions suggest that this error should be less than 20%. The use of the Monod kinetic model has limitations when determining growth rates of multiple species in actual heap systems as one has to account for the

attachment and accumulation of micro-organisms within the system, as well as the detachment and washout of planktonic cells during the leaching process.

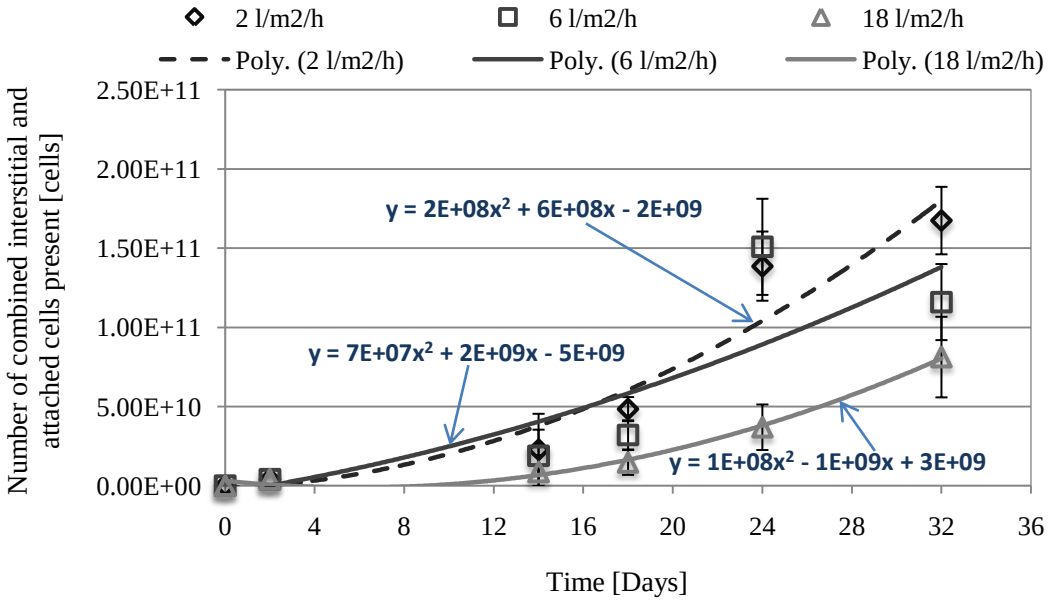

(a) Run 2

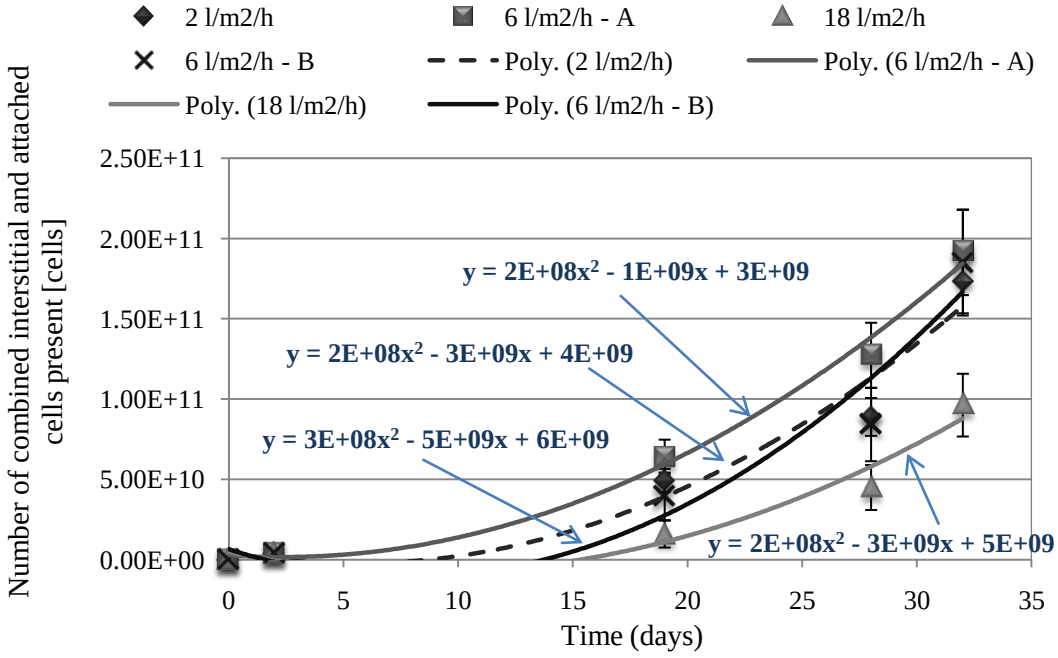

(b) Run 3

Figure 4-16: Microbial growth curve obtained by combining the interstitial and attached cells accumulated in the ore bodies, determined from the mechanical detachment of cells from the ore samples periodically removed from the heap systems using the in-bed sampling technique, given for experimental (a) run 2 at irrigation rates ◊ - 2 L/m^2.h, □ - 6 L/m^2.h and Δ - 18 L/m^2.h, and (b) run 3 at irrigation rates ♦ - 2 L/m^2.h, ■ - 6 L/m^2.h – A, x - 6 L/m^2.h – B and ▲ - 18 L/m^2.h. Error bars represent the standard deviation of the ore-associated cell counts. The 'poly.' lines were generated in excel using the trendline option for polynomials of order 2.

Figure 4-17 shows the progression of the microbial growth whilst identifying the difference between the exported planktonic cells (accumulated within the time intervals between the in-bed sampling points), interstitial and attached cells during leach runs 2 and 3, at an irrigation rate of 6 L/m^2.h. The data was obtained from the microscopic analysis of the cells mechanically detached from the ore extracted using the in-bed ore sampler. Increased bacterial adherence to the ore was observed over the 32 day leaching period across the runs with the exception of run 2. In run 2 the total cell count increased to a peak (1.6 x10^{11} cells) and then decreased slightly to (1.4 x10^{11} cells). This difference could be attributed to the error introduced at each analysis stage i.e. from the in-bed sampling procedure, detachment protocol and microscopic cell counting limitations. Increasing cell numbers in stagnant fluid were also observed. The interstitial cells were the most dominant form of cells accumulated within the heap systems (58 %), compared to 20 % exported (in the interval between 24 to 32 days) and 22 % attached cells after 32 days leaching. Where data are considered over the whole time period, 17.6 % were attached, 46.2 % in the interstitial phase and the remaining 36.2 % eluted from the column over the overall time period during run 2, and 26.9 % were attached, 54.1 % interstitial cells and 19 % planktonic cells over the overall time period during run 3.

Figure 4-18 shows the progression of the microbial growth and the relative proportions of exported planktonic cells, interstitial and attached cells at the three irrigation rates, during run 2 (similar data for run 3 can be found in Appendix D). Increasing bacterial association with the ore, i.e. attachment, was observed over the 32 day leaching period for 2 and 18 L/m^2.h, with a slight decrease at the end for 6 L/m^2.h. A greater number of bacteria adhere to ore under low flow conditions (2 and 6 L/m^2.h), due to reduced detachment of microorganisms by the fluid shear and slower exportation of microorganisms from the systems, providing greater time for initial attachment (Lizama *et al*., 2005). Higher attachment of microorganisms to the ore at low flow rates could also be a response to nutrient and ferrous iron limitations due to the low availability as a consequence of slower supply to the system. Increased cell numbers in stagnant fluid were also observed. Cell balances over the systems are shown in Table 4-7 and Table 4-8. For 2 and 6 L/m^2.h, the interstitial cells were the most dominant form of cells accumulated within the heap systems. The interstitial cell were not dominant at high flow (18 L/m^2.h) because of the high exportation of cells that was observed.

Table 4-7: Cell balance over the 3 flow systems during leaching run 2 at day 32

	Irrigation rate [L/m^2.h]		
	2	6	18
Inoculated [cells]	4.00E+09	4.00E+09	4.00E+09
Total planktonic [cells]	2.27E+10	6.57E+10	7.17E+10
Total interstitial [cells]	9.94E+10	8.40E+10	6.13E+10
Total attached [cells]	6.80E+10	3.19E+10	1.98E+10
Total cells [cells]	1.90E+11	1.82E+11	1.53E+11
% planktonic	**12.0**	**36.2**	**46.9**
% interstitial	**52.3**	**46.2**	**40.1**
% attached	**35.8**	**17.6**	**13.0**

(a)

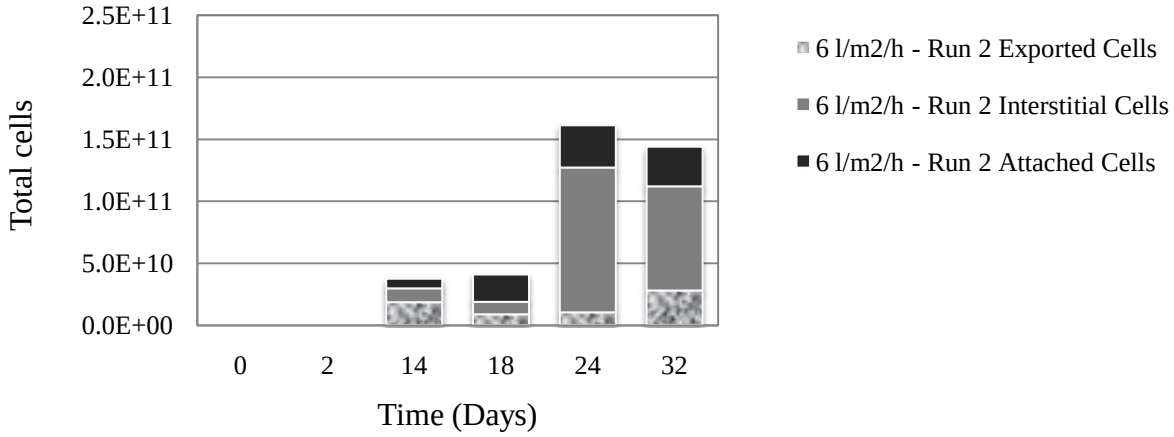

(b)

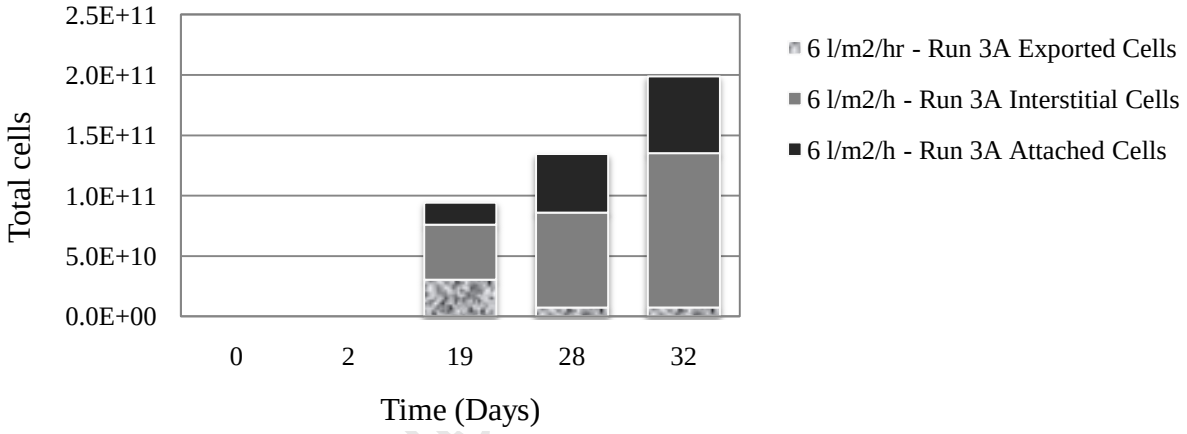

(c)

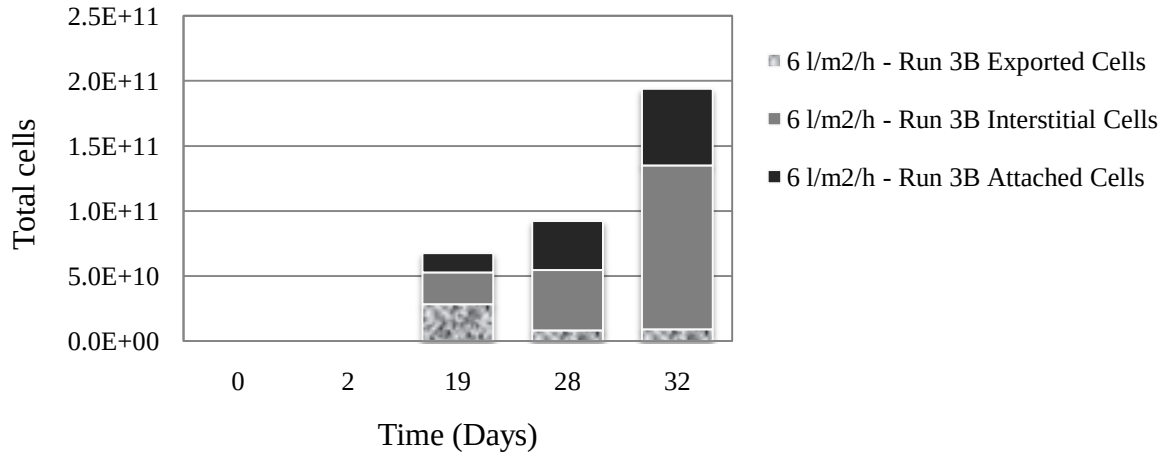

Figure 4-17: Comparison of planktonic cells (removed within each time period), interstitial, and attached microorganisms present in the column reactors, determined from the mechanical detachment of cells from the ore samples periodically removed from the heap systems using the in-bed sampling technique, given for replicate runs (a) Run 2 (b) Run 3A and (c) Run 3B, at an irrigation rate of 6 L/m^2.h.

(a)

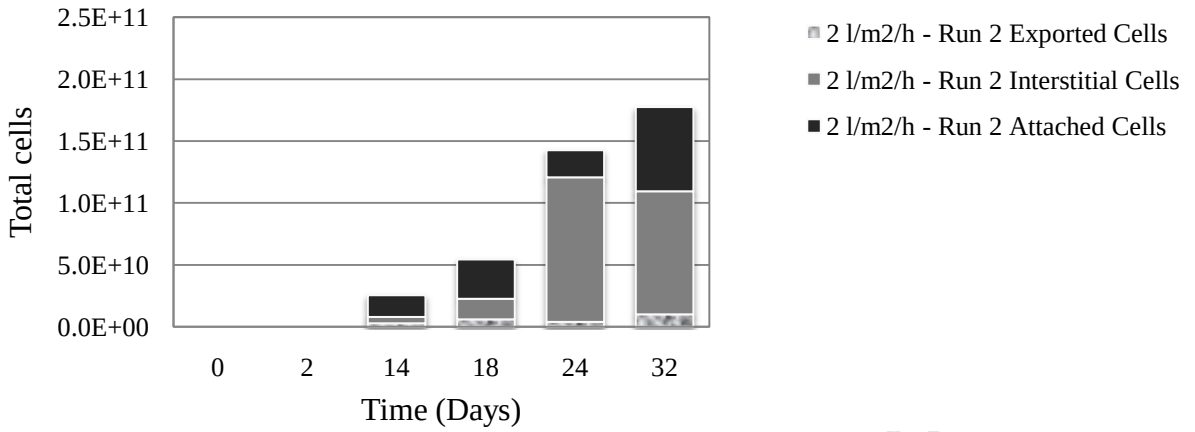

(b)

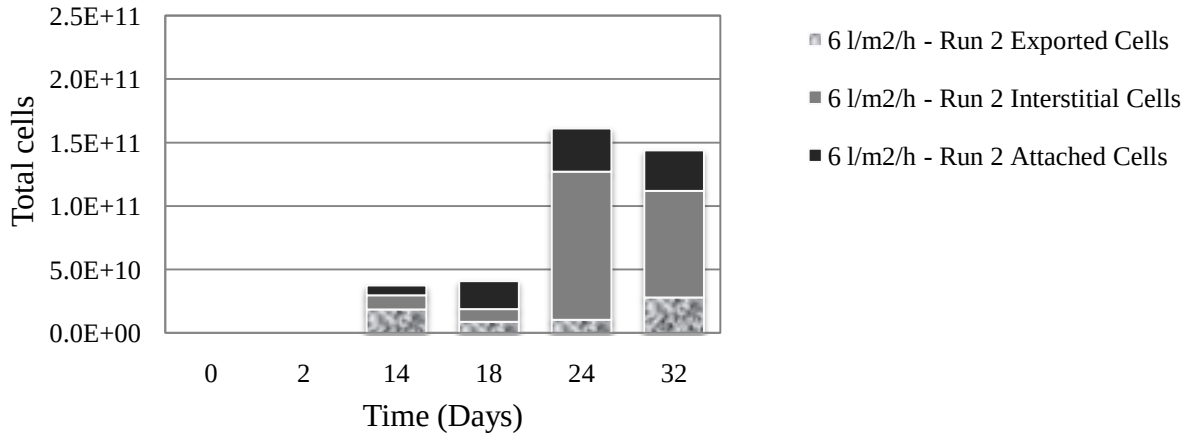

(c)

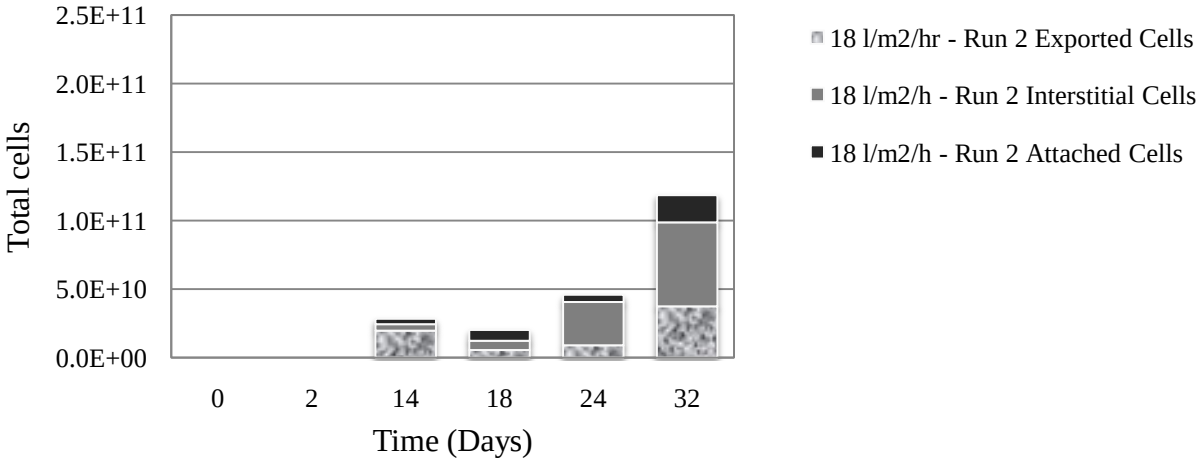

Figure 4-18: Microbial attachment to the low grade copper bearing ore body in the column reactors, determined from the mechanical detachment of cells from the ore samples periodically removed from the heap systems using the in-bed sampling technique, given for different irrigation rates 2, 6 and L/m^2.h for run 2.

Table 4-8: Cell balance over the 3 flow systems during leaching run 3 at day 32

	Irrigation rate [L/m^2.h]			
	2	6	6 rpt	18
Inoculated [cells]	4.00E+09	4.00E+09	4.00E+09	4.00E+09
Total planktonic [cells]	1.18E+10	4.50E+10	4.55E+10	5.88E+10
Total interstitial [cells]	1.13E+11	1.28E+11	1.26E+11	7.29E+10
Total attached [cells]	6.02E+10	6.35E+10	5.89E+10	2.32E+10
Total cells [cells]	1.85E+11	2.36E+11	2.30E+11	1.55E+11
% planktonic	**6.4**	**19.0**	**19.7**	**38.0**
% interstitial	**61.0**	**54.1**	**54.7**	**47.0**
% attached	**32.6**	**26.9**	**25.6**	**15.0**

4.4.5 *Reproducibility of Experiment*

The reproducibility of the colonisation experiment was evaluated by comparison of the growth of the ore-associated bacterial population over repetitive runs under each of the flow conditions. The duplicate or triplicate data sets are presented in Figure 4-19, Figure 4-20, and Figure 4-21. An assessment of the growth curves for each set of conditions showed good reproducibility. The error bars shown represent the standard deviation of the triplicate cell counts for each data point. Note: the in-bed sampling points were different across experimental runs. Hence mean values could not be determined.

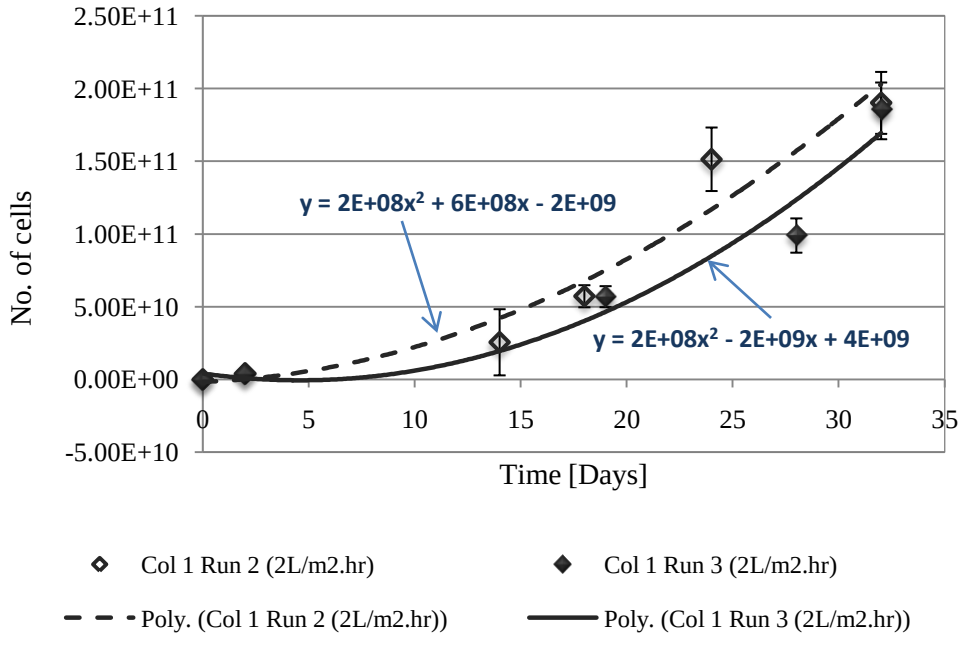

Figure 4-19: Microbial growth curve obtained by combining the interstitial and attached cells accumulated in the ore bodies, determined from the mechanical detachment of cells from the ore samples periodically removed from the heap systems using the in-bed sampling technique, obtained from duplicate experimental runs at 2 L/m^2.h. Error bars represent the standard deviation of the ore-associated cell counts. The 'poly.' lines were generated in excel using the trendline option for polynomials of order 2.

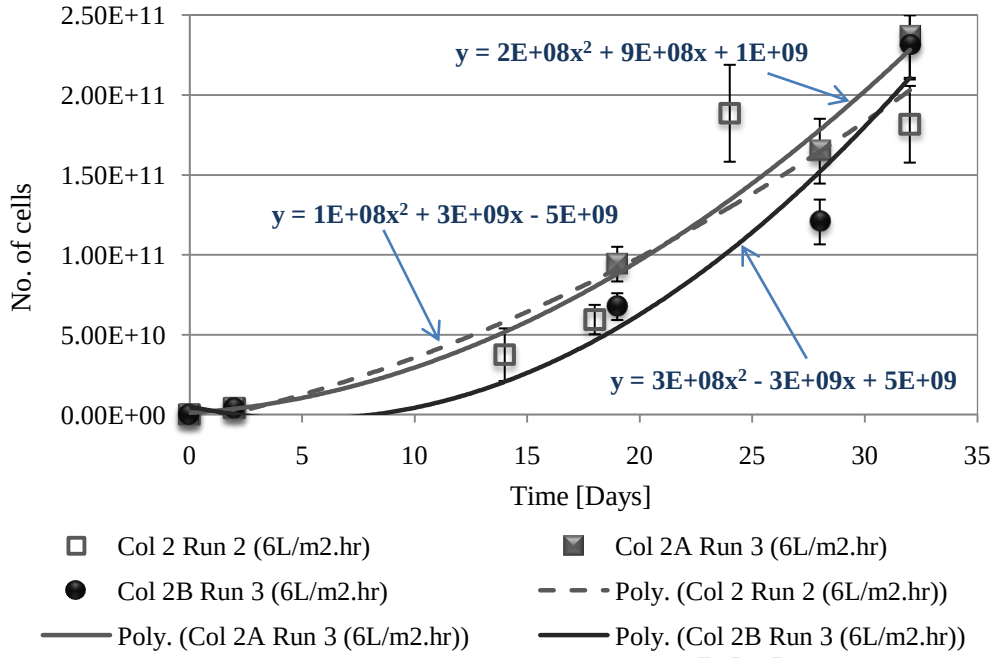

Figure 4-20: Microbial growth curve obtained by combining the interstitial and attached cells accumulated in the ore bodies, determined from the mechanical detachment of cells from the ore samples periodically removed from the heap systems using the in-bed sampling technique, obtained from triplicate experimental runs at 6 L/m^2.h. Error bars represent the standard deviation of the ore-associated cell counts. The 'poly.' lines were generated in excel using the trendline option for polynomials of order 2.

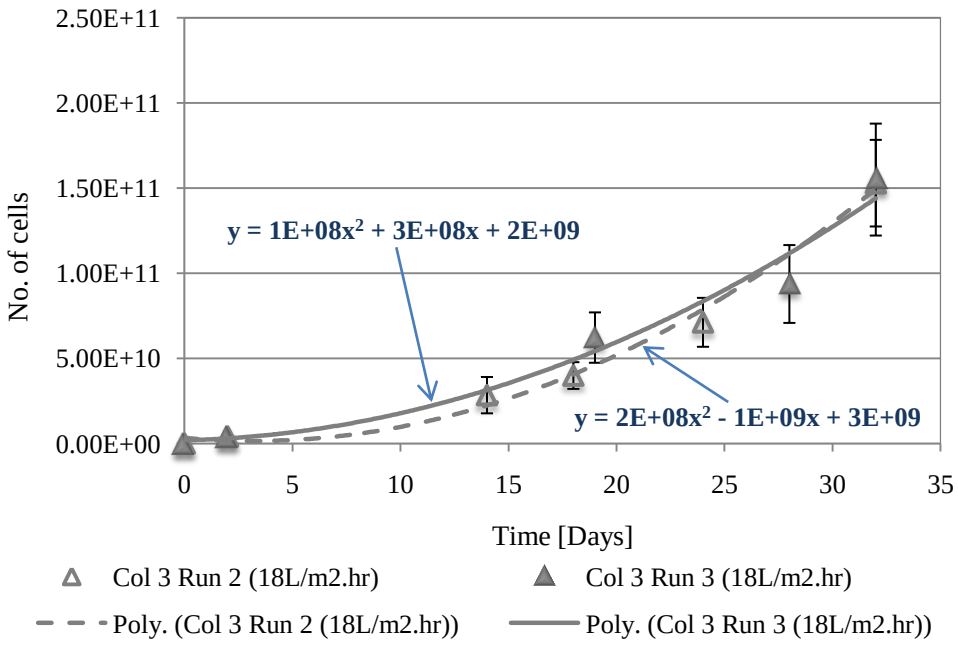

Figure 4-21: Microbial growth curve obtained by combining the interstitial and attached cells accumulated in the ore bodies, determined from the mechanical detachment of cells from the ore samples periodically removed from the heap systems using the in-bed sampling technique, obtained from duplicate experimental runs at 18 L/m^2.h. Error bars represent the standard deviation of the ore-associated cell counts. The 'poly.' lines were generated in excel using the trendline option for polynomials of order 2.

4.5 Discussion and Conclusions

The purpose of the research presented in Chapter 4 was to investigate the effect of irrigation application rates on the growth and accumulation of a mixed mesophilic culture within heap environments, during the bioleaching of low grade copper-bearing mineral ore. To date, the effect of fluid dynamics on the ability of microbial populations to thrive within heap environments has not been considered rigorously. Few investigations have reflected on the effect of irrigation rates on microbial colonisation. Typical industrial irrigation rates employed range from 5 to 20 L/m^2.h (Petersen and Dixon, 2007a). Lizama *et al*. (2005) conducted experiments assessing the influence of irrigation to height ration on microbial growth. Irrigation rates in the region of 1.8 to 21.6 L/m^2.h were used in their experimental studies. The irrigation rates used in the investigation herein were 2, 6 and 18 L/m^2.h, and the study showed that the rate at which micro-organisms multiply and attach to ore in simulated heap bioleaching systems was influenced slightly by the irrigation rate.

The new in-bed sampling technique demonstrated the ability for ore samples to be obtained without significant disruption of the ore bed under low to moderate flow conditions. The data collected from this provided useful information on the relative degrees of attachment of the micro-organisms accumulated within the heap structures. This is the first analysis and report of the data obtained from the in-bed sampling technique. This instrument can also be extrapolated and used to assess colonisation at different heights within the bed of a particular leaching system.

In particular, the enhancement of microbial surface colonisation at lower irrigation rates was observed, as illustrated by the increase in bacterial adherence to the ore surface and interstitial cell numbers with time and with respect to replicate runs. Greater accumulation of cells within the ore bed was observed at low flow. The total quantity of cells retained in the ore bed for an irrigation rate of 18 L/m^2.h was much lower than for the other flows, inferring that under higher flow conditions the detachment and transport of microbial species out of the column affected the microbial growth. Lizama *et al.* (2005) also attributed the low attachment of bacteria to the mineral surface at high flow rates to shorter residence times of solution within the system. Hence the micro-organisms are generally transported through the ore bed without sufficient time to attach to mineral surfaces. Inversely, under low flow conditions, microorganism-ore contact time increased within the leaching system, allowing the cells to form stronger surfaces bonds and remain attached for longer periods. Further, Wan *et al*. (1994) conducted an investigation using glass micro-models of porous systems filled with quartz sand, and reported the relationship between microbial retention rate and gas saturation as directly proportional. Therefore, the preferential sorption of microbes onto the gas-water interface over the solid-water interface should result in higher attachment and colonisation for lower flow rates. This is attributed to the presence of a less liquid saturated system under low flow conditions, as the irrigation rate partially controls the quantity of void space available (Bouffard and West-Sells, 2009). Strong bacterial adhesion to the ore at various irrigation rates ranged from 13 to 36 %.

There was preferential accumulation of the microbes in the stagnant regions over both those in the PLS and on the ore surfaces, as illustrated by the dominant interstitial population. Higher affinity to the interstitial spaces could be attributed to the microbial density of ore-associated micro-organisms reaching maximum capacity given that only monolayer biofilms can be formed (Africa, 2009; Africa *et al.*, 2010). Since the microbial species used were first cultivated on pyrite and then introduced into the low grade ore heap, the relative dominance of interstitial cells over attached could be attributed to the slight influence cultivation conditions have on the ability of cells to attach to mineral surfaces

(Devasia *et al*. 1993). Additionally, the low-grade ore provided a large gangue mineral surface area to which adherence of cells may have been less favourable. Africa *et al*. (2010) reported attachment to sulphide minerals to occur preferentially over gangues. Attachment to gangue minerals was low. This is consistent with Rodriguez *et al*. (2003) showing adhesion to various substrates to be a preferential.

Average specific growth rates of ore-associated micro-organisms, i.e. interstitial and attached, of 0.0053, 0.0052 and 0.0043 h^{-1} were found for 2, 6 and 18 $L/m^2.h$, showing faster colonisation under low flow regimes. Growth rates on whole ore in the column geometry were shown to be significantly lower than those measured in continuous culture studies using ferrous iron as the substrate (Breed and Hansford, 1999; Dempers *et al.,* 2003; Karavaiko *et al.,* 2006) and slightly lower than those reported by Minnaar *et al*., 2010. It is difficult to attain a fair comparison of the growth rates attained with literature because of the differing experimental parameters used, from varied reactor systems, mode of operation, pH, temperature, substrate and ore mineralogy, microbial species employed, and the lack of studies distinguishing between planktonic, interstitial and attached cell growth. Sub-optimal growth conditions were used in this investigation, *i.e*. RT ± 23 °C, therefore the growth rates were expected to be lower than those obtained at conditions specific to the microbial species optimal activity.

The proportion of planktonic cells relative to the total ore-associated community was low for all flow conditions. Despite the increased planktonic cell numbers at high flow (18 $L/m^2.h$), oxidation of ferrous to ferric iron was observed, shown by the low ferrous iron concentrations. This is indicative of the indirect non-contact mechanism in which cells present in the bulk mobile solution were contributing to bioleaching (Devasia *et al*. 1993; Tributsch, 2001; Sand and Gehrke, 2006). Similarly the microbes which were attached to the ore may have been able to form an EPS biofilm which helped to mediate the ferric ion regeneration via the indirect contact mechanism (Tributsch, 2001). Consequently, the interstitial cells present, due to the stagnant regions and the exchange between planktonic and ore-associated cells, also contribute to mineral dissolution. The relative dominance of cells within the interstitial phase could be an indication that ferrous ion oxidation occurs mainly via the activity of micro-organisms suspended within these regions. This may be an indication of the co-operative leaching mechanism in which the planktonic, interstitial and attached microbes synergistically work together to create an environment conducive to mineral dissolution (Tributsch, 2001). The preliminary study showed that *L. ferriphilum* was the dominant species accumulating within the interstitial phase, followed by some growth of *At. caldus* over the leaching period. Therefore the oxidation of ferrous to ferric ion by *L. ferriphilum* could have been complemented by the oxidation of sulphur compounds by *At. caldus* (Schippers, 2007).

The solution chemistry may have also had an effect on the cell attachment. The greater proportion of ore-associated cells than the mobile planktonic proportion could be due to the low ferrous iron concentration in solution causing the cells to move along chemical gradients in search of regions with high ferrous iron accumulation (Rossi, 1990; van Loosdrecht *et al*., 1990).

The supply of ferrous iron and acid to the system were determined to be factors which influenced the low flow system (2 $L/m^2.h$). The slow pH stabilisation at low flow conditions was characterised by the pH profiles which indicated that the pH was higher at 2 $L/m^2.h$ than for the other irrigation conditions. This could be attributed to acid consumption via gangue dissolution occurring at a faster rate than the delivery of acid to the leaching environment at low flow conditions and the microbially assisted acid regeneration. Mass transfer limitation was also responsible for the slower rate of ferric iron generation at 2 $L/m^2.h$, which is a function of the delivery of nutrients (Fe^{2+}) to within the vicinity of active

micro-organisms within the leaching environment. Additionally, the slower oxidation of ferrous iron at 2 L/m^2.h observed could be related to Du Plessis *et al*'s (2007) statement that reduced irrigation rates may cause increased gradient effects, resulting in the accumulation of soluble salts and the development of high osmotic potential which has a detrimental impact on microbial activity.

Theory suggested that a well colonised heap will result more efficient leaching rates. Since better colonisation of the heap was observed under low flow conditions the bioleaching capabilities should have been more evident than for 18 L/m^2.h. However, the data obtained contradicted this phenomenon, implying that parameters other than the degree of colonisation were limiting factors. Hence, there must be a threshold at which the degree of bioleaching is independent of the degree of colonisation. Colonisation should play an even greater role within a higher temperature regime. Since the irrigation rates are varied, the differences in Cu extraction can be linked to the differing acid, ferrous and ferric iron volumetric loading rates. Additionally, higher Cu concentrations in the leachate under low flow could result in easier Cu recovery from solution by solvent extraction and electro-winning processes.

5 CHAPTER 5: PROPAGATION OF MICRO-ORGANISMS FROM A POINT SOURCE

5.1 Introduction

The experimental investigation presented in the Chapter 4 showed that attachment and subsequent colonisation of the heap systems was dependent on the irrigation rates and thus flow regime employed. The flow dynamics within heap environments affects the attachment and colonisation process because the propagation of micro-organisms through the heap to sites within the vicinity of the mineral surface is a function of the convective transport caused by fluid flow (Rossi, 1990; van Loosdrecht *et al*., 1990).

The transportation of solutes and micro-organisms through the porous media is governed by the hydraulic and geochemical properties of the heap (Decker and Tyler, 1999). Transport occurs via several modes: gravity, diffusion, convection and chemotaxis (Rossi, 1990; van Loosdrecht *et al*., 1990). The mechanisms required for initial adhesion of the micro-organisms to the mineral surface such as chemotaxis, Brownian motion, electrostatic attraction and cell surface hydrophobicity are short range and thus only effective when micro-organisms are transported within close proximity of active surface sites (Rossi, 1990).

The transport of micro-organisms within the heap bioleaching environment plays an important role in microbe-mineral contacting and subsequent adhesion to the ore surface. To enhance attachment and colonisation of ore surfaces, research should focus on promoting the transport and propagation of the micro-organisms through the heap in search of preferential conditions and active sites on the mineral surfaces. Hydrology and soil engineering investigations (Thullner *et al*., 2002; Yarwood *et al*., 2006; Seitert and Engesgaard, 2007; Thullner, 2010) have studied the relationship between fluid flow and suggested significant interactions between microbial colonisation and fluid flow in porous systems. To date, such investigations have been overlooked within the bioleaching space. The study presented in this section aimed to address this. The results and discussion of the preliminary experiment conducted to assess the propagation of micro-organisms through the box heap system in relation to the distribution of solution from a single point source of irrigation. A brief outline of the experiment was provided in Section 5.2.

5.2 Experimental Approach

This experiment was a preliminary study conducted to establish the likely trends that occur within heaps systems with regards to the changing moisture content and the propagation of micro-organisms through a porous ore bed. This data will provide a basic quantification of impact of solution flow channels on transport of the micro-organisms within the heap.

5.2.1 *Experimental procedure*

A more detailed experimental approach is provided in Section 3.6. The experiment was conducted in a large box reactor system described in Chapter 3. The box was packed with 132 kg of ore using an irrigation rate of 6 L/m^2.h, whilst being aerated at 1.75 L/min. The irrigation feed composition used is presented in Chapter 3.

The ore bed was acid washed for 26 days to establish fluid flow, decrease the pH of the system to close within the range of the specification (pH 1.15), to remove inhibitory substances and create an environment conducive to microbial attachment to the ore surface. The box was inoculated on day 27

with 10^{12} cells/ton of ore using a mesophilic stock culture containing *At. caldus, At. ferrooxidans, At. thiooxidans* and predominantly *L. ferriphilum*.

The experiment ran for 83 days with periodic monitoring of the effluent collected in the 13 bottom ports. Daily analyses were conducted where possible. The effluent collected was analysed daily.

The ore bed was divided into 9 sampling zones as outlined in Figure 3-5 and Figure 3-6, from which 20 g ore samples were removed (using tweezers) at intervals during the leaching process, i.e. day 24, 49, 63 and 83. The ore samples collected from each of the 9 zones were analysed for moisture content to give an indication of the solution distribution with the ore bed. This was determined by drying the ore samples in the 80°C oven over a 24 hr period. The cells present in the ore samples were mechanically detached using the protocol developed by Bryan *et al.* (2011). The cell densities within the interstitial, loosely and strongly attached phases were determined.

5.3 Results and Discussion of Microbial Propagation

5.3.1 *Solution Flow and Moisture Content*

The total effluent flow rate out of the box system as a function of time is presented in Figure 5-1. The outlet flow rate fluctuated during the course of the experimental run. The dips in the profile correspond to either the feed reservoir running out or the tubing being blocked by precipitates. The evaporation rate calculated was approximately 15 ml/h which translates to 4.2% of feed rate of 360 ml/h.

The trend in effluent flow out of the 13 different ports is presented in Figure 5-2. Again, the flow rate fluctuated during the leaching period, partially a consequence of the changing solution flow channels. The majority of the solution flowing out was collected in the first six ports (average of 97.7 %), showing some lateral distribution from the point source. Solution flowed preferentially out port 5, accounting for approximately 62 % of the total flow.

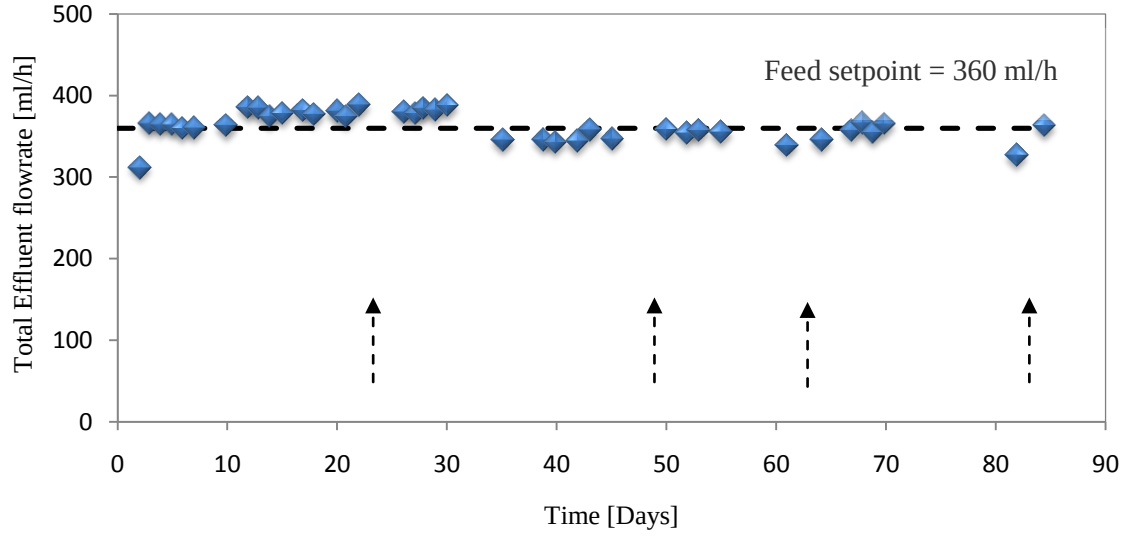

Figure 5-1: Total effluent flow rate profile as a function of time during the bioleaching of low grade copper-bearing ore in a box reactor, at an irrigation rate of 6 l/m^2/h, corresponding to 360 ml/h. The arrows are indicative of the in-bed sampling points.

(a) High flow

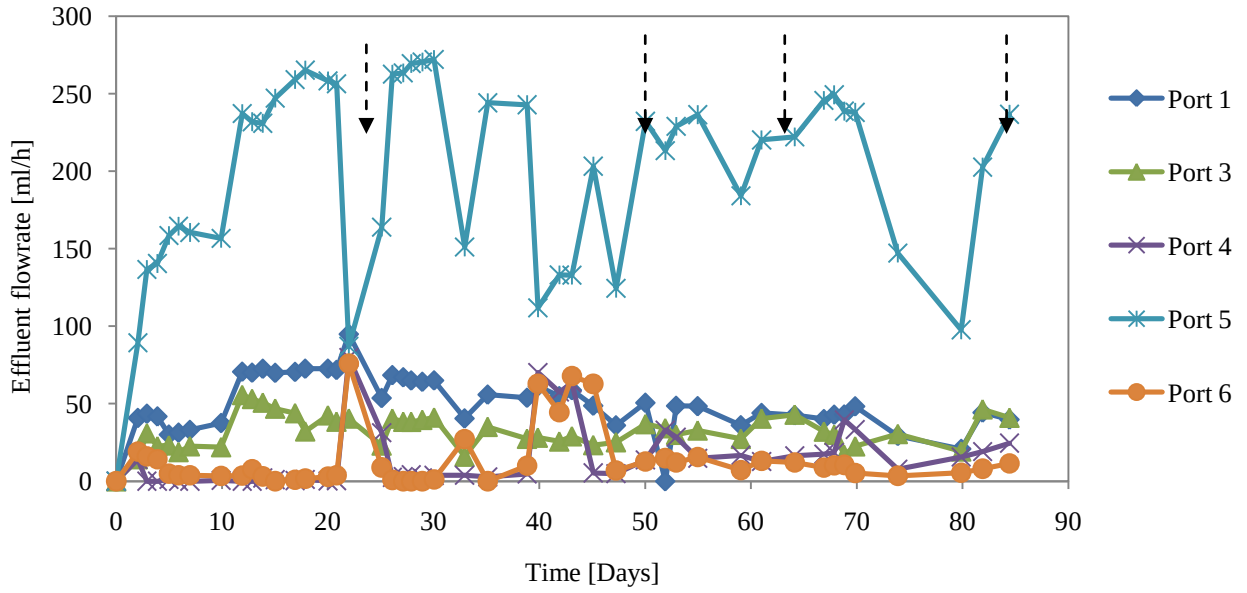

(b) Low flow

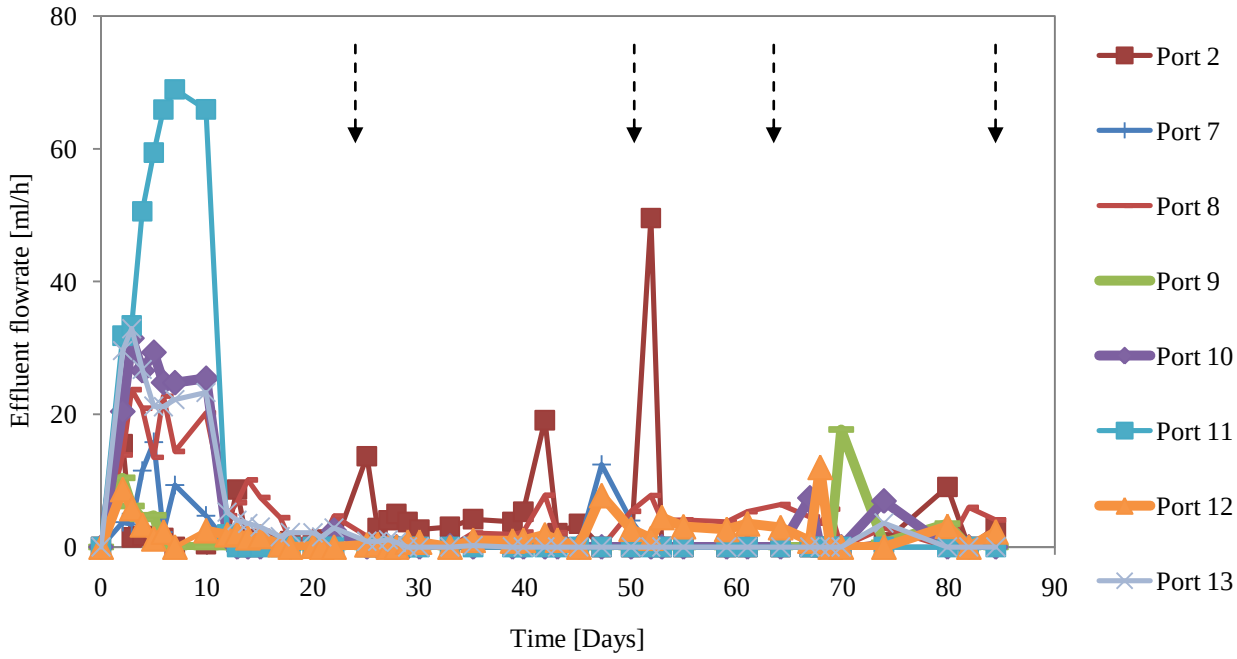

Figure 5-2: Profile of fluctuating effluent flow rates during the bioleaching of low grade copper bearing ore in a box reactor, given for each of the 13 outlet ports. The arrows are indicative of in-bed sampling points.

The moisture content of the nine zones in the ore bed determined at intervals during the bioleaching run is displayed in Figures 5-3 and 5-4. The plots were generated in MATLAB®, shown by the code presented in Appendix E. The average moisture content over the box was calculated at each in-bed sampling interval. The small red squares represent the zones whose moisture contents are **not** within the 10 % margin from the average value, whilst the small yellow squares represent the zones that **do not** fall within the 20 % margin.

(a) Day 24

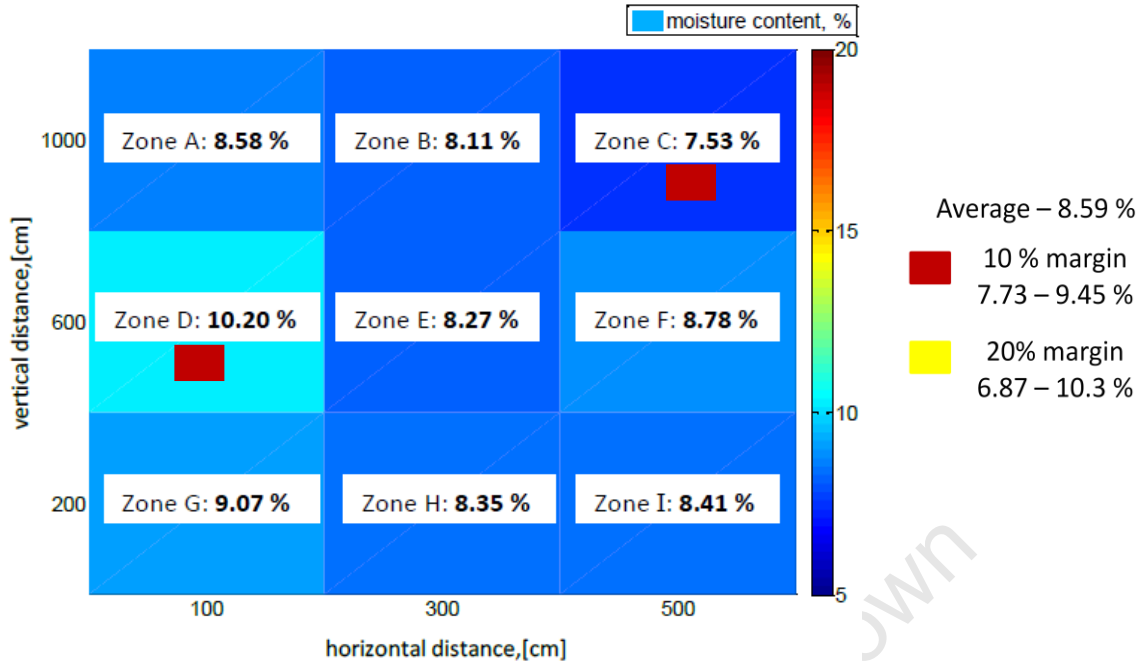

(b) Day 49

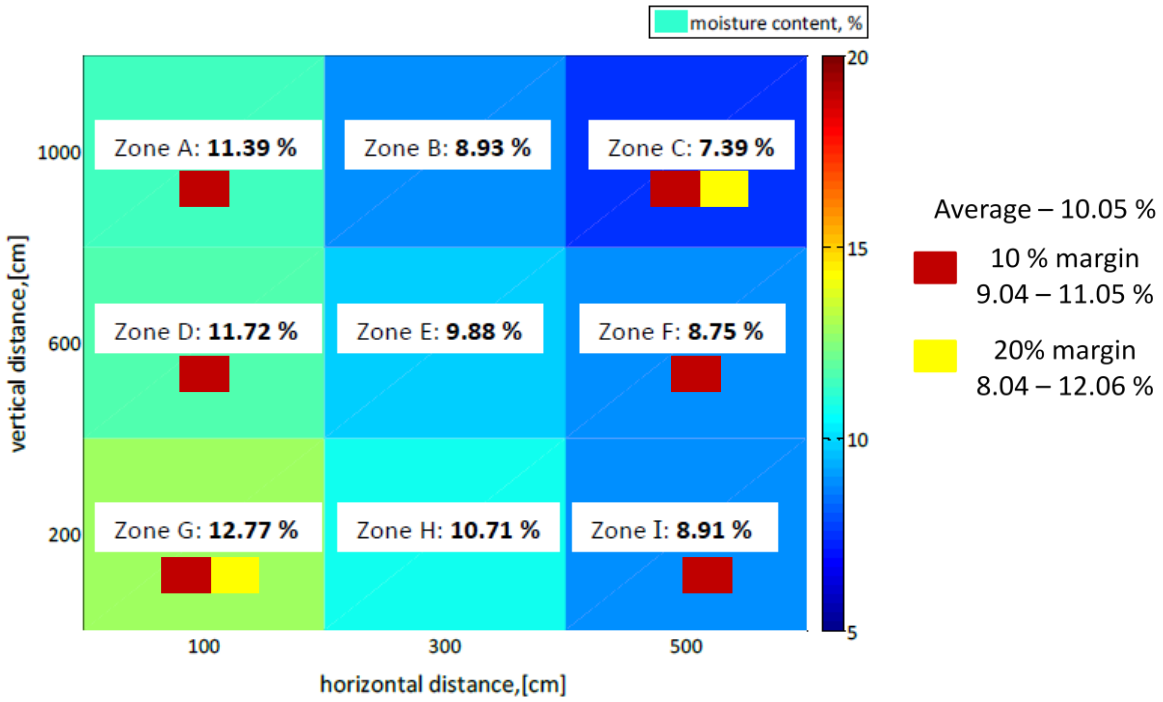

Figure 5-3: Moisture content of the ore bed during leaching, determined from the ore samples periodically removed from the heap systems, given for sampling times (a) day 24 and (b) day 49.

The initial moisture contents of all the zones obtained on day 24 during irrigation from multiple ports ranged from 7.5 to 10.2 %. The average moisture content was 8.6 % with all the zones, except zones C and D, falling within 10 % of the average. During the next 25 days, the moisture content increased for the zones within the first two thirds of the ore bed along the horizontal axis. The moisture contents in the first third were the highest at 11.4, 11.7 and 12.8 % for zones A, D and G respectively, shown by the colour coded matrix in Figure 5-3 (b). The moisture contents in the middle zones had increased slightly to 8.9, 9.9 and 10.7 % for zones B, E and H respectively, whilst moisture contents of the zones

furthest from the point source in the horizontal direction remained within the range of the initial moisture contents at 7.4, 8.8 and 8.9% for zones C, F and I respectively. The average moisture content over the system had increased to 10.1 %. The moisture content in zones A, C, D, F, G and I, did not fall within the 10 % margin as indicated in Figure 5.3 (b). Further, the moisture content in zones G and C fell out of the 20 % margin. Zone G had the highest moisture content on day 49, indicating the movement of fluid downwards, whilst zone C contained the lowest moisture content indicating low lateral fluid movement.

(a) Day 63

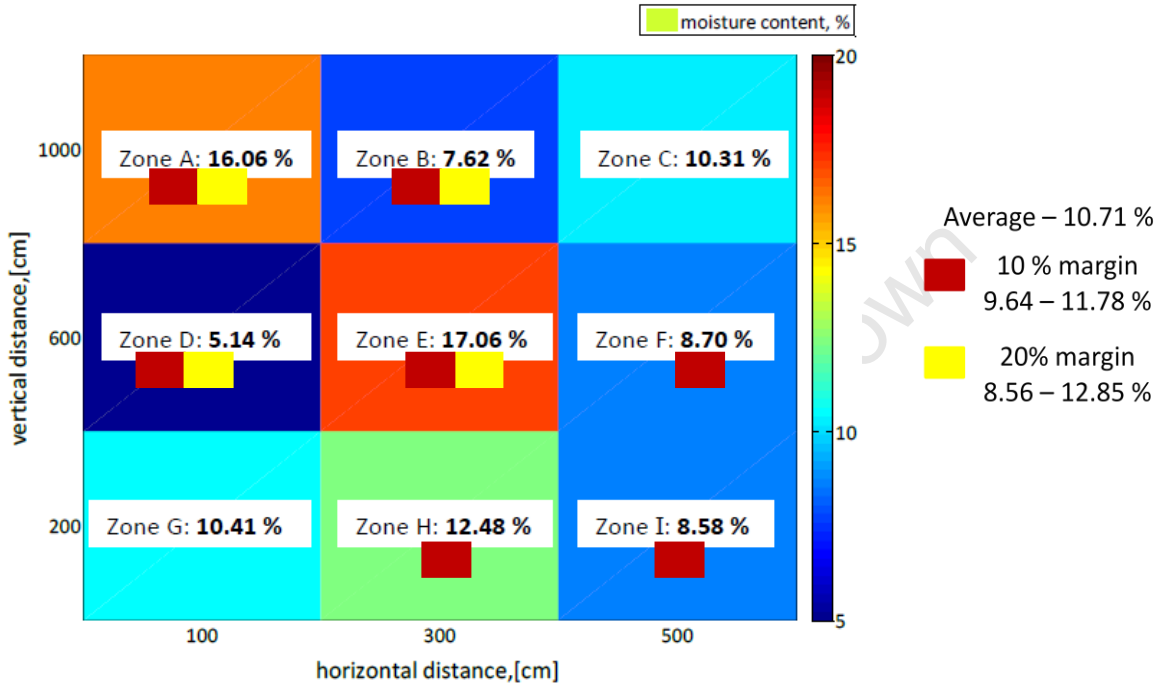

(b) Day 83

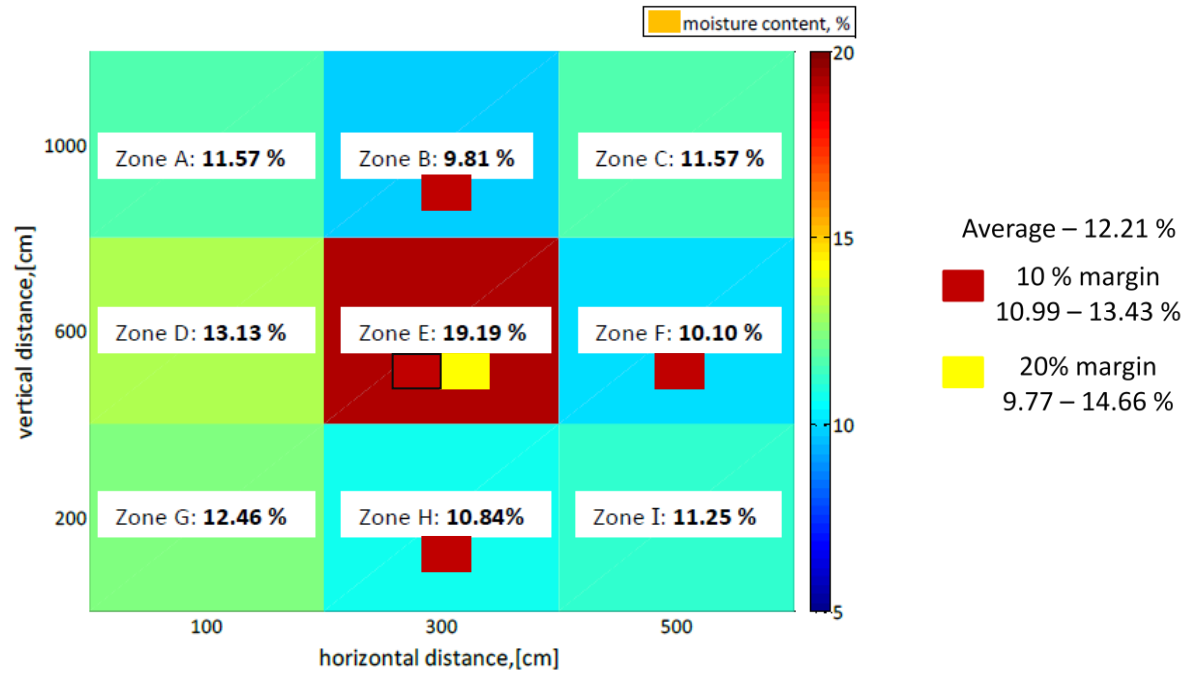

Figure 5-4: Moisture content of the ore bed during leaching, determined from the ore samples periodically removed from the heap systems, given for sampling times (a) day 63 and (b) day 83.

On day 63, the average moisture content had increased further to 10.7 %. The moisture content in zones C and G were within the 10 % margin, whilst the moisture content in zones F, H, and I were within 20 % of the average moisture content. The highest increases in moisture content were for zones A, E and H to 16.1, 17.1 and 12.5 % respectively, indicating increased wetness of the ore bed and the lateral distribution of fluid within the first two thirds (Figure 5-4 (a)). One anomaly was the moisture content value for zone D on day 63, given as 5.1 %. This value was expected to be higher as solution flow through the outlet ports below this zone was also high. However, the low value may have been due to the changing solution flow paths along the pore network within the box heap.

The saturation of the bed increased further with depth and laterally, shown by the increasing moisture contents colour coded in Figure 5-4 (b), corresponding the lateral and downward expansion of the water saturation observed by Yarwood *et al*., 2006. The moisture contents on day 83 were 11.6, 13.1 and 12.5 % in the first third of the bed closest to the point source *i.e*. zones A, D and G respectively. The middle zones B, E and H had moisture contents of 9.8, 19.2 and 10.8 % respectively. The furthest zones from the point source, zones C, F and I, had moisture contents of 11.6, 10.1 and 11.3 % respectively. These values gave an increased average moisture content of 12.2 %, with the moisture content of all the middle zones falling outside of the 10 % margin. The highest moisture content attained was 19.2 % in zone E.

An increase in the average moisture content over time was evident, shown by the change from 8.6% (day 24) to 10.1 % (day 49) to 10.7 % (day 63) up to 12.2 % (day 83). During the initial wetting of the bed, post day 24, the ore bed was wet evenly. When irrigation from the point source on the left began, the zones on the left (A, D, G) were the wet zones. However, over time there was a shift to the middle and downwards (zones B, E, H). The dry zones started in the right top corner of the box heap, and showed little increase in the moisture content over time. These moisture contents displayed in Figure 5-3 and Figure 5-4 showed that the solution distribution across the bed was non-uniform. This observation confirms the existence of preferential flow paths described by Rossi (1990), Decker and Tyler (1999) and O'kane *et al*. (2000). Consequently, areas of the ore bed will remain partially leached due to the lack of fluid-ore contacting. Assuming this is true for zones B, C and F, an estimated 33% of the ore bed was poorly contacted with solution.

5.3.2 *Bioleaching Performance*

The mineralogy of the low grade copper bearing ore used in the leaching experiment contained 0.69 % copper and 2.95 % iron, i.e. 911 g and 3894 g respectively in 132 kgs. Figure 5-5 (a) and (b) shows the copper concentration profile and the cumulative copper removal as a function of time, given for each of the outlet ports.

Initially, the copper concentrations of the leachate expelled from all the ports were high between days 3 to 7. The concentrations were approximately 1.5, 1.8, 1.6, 1.6, 1.5, 1.6, 1.4, 1.6 1.5, 2.0 and 1.5 g/l for ports 1, 2, 3, 4, 5, 6, 7, 8, 9, 10, 11, 12, and 13. Thereafter the concentrations decrease over time with respect to the available mineral surface contacted by fluid (Figure 5-5 (a)). The concentration in ports 1, 2 and 3 fluctuated for the duration of the leaching period remaining at concentrations below 0.1 g/l. The copper concentration in ports 4 and 5 fluctuated below 0.15 g/l whilst the concentrations in ports 6 and 7 were slightly higher, fluctuating around 0.3 g/l. The concentration of the leachate collected in port 8 fluctuated between 0.5 and 1.3 g/l. The copper concentration in port 12 was the highest on day 20 (0.34 g/l) decreasing gradually to 1.7 g/l on day 39, and further to below 0.4 g/l for the remainder of the leach run. The rest of the ports, i.e. 9, 10, 11 and 13, expelled very low concentrations (~ 0 g/l) of copper post day 30. The ports which expelled the largest volumes of leach

solution were responsible for the extraction of the majority of the copper. The largest quantities of copper were extracted via ports 1, 3, 5, 8 and 11, contributing to 12, 6.5, 48.7, 5.9 and 7.5 % of the extracted copper. Port 5 was accountable for almost 50% of the copper recovered which corresponded to the elution of 62% of the solution flow. The observed effluent colour was a bright blue during the acid-wash stage, followed by a pale blueish green colour which as copper concentrations decreased. Of the available copper, the majority was removed from the box system through ports 1 and 5, eluting 19 and 83 g respectively, giving a combined 58% of the total copper liberated over the first 90 days (Figure 5-5 (b)). Since the copper extraction rate is a function of the available exposed mineral surface contacted by the leach solution (Rossi, 1990), the observed copper removal confirms that most of the fluid-ore contacting took place within the first 2 thirds of the ore bed, i.e. zones A, D, E, G and H.

Figure 5-6 shows the total cumulative % copper liberation as a function of time, giving an indication of the leaching performance of a system irrigated from a single point source. The majority of the copper extraction was achieved during the acid-wash stage. 9.8% of the total copper available in the ore bed was liberated at a rapid rate of 1.30 g/day during the first 10 days, due to the dissolution of the available acid-soluble copper. Thereafter, the copper extraction rate decreased, continuing at a constant rate of 0.14 g/day for the duration of the leaching process to yield 18% extraction after 90 days. The rate and extent of copper extraction is dependent on factors such as the operation temperature regime, solution chemistry, microbial species present, ore mineralogy and the accessibility of leach solution to the exposed mineral surface (Watling, 2008). Typically, of the available copper within the low grade ore, 42 % is chalcocite and 15 % bornite. According to Watling (2008), 40 % of the available chalcocite and bornite is typically recovered during the first 10 days of leaching, along with 80% of the available copper oxides. This coincides with the total copper extracted during the first 10 days (10 %). The ore contains 28.4 % chalcopyrite, which is difficult to leach at such low temperatures (Watling, 2008). These facts, combined with the short leach duration (83 days) and the large proportion of gangue material with which the leach solution was contacted, resulted in the low copper extraction observed.

5.3.1 *Solution Chemistry of Leachate*

Figure 5-7 (a) and (b) show the redox and pH profiles of the eluted leachate as a function of leach time, given the each of 13 outlet ports. The feed solution was at a pH of 1.15. The pH was initially high (> pH 5) due to the water washing of the ore in a preliminary flow experiment. During the acid-wash stage, the pH within the ore bed fell gradually. Thereafter, the pH of the effluent from all outlet ports remained above the feed specification, due to rapid depletion of acid by the gangue material and the ferrous iron oxidation, fluctuating ranging from pH 1.16 to 1.4 for the duration of the experiment. The redox potential of the feed solution was ~ 380 mV. Initially, the redox potential of the leachate was very low at 300 mV, partially attributed to the pre-experiment water-washing of the heap during flow studies. The redox potential of the leachate increased slowly from 300 to 400 mV during the first 14 days of acid-washing, followed by a 15 day lag period in which the redox potential stayed constant at 400mV. Following inoculation on day 27, a rapid increase in redox potential from 400 to 700 mV was observed between days 30 to 45. This indicated the increased oxidation of ferrous to ferric iron attributed to microbial growth and activity. The redox potential of the leachate collected in the ports furthest from the point source lagged behind slightly during this period, shown in Figure 5-7 (b) by ports 8 and 12. From day 55 onwards, the redox potential of the eluted solution collected in all ports, fluctuated around 700 mV for the rest of the leaching run.

(a) Copper concentration

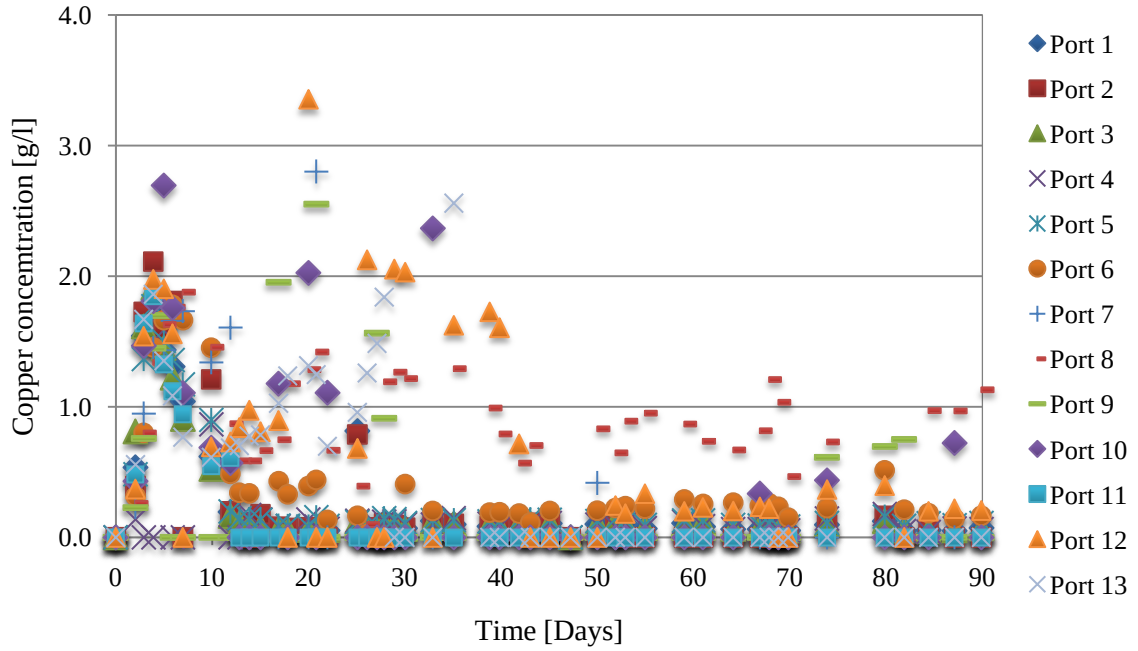

.

(b) Cumulative copper

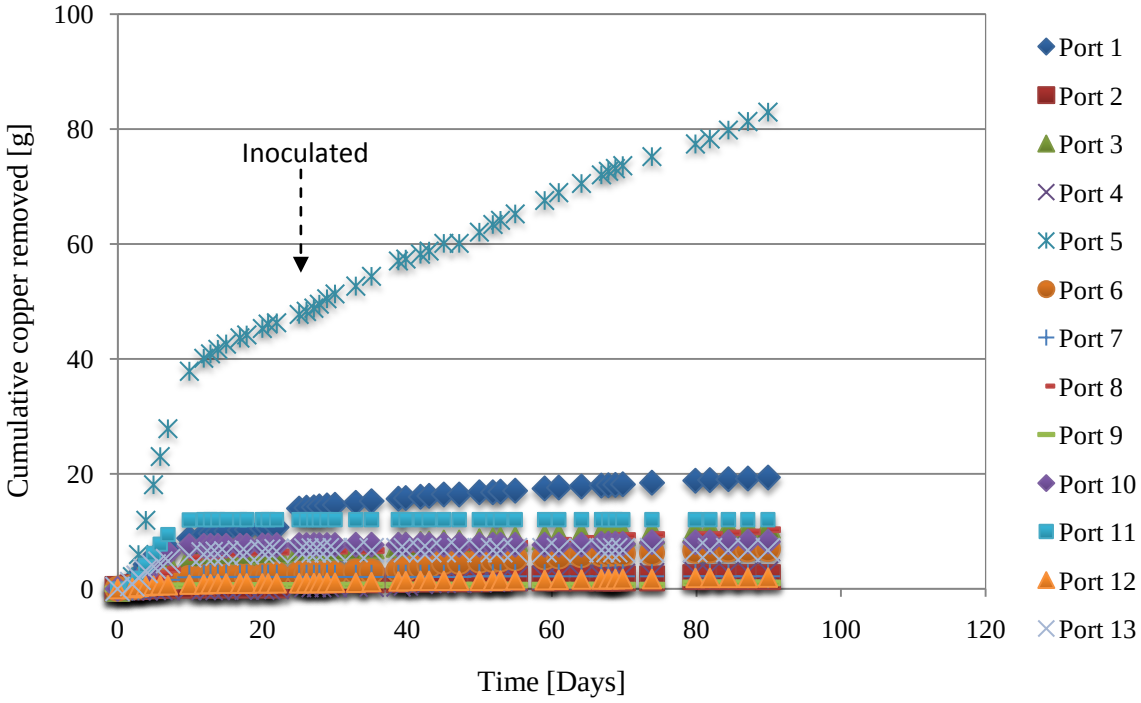

Figure 5-5: Copper analysis showing (a) the concentration profile and (b) the cumulative copper removal as a function of time during the bioleaching of low grade copper bearing ore, given for each of the 13 effluent collection ports, determined from atomic absorption spectroscopy.

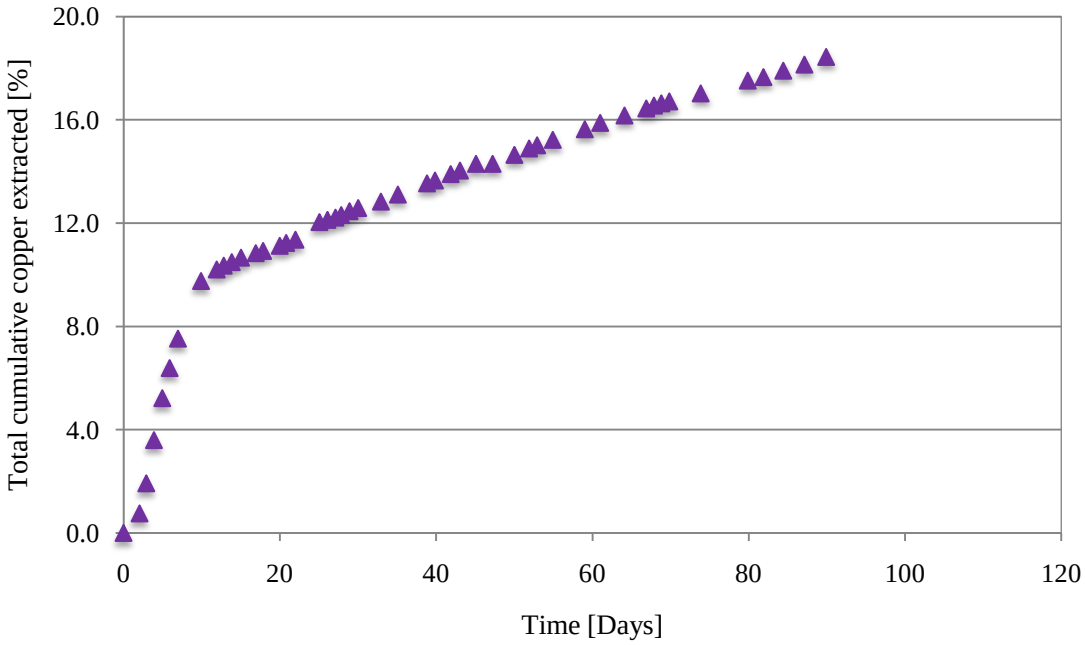

Figure 5-6: Total cumulative copper liberation as a function of time during the bioleaching of low grade copper bearing ore, determined from atomic absorption spectroscopy.

Figures 5-8 (a) and (b) show the ferrous and total iron concentrations of the leachate as a function of time, given for outlet ports 1, 2, 3, 4, 5, 6, 8, and 12. The iron concentration in the feed was 0.5 g/l, supplied in the ferrous form. Initially the ferrous iron concentration of the effluent was high ranging from 0.4 to 1.0 g/l. The leachate eluted in the ports furthest from the point source, i.e. ports 8 and 12, contained the highest ferrous iron concentrations (0.8 g/l and 0.9 g/l respectively) and the highest initial total iron concentrations (1.1 g/l and 1.2 g/l respectively). The high concentration could be attributed to the accumulation of iron within the system due to the low flow within the regions above these ports. Additionally, the acid leaching that occurred the region furthest from the point source of irrigation was not accompanied by microbial conversion of ferrous iron. Post inoculation, rapidly decreasing ferrous iron concentrations were observed from day 28 to 43, due to the microbial oxidation of ferrous to ferric iron, corresponding to the increased redox potential during the same time period. Thereafter, the ferrous iron concentration present in the eluted solution was ~ 99% depleted. The total iron concentration decreased from day 27 to 43 reaching levels ranging from 0.24 to 0.5 g/l between days 42 and 52. The concentrations then increased again to final concentrations of 0.34 g/l (ports 1 to 4), 0.40 g/l (port 5), 0.64 g/l (port 6), 0.98 g/l (port 8) and 0.53 g/l (port 12). Higher concentrations correlated to lower flow rates. The decreased total iron concentration suggests precipitation, which is generally not expected at pH 1.15. Precipitation could be attributed to the pH of the effluent differing from the ore bed, requiring further analysis of the ore.

(a) pH

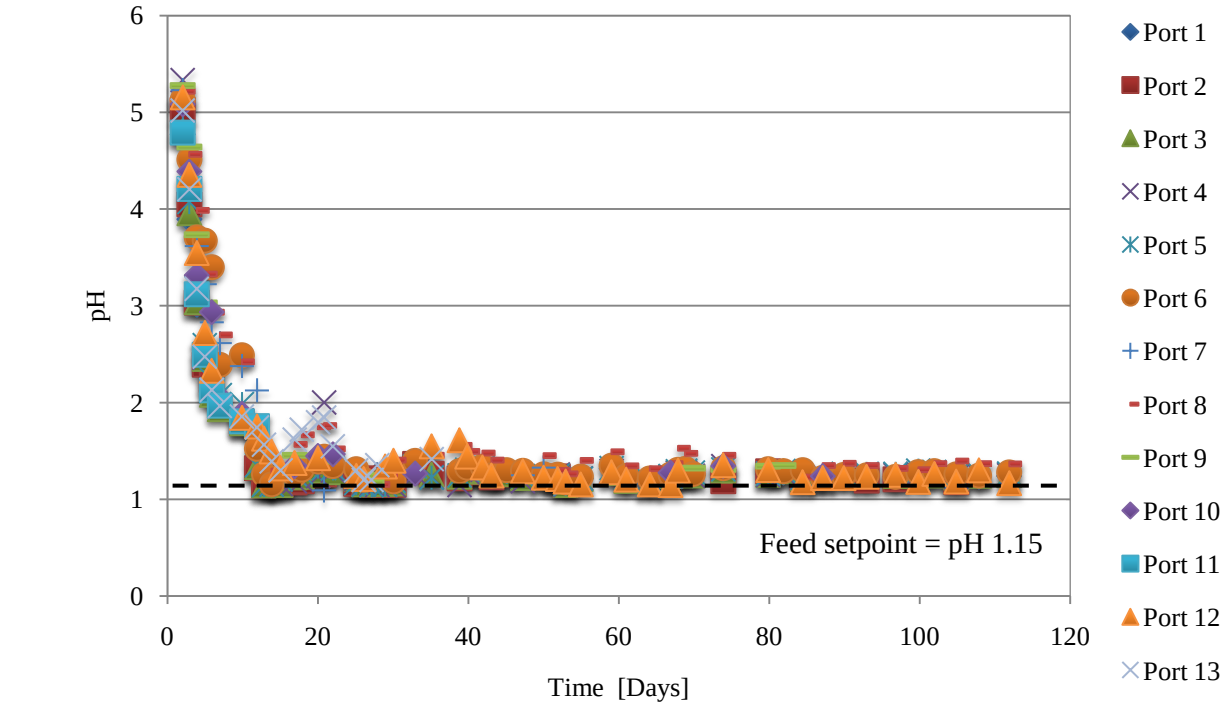

(b) Redox potential

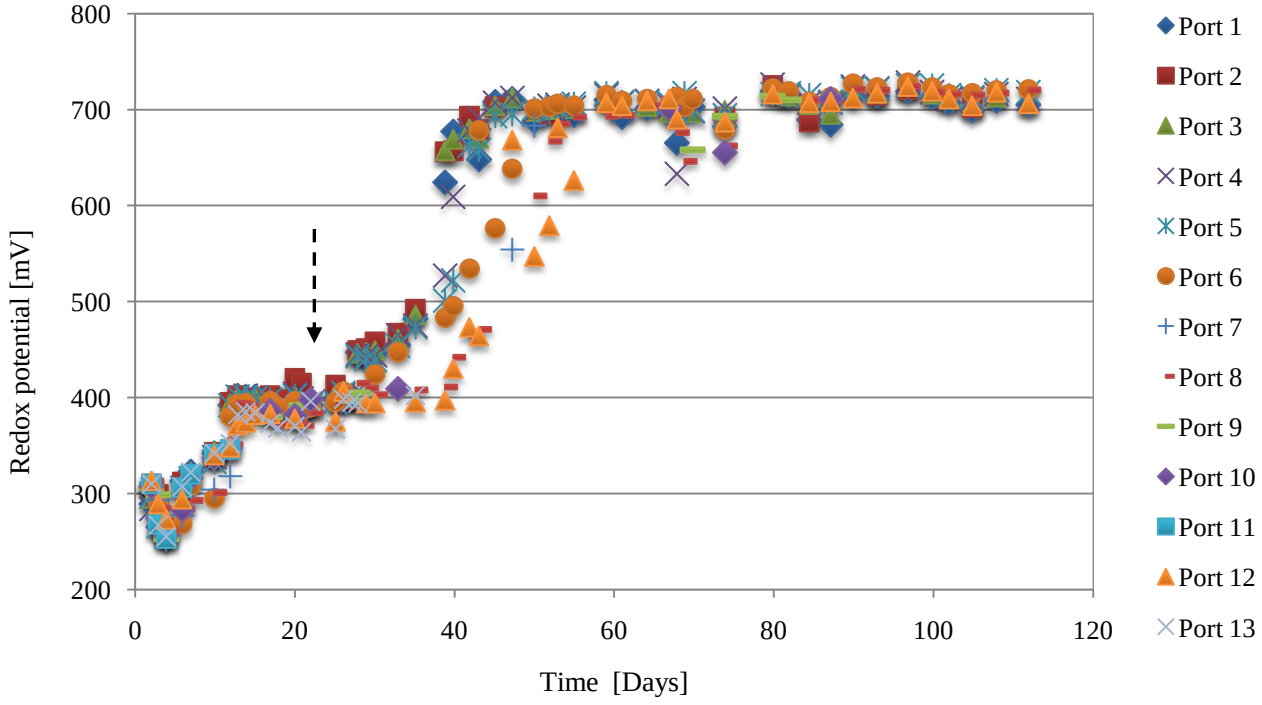

Figure 5-7: Trend in (a) the pH and (b) the redox potential, of the eluted solution passing through the box heap, given for each of the 13 effluent collection ports. The arrow is indicative of the inoculation point.

(a) Ferrous iron

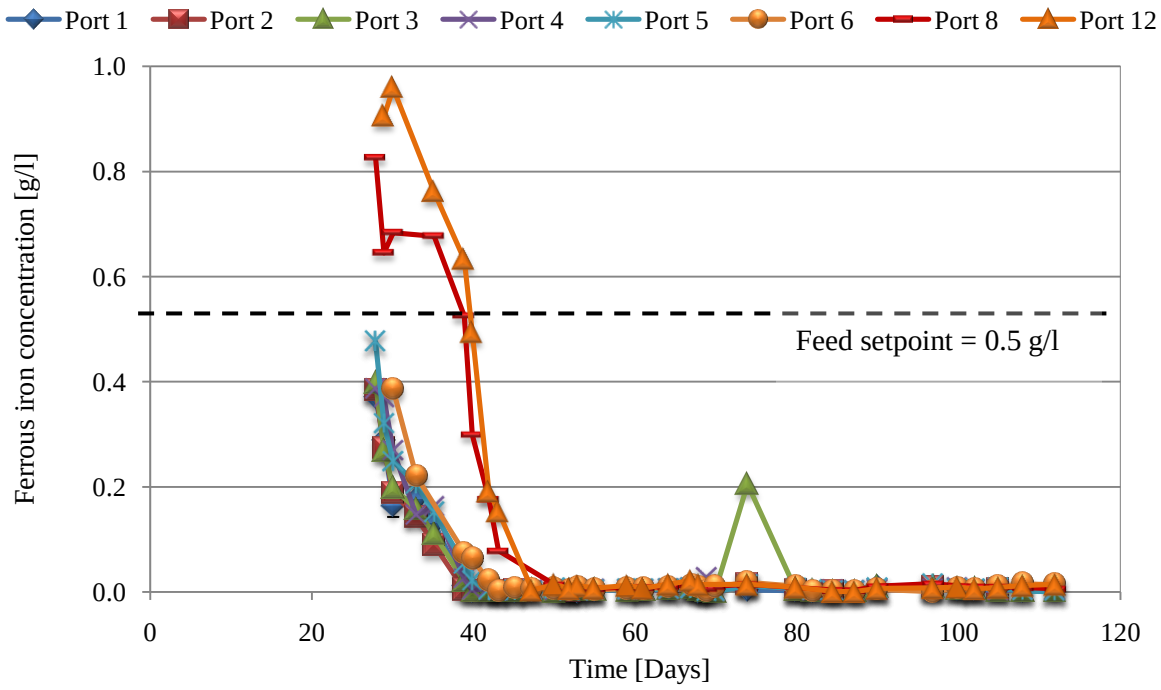

(b) Total iron

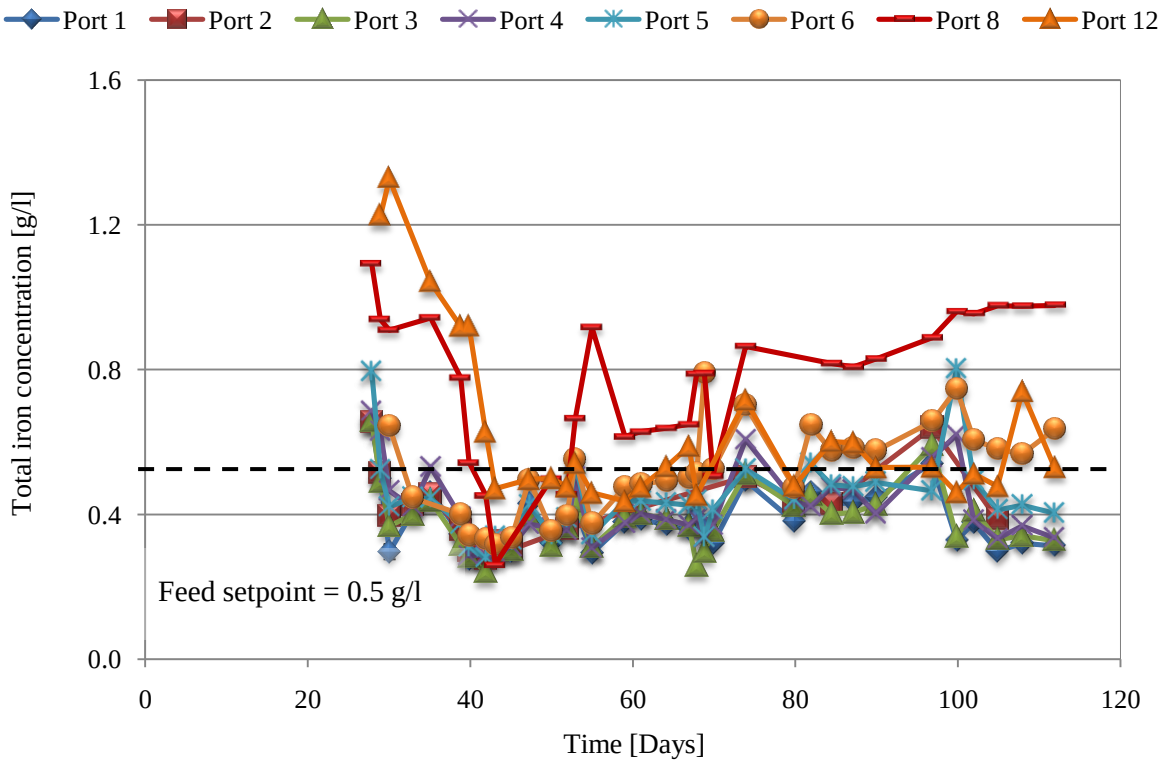

Figure 5-8: Iron analysis showing (a) the ferrous iron concentration and (b) the total iron concentration as a function of time, determined spectrophotometrically using the colorimetric 1-10 phenanthroline method, given for ports 1, 2, 3, 4, 5, 6, 8 and 12.

5.3.2 *Microbial Propagation and Colonisation*

Understanding the relationship between fluid flow channels and the transportation of micro-organisms within heaps environments is essential to providing adequate dispersion of microbial communities in the ore bed and enhancing bioleaching capabilities. Monitoring of the microbial cells eluted in the pregnant leach solution (PLS) and the cell densities within different locations in the ore bed was conducted. The cells in the PLS may be expected to correlate to the solution flow out of the box, whilst the cell densities within different zones can be linked to the movement of fluid through the ore bed characterised by the moisture contents presented in Section 5.3.1.

Figure 5-9 (a) and (b) shows the leachate cell concentration and the cumulative amount of planktonic cells eluted from the ore bed as a function of time, given for outlet ports 1, 2, 3, 4, 5, 6, 8, and 12. Microbial cells were detected in the eluted solution on the day after inoculation which had occurred on day 27, indicating the loss of some cells before their attachment and growth within the system. The initial cell concentrations ranged from below the detection limit to $9.4x10^5$cells/ml. For all the outlet ports displayed in Figure 5-9, a gradual increase in effluent cell concentration was observed, attributed to microbial growth. Cell concentrations increased to a maximum of $4.4x10^6$cells/ml (port 5) on day 70. Thereafter, on day 83, the effluent cell concentrations decreased, the final cell concentrations in the PLS were $3.1x10^5$cells/ml (port 1), $3.1x10^5$cells/ml (port 2), $3.1x10^5$cells/ml (port 3), $7.3\ x10^5$cells/ml (port 4), $7.5x10^5$cells/ml (port 5), $9.4x10^5$cells/ml (port 6), $1.6\ x10^6$cells/ml (port 8) and $6.3\ x10^5$cells/ml (port 12).

Initially, the cumulative amount of cells exported from the heap system, from day 28 to 38, were very low. From day 39 onwards, the cell exportation increased gradually due to the increase in cell numbers within the ore bed as a result of microbial growth. The majority of cells were eluted through port 5, shown by the high cell removal between days 50 to 90 totalling $2.4x10^{11}$cells. This observation corresponded to the highest outlet flow being through port 5. After 83 days of leaching, the total cell exportation from the box was $3.1x10^{11}$cells, where $3.0\ x10^{10}$cells, $3.0\ x10^9$cells, $2.9\ x10^{10}$cells, $2.4\ x10^{10}$cells, $2.1\ x10^{11}$cells, $6.9\ x10^9$cells, $3.9\ x10^9$cells and $3.6\ x10^9$cells were removed through ports 1, 2, 3, 4, 5, 6, 8, and 12 respectively. The cells present within the other ports were not detectable under the microscope. However, the data is negligible as the effluent collected in ports 7, 9, 10, 11 and 13, make up less than 3 % of the total flow. Approximately 68% of the total cells eluted were removed from the system via port 5. Again, suggesting that fluid passing through the system had mainly contacted the first two thirds of the ore bed (i.e. zones A, D, E, G, and H) inferring that the cell densities within these zones will be greater than in the zones furthest from the point source. This is supported by the data presented in Figures 5-10 and 5-11.

Figures 5-10, 5-11 and 5-12 show the cell densities within the 9 zones of the ore bed at intervals during the leaching period, obtained from the microscopic analysis of the cells mechanically detached from the ore samples extracted. These cell densities give an indication of the spatial distribution of the micro-organisms within the system.

The heap was inoculated on day 27 at a concentration of $1.0x10^{12}$cells/ton ore, after which the cells transport through the heap and retention of cells within the system was observed. On day 49 (22 days after inoculation), the average overall cell density accumulated within the ore bed was $1.4x10^{10}$cells/kg ore ($1.4x10^7$cells/ton ore). This was distributed across the system with the three vertical regions as follows: the left vertical region I (containing zones A, D, and G) had the highest cell density of $\sim10^{10}$cells/kg ore, the middle region II (containing zones B, E, and H) had an average cell density of

10^8cells/kg ore, whilst cell densities within the right region III furthest from the point source of irrigation (zone C, F, and I) were below 10^7cells/kg ore. Already on day 49, an increase in cell numbers with depth in the bed was observed (Figure 5-10). This was shown by the higher cell density in zones D ($5.1x10^{10}$cells/kg ore) and E ($3.9x10^8$cells/kg ore) in comparison to zones A ($4.1x10^{10}$cells/kg ore) and B ($1.7x10^8$cells/kg ore) respectively.

(a) Cell concentration

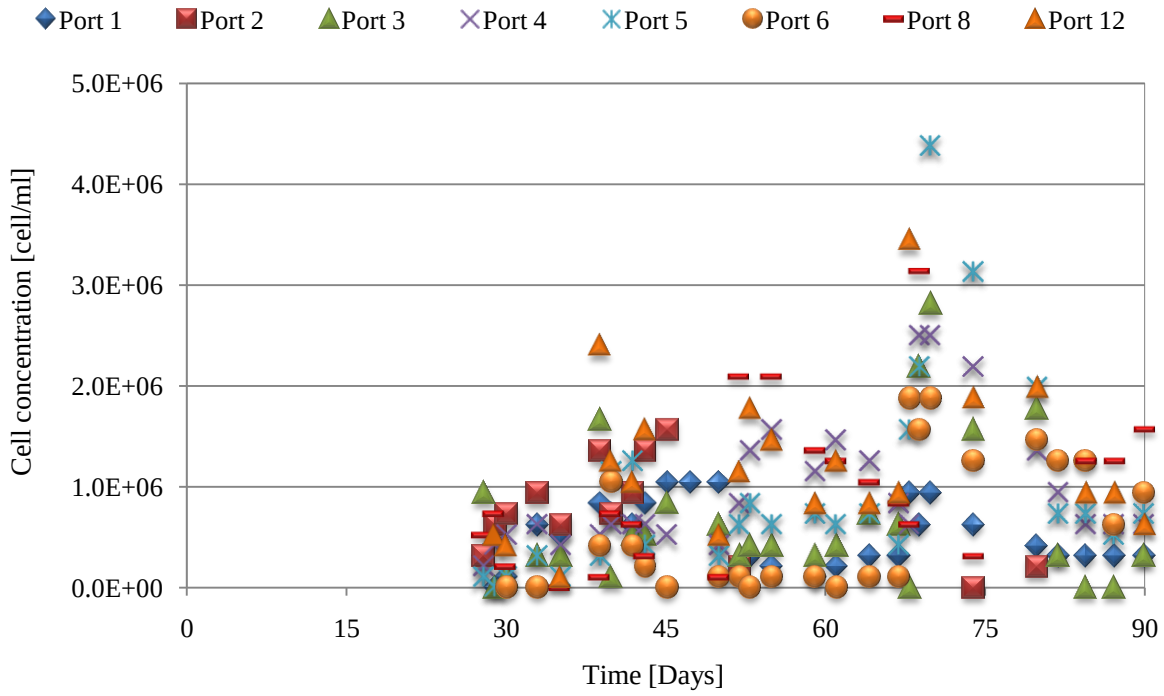

(b) *Cumulative cells*

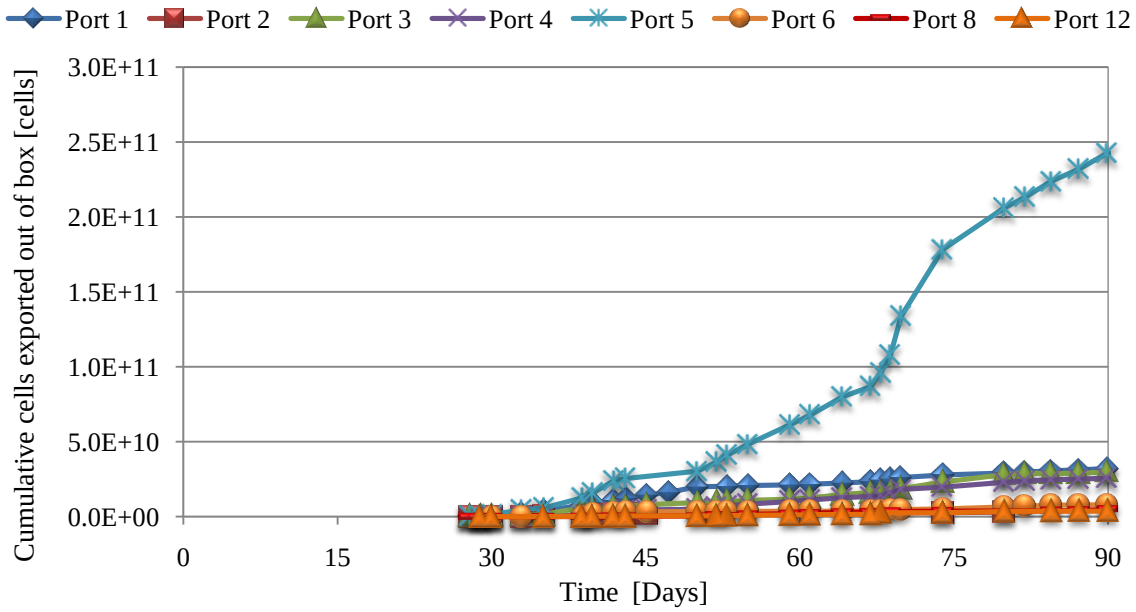

Figure 5-9: Trend in (a) the cell concentration and (b) the cumulative number of cells, exported in the leachate passing through the heap, given for outlet ports 1, 2, 3, 4, 5, 6, 8, and 12.

On day 63 (36 days post inoculation), the cell concentrations increased to ~10^{11}cells/kg ore in the left vertical region I (Figure 5-11). This was higher than the cell density of the middle vertical region II, which contained ~10^{7} to 10^{10}cells/kg ore. The cell density in the right region III was lower than 10^{8}cells/kg ore due to the inability to detect cells within zones C and F as a consequence of the low detection limit (10^{5}cells/ml = $5x10^{7}$cells/kg ore) of the microscopic cell counting method. Further increases in the cell density laterally and with depth were observed, corresponding to $1.31x10^{11}$cells/kg ore in zones D and G in comparison to zone A ($1.1x10^{11}$cells/kg ore), and $5.1x10^{9}$ and $2.8x10^{10}$cells/kg ore for zones E and H respectively in comparison to zone B ($6.7x10^{7}$cells/kg ore). The average overall cell density was $4.5x10^{10}$cells/kg ore ($4.5\ x10^{7}$cells/ton ore) on day 63.

Figure 5-12 shows further increased cell densities within the bed at day 83 (56 days after inoculation), indicating active microbial growth and subsequent retention in the system. After 83 days of leaching, the average overall cell density of the ore bed increased to $6.7x10^{10}$cells/kg ore ($6.7x10^{7}$cells/ton ore). The cell densities in the left vertical region I remained the highest at values greater than 10^{11}cells/kg ore. The middle vertical region II showed the most growth with cell densities increasing from 10^{8} to 10^{10}cells/kg ore over the 56 days post inoculation. The cell densities in the right vertical region III were lower than 10^{8} cells/kg ore, as cells within zones C and F remained undetectable.

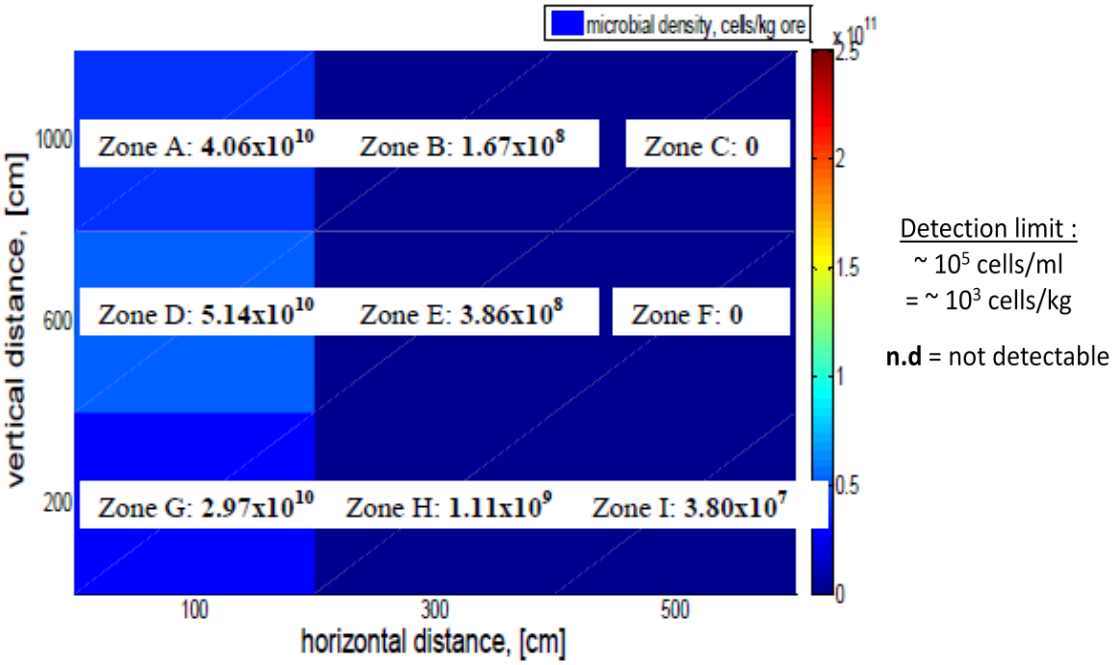

Figure 5-10: Cell densities of the 9 zones in the ore bed, determined from mechanical detachment and microscopic analysis of the ore samples periodically removed from the heap systems, given for day 49 (22 days post inoculation).

A clear increase in cell density across the whole ore bed was observed over time. The average cell density increased from $1.4x10^{10}$cells/kg ore at 22 days post inoculation to $4.5\ x10^{10}$cells/kg ore (36 days after inoculation) to $6.7x10^{10}$cells/kg ore (56 days after inoculation). Increased accumulation of micro-organisms within the system was observed over the leaching period in zones A, B, D, E, G, H, and I. The zones in the left vertical section continually contained the highest cell densities. The higher microbial retention within these zones can be attributed to a higher degree on fluid-mineral contacting in these regions as result of the preferential distribution of micro-organisms along preferential flow paths (Rossi, 1990; Decker and Tyler, 1999; O'kane *et al.*, 2000) and near the point source of

irrigation (Seitert and Engesgaard, 2007). However, the movement of micro-organisms within heaps environment is not independent of the active movement along chemical concentration gradients (van Loosdrecht *et al.*, 1990).

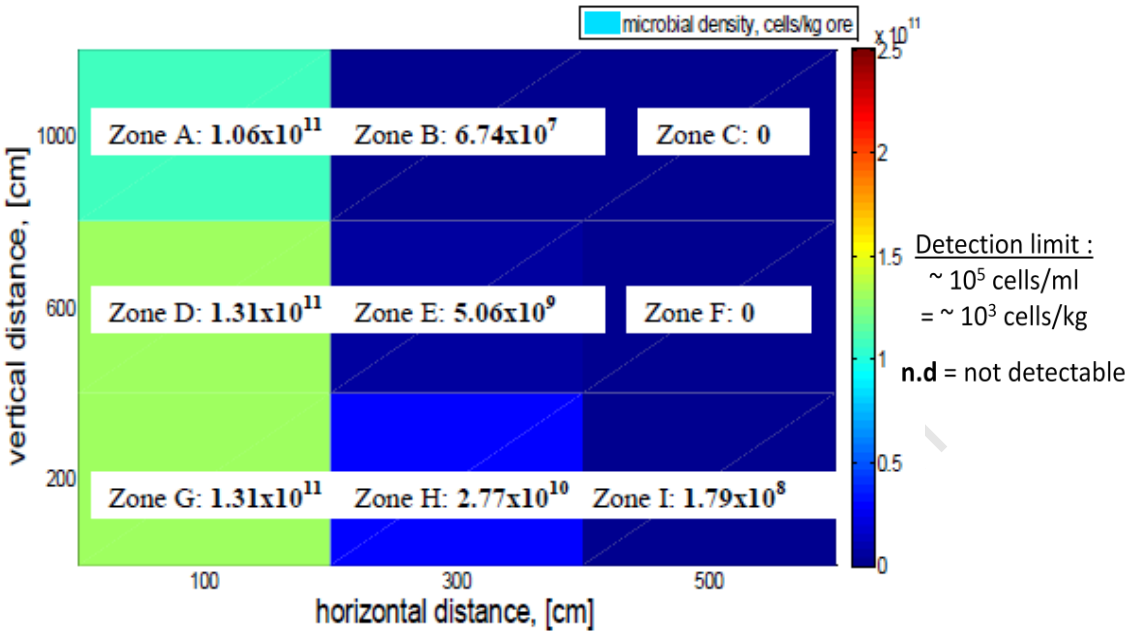

Figure 5-11: Cell densities of the 9 zones in the ore bed, determined from mechanical detachment and microscopic analysis of the ore samples periodically removed from the heap systems, given for day 63 (36 days after inoculation).

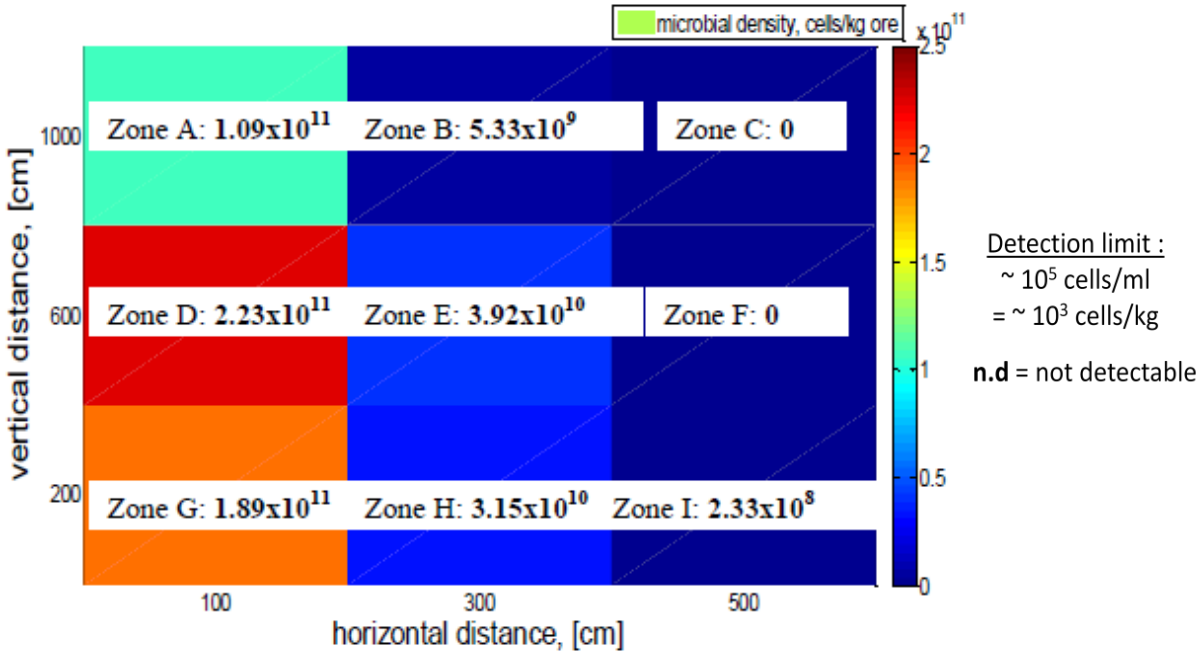

Figure 5-12: Cell densities of the 9 zones in the ore bed, determined from mechanical detachment and microscopic analysis of the ore samples periodically removed from the heap systems, given for day 83 of the leaching duration (56 days post inoculation).

Table 5-1: The relative proportions of ore-associated micro-organisms present in each of the 9 zones in the ore bed, determined from the mechanical detachment and microscopic analysis of cells obtained from the ore samples periodically removed from the box, given for intervals during the leaching run on days 49, 63 and 83 corresponding to 22, 36 and 56 days post-inoculation (n.d = not detectable)

		ZONE								
Day post inoculation	**Cell phase**	**A**	**B**	**C**	**D**	**E**	**F**	**G**	**H**	**I**
22	% Interstitial (i)	34.1	100.0	n.d	38.1	100.0	n.d	43.2	35.6	100.0
	% Weakly attached (ii)	19.5	n.d	n.d	14.6	n.d	n.d	17.0	64.4	n.d
	% Strongly attached (iii)	46.3	n.d	n.d	47.3	n.d	n.d	39.7	n.d	n.d
36	(i)	35.8	100.0	n.d	23.1	53.2	n.d	37.5	54.4	100.0
	(ii)	41.8	n.d	n.d	51.4	14.9	n.d	25.0	25.5	n.d
	(iii)	22.4	n.d	n.d	25.5	31.9	n.d	37.5	20.1	n.d
56	(i)	24.2	34.6	n.d	25.6	49.9	n.d	37.2	11.3	100.0
	(ii)	38.3	59.8	n.d	51.8	27.2	n.d	21.7	53.9	n.d
	(iii)	37.5	5.6	n.d	22.6	22.8	n.d	41.1	34.8	n.d

Table 5-1 shows the relative proportions of the ore-associated cells, obtained for three intervals during the leaching run. On day 49 (day 22 post-inoculation), zone A contained a fair distribution of cells across the three phases. 34 % of the cells were found in the interstitial phases, with 20 and 46 % found in the weakly and strongly attached phases, respectively. The proportion of weakly attached cells increased to 42 % on day 63 (day 36 post-inoculation), then decreased slightly to 38 % on day 83 (day 56 post-inoculation), corresponding to decreases in the interstitial phase to 24 %. Similarly, zone D contained 38 % interstitial cells, 15 weakly attached, and 47 % strongly attached on day 49. The proportion of weakly attached cells increased to 51 % on day 63, corresponding to decreases in the interstitial phase to 26 %. In zone G, the cells were distributed as 43 % interstitial, 17 % weakly attached and 40 % strongly attached, with stronger adherence to the mineral increasing with time.

In zone B, cells within the weakly and strongly attached phases were not detected on days 49 and 63. By day 83 the cells were distributed across zone B as follows: 34 % interstitial, 60 % weakly attached, 6 % strongly attached. Cells in the attached phases were also not detectable for zones C, F, and I. In zone I, cell accumulation occurred within the stagnant region only. In zone E the proportion of interstitial cells was higher than strongly attached, i.e. 53 % vs. 32 % on day 63 and 50 % vs. 23 % on day 83.

5.4 Discussion and conclusions

The purpose of the preliminary research presented in Chapter 5 was to investigate the influence of the solution flow distribution on the propagation and spatial distribution of the microbial species present within the heap environment, establishing the main trends to inform future research. The influence of fluid flow on microbial attachment and subsequent colonisation has been shown through an assessment of the moisture contents in zones in the ore bed in relation to the microbial cell densities and cell concentrations. Reproducibility of the experiment was beyond the scope of the study due to time constraints. However, all analyses were done in triplicate to ensure good reproducibility with the experimental run.

The moisture content of the ore bed showed that the flow and subsequent saturation of the bed occurred mainly within region I (zones A, D, G) of the ore bed, with increased bed wetness downwards in the vertical direction. Channelling and preferential flow were observed leaving approximate 33% of the ore bed poorly contacted with acidified solution (Rossi, 1990). The majority of the copper was extracted from the regions with the higher fluid throughput.

The decreased cell density of the top zones (A and B) over time and the increased in cell densities with depth, can be attributed to the downward migration of micro-organisms as a result of cell detachment, and fluid flow (Seitert and Engesgaard, 2007; Thullner, 2010). This corresponded to increased wetness of the ore bed in the lateral and downward direction as a function of time. Additionally, the downward movement of the cells could be due to micro-organisms' search for favourable leaching conditions (Rossi, 1990; van Loosdrecht, 1990). Petersen and Dixon (2007a) also reported increasing cell numbers with time and decreasing depth within their column studies. However, Petersen and Dixon (2007a) only quantified the micro-organisms present in the PLS samples drawn, with no measure of the micro-organisms accumulating within the ore bed.

The low cell numbers within the right region II corresponded to the low moisture contents attained in the zones furthest from the irrigation point i.e. zones C, F and I. No cells were observed in zone C and F for the whole duration of the leaching run, confirming the lack of fluid supply to these regions resulting in proportions of the heap remaining un-colonised which could lead to inefficient leaching of the ore bed.

Significant microbial growth and retention within the system was observed. The dispersion of the microbial colonies across the ore bed was shown. Zones through which the solution flowed predominantly allowed for micro-organism-mineral contacting as the micro-organisms were transported into these regions, enhancing bacterial adherence and subsequent colonisation of these regions (Rossi, 1990). The majority of the colonies accumulated radially near and axially below the point source of irrigation similar to the movement of cells as reported by Yarwood *et al.* (2006).

Initially, the interstitial phase was the more dominant phase. As the micro-organisms began to reproduce, attach and colonise the mineral surface, the interstitial phase only remained dominant in regions of low flow throughput. The relative proportions between the microbial phases vary for the duration of the leach run, suggesting an inter-phase transition. Movement of cells from the interstitial phase to the ore surface would occur via attachment. Inversely, detachment of cells from the ore surface could also occur as a function of the attachment threshold was being attained within localised zones of the ore bed, absorption studies would help to inform this.

6 CHAPTER 6: CONCLUSIONS AND RECOMMENDATIONS

6.1 Introduction

In the heap bioleaching process the microbially assisted dissolution of low grade mineral ores involves a number of sub-processes which occur simultaneously and therefore it is pertinent to understand how these sub-processes are interlinked. Particularly, the relationships between fluid flow dynamics and microbial colonisation of the heap are of interest, due to the transport of micro-organisms to within close proximity of the mineral surface and the subsequent microbe-mineral contacting being a function of the heap hydrodynamics. To date, this has been investigated in agricultural and soil engineering fields but seldom within the heap bioleaching space. Only one investigation (Lizama *et al*., 2005) has thoroughly assessed the impact of irrigation rates on microbial colonisation of heap bioleaching systems. Lizama *et al*. (2005) showed that the microbial growth rate was influenced by the irrigation rate to height ratio.

The purpose of this study was two-fold. Firstly the effect of irrigation application rates on the accumulation of a mixed mesophilic microbial community within simulated column heap environments containing an acid-agglomerated low grade copper-bearing ore was examined. Secondly, the relationship between the dispersion of solution from a point source of irrigation, subsequent moisture of the ore bed and the successive spatial distribution of microbial colonies post inoculation was sought using a box reactor under simulated heap conditions.

Specifically, the research intended to answer the following key questions:

- How does microbial colonisation vary with time during bioleaching?
- How does the distribution of cells between the PLS, interstitial and attached locations varies with time and irrigation rate?
- Will decreased irrigation rates facilitate increased attachment and colonisation of the minerals surface?
- Do higher flow velocities mediate the detachment of microbes from the mineral surface?
- How does the microbial population density change with time and location during the heap leaching process, relative to the irrigant source?
- How does moisture content and solution flow path change with time and location with respect to irrigation from a single point source?
- Do moisture contents and flow paths affect the propagation and distribution of microbial populations through the heap?

6.2 Irrigation Rate and Colonisation

The results of experiments conducted in the leach columns presented herein have not been presented previously. A new in-bed sampling technique was adopted and commissioned in this investigation. This allowed for the quantification of the microbial community associated with the mineral ore bed through the attainment of time progression data relating to the solid phase at a laboratory scale, not previously reported. The technique demonstrated the ability to obtain representative ore samples without significant disruption of the ore bed under low to moderate flow conditions.

A protocol to mechanically detach cells from ore samples, reported by Bryan *et al.* [submitted for publication], was used as a novel approach to quantify the different microbial phases such as the PLS, interstitial and attached cells.

The experiments were conducted in small scale heap leach columns, 100 mm wide and 360 mm high, as presented in Chapter 3. The range of irrigation rates used was based on industrial practice and previous investigations: 5 to 20 L/m^2.hr (Petersen and Dixon, 2007a) and 1.8 to 21.6 L/m^2.h (Lizama *et al*., 2005). The irrigation conditions utilised in this investigation were 2, 6 and 18 L/m^2.h.

The leaching profiles were typical of heap leach systems. The acid-soluble copper was leached out rapidly during the initial acid-wash stage. Thereafter, the copper was extracted at a low rate across all irrigation rates and experimental runs. Slower increase in redox potential and decrease in the ferrous iron concentration was observed with low flow (2 L/m^2.h). Despite the higher effluent copper and iron concentrations at low flow, the copper extraction achieved over the 32 day leaching period was slightly higher for the high flow (18 L/m^2.h).

Increases in bacterial adherence to the ore surface and interstitial cell numbers with time were observed. This was more prominent in the low to moderate flow regimes. The enhanced microbial surface colonisation at low flow was attributed to the retardation of microbial growth at high flow due to a number of factors such as the microbial breakthrough rate resulting in insufficient time for microbe-mineral contacting for bacterial adherence to the ore surface (Lizama *et al*., 2005), and the fluid shear causing cell detachment (Rossi, 1990; van Loosdrecht *et al*., 1990). Inversely, higher flow (18 L/m^2.h) tended to mediate the detachment and removal of cells from the ore bed. These are supported by the higher number of planktonic cells under high flow (18 L/m^2.h).

There was a higher affinity for cell retention in the stagnant regions over cells in the free-flowing liquids and ore surface-associated micro-organisms. It can be hypothesised that the accumulation of micro-organisms on the accessible ore surfaces post initial microbe-mineral contacting approached an equilibrium resulting in the release of new micro-organisms into the interstitial zones around the clustered ore particles, showing the effect of reversible adhesion described by Rossi (1990) and van Loosdrecht *et al*. (1990). Typical ratios of PLS to interstitial to attached cells (P/I/A) were 1:4:3 and 1:10:5 for an irrigation rate of 2 L/m^2.h during run 2 and 3 respectively. The P/I/A value was 1:3:1for 6 L/m^2.h and 1:1:− for 18 L/m^2.h, confirming the relative dominance of the cells within the stagnant regions.

The average specific growth rates of the ore-associated micro-organisms were 0.0053, 0.0052 and 0.0043 h^{-1} for 2, 6 and 18 L/m^2.h respectively, showing faster colonisation under low to moderate flow regimes. The growth rates obtained in this study were lower than those previously reported by Dempers *et al.* (2003) for a mixed culture of planktonic mesophilic bacteria under chemostat conditions typical of a *Leptospirillum* dominated culture using ferrous iron in the absence of pyrite as an energy source. The lower growth rates attained in this investigation over the growth rates reported by Dempers *et al.* (2003) were attributed to the differences between the systems used to determine the rates. Dempers *et al.* (2003) measured the growth rates of submerged continuous culture systems, whilst this study used the bioleaching of whole-ore within the column geometry operating under continuous flow. Additionally, the temperature regimes used by Dempers *et al.* (2003) was between 30 to 40 °C compared to the ambient temperature conditions employed in this study, possibly resulting in sub-optimal growth conditions. Hence the lower growth rates attained. However, the growth rates determined in this study give a reliable representation of growth rates on whole-ore leaching systems in comparison to the study by Minnaar *et al*. (2010). Additionally, there was good reproducibility of the column data.

The investigation showed that a variety of irrigation rates should be employed to achieve a particular result. For instance, in industry practices the irrigation rate should be set low (< 6 $L/m^2.h$) initially, to promote colonisation of the heap. After sufficient colonisation has occurred the irrigation rate can be increased to greater than 6 $L/m^2.h$ to promote metal extraction, but kept lower than 18 $L/m^2.h$ to avoid detachment of micro-organisms from the mineral surface.

6.3 Fluid Flow from Discrete Irrigation Points

The packed box system provided a preliminary means of assessing the propagation and spatial distribution of the micro-organisms in relation to the distribution of solution from a single point source of irrigation. Previously preferential solution flow distribution was implicated to influence contacting of fluid with exposed mineral surfaces (Rossi, 1990). 'Dry partially-leached zones' were identified within the system. An increase in the moisture content over time was observed. The wettest zones in the ore bed were those located in the vertical regions closest to the irrigant source. The lateral distribution of leach solution occurred mainly across the first two thirds of the box reactor in the vertical direction, corresponding to 97 % of the effluent recovery through the collection ports within the first 275 mm of the irrigant point. The majority of the fluid was expelled via port 5 (62 % of the flow). Two of the 9 zones (Zones C and F) remained at undetectable cell counts due to limited lateral movement of fluid and micro-organisms through the system into these regions. Therefore, the preferential fluid flow through the ore bed affected the transportation and dispersion of microbial communities within the heap. Increasing cell density beneath the point source of irrigation occurred. The cell density also increased with depth in the ore bed. This was postulated to be a consequence of microbial detachment and the successive migration downwards, as shown by Seitert and Engesgaard (2007). Initial cell retention within the box heap occurred in the stagnant regions. Thereafter, increased attachment, i.e. $6.7x10^{10}$cells/kg, to the surface was observed as a function of time over a 56 day leaching period following inoculation.

The preliminary box data presented has not been replicated for reproducibility, as the experiment was only conducted to establish the trends that would be expected, in order to inform future investigations. Additionally, the ore samples used to obtain the data were relatively small in comparison to the zones analysed, introducing uncertainty into the cell densities and moisture contents obtained.

6.4 Recommendations

Further studies can follow on from the work conducted within this thesis. Some suggestions on the avenues to explore and the discrepancies that need to be addressed are presented herein.

- The column systems should operate using the in-bed sampling technique to specifically obtain fully characterised microbial species analysis in order to understand the complete column leach system.
- The in-bed sampling apparatus can also be extrapolated to assess colonisation at different heights within the bed of a particular leaching system and characterise the microbial species present in the ore samples.
- To improve the reproducibility of the ore sampling method used during the preliminary box experiment, increasing the size of the sampling ports or extracting larger samples could be considered. However, upon removal of larger samples, changes in solution flow paths would occur, creating biased results.

- Assessment of the influence of ferrous iron concentration on the attachment and retention of cells within heap systems needs to be conducted. The influence of ferrous iron concentration in the feed solution on the rate and extent of attachment needs investigation as this will verify whether the higher degree of attachment observed at low flow was a response to nutrient and ferrous iron limitations, besides being a function of fluid shear.
- Further box reactor experimental runs with adaptation and expansion of the procedure are recommended. Moving forward, there is a need to conduct a physico-chemical experiment during which the lateral movement of fluid over a limited depth is analysed, allowing for ample sampling and characterisation of the zones furthest from the point source of irrigation (Zones C and F).
- Tracer studies can be conducted in the box reactor to attain a better sense of the flow distribution across the bed and the residence time of solution, solutes and cells within the system. The tracer used should be inert, for instance NaCl which is detectable using a spectrophotometer or conductivity meter.
- Further, extensive analysis on the ore samples extracted should be conducted to assess mineral compositions, iron precipitation, microbial activity and characterise the microbial species present.
- Comparison of microbial propagation and subsequent colonisation from the single point with microbial migration in systems containing multiple drip points should be conducted, complementing the dripper spacing studies conducted previously by Petersen and Dixon (2007a).
- The ore used in study was not sterilised prior to use, therefore the indigenous species present could have altered results. qPCR tests should be conducted on initial ore samples to identify native species, which could also indicate why *L. ferriphilum* remained the dominant species within the interstitial phase.
- It would also be useful to compare microbial colonisation alongside extensive quantitative copper leaching data. However, the duration of the leach period was short and thus did not allow for adequate time to draw concrete relationships between the two parameters. As such future investigations within these heap systems should be operated for an extended period of time (> 4 months) to enable substantial monitoring of copper bioleaching.
- Test work to further investigate the relationship between colonisation and Cu recovery should be conducted, to determine the threshold point where colonisation no longer affects the rate and extent of leaching.
- A solution balance over heap systems should indicate that lower irrigation rates have potential to minimise water usage and waste disposal, and reduce effluent processing costs.

REFERENCES

Africa, C., Harrison, S.T.L., Becker, M., van Hille, R.P. (2010). In-situ investigation and visualisation of microbial attachment and colonisation in a heap bioleach environment: The novel biofilm reactor. Minerals Engineering, **23**, 486-491.

Africa, C. (2009). Microbial attachment to sulfide minerals in a bioleach environment. MSc Thesis. University of Cape Town.

American Public Health Association (APHA). (1985). Standard methods for the examination of water and wastewater. 16th edition, APHA, Washington DC.

Bailey, J.E., Ollis, D.F. (1986). Biochemical Engineering Fundamentals. McGraw Hill, New York.

Bartlett, R.W. (1992). Leaching and fluid recovery of materials. Solution Mining. Gordon & Breach Science Publishers.

Bartlett, R.W. (1997). Metal extraction from ores by heap leaching. Metallurgical & Materials Transactions, **28B**, 529-537.

Bouffard, S.C., Dixon, D.G. (2001). Investigative study into the hydrodynamics of heap leaching processes. Metallurgical & Materials Transactions, **32B**, 763-776.

Bouffard, S.C. (2008). Agglomeration for heap leaching: Equipment design, agglomerate quality control, and impact on the heap leach process. Minerals Engineering, **21**, 1115-1125.

Bouffard, S.C., Dixon, D.G. (2009). Modeling the performance of pyritic biooxidation heaps under various design and operating conditions. Hydrometallurgy, **95**, 227-238.

Breed, A.W., Hansford, G.S. (1999). Effect of pH on ferrous-iron oxidation kinetics of *Leptospirillum ferrooxidans* in continuous culture. Biochemical Engineering Journal, **3**, 193-201.

Brierley, C.L. (2001). Bacterial succession in bioheap leaching. Hydrometallurgy, **59**, 249-255.

Bromfield, L., Africa C.-J., Harrison S.T.L. and van Hille R.P. (2010). The effect of temperature on the attachment of *Metallosphaera hakonensis* to a copper sulphide concentrate with application to heap bioleaching. In Proceedings of Bio & Hydrometallurgy Conference, Cape Town, South Africa.

Bryan, C.G., Jones, G., van Wyk, N., Tupikina, O.V., Harrison S.T.L. and van Hille R.P. (2011). A critical evaluation of techniques for the selective isolation and analysis of microbial populations involved in heap bioleaching. Environmental Microbiology submitted.

Cariaga E., Concha, F., Sepúlveda, M. (2005). Flow through porous media with applications to heap leaching copper ores. Chemical Engineering Journal, **111**, 151-165.

Chen, G. (2008). Bacterial interactions and transport in unsaturated porous media. Colloids and Surfaces B: Biointerfaces, **67**, 265-271.

Chiume, R., Minnaar, S., Ngoma, E., Harrison, S.T.L. (2010). Investigating microbial colonisation in bioheaps with varying irrigation rate. In Proceedings of Bio & Hydrometallurgy Conference, Cape Town, South Africa.

Cooper, G., Dixon, S. (2006). Modeling Chalcocite leaching, In Proceedings of SME Annual Meeting. St. Louis, USA. **Vol 4**.

Coram, N.J., Rawlings, D.E. (2002). Molecular relationship between two groups of the genus *Leptospirillum* and the finding that *Leptospirillum ferriphilum* sp. nov. dominates in South African commercial biooxidation tanks that operate at 40 °C. Applied and Environmental Microbiology, **68**, 838-845

Córdoba, E.M., Muñoz, J.A., Blázquez, M.L., González, F., Ballester, A. (2008). Leaching of chalcopyrite with ferric ion. Part II: Effect of redox potential. Hydrometallurgy, **93**, 88-96.

Decker, D.L., Tyler, S.W. (1999). Hydrodynamics and solute transport in heap leach mining. Closure, Remediation & Management of Precious Metals Heap Leach Facilities.

Dempers, C.J.N., Breed, A.W., Hansford, G.S. (2003). The kinetics of ferrous-iron oxidation by *Acidithiobacillus ferrooxidans* and *Leptospirillum ferrooxidans*; effect of cell maintenance. Biochemical Engineering Journal, **16**, 337-346.

Devasia, P., Natarajan K.A., Sathyanarayana D.N., Rao, G.R. (1993). Surface chemistry of *Thiobacillus ferrooxidans* relevant to adhesion to mineral surfaces. Applied & Environmental Microbiology, **59** (12), 4051-4055.

Du Plessis C.A., Batty, J.D., Dew, D.W. (2007). Commercial applications of thermophile bioleaching. In Biomining (Eds. Rawlings D.E. and Johnson D.B.), Springer-Verlag, pp 57-78.

Escobar, B., Hevia, M.J., Vargas, T. (2004). Evaluating the growth of free and attached cells during the bioleaching of chalcopyrite with *Sulfolobus metallicus*. In: Tzesos, M., Hatzikioseyan, A., Remoundaki, E. (Eds.), Biohydrometallurgy: A Sustainable Technology in Evolution (Athens, 2003), 1091-1097.

Escobar, B., Lazo, D. (2003). Activation of bacteria in agglomerated ores by changing the composition of the leaching solution. Hydrometallurgy, **71**, 173-178.

Gehrke, T., Telegdi, J., Dominique, T., Sand, W. (1998). Importance of extracellular polymeric substances from *Thiobacillus ferrooxidans* for bioleaching. Applied and Environmental Microbiology, **64** (7), 2743-2747.

Ghauri, M.A., Okibe, N., Johnson, D.B. (2007). Attachment of acidophilic bacteria to solid surfaces: The significance of species and strain variations. Hydrometallurgy, **85**, 72-80.

Ginn, T.R., Wood, B.D., Nelson, K.E., Scheibe, T.D., Murphy, E.M, Clement, T.P. (2002). Processes in microbial transport in the natural subsurface. Advances in Water Resources, **25**, 1017-1042.

Graf von der Schulenburg, D.A., Akpa, B.S., Gladden, L.F., Johns, M.L. (2008). Non-invasive mass transfer measurements in complex biofilm-coated structures. Biotechnology and Bioengineering, **101**, 602-608. Wiley Periodicals, Inc.

Graf von der Schulenburg, D.A., Paterson-Beedle, M., Macaskie, L.E., Gladden, L.F., Johns, M.L. (2007). Flow through an evolving porous media – compressed foam. Journal of Material Science, **42**, 6541-6548. Springer.

Karavaiko, G.I., Dubinina, G.A., Kondratieva, T F. (2006). Lithotrophic microorganisms of the oxidative cycles of sulphur and iron. Microbiology, **75 (5)**, 512-545.

Kinzler, K. Gehrke, T., Telegdi, J., Sand, W. (2003). Bioleaching – a result of interfacial processes caused by extracellular polymeric substances (EPS). Hydrometallurgy, **71**, 83-88.

Komadel, P., Stucki, J.W. (1988). Quantitative assay of minerals for Fe^{2+} and Fe^{3+} using 1,10-phenanthroline: III. A rapid photochemical method. Clays and Clay Minerals, **36**, 379–381.

Lehman, R.M., Colwell, F.S., Bala, G.A. (2001). Attached and unattached microbial communities in a simulated basalt aquifer under fracture- and porous-flow conditions. Applied and Environmental Microbiology, **67**, 2799-2809.

Lin, C.L., Miller, J.D., Garcia, C. (2005). Saturated flow characteristics in column leaching as described by LB simulation. Minerals Engineering, **18**, 1045-1051.

Lizama, H.M., Harlamovs, J.R., McKay, D.J., Dai, Z. (2005). Heap leaching kinetics are proportional to the irrigation rate divided by heap height. Minerals Engineering, **18**, 623-630.

Michel, C., Bény, C., Delorme, F., Poirier, L., Spolaore, P., Morin, D., d'Hugues, P. (2009). New protocol for the rapid quantification of exopolysaccharides in continuous culture systems of acidophilic bioleaching bacteria. Applied Microbiology and Biotechnology, **82**, 371-378.

Minnaar S., Tupikana O.V., van Hille R.P., van Wyk N., Janse van Rensberg S. Harrison S.T.L. (2010). Microbial growth rates on mesophilic acidophiles on low grade whole ore containing chalcopyrite. In Proceedings of Bio & Hydrometallurgy Conference, Cape Town, South Africa.

Monod, J. (1949). The growth of bacterial cultures. Annual Review of Microbiology, **3**, 371-394.

Morin, D.H.R. (2007). Bioleaching of sulfide minerals in continuous stirred tanks, In: Donati, D.E., Sand, W. (eds) Microbial processing of metal sulphides, 193-218. Springer.

Muira, Y., Hiraiwa, M.N., Ito, T., Watanabe, Y., Okabe, S. (2007). Bacterial community structures in MBRs treating municipal wastewater: relationship between community stability and reactor performance. Water Research, **41**, 627-637.

Ndlovu, S. (2008). Biohydrometallurgy for sustainable development in the African minerals industry. Hydrometallurgy, **97**, 20-27.

O'Kane Consultants Inc. (2000). Demonstration of the application of unsaturated zone hydrology for heap leach optimization. Industrial Research Assistance Program Contract # 332407, Report No. 628-1.

Oyekola, O.O. (2008). An investigation into the relationship between process kinetics and microbial population dynamics in a lactate-fed sulphidogenic CSTR as a function of residence time and sulphate loading. PhD Thesis. University of Cape Town.

Petersen, J., Dixon, D.G. (2003). The dynamics of chalcocite heap bioleaching. In: Young, C.A., Alfantazi, A.M., Anderson, C.G., Dreisinger, D.B., Harris, B., and James, A. (Eds), Hydrometallurgy, **1**, 351-364.

Petersen, J., Dixon, D.G. (2007a). Principles, mechanisms and dynamics of chalcocite heap bioleaching, In: Donati, D.E., Sand, W. (eds) Microbial Processing of Metal Sulphides, 193-218. Springer.

Petersen, J., Dixon, D.G. (2007b). Modeling and optimization of heap bioleach processes. In Biomining (Eds. Rawlings D.E. and Johnson D.B.). Springer-Verlag, pp 153-175.

Pintelon, T.R.R., Graf von der Schulenburg, D.A., Johns, M.L. (2009). Towards optimum permeability reduction in porous media using biofilm growth simulations. Biotechnology and Bioengineering, **103**, 767-779.

Pirt, S.J. (1975). Principles of microbe and cell cultivation. Blackwell Scientific publications, Oxford.

Plumb, J.J., McSweeney, N.J., Franzmann, P.D. (2008). Growth and activity of pure and mixed bioleaching strains on low grade chalcopyrite ore. Minerals Engineering, **21**, 93-99.

Pradhan N., Nathsarma, K.C., Srinivasa Rao, K., Sukla, L.B., Mishra, B.K. (2008). Bacterial heap bioleaching of chalcopyrite: A review. Minerals Engineering, **21**, 355-365.

Rawlings, D.E. (2002). Heavy metal mining using microbes. Annual Review: Microbiology, **56**, 65-91.

Rawlings, D.E., Dew, D., du Plessis, C. (2003). Biomineralization of metal-containing ores and concentrates. TRENDS in Biotechnology, **21**, 38-44.

Rawlings, D.E., Johnson, D.B. (2007). Review: The microbiology of biomining: development and optimization of mineral-oxidizing microbial consortia. Microbiology, **153**, 315-324.

Rockhold, M.L., Yarwood, R.R., Niemet, M. R., Bottomley, P.J., Selker, J.S. (2002). Review: Considerations for modelling bacterial-induced changes in hydraulic properties of variably saturated porous media. Advances in Water Resources, **25**, 477-495.

Rockhold, M.L., Yarwood, R.R., Niemet, M. R., Bottomley, P.J., Brockman, F.J., Selker, J.S. (2007). Visualization and modeling of the colonization dynamics of a bioluminescent bacterium in variably saturated, translucent quartz sand. Advances in Water Resources, **30**, 1593-1607.

Rodriguez, Y., Ballester, A., Blazquez, M.L., Gonzalez, F., Munoz, J.A. (2003). Study of bacterial attachment during the bioleaching of pyrite, chalcopyrite and sphalerite. Geomicrobiology Journal, **20**, 131-141.

Rohwerder, T., Sand, W. (2007). Mechanisms and biochemical fundamentals of bacterial metal sulfide oxidation, In: Donati, D.E., Sand, W. (eds) Microbial processing of metal sulphides, 193-218. Springer.

Rossi G. (1990). Biohydrometallurgy, McGraw-Hill, Hamburg

Roychoudhury, A.N. (2004). Sulfate respiration in extreme environments: A kinetic study. Geomicrobiology, **21**, 33-43.

Sampson, M.I., Phillips, C.V, Blake, R.C. (2000). Influence of attachment of acidophilic bacteria during the oxidation of mineral sulfides. Minerals Engineering, **13**(4), 373-389.

Sand, W., Gehrke T., Jozsa P.G., Schippers A. (2001). (Bio)chemistry of bacterial leaching – direct vs. indirect bioleaching. Hydrometallurgy **59**, 159-175.

Sand, S., Gehrke, T. (2006). Extracellular polymeric substances mediate bioleaching/biocorrosion via interfacial processes involving iron(III) ions and acidophilic bacteria. Research in Microbiology, **157**, 49-56.

Schippers, A. (2007) Microorganisms involved in bioleaching, In: Donati, D.E., Sand, W. (eds) Microbial Processing of Metal Sulphides, 193-218. Springer.

Schippers, A., Jozsa, P-G., Sand, W. (1996). Sulfur chemistry in bacterial leaching of pyrite. Applied and Environmental Microbiology, **62**, 3424-3431.

Seitert, D., Engesgaard, P. (2007). Use of tracer tests to investigate changes in flow and transport properties due to bioclogging of porous media. Journal of Contaminant Hydrology, **93**, 58-71.

Sen, T.K., Das, D., Khilar, K.C., Suraishkumar, G.K. (2005). Bacterial transport in porous media: New aspects of the mathematical model. Colloids & Surfaces A: Physicochemical Engineering Aspects, **260**, 53-62.

Shuler, L., Kargi, F. (1992). "Bioprocess Engineering – Basic Concepts." Prentice-Hall, pp. 232-248.

Thullner, M., Mauclaire, L., Schroth, M.H., Kinzelbach, W., Zeyer, J. (2002). Interaction between water flow and spatial distribution of microbial growth in a two-dimensional flow field in unsaturated porous media. Journal of Contaminant Hydrology, **58**, 169-189.

Thullner, M., Schroth, M.H., Zeyer, J., Kinzelbach, W. (2004). Modeling of a microbial growth experiment with bioclogging in a two dimensional flow field. Journal of Contaminant Hydrology, **70**, 37-62.

Thullner, M. (2010). Comparison of bioclogging effects in saturated porous media with one- and two-dimensional flow systems. BioGeoCivil Engineering **36 (2)**, 176-196.

Tributsch, H. (2001). Direct versus indirect bioleaching. Hydrometallurgy, **59**, 177 – 185.

Tupikana O.V., Ngoma, I.E., Minnaar S., Harrison S.T.L. (2010). Some aspects of the effect of pH and stress in heap bioleaching. In Proceedings of Bio & Hydrometallurgy Conference, Cape Town, South Africa.

Vandevivere, P., Baveye, P. (1992). Relationship between transport of bacteria and their clogging efficiency in sand columns. Applied and Environmental Microbiology, **58** (8), 2523-2530.

Van Hille, R.P., van Zyl, A. W., Spurr, N.R.L., Harrison, S.T.L. (2010). Investigating heap bioleaching: effect of feed iron concentration on bioleaching performance, Minerals Engineering, **23**(6), 518-525.

Van Loosdrecht, M.C.M., Lyklema, J., Norde, W., Zehnder, A.J.B. (1990). Influence of interfaces on microbial activity. Microbiological Reviews, **54**(1), 75-87.

Viera, M., Pogliani, C., Donati, E. (2007). Recovery of zinc, nickel, cobalt and other metals by bioleaching. In: Donati, D.E., Sand, W. (eds) Microbial processing of metal sulphides, 193-218. Springer.

Wan, J., Wilson, J.L., Kieft, T.L. (1994). Influence of the gas-water interface on transport of microorganisms through unsaturated porous media. Applied and Environmental Microbiology, **60** (2), 509-516.

Watling, H.R. (2006). The bioleaching of sulphide minerals with emphasis on copper sulphides – a review. Hydrometallurgy, **84**, 81-108.

Wu, A., Yin, S., Yang, B., Wang, J., Qiu, G. (2007). Study on preferential flow in dump leaching of low grade ores. Hydrometallurgy, **87**, 124-132.

Wu, A., Yin, S., Qin, W., Liu, J., Qiu G. (2009). The effect of preferential flow on extraction and surface morphology of copper sulphides during heap leaching. Hydrometallurgy, **95**, 76-81.

Yarwood, R.R., Rockhold, M.L., Niemet, M.R., Selker, J.S., Bottomley, P.J. (2006). Impact of microbial growth on water flow and solute transport in unsaturated porous media. Water Resources Research, **42**, W10405.

APPENDICES

Appendix A – Feed Solution and Culture Preparation

Acid Solution for Agglomeration

The acid water agglomeration solution is prepared using a ratio of 50 ml H_2O/kg ore and 3.7 ml 96% H_2SO_4/kg ore. Table A.1 shows the volume required for the different systems.

Table A.1: Agglomeration media composition

Volume 96% H_2SO_4	Volume deionised H_2O	
14.8	200	ml/ 4 kg
488.4	6600	ml/ 132 kg

Acid-wash Feed Solution

Prepare 20 L of acidified solution for the acid-wash stage. This stage is required to stabilise the pH of the system at a specified design condition (pH 1.15) and to remove copper oxides, and other inhibitory compounds.

Feed Solution

The feed solution was prepared with the following composition:

Table A.2: Media composition

Chemical Compound	Composition
Deionised H_2O	20 L
Conc. H_2SO_4	Adjust to pH 1.15
$FeSO_4.7H_2O$ (ferrous sulphate)	500 mg/L
$(NH_4)_2SO_4$	183.3mg/L
$NH_4H_2PO_4$	60.5 mg/L
K_2SO_4	111.2 mg/L

The salts were dissolved in distilled water. Thereafter then the pH was adjusted to pH 1.15 using concentrated H_2SO_4 before making the solution up to its specified volume. A sample of the feed solution was taken for analysis, measuring the pH and redox potential when new feed was made.

Microbial Cultures

A mixed mesophilic culture was used (UCT stock) containing *At. caldus*, *At. ferrooxidans*, *At. thiooxidans*, *L. ferriphilum* grown on pyrite in a batch stirred tank reactor at 30°C. The reactor was sub-cultured twice weekly to ensure activity.

Appendix B – Analytical methods

Microscopic Cell Counting Method

Cell counts were done using a Thoma Counting Chamber under an Olympus BX40 Microscope. The microscopic analysis of the PLS gives the planktonic cell counts. The microscopic analysis of the solution from the mechanical detachment of cells from the ore samples extracted from the systems, gives the interstitial and attached cells counts.

Formulae for calculation cell concentration:

$$Volume\ \_of\ \_1\_small\ \_square\ \_[mm^3] = depth \times area$$

$$Cell\ \_concentrat\ ion\ \_[cells\ /ml\ ] = \frac{cells\ \_counted\ \times \frac{total\ \_no\ \_of\ \_big\ \_squares\ \_(16)}{no\ \_of\ \_squares\ \_counted\ \_(4)}}{volume\ \_of\ \_1\_small\ \_square \times total\ \_no.\_of\ \_small\ \_squares}$$

Ferrous and Total Iron Concentration via Spectrophotometry

The protocol presented here-in was obtained from the CeBER database of analytical laboratory methods. The ferrous and total iron concentrations of the leachate were determined colormetrically using the 1-10 phenanthroline method developed by Komadel and Stucki (1988). The reagents were prepared as follows:

1. A fresh stock of ferrous iron solution at 100ppm was used as the standard. First, 20 ml of concentrated H_2SO_4 was added to 50 ml distilled water in a volumetric flask. Then, 497.6 mg of $FeSO_4.7H_2O$ was dissolved in the acidified water. The solution was diluted with distilled water to make up 1000 ml of the standard solution. The solution was shaken vigorously to ensure that it was well mixed. Constant monitoring of the ferrous iron concentration in the standard solution was required to assess whether ferrous iron oxidation had occurred.
2. An ammonium acetate buffer solution is made by dissolving 250 g of ammonium acetate ($NH_4C_2H_3O_2$) in 150 ml of distilled water, followed by the addition of 700 ml of concentrated glacial acetic acid.
3. To make the 1-10 phenanthroline indicator solution, 2127.7 mg of 1-10 phenanthroline ($C_{12}H_8N_2.H_2O$) was dissolved in 100 ml of distilled water i.e. volumetric flask. The solution was diluted with distilled water to 1000 ml, providing a concentration in excess of the stoichiometric requirements.
4. To obtain the total iron concentration, a spatula tip of hydroxylamine was added to each sample to convert all iron present to the ferrous form, where after the ferrous assay was performed.

Standard curves of the relationship between ferrous concentration and absorbance were constructed. 2 ml aliquot of acetate buffer, followed by 2 ml of 1-10 phenanthroline solution was put into test-tubes. The standard ferrous iron stock solution was diluted to provide samples of 0, 10, 20, 30, 40, and 50 ppm. From these, 1 ml was pipetted into the respective test-tubes. On addition of samples containing ferrous iron, solution reacted to form an orange-red colour. The concentration of 0 ppm was made up of pure Millipore water, and was required to zero the spectrophotometer. The absorbance maximum was determined through a scan of a ferrous sample and confirmed to be 510 nm. The standard curves

generated are presented in Figures B1 and B2. Note that the concentrated effluent sample should be diluted to determine the concentration from the standard curves, such that an $A_{510} < 2$ results.

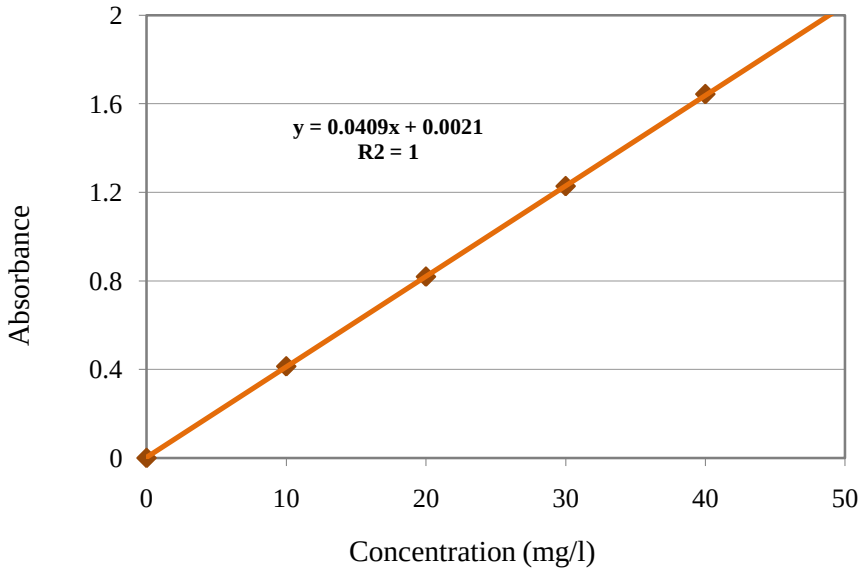

Figure B.1: Standard curve used to obtain the ferrous and total iron concentrations during the column experiments

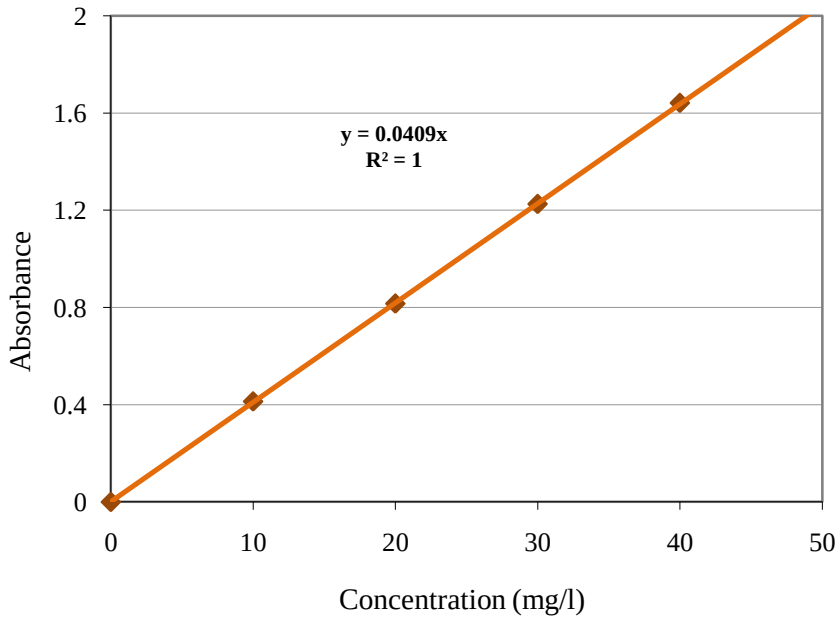

Figure B.2: Standard curve used to obtain the ferrous and total iron concentrations during the box experiment

Table B.1: Data generated to produce the standard curve for the determination of ferrous and total iron concentrations during the column experiments

Concentration [mg/l]	Absorbance			
	Sample 1	Sample 2	Sample 3	Average
0	0	0	0	0
10	0.418	0.412	0.411	0.414
20	0.815	0.817	0.824	0.819
30	1.237	1.219	1.226	1.227
40	1.638	1.648	1.643	1.643
50	2.037	2.047	2.043	2.042

Table B.2: Data generated to produce the standard curve for the determination of ferrous and total iron concentrations during the box experiment

Concentration [mg/l]	Absorbance			
	Sample 1	Sample 2	Sample 3	Average
0	0	0	0	0
10	0.412	0.414	0.415	0.414
20	0.813	0.82	0.816	0.816
30	1.22	1.227	1.231	1.226
40	1.641	1.645	1.639	1.642
50	2.042	2.039	2.046	2.042

Appendix C – Raw Data Calculations

The volume, pH, redox potential, ferrous iron concentration, total iron concentration and the copper concentration were all provided as measured values.

Moisture content calculation:

$$Moisture\ \_content\ \_[\%] = \frac{(Wet\ \_mass\ \_[g]) - (Dry\ \_mass\ \_[g])}{Wet\ \_mass\ \_[g\}} \times 100\ \%$$

Copper recovery calculations:

$$Mass\ \_copper\ \_extracted\ \_[g] = \frac{Copper\ \_concentrat\ ion\ \_[mg\ /l]) \times (Effluent\ \_volume\ \_[ml]}{1000\ \times 1000}$$

$$Copper\ \_re\ \mathrm{cov}\ ery\ \_[\%] = \frac{Mass\ \_copper\ \_extracted\ \_[g]}{Total\ \_mass\ \_copper\ \_in\ \_ore\ \_[g]} \times 100\ \_[\%]$$

The planktonic cell counts were determined by:

$$Planktonic\ \_cells = Effluent\ \_sample\ \_volume\ \_[ml] \times Effluent\ \_cell\ \_concentrat\ ion\ \_[cells\ /ml]$$

The interstitial cell densities were determined from:

$$Interstiti\ al\ \_cell\ \_density\ \_[cell\ /kg\ \_ore] = \frac{Volume\ \_collected\ \_in\ \_wash\ \_1\ \_[ml] \times Cell\ \_concentrat\ ion\ \_[cells\ /ml]}{Mass\ \_of\ \_ore\ \_sample}$$

The loosely attached cell densities were determined from:

$$Loosely\ \_cell\ \_density\ \_[cell\ /kg\ \_ore] = \frac{Volume\ \_collected\ \_in\ \_wash\ \_2,3\ \&\ 4\ \_[ml] \times Cell\ \_concentrat\ ion\ \_[cells\ /ml]}{Mass\ \_of\ \_ore\ \_sample}$$

The strongly attached cell densities were determined from:

$$Interstiti\ al\ \_cell\ \_density\ \_[cell\ /kg\ \_ore] = \frac{Volume\ \_collected\ \_in\ \_wash\ \_5\ \&\ 6\ \_[ml] \times Cell\ \_concentrat\ ion\ \_[cells\ /ml]}{Mass\ \_of\ \_ore\ \_sample}$$

Plots of Ln [cell number] as a function of the leaching time were used to obtain the growth rates, assuming exponential growth illustrated by the Malthus equation.

$$\frac{dX}{dt} = \mu X$$

Figure D1 and D2 show the growth rates attained from the gradient of the straight line graph. Units were converted from day^{-1} to h^{-1}. Note: Col 1, 2 and 3 represent 2, 6 and 18 l/m^2/h respectively.

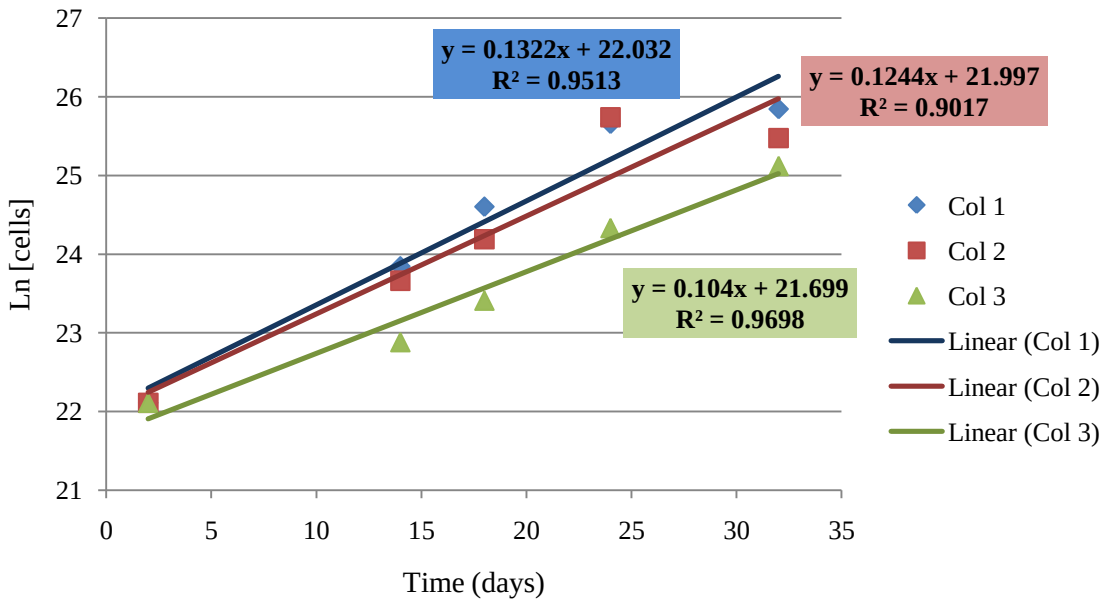

Figure C.1: Growth rate calculation for the column leaching of low grade copper-bearing ore with a mixed mesophilic culture, given for run 2.

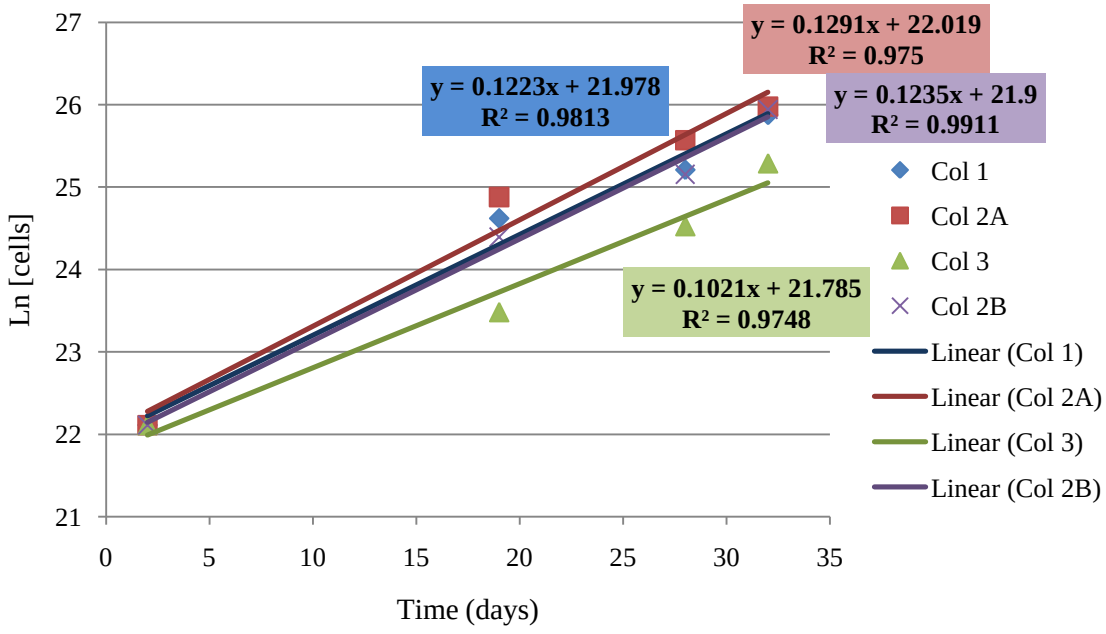

Figure C.2: Growth rate calculation for the column leaching of low grade copper-bearing ore with a mixed mesophilic culture, given for run 3.

Appendix D – Supporting Data

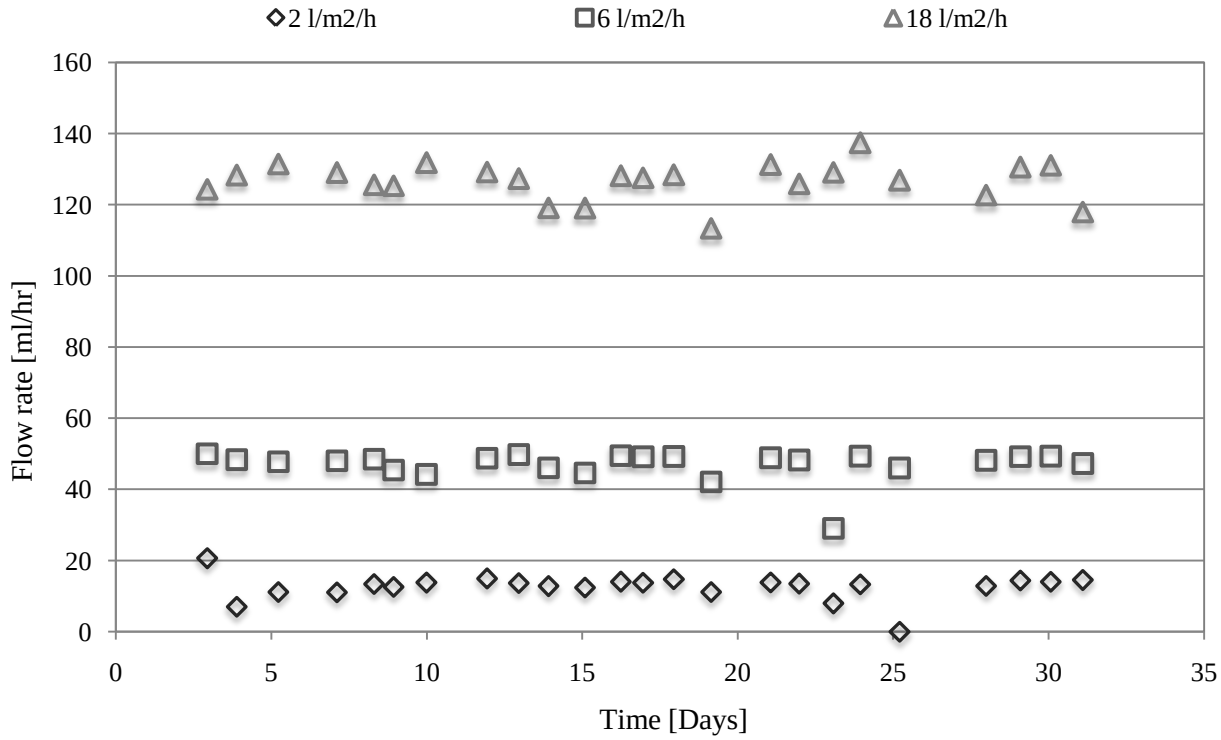

Figure D.1: Effluent flow rate profile during the column leaching of low grade copper-bearing ore with a mixed mesophilic culture, given for irrigation rates 2, 6 and 18 l/m^2/h in run 2

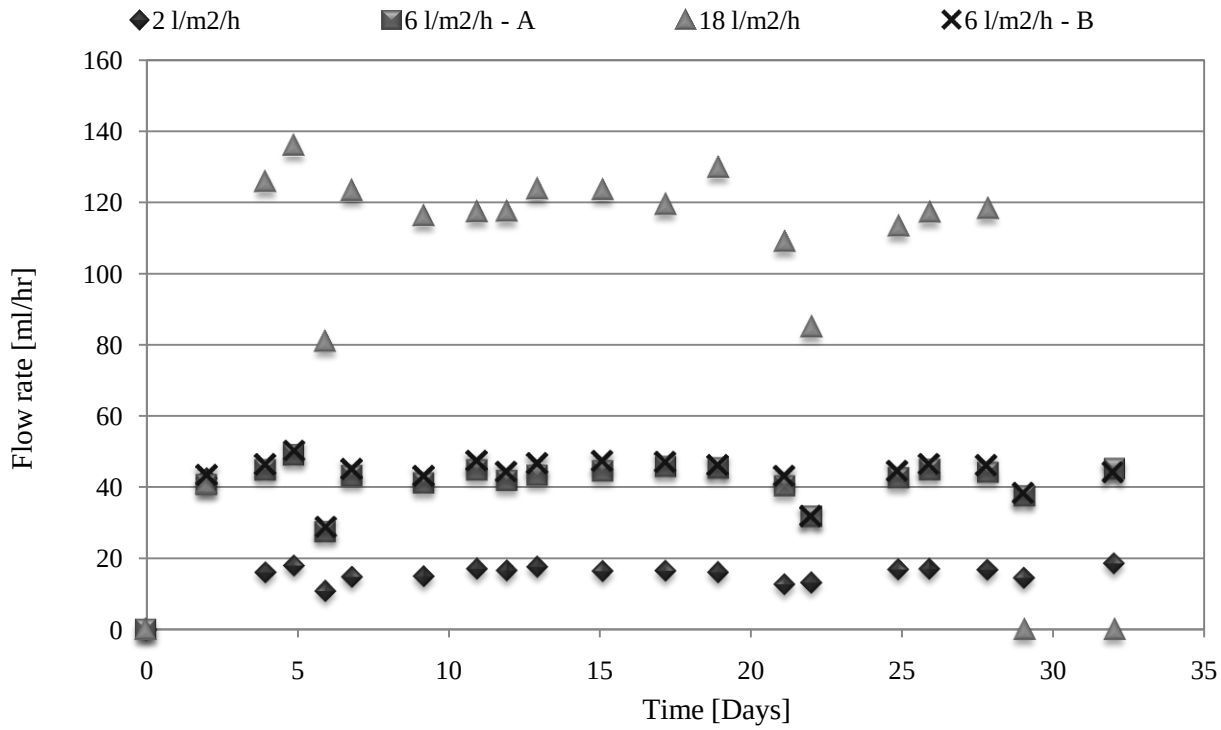

Figure D.2: Effluent flow rate profile during the column leaching of low grade copper-bearing ore with a mixed mesophilic culture, given for irrigation rates 2, 6 and 18 l/m^2/h in run 3

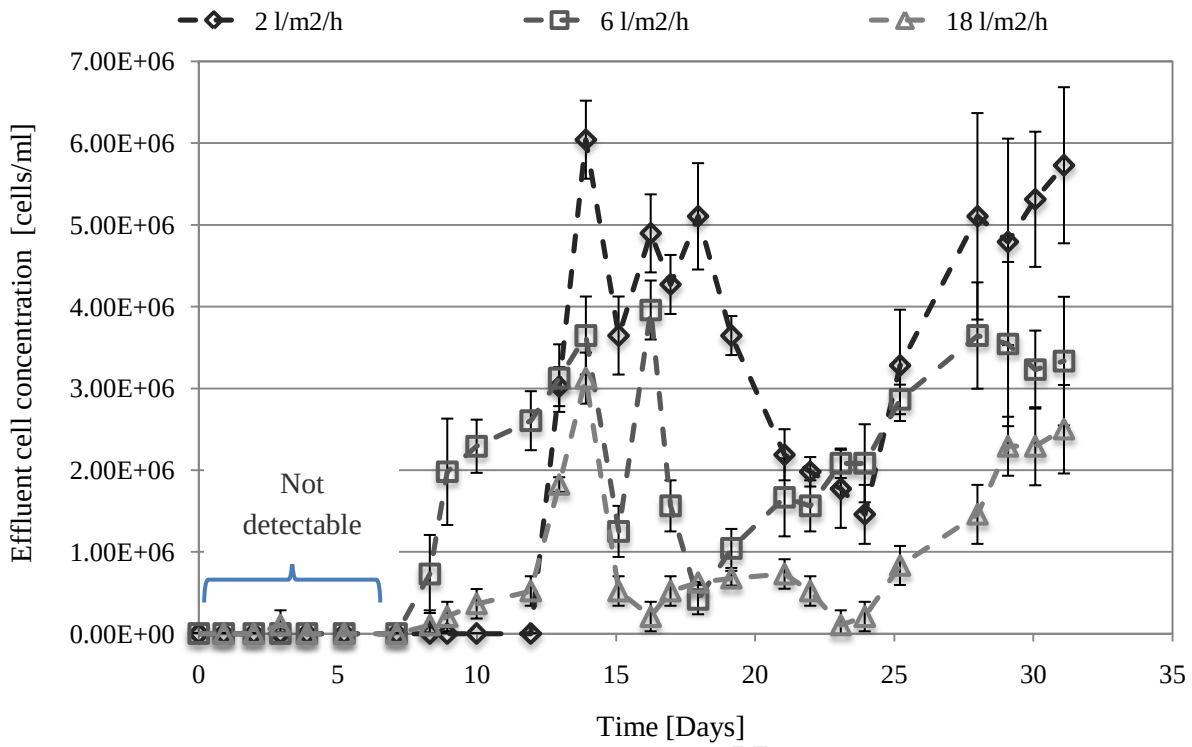

Figure D.3: Trend in cell concentration exported from the heap during the column leaching of low grade copper-bearing ore with a mixed mesophilic culture, given for irrigation rates 2, 6 and 18 l/m^2/h in r un 2.

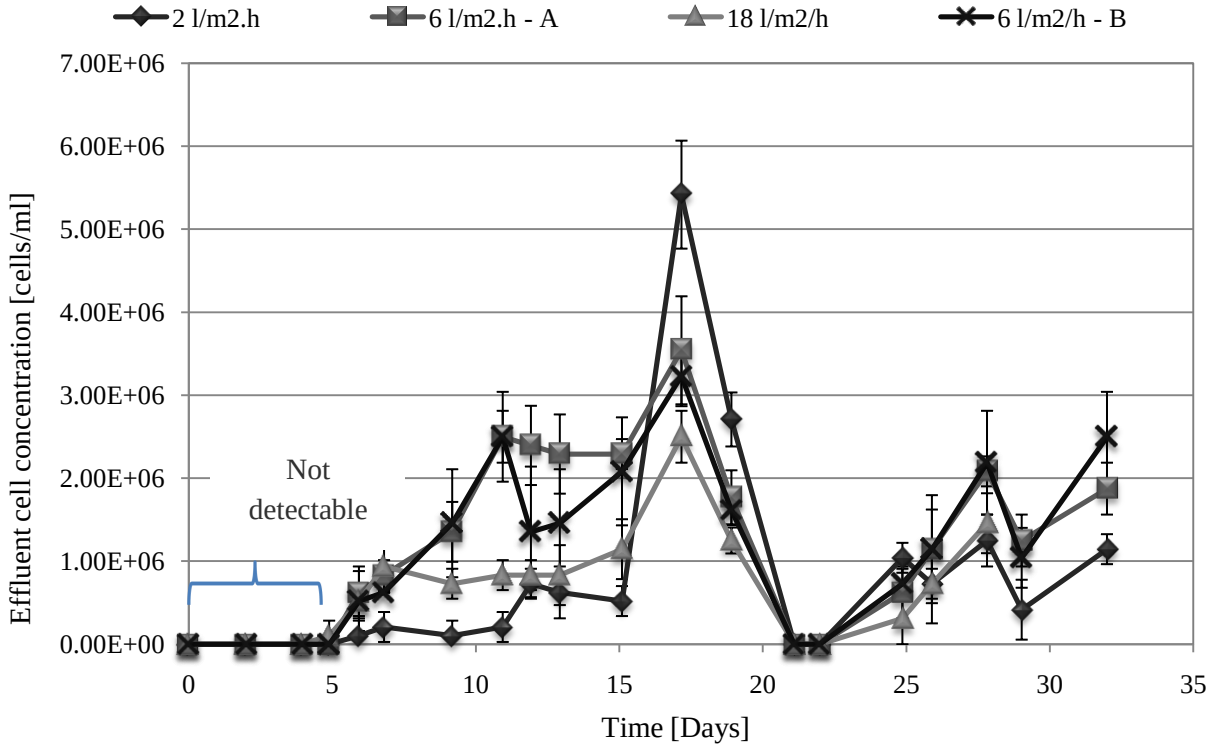

Figure D.3: Trend in cell concentration exported from the heap during the column leaching of low grade copper-bearing ore with a mixed mesophilic culture, given for irrigation rates 2, 6 and 18 l/m^2/h in run 3.

(a)

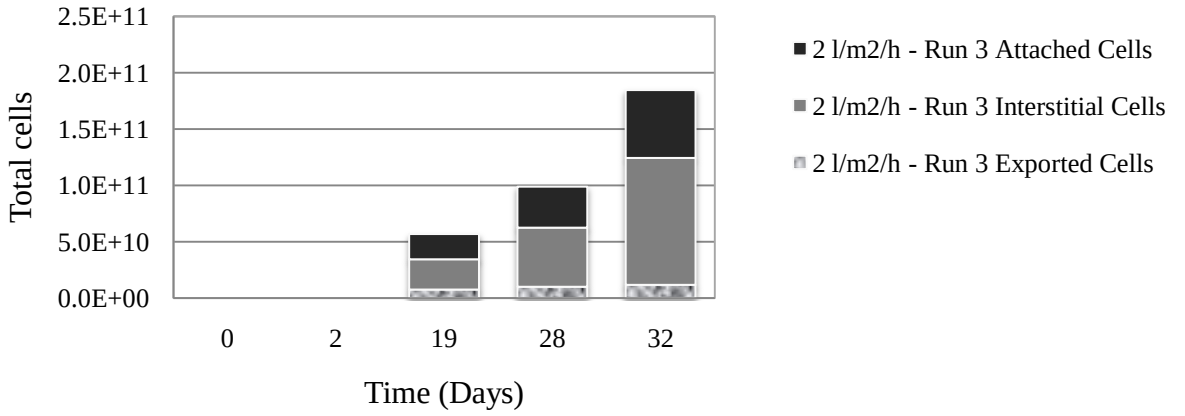

(b)

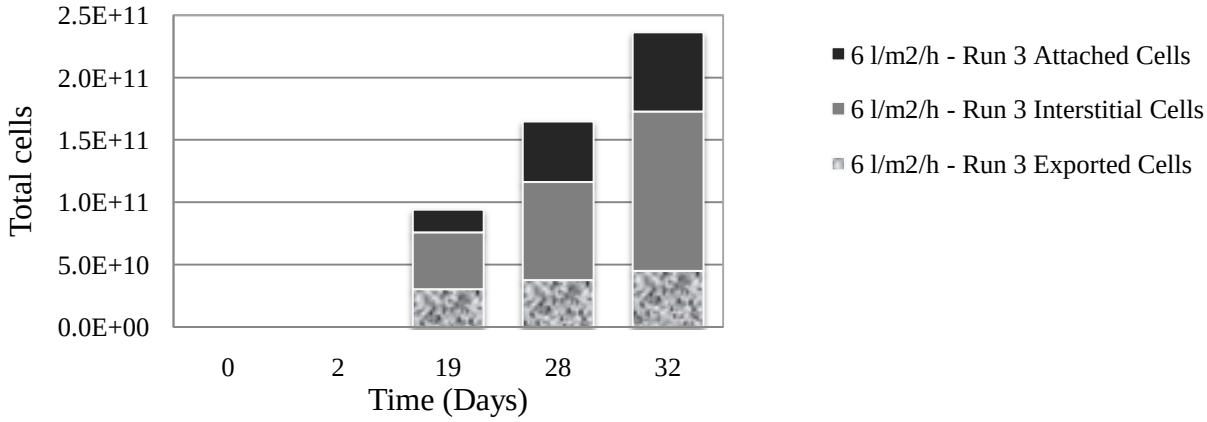

(c)

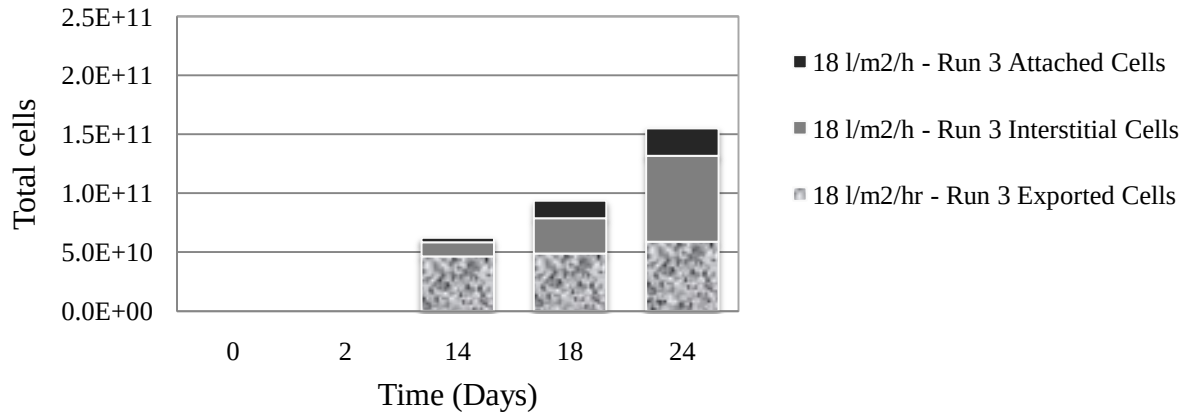

Figure D:4 Microbial attachment to the low grade copper bearing ore body in the column reactors, determined from the mechanical detachment of cells from the ore samples periodically removed from the heap systems using the in-bed sampling technique, given for different irrigation rates 2, 6 and L/m^2.h for run 2.

Appendix E – MATLAB® Code

This is an example of the MATLAB® code used to generate the colour coded plots for the moisture contents and the cell densities, given for the initial moisture contents determined on day 24.

```
% CODE STARTS
% .....................................................................
clear all
clc
close all

A = [9.07 10.21 8.58;
   8.35 8.27 8.11;
   8.41 8.78 7.53;];

x = [100 300 500];
y = [200 600 1000];

figure(1)
pixplot(x,y,A)
caxis([5 20])
colorbar
xlabel('horizontal distance,[cm]')
ylabel('vertical distance, [cm]')
% .....................................................................
% CODE ENDS
```

Appendix F – Raw Data

Preliminary Run Data

Leach Run Time [Days]	Effluent Volume [ml]			Effluent redox potential [mV]			Effluent pH			Fe^{2+} Absorbance on Spectrophotometer			Fe^{2+} [g/L] in pls			Cu extracted [g]			% Cumulative Cu extracted		
	Col 1	Col 2	Col 3	Col 1	Col 2	Col 3	Col 1	Col 2	Col 3	Col 1	Col 2	Col 3	Col 1	Col 2	Col 3	Col 1	Col 2	Col 3	Col 1	Col 2	Col 3
00:00																					
0.78	805	845	830	390	390	365	0.89	0.86	0.91				0.391	0.331	0.615	0.55	0.45	1.32	2.0	1.7	4.9
1.72	1041	1109	1145	386	388	366	1.17	1.12	1.30												
1.99	240	260	320	384	387	371	1.17	1.16	1.30												
2.11	36	134	374	387	434	392	1.23	1.22	1.30												
2.24	43	134	367	392	454	396	1.29	1.21	1.26												
2.35	38	103	320	396	437	400	1.34	1.24	1.27												
2.72	136	410	1130	407	423	403	1.40	1.24	1.27	0.53	0.65	0.57	0.130	0.158	0.140						
2.80	28	86	245	419	425	413	1.44	1.26	1.28												
2.89	25	81	228	420	426	407	1.43	1.23	1.28												
3.84	292	1020	2790	425	434	416	1.44	1.22	1.25	0.46	0.41	0.60	0.113	0.099	0.146	0.12	0.18	0.34	2.5	2.3	6.1
6.82	990	3260	8580	482	638	557	1.46	1.23	1.25	0.77	0.09	0.12	0.094	0.002	0.003						
7.91	365	1162	3128	626	645	648	1.39	1.23	1.20	0.11	0.09	0.07	0.003	0.002	0.002						
8.78	284	950	2480	610	622	630	1.25	1.21	1.22	0.28	0.16	0.11	0.007	0.004	0.003						
9.84	355	1180	3110	617	624	632	1.39	1.28	1.30	0.11	0.09	0.08	0.003	0.002	0.002						
11.01	375	1270	3425	614	615	632	1.47	1.32	1.28	0.12	0.09	0.08	0.003	0.002	0.002	0.12	0.14	0.29	2.9	2.9	7.2
13.82	930	3060	8360	644	648	646	1.26	1.16	1.15	0.19	0.18	0.16	0.005	0.004	0.004						
14.84	340	1120	3030	635	638	642	1.23	1.11	1.08	0.14	0.10	0.09	0.004	0.002	0.002						
15.78	300	1020	2720	650.5	646	644	1.25	1.15	1.13	0.17	0.14	0.12	0.004	0.003	0.003						
16.95	375	1260	3390	592	606	586	1.21	1.14	1.09	0.12	0.08	0.08	0.003	0.002	0.002						

Leach Run Time [Days]	Effluent Volume [ml]			Effluent redox potential [mV]			Effluent pH			Fe^{2+} Absorbance on Spectrophotometer			Fe^{2+} [g/L] in pls			Cu extracted [g]			% Cumulative Cu extracted		
	Col 1	Col 2	Col 3	Col 1	Col 2	Col 3	Col 1	Col 2	Col 3	Col 1	Col 2	Col 3	Col 1	Col 2	Col 3	Col 1	Col 2	Col 3	Col 1	Col 2	Col 3
17.85	275	960	2530	524	579	606	1.22	1.10	1.08	0.11	0.08	0.08	0.003	0.002	0.002	0.68	0.71	1.12	5.5	5.5	11.3
20.84	920	3240	8600	635.5	625	648.5	1.25	1.13	1.09	0.11	0.09	0.07	0.003	0.002	0.002				5.5	5.5	11.3
21.82	300	1000	2740	638	633	607	1.35	1.23	1.22	0.14	0.10	0.08	0.004	0.002	0.002						
22.83	310	1100	2960	560	593	585	1.40	1.25	1.22	0.17	0.09	0.09	0.004	0.002	0.002						
23.84	300	1080	2980	651	583	648	1.42	1.26	1.22	0.13	0.09	0.08	0.003	0.002	0.002						
24.80	300	1080	2820	599	586	616	1.38	1.25	1.22	0.17	0.09	0.07	0.004	0.002	0.002	0.58	0.53	0.89	7.6	7.5	14.6
27.86	940	3260	8950	675	675	667.5	1.39	1.22	1.21	0.12	0.07	0.07	0.003	0.002	0.002						
28.79	285	1030	2745	677	674	674	1.36	1.19	1.19	0.10	0.06	0.06	0.002	0.001	0.001						
29.92	350	1240	3450	666	667	668	1.37	1.19	1.21	0.10	0.07	0.06	0.002	0.002	0.001						
31.89	620	2160	5960	639	638	635	1.38	1.19	1.18	0.10	0.07	0.06	0.002	0.002	0.002	0.541	0.4	0.83	9.6	8.9	17.7
34.82	900	3160	8340	675	657	669	1.35	1.19	1.18	0.10	0.05	0.06	0.002	0.001	0.001						
36.02	360	1300	3420	683	672	655	1.36	1.16	1.20	0.10	0.04	0.05	0.002	0.001	0.001						
36.81	240	840	2220	655	656	654	1.37	1.18	1.20	0.10	0.05	0.06	0.003	0.001	0.001						
37.81	300	1090	2840	684	677	671	1.36	1.17	1.18	0.10	0.05	0.06	0.002	0.001	0.001						
42.06	1160	5350	12700	661	623	615	1.37	1.19	1.19	0.11	0.05	0.06	0.003	0.001	0.001	0.67	0.67	0.97			
42.95	285	960	2380	640	650	642	1.37	1.20	1.20	0.11	0.05	0.06	0.003	0.001	0.001						
43.90	290	1200	2500	677	672	669	1.37	1.22	1.21	0.11	0.06	0.07	0.003	0.002	0.002						
44.90	300	1040	2580	678	684	682	1.36	1.20	1.19	0.11	0.06	0.07	0.003	0.002	0.002						
45.79	305	1000	2510	665	662	663	1.35	1.19	1.18	0.11	0.10	0.08	0.003	0.003	0.002						
48.91	940	3370	9670	676	670	671	1.36	1.20	1.19	0.11	0.10	0.07	0.003	0.002	0.002						
49.99	355	1180	2980	685	673	674	1.38	1.21	1.20	0.12	0.07	0.06	0.003	0.002	0.001						
52.84	900	3080	7650	657	648	646	1.38	1.26	1.20	0.12	0.07	0.06	0.003	0.002	0.001						
56.91	1030	3560	10250	668	620	638	1.36	1.20	1.16	0.12	0.08	0.06	0.003	0.002	0.001						

2 l/m^2/h

	Cell concentration [cells/ml]							
Days	Sample 1	Sample 2	Sample 3	Average	Stddev	Cells	Cumulative cells no.	Cumulative error
0.00				0.00E+00		0.00E+00	0.00E+00	0.00E+00
				0.00E+00		0.00E+00	0.00E+00	0.00E+00
1.99	0.00E+00	0.00E+00	0.00E+00	0.00E+00	0.00E+00	0.00E+00	0.00E+00	0.00E+00
2.11	6.25E+05	3.13E+05	3.13E+05	4.17E+05	1.80E+05	1.50E+07	1.50E+07	6.50E+06
2.24	1.56E+06	2.50E+06		2.03E+06	6.63E+05	8.73E+07	1.02E+08	3.50E+07
2.35	2.19E+06	1.25E+06	3.44E+06	1.00E+00	1.10E+06	3.80E+01	1.02E+08	7.67E+07
2.72	2.81E+06	1.25E+06	2.19E+06	2.08E+06	7.86E+05	2.83E+08	3.86E+08	1.84E+08
3.84	0.00E+00	0.00E+00	0.00E+00	0.00E+00	0.00E+00	0.00E+00	3.86E+08	1.84E+08
6.82	9.38E+05	3.13E+05	6.25E+05	6.25E+05	3.13E+05	6.19E+08	1.00E+09	4.93E+08
7.91	2.81E+06	3.13E+06	2.81E+06	2.92E+06	1.80E+05	1.06E+09	2.07E+09	5.59E+08
8.78	1.88E+06	2.81E+06	2.19E+06	2.29E+06	4.77E+05	6.51E+08	2.72E+09	6.94E+08
9.84	1.88E+06	1.88E+06	1.56E+06	1.77E+06	1.80E+05	6.29E+08	3.35E+09	7.59E+08
11.01	1.25E+06	1.25E+06	6.25E+05	1.04E+06	3.61E+05	3.91E+08	3.74E+09	8.94E+08
13.82	6.25E+05	9.38E+05	1.25E+06	9.38E+05	3.13E+05	8.72E+08	4.61E+09	1.18E+09
14.84	9.38E+05	6.25E+05	9.38E+05	8.33E+05	1.80E+05	2.83E+08	4.89E+09	1.25E+09
15.78	6.25E+05	1.25E+06	3.13E+05	7.29E+05	4.77E+05	2.19E+08	5.11E+09	1.39E+09
16.95	6.25E+05	9.38E+05	9.38E+05	8.33E+05	1.80E+05	3.13E+08	5.43E+09	1.46E+09
17.85	3.13E+05	6.25E+05	3.13E+05	4.17E+05	1.80E+05	1.15E+08	5.54E+09	1.51E+09
20.84	1.25E+06	3.13E+05	3.13E+05	6.25E+05	5.41E+05	5.75E+08	6.12E+09	2.00E+09

2 l/m^2/h								
	Cell concentration [cells/ml]							
Days	Sample 1	Sample 2	Sample 3	Average	Stddev	Cells	Cumulative cells no.	Cumulative error
21.82	6.25E+05	1.25E+06	3.13E+05	7.29E+05	4.77E+05	2.19E+08	6.33E+09	2.15E+09
22.83	9.38E+05	1.25E+06	9.38E+05	1.04E+06	1.80E+05	3.23E+08	6.66E+09	2.20E+09
23.84	2.50E+06	2.19E+06	2.19E+06	2.29E+06	1.80E+05	6.88E+08	7.34E+09	2.26E+09
24.80	2.19E+06	2.19E+06	2.19E+06	2.19E+06	0.00E+00	6.56E+08	8.00E+09	2.26E+09
27.86	1.25E+06	1.25E+06	1.88E+06	1.46E+06	3.61E+05	1.37E+09	9.37E+09	2.60E+09
28.79	1.88E+06	1.25E+06	1.56E+06	1.56E+06	3.13E+05	4.45E+08	9.82E+09	2.69E+09
29.92	1.25E+06	1.88E+06	1.88E+06	1.67E+06	3.61E+05	5.83E+08	1.04E+10	2.81E+09
31.89	1.56E+06	1.25E+06	1.56E+06	1.46E+06	1.80E+05	9.04E+08	1.13E+10	2.92E+09
34.82	1.25E+06	1.25E+06	1.25E+06	1.25E+06	0.00E+00	1.13E+09	1.24E+10	2.92E+09
36.02	9.38E+05	1.56E+06	9.38E+05	1.15E+06	3.61E+05	4.13E+08	1.28E+10	3.05E+09
36.81	1.25E+06	1.56E+06	9.38E+05	1.25E+06	3.13E+05	3.00E+08	1.31E+10	3.13E+09
37.81	9.38E+05	1.56E+06	9.38E+05	1.15E+06	3.61E+05	3.44E+08	1.35E+10	3.24E+09
42.06	1.56E+06	1.25E+06	1.56E+06	1.46E+06	1.80E+05	1.69E+09	1.52E+10	3.45E+09
42.95	2.19E+06	1.56E+06	1.56E+06	1.77E+06	3.61E+05	5.05E+08	1.57E+10	3.55E+09
43.90	1.56E+06	1.88E+06	1.56E+06	1.67E+06	1.80E+05	4.83E+08	1.62E+10	3.60E+09
44.90	1.88E+06	2.19E+06	2.19E+06	2.08E+06	1.80E+05	6.25E+08	1.68E+10	3.66E+09
45.79	1.56E+06	1.88E+06	1.88E+06	1.77E+06	1.80E+05	5.40E+08	1.73E+10	3.71E+09
48.91	1.25E+06	1.56E+06	1.56E+06	1.46E+06	1.80E+05	1.37E+09	1.87E+10	3.88E+09

6 l/m^2/h

	Cell concentration [cells/ml]							
Days	Sample 1	Sample 2	Sample 3	Average	Stddev	Cells	Cumulative cells no.	Cumulative error
0.00				0.00E+00			0.00E+00	0.00E+00
				0.00E+00		0.00E+00	0.00E+00	0.00E+00
1.99	0.00E+00	0.00E+00	0.00E+00	0.00E+00	0.00E+00	0.00E+00	0.00E+00	0.00E+00
2.11	2.50E+06	2.19E+06		2.34E+06	2.21E+05	3.14E+08	3.14E+08	2.96E+07
2.24	5.63E+06	8.13E+06		6.88E+06	1.77E+06	9.21E+08	1.24E+09	2.66E+08
2.35	4.38E+06	6.25E+06	2.81E+06	4.48E+06	1.72E+06	4.61E+08	1.70E+09	4.44E+08
2.72	0.00E+00	6.25E+05	3.13E+05	3.13E+05	3.13E+05	1.28E+08	1.82E+09	5.72E+08
3.84	6.25E+05	9.38E+05	0.00E+00	5.21E+05	4.77E+05	5.31E+08	2.36E+09	1.06E+09
6.82	2.19E+06	1.56E+06	2.19E+06	1.98E+06	3.61E+05	6.45E+09	8.81E+09	2.24E+09
7.91	3.13E+06	2.50E+06	3.13E+06	2.92E+06	3.61E+05	3.39E+09	1.22E+10	2.65E+09
8.78	3.13E+06	2.81E+06	2.81E+06	2.92E+06	1.80E+05	2.77E+09	1.50E+10	2.83E+09
9.84	2.50E+06	2.81E+06	2.50E+06	2.60E+06	1.80E+05	3.07E+09	1.80E+10	3.04E+09
11.01	2.19E+06	2.50E+06	2.50E+06	2.40E+06	1.80E+05	3.04E+09	2.11E+10	3.27E+09
13.82	2.50E+06	1.88E+06	1.88E+06	2.08E+06	3.61E+05	6.38E+09	2.75E+10	4.37E+09
14.84	6.25E+05	1.56E+06	1.25E+06	1.15E+06	4.77E+05	1.28E+09	2.87E+10	4.91E+09
15.78	3.13E+05	1.25E+06	1.25E+06	9.38E+05	5.41E+05	9.56E+08	2.97E+10	5.46E+09
16.95	1.25E+06	9.38E+05	6.25E+05	9.38E+05	3.13E+05	1.18E+09	3.09E+10	5.85E+09
17.85	6.25E+05	6.25E+05	9.38E+05	7.29E+05	1.80E+05	7.00E+08	3.16E+10	6.03E+09

6 l/m^2/h								
	Cell concentration [cells/ml]							
Days	Sample 1	Sample 2	Sample 3	Average	Stddev	Cells	Cumulative cells no.	Cumulative error
20.84	9.38E+05	1.25E+06	9.38E+05	1.04E+06	1.80E+05	3.38E+09	3.50E+10	6.61E+09
21.82	1.88E+06	1.25E+06	2.19E+06	1.77E+06	4.77E+05	1.77E+09	3.67E+10	7.09E+09
22.83	1.25E+06	1.88E+06	2.19E+06	1.77E+06	4.77E+05	1.95E+09	3.87E+10	7.61E+09
23.84	2.50E+06	3.13E+06	2.50E+06	2.71E+06	3.61E+05	2.93E+09	4.16E+10	8.00E+09
24.80	9.38E+05	1.56E+06	1.88E+06	1.46E+06	4.77E+05	1.58E+09	4.32E+10	8.52E+09
27.86	2.81E+06	1.56E+06	2.19E+06	2.19E+06	6.25E+05	7.13E+09	5.03E+10	1.06E+10
28.79	2.19E+06	3.44E+06	2.19E+06	2.60E+06	7.22E+05	2.68E+09	5.30E+10	1.13E+10
29.92	9.38E+05	2.19E+06	1.25E+06	1.46E+06	6.51E+05	1.81E+09	5.48E+10	1.21E+10
31.89	1.56E+06	3.13E+05	9.38E+05	9.38E+05	6.25E+05	2.03E+09	5.68E+10	1.35E+10
34.82	9.38E+05	1.56E+06	9.38E+05	1.15E+06	3.61E+05	3.62E+09	6.04E+10	1.46E+10
36.02	1.88E+06	1.25E+06	1.88E+06	1.67E+06	3.61E+05	2.17E+09	6.26E+10	1.51E+10
36.81	1.88E+06	1.88E+06	2.19E+06	1.98E+06	1.80E+05	1.66E+09	6.43E+10	1.52E+10
37.81	1.56E+06	1.88E+06	1.88E+06	1.77E+06	1.80E+05	1.93E+09	6.62E+10	1.54E+10
42.06	1.25E+06	1.88E+06	6.25E+05	1.25E+06	6.25E+05	6.69E+09	7.29E+10	1.88E+10
42.95	9.38E+05	6.25E+05	1.25E+06	9.38E+05	3.13E+05	9.00E+08	7.38E+10	1.91E+10
43.90	1.25E+06	1.25E+06	6.25E+05	1.04E+06	3.61E+05	1.25E+09	7.50E+10	1.95E+10
44.90	6.25E+05	6.25E+05	9.38E+05	7.29E+05	1.80E+05	7.58E+08	7.58E+10	1.97E+10
45.79	9.38E+05	9.38E+05	1.25E+06	1.04E+06	1.80E+05	1.04E+09	7.68E+10	1.99E+10
48.91	1.25E+06	6.25E+05	9.38E+05	9.38E+05	3.13E+05	3.16E+09	8.00E+10	2.09E+10

18 l/m^2/h

	Cell concentration [cells/ml]							
Days	Sample 1	Sample 2	Sample 3	Average	Stddev	Cells	Cumulative cells no.	Cumulative error
0.00				0.00E+00			0.00E+00	0.00E+00
				0.00E+00		0.00E+00	0.00E+00	0.00E+00
1.99	0.00E+00	0.00E+00	0.00E+00	0.00E+00	0.00E+00	0.00E+00	0.00E+00	0.00E+00
2.11	1.56E+06	2.19E+06		1.88E+06	4.42E+05	7.01E+08	7.01E+08	1.65E+08
2.24	3.13E+05	3.13E+05	0.00E+00	2.08E+05	1.80E+05	7.65E+07	7.78E+08	2.32E+08
2.35	0.00E+00	3.13E+05	0.00E+00	1.04E+05	1.80E+05	3.33E+07	8.11E+08	2.89E+08
2.72	0.00E+00	0.00E+00	0.00E+00	0.00E+00	0.00E+00	0.00E+00	8.11E+08	2.89E+08
3.84	0.00E+00	0.00E+00	0.00E+00	0.00E+00	0.00E+00	0.00E+00	8.11E+08	2.89E+08
6.82	2.19E+06	4.69E+06	3.44E+06	3.44E+06	1.25E+06	2.95E+10	3.03E+10	1.10E+10
7.91	3.75E+06	3.13E+06	2.50E+06	3.13E+06	6.25E+05	9.78E+09	4.01E+10	1.30E+10
8.78	3.13E+06	3.75E+06	3.13E+06	3.33E+06	3.61E+05	8.27E+09	4.83E+10	1.39E+10
9.84	3.44E+06	4.69E+06	4.06E+06	4.06E+06	6.25E+05	1.26E+10	6.10E+10	1.58E+10
11.01	4.38E+06	3.13E+06	3.75E+06	3.75E+06	6.25E+05	1.28E+10	7.38E+10	1.79E+10
13.82	3.13E+06	3.75E+06	3.75E+06	3.54E+06	3.61E+05	2.96E+10	1.03E+11	2.10E+10
14.84	1.56E+06	2.19E+06	2.81E+06	2.19E+06	6.25E+05	6.63E+09	1.10E+11	2.29E+10
15.78	9.38E+05	2.50E+06	2.19E+06	1.88E+06	8.27E+05	5.10E+09	1.15E+11	2.51E+10
16.95	1.56E+06	2.19E+06	9.38E+05	1.56E+06	6.25E+05	5.30E+09	1.20E+11	2.72E+10
17.85	9.38E+05	1.56E+06	1.88E+06	1.46E+06	4.77E+05	3.69E+09	1.24E+11	2.84E+10
20.84	2.19E+06	2.19E+06	1.25E+06	1.88E+06	5.41E+05	1.61E+10	1.40E+11	3.31E+10

18 l/m^2/h

Cell concentration [cells/ml]								
Days	Sample 1	Sample 2	Sample 3	Average	Stddev	Cells	Cumulative cells no.	Cumulative error
21.82	1.56E+06	2.81E+06	2.50E+06	2.29E+06	6.51E+05	6.28E+09	1.47E+11	3.49E+10
22.83	2.19E+06	2.81E+06	1.56E+06	2.19E+06	6.25E+05	6.48E+09	1.53E+11	3.67E+10
23.84	2.81E+06	3.75E+06	3.13E+06	3.23E+06	4.77E+05	9.62E+09	1.63E+11	3.81E+10
24.80	2.19E+06	2.50E+06	2.81E+06	2.50E+06	3.13E+05	7.05E+09	1.70E+11	3.90E+10
27.86	2.81E+06	2.50E+06	2.50E+06	2.60E+06	1.80E+05	2.33E+10	1.93E+11	4.06E+10
28.79	2.50E+06	2.19E+06	2.81E+06	2.50E+06	3.13E+05	6.86E+09	2.00E+11	4.15E+10
29.92	2.81E+06	1.88E+06	2.19E+06	2.29E+06	4.77E+05	7.91E+09	2.08E+11	4.31E+10
31.89	9.38E+05	1.88E+06	6.25E+05	1.15E+06	6.51E+05	6.83E+09	2.15E+11	4.70E+10
34.82	2.50E+06	1.56E+06	1.88E+06	1.98E+06	4.77E+05	1.65E+10	2.31E+11	5.10E+10
36.02	1.56E+06	2.19E+06	1.56E+06	1.77E+06	3.61E+05	6.06E+09	2.37E+11	5.22E+10
36.81	1.88E+06	2.50E+06	2.19E+06	2.19E+06	3.13E+05	4.86E+09	2.42E+11	5.29E+10
37.81	1.25E+06	1.56E+06	2.19E+06	1.67E+06	4.77E+05	4.73E+09	2.47E+11	5.43E+10
42.06	9.38E+05	6.25E+05	1.56E+06	1.04E+06	4.77E+05	1.32E+10	2.60E+11	6.03E+10
42.95	6.25E+05	1.56E+06	3.13E+05	8.33E+05	6.51E+05	1.98E+09	2.62E+11	6.19E+10
43.90	9.38E+05	9.38E+05	1.88E+06	1.25E+06	5.41E+05	3.13E+09	2.65E+11	6.33E+10
44.90	1.25E+06	6.25E+05	1.56E+06	1.15E+06	4.77E+05	2.96E+09	2.68E+11	6.45E+10
45.79	6.25E+05	9.38E+05	6.25E+05	7.29E+05	1.80E+05	1.83E+09	2.70E+11	6.49E+10
48.91	3.13E+05	6.25E+05	1.25E+06	7.29E+05	4.77E+05	7.05E+09	2.77E+11	6.96E+10

Run 2 Column Data

		Detachment on 23/11/09			Detachment on 27/11/09			Detachment on 3/12/09			Detachment on 11/12/09		
		Column 1	Column 2	Column 3	Column 1	Column 2	Column 3	Column 1	Column 2	Column 3	Column 1	Column 2	Column 3
	Mass of Ore [g]	99.9	100.1	99.8	50.9	50.66	50.83	50.32	50.45	50.63	200.66	200.18	200.32
	Volume of Media added per wash [ml]	50	50	50	25	25	25	25	25	25	100	100	100
Media wash	Mass of centrifuge tube [g]	68.7	68.8	68	68.4	67.9	67.9	68.4	67.9	67.9	68.4	67.9	67.9
	Mass after sol + adjustment	129.7	129.7	129.7	95.1	95.1	95.1	96	96	96	177.5	177.5	177.5
	Mass Media added [g]	61	60.9	61.7	26.7	27.2	27.2	27.6	28.1	28.1	109.1	109.6	109.6
	Mass of centrifuge bottle after removal	82	80.3	85.5	75.4	74.5	77.6	77.1	74.8	77	95.2	99.3	105.7
	Mass of supernatant collected [g]	47.7	49.4	44.2	19.7	20.6	17.5	18.9	21.2	19	82.3	78.2	71.8
Media wash + vortex 1	Mass of centrifuge tube [g]	68.7	68.8	68	68.4	67.9	67.9	68.4	67.9	67.9	68.4	67.9	67.9
	Mass after sol + adjustment	128.5	128.5	128.5	102.2	102.2	103.7	102.9	102.9	102.9	214.9	214.9	214.9
	Mass Media added [g]	59.8	59.7	60.5	33.8	34.3	35.8	34.5	35	35	146.5	147	147
	Mass of centrifuge bottle after removal	71	70.3	72.8	76.6	75.8	79.1	78.3	75.7	78.6	98.5	103	117.8
	Mass of supernatant collected [g]	57.5	58.2	55.7	25.6	26.4	24.6	24.6	27.2	24.3	116.4	111.9	97.1
Media wash + vortex 2	Mass of centrifuge tube [g]	68.7	68.4	67.9	68.4	67.9	67.9	68.4	67.9	67.9	68.4	67.9	67.9
	Mass after sol + adjustment	123.6	123.6	123.6	102.7	102.7	105.9	104.4	104.4	104.4	199.3	199.3	199.3
	Mass Media added [g]	54.9	55.2	55.7	34.3	34.8	38	36	36.5	36.5	130.9	131.4	131.4
	Mass of centrifuge bottle after removal	71.9	70.5	72.9	76.8	75.9	79.2	78.3	76	78.8	101.4	104.4	102.7
	Mass of supernatant collected [g]	51.7	53.1	50.7	25.9	26.8	26.7	26.1	28.4	25.6	97.9	94.9	96.6
Media wash + vortex 3	Mass of centrifuge tube [g]	68.7	68.4	67.9	68.4	67.9	67.9	68.4	67.9	67.9	68.4	67.9	67.9
	Mass after sol + adjustment	123.8	123.8	123.8	102	102	104.1	102.6	102.6	102.6	207.2	207.2	207.2
	Mass Media added [g]	55.1	55.4	55.9	33.6	34.1	36.2	34.2	34.7	34.7	138.8	139.3	139.3
	Mass of centrifuge bottle after removal	71.9	70.7	74.3	76.9	75.8	79.5	78.4	75.8	79.4	102.7	105.6	106.2
	Mass of supernatant collected [g]	51.9	53.1	49.5	25.1	26.2	24.6	24.2	26.8	23.2	104.5	101.6	101
Tween wash + vortex 3	Mass of centrifuge tube [g]	68.7	68.4	67.9	68.4	67.9	67.9	68.4	67.9	67.9	68.4	67.9	67.9
	Mass after sol + adjustment	126.3	126.3	126.3	103.9	103.9	107.3	105.6	105.6	105.6	211.1	211.1	211.1
	Mass Media added [g]	57.6	57.9	58.4	35.5	36	39.4	37.2	37.7	37.7	142.7	143.2	143.2
	Mass of centrifuge bottle after removal	72.2	71	74.2	76.8	75.9	79.7	78.2	78.9	79.2	103.8	105.4	111.6
	Mass of supernatant collected [g]	54.1	55.3	52.1	27.1	28	27.6	27.4	26.7	26.4	107.3	105.7	99.5
Tween wash + vortex 3	Mass of centrifuge tube [g]	68.7	68.4	67.9	68.4	67.9	67.9	68.4	67.9	67.9	68.4	67.9	67.9
	Mass after sol + adjustment	124.1	124.1	124.1	103.5	103.5	106.7	103.2	103.2	103.2	207.7	207.7	207.7
	Mass Media added [g]	55.4	55.7	56.2	35.1	35.6	38.8	34.8	35.3	35.3	139.3	139.8	139.8
	Mass of centrifuge bottle after removal	70.2	71.4	73.6	76.9	76.2	79.9	78	76	79.4	103.7	105.8	108.3
	Mass of supernatant collected [g]	53.9	52.7	50.5	26.6	27.3	26.8	25.2	27.2	23.8	104	101.9	99.4

The volume, pH, redox, Fe^{2+}, Fe^{tot} and Cu data are not shown because it is similar to the data presented for the preliminary. The cell density data is not shown, to see typical data viz. the extensive raw data section for the box reactor experiment.

Run 3 Column Data

(No data displayed as the data similarity to the preliminary run and run 2.

Box Data

Effluent Volume [ml]															
Leach Run Time [Days]	Port 1	Port 2	Port 3	Port 4	Port 5	Port 6	Port 7	Port 8	Port 9	Port 10	Port 11	Port 12	Port 13	Total	Flow rate (ml/hr)
0.00	0	0	0	0	0	0	0	0	0	0	0	0	0	0	0
2.04	2000	760	700	690	4380	940	183	680	510	1000	1560	425	1450	15278	312
2.90	900	30	640	0	2825	330	70	490	128	650	690	120	680	7553	365
3.90	1000	40	540	0	3360	340	275	500	102	635	1210	80	640	8722	365
4.98	780	30	600	30	4110	126	410	350	124	760	1540	32	550	9442	364
5.90	690	30	415	0	3620	85	50	500	0	545	1450	50	465	7900	359
6.97	850	0	580	0	4120	100	240	370	0	635	1770	0	570	9235	360
9.92	2660	30	1560	42	11100	245	335	1430	0	1800	4670	175	1650	25697	363
11.91	3380	85	2660	0	11350	175	30	225	0	73	92	89	250	18409	385
12.84	1570	194	1190	0	5200	175	0	150	0	0	0	46	90	8615	384
13.85	1760	0	1230	50	5600	75	0	245	0	0	0	34	86	9080	374
15.03	1970	34	1320	30	6960	0	0	210	0	0	0	45	85	10654	378
16.91	3180	18	1980	18	11680	40	0	200	7	9	0	16	70	17218	382
17.86	1670	21	740	26	6100	38	0	24	0	0	0	0	50	8669	377
20.01	3740	24	2190	6	13300	150	0	67	0	15	0	7	110	19609	381
20.82	1400	22	750	5	5000	75	4	14	7	0	0	0	30	7307	375
21.99	2650	0	1130	2230	2430	2120	0	130	0	70	0	0	80	10840	388
25.09	4000	1020	1720	2330	12210	660	0	120	0	0	0	25	65	22150	297
26.10	1660	70	980	60	6370	21	0	18	0	0	0	10	21	9210	380
27.13	1660	100	950	75	6520	0	0	0	20	0	0	0	27	9352	378
27.88	1170	90	690	75	4850	0	0	13	11	0	0	0	13	6912	384
28.93	1620	95	1000	55	6830	0	0	28	0	0	0	19	0	9647	382
30.05	1740	70	1100	100	7280	32	0	31	0	0	0	20	0	10373	388
32.93	2800	210	1100	265	10440	1880	0	0	0	10	0	0	0	16705	242

Effluent Volume [ml]															
Leach Run Time [Days]	Port 1	Port 2	Port 3	Port 4	Port 5	Port 6	Port 7	Port 8	Port 9	Port 10	Port 11	Port 12	Port 13	Total	Flow rate (ml/hr)
35.11	2930	220	1840	150	12800	0	0	110	0	0	0	54	11	18115	346
38.83	4810	340	2450	415	21700	900	0	170	0	0	0	82	0	30867	346
39.85	1500	130	690	1720	2740	1540	0	55	0	0	0	25	0	8400	343
41.88	2670	930	1250	2800	6480	2165	0	380	0	0	0	90	0	16765	344
43.07	1680	60	830	1810	3800	1940	0	62	0	0	0	30	0	10212	357
45.09	2360	170	1130	260	9840	3040	0	0	0	0	0	0	0	16800	347
47.24	1860	0	1300	250	6420	360	640	0	0	0	0	400	0	11230	218
50.02	3380	0	2460	920	15500	850	265	360	0	0	0	180	0	23915	358
51.90	0	2230	1540	1480	9600	670	0	350	0	0	0	60	0	15930	354
52.92	1200	0	740	700	5650	300	0	100	0	0	0	110	0	8800	357
54.96	2365	0	1600	720	11550	760	0	200	0	0	0	150	0	17345	355
59.04	3540	0	2680	1640	18050	700	0	370	0	0	0	260	0	27240	278
61.00	2070	0	1900	600	10350	620	0	250	0	0	0	165	0	15955	339
64.13	3200	0	3230	1230	16700	910	0	480	0	0	0	220	0	25970	345
66.90	2660	0	2125	1160	16300	580	0	300	0	490	0	60	0	23675	357
67.87	1000	0	700	430	5810	240	0	84	0	0	0	280	0	8544	367
68.82	980	0	390	900	5440	240	0	130	0	0	0	0	0	8080	355
69.85	1200	0	560	830	5910	130	0	0	440	0	0	0	0	9070	365
73.88	2830	67	2950	750	14240	340	0	280	62	670	0	0	350	22539	233
79.88	3000	1300	2770	2240	14050	790	0	0	510	0	0	450	0	25110	175
81.90	2150	0	2250	930	9830	390	0	290	0	0	0	0	0	15840	327
84.44	2430	180	2500	1500	14440	700	0	250	0	0	0	140	0	22140	363
87.13	2500	0	2880	770	15600	145	0	210	0	160	0	100	0	22365	347
89.92	2430	0	3840	1060	14800	190	0	350	0	0	0	120	0	22790	340

Effluent Volume [ml]

Leach Run Time [Days]	Port 1	Port 2	Port 3	Port 4	Port 5	Port 6	Port 7	Port 8	Port 9	Port 10	Port 11	Port 12	Port 13	Total	Flow rate (ml/hr)
92.96	2940	60	1880	3150	16500	220		580				350		25680	352
96.81	3800	100	570	4600	22500	260		640				380		32850	355
99.83	3000		2350	2630	14600	280		320				300		23480	324
101.95	2100		1940	1240	11150	170		300				120		17020	335
104.88	2880	70	2050	2700	14430	290		350				160		22930	326
107.90	3020		2110	2980	15600	220		280				370		24580	339
111.90	4000		4380	1620	19940	400		510				100		30950	322

Effluent pH

Leach Run Time [Days]	Port 1	Port 2	Port 3	Port 4	Port 5	Port 6	Port 7	Port 8	Port 9	Port 10	Port 11	Port 12	Port 13	Average
0.00	-	-	-	-	-	-	-	-	-	-	-	-	-	-
2.04	4.773	5.026	4.806	5.331	5.013	5.129	5.228	5.216	5.277	5.082	4.791	5.155	5.019	5.065
2.90	3.896	4.048	3.955		4.07	4.509	4.275	4.565	4.641	4.386	4.206	4.352	4.203	4.259
3.90	3.009	3.033	3.037		3.183	3.706	3.616	3.984	3.733	3.314	3.118	3.546	3.174	3.371
4.98	2.481	2.39	2.45	2.462	2.594	3.674	3.223	3.327	3.031	2.608	2.494	2.719	2.473	2.764
5.90	2.126	2.23	2.08		2.233	3.399	2.83	2.935		2.934	2.127	2.327	2.13	2.486
6.97	1.987		1.93		2.078	2.389	2.613	2.698		2.052	1.968		1.963	2.186
9.92	1.83	1.798	1.785	1.814	1.983	2.488	2.376	2.421		1.884	1.806	1.843	1.856	1.990
11.91	1.357	1.322	1.331		1.351	1.523	2.125	1.848		1.749	1.756	1.753	1.741	1.623
12.84	1.146	1.145	1.145		1.148	1.259		1.437				1.627	1.564	1.309

Effluent pH														
Leach Run Time [Days]	Port 1	Port 2	Port 3	Port 4	Port 5	Port 6	Port 7	Port 8	Port 9	Port 10	Port 11	Port 12	Port 13	Average
13.85	1.143		1.146	1.153	1.15	1.156		1.293				1.495	1.392	1.241
15.03	1.151	1.149	1.147	1.156	1.203			1.234				1.319	1.3	1.207
16.91	1.237	1.173	1.227	1.186	1.26	1.253		1.566	1.456	1.343		1.376	1.617	1.336
17.86	1.229	1.187	1.233	1.196	1.27	1.306		1.665					1.72	1.351
20.01	1.332	1.254	1.326	1.241	1.338	1.389		1.749		1.447		1.425	1.795	1.430
20.82	1.302	1.256	1.294	2.001	1.323	1.44	1.092	1.761	1.394				1.844	1.471
21.99	1.275		1.28	1.294	1.319	1.345		1.519		1.465			1.546	1.380
25.09	1.157	1.159	1.214	1.209	1.168	1.312		1.19				1.244	1.3	1.217
26.10	1.149	1.157	1.152	1.159	1.149	1.201		1.198				1.211	1.2	1.175
27.13	1.148	1.149	1.162	1.157	1.144				1.184				1.201	1.164
27.88	1.248	1.215	1.191	1.147	1.19			1.153	1.248				1.351	1.218
28.93	1.152	1.147	1.156	1.15	1.149			1.256				1.34		1.193
30.05	1.178	1.149	1.163	1.147	1.19	1.184		1.404				1.397		1.227
32.93	1.39	1.364	1.354	1.261	1.34	1.397				1.265				1.339
35.11	1.297	1.264	1.255	1.231	1.222			1.455				1.546	1.416	1.336
38.83	1.227	1.216	1.233	1.148	1.245	1.291		1.557				1.61		1.316
39.85	1.281	1.278	1.287	1.281	1.304	1.327		1.493				1.441		1.337
41.88	1.294	1.295	1.301	1.304	1.325	1.336		1.476				1.329		1.333
43.07	1.229	1.227	1.249	1.242	1.259	1.246		1.405				1.247		1.263
45.09	1.258	1.256	1.259	1.258	1.284	1.3								1.269
47.24	1.236		1.219	1.187	1.24	1.294	1.248					1.289		1.245
50.02	1.232		1.229	1.212	1.243	1.257	1.328	1.45				1.224		1.272
51.90		1.237	1.213	1.256	1.246	1.255		1.298				1.211		1.245
52.92	1.16		1.148	1.146	1.157	1.174		1.263				1.184		1.176

Effluent pH														
Leach Run Time [Days]	Port 1	Port 2	Port 3	Port 4	Port 5	Port 6	Port 7	Port 8	Port 9	Port 10	Port 11	Port 12	Port 13	Average
54.96	1.216		1.21	1.216	1.213	1.235		1.402				1.154		1.235
59.04	1.318		1.274	1.293	1.321	1.346		1.491				1.28		1.332
61.00	1.192		1.189	1.209	1.226	1.24		1.345				1.204		1.229
64.13	1.168		1.164	1.161	1.188	1.214		1.316				1.153		1.195
66.90	1.226		1.238	1.234	1.241	1.254		1.368		1.273		1.147		1.248
67.87	1.261		1.272	1.271	1.288	1.303		1.528				1.295		1.317
68.82	1.265		1.285	1.277	1.295	1.314		1.474						1.318
69.85	1.246		1.247	1.244	1.276	1.26			1.321					1.266
73.88	1.304	1.186	1.295	1.343	1.308	1.319		1.456	1.309	1.345		1.351		1.322
79.88	1.257	1.289	1.253	1.248	1.266	1.31			1.343			1.302		1.284
81.90	1.277		1.289	1.274	1.292	1.291			1.347					1.295
84.44	1.209	1.21	1.213	1.227	1.218	1.302		1.229				1.178		1.223
87.13	1.218		1.219	1.231	1.237	1.222		1.348		1.238		1.221		1.242
89.92	1.248		1.25	1.24	1.264	1.252		1.372				1.219		1.264
92.96	1.239	1.194	1.246	1.243	1.264	1.247		1.349				1.234		1.252
96.81	1.234	1.206	1.24	1.248	1.263	1.231		1.318				1.253		1.249
99.83	1.248		1.249	1.261	1.294	1.28		1.304				1.179		1.259
101.95	1.257		1.245	1.261	1.283	1.291		1.37				1.262		1.281
104.88	1.218	1.176	1.224	1.231	1.247	1.258		1.396				1.183		1.242
107.90	1.233		1.242	1.247	1.259	1.244		1.368				1.299		1.270
111.90	1.241		1.25	1.25	1.266	1.279		1.365				1.166		1.260

Effluent redox potential [mV]														
Leach Run Time [Days]	Port 1	Port 2	Port 3	Port 4	Port 5	Port 6	Port 7	Port 8	Port 9	Port 10	Port 11	Port 12	Port 13	Average
0.00	-	-	-	-	-	-	-	-	-	-	-	-	-	-
2.04	289	310	295	284	297	306	311	313	306	307	310	313	310	304
2.90	265	299	268		266	289	293	285	299	274	268	289	267	280
3.90	257	264	257		255	253	252	261	253	256	253	273	255	257
5.90	313	312	310		306	268	277	284		283	306	294	307	296
6.97	323		322		316	308	290	293		316	320		322	312
9.92	342	343	344	338	333	295	304	301		337	341	340	342	330
11.91	392	395	394		392	380	318	351		347	346	348	352	365
12.84	402	402	401		401	393		394				371	382	393
13.85	401		400	402	400	394		392				374	385	394
15.03	401	399	400	400	399			383				382	384	394
16.91	399	402	397	398	398	396		373	380	386		383	373	390
17.86	394	398	392	393	391	390		372					368	387
20.01	403	420	402	404	402	396		373		381		378	370	393
20.82	397	415	395	399	394	386	392	371	392				364	391
21.99	392		394	394	392	390		384		398			396	393
25.09	398	413	404	396	395	395		395				375	367	393
26.10	405	403	400	403	405	406		406				406	398	404
27.13	402	398	401	395	400				397				395	398
27.88	447	449	446	445	443			415	405				394	431
28.93	445	451	447	443	440			410				394		433
30.05	446	458	449	444	439	424		403				394		432
32.93	455	467	461	465	454	447				409				451
Effluent redox potential [mV]														

Leach Run Time [Days]	Port 1	Port 2	Port 3	Port 4	Port 5	Port 6	Port 7	Port 8	Port 9	Port 10	Port 11	Port 12	Port 13	Average
35.11	482	492	486	475	473			408				395	402	452
38.83	624	656	657	527	501	483		411				397		532
39.85	677	657	669	609	522	495		442				430		563
41.88	674	693	680	678	662	534		465				473		607
43.07	648	679	670	691	658	678		471				464		620
45.09	708	703	704	707	693	576								682
47.24	711		712	712	695	638	554					668		670
50.02	688		698	698	701	701	683	610				547		666
51.90		695	700	704	698	703		667				579		678
52.92	697		702	705	703	706		685				681		697
54.96	694		701	702	706	704		692				626		689
59.04	710		712	715	717	715		693				707		710
61.00	692		702	707	708	709		694				704		702
64.13	701		703	709	708	711		704				709		706
66.90	698		697	704	707	705		701		701		711		703
67.87	665		709	633	697	713		676				690		683
68.82	706		708	711	717	703		646						699
69.85	703		697	698	699	711			658					694
73.88	682	692	699	701	694	679		662	693	655		687		684
79.88	719	725	720	726	716	722			714			716		720
81.90	714		714	714	717	719			710					715
84.44	689	687	705	707	715	708		710				707		704
87.13	684		695	707	708	713		709		711		708		704
89.92	715		724	724	722	727		721				712		721

Effluent redox potential [mV]

Leach Run Time [Days]	Port 1	Port 2	Port 3	Port 4	Port 5	Port 6	Port 7	Port 8	Port 9	Port 10	Port 11	Port 12	Port 13	Average
92.96	714	715	717	722	721	723		720				717		719
96.81	719	721	724	728	725	728		724				724		724
99.83	713		716	718	725	723		718				719		719
101.95	707		711	710	715	716		716				711		712
104.88	699	702	708	711	713	717		715				704		709
107.90	709		713	716	720	720		717				718		716
111.90	705		707	711	718	721		720				706		713

IN-BED SAMPLING 1	Zone 1	Zone 2	Zone 3	Zone 4	Zone 5	Zone 6	Zone 7	Zone 8	Zone 9
mass empty vessel (kg)	77.26	86.86	84.86	75.96	78.88	78.26	83.76	79.92	73.6
mass ore added (kg)	21.42	22.18	20.3	20.9	20.04	21.72	22	21.84	20.66
mass after drying (kg)	96.24	107.06	103.66	94.41	96.94	98.08	102.95	99.42	92.42
mass difference (kg)	18.98	20.2	18.8	18.45	18.06	19.82	19.19	19.5	18.82
moisture content (%)	**11.39**	**8.93**	**7.39**	**11.72**	**9.88**	**8.75**	**12.77**	**10.71**	**8.91**

IN-BED SAMPLING 2	Zone 1	Zone 2	Zone 3	Zone 4	Zone 5	Zone 6	Zone 7	Zone 8	Zone 9
mass empty vessel (kg)	77.8	86.94	85.22	76.06	79.59	75.74	63.28	80.62	73.69
mass ore added (kg)	20.74	21.39	20.65	21.22	20.46	20.08	20.92	21.32	21.55
mass after drying (kg)	95.21	106.7	103.74	96.19	96.56	94.08	82.02	99.28	93.39
mass difference (kg)	17.41	19.76	18.52	20.13	16.97	18.34	18.74	18.66	19.7
moisture content (%)	**16.06**	**7.62**	**10.31**	**5.14**	**17.06**	**8.67**	**10.42**	**12.48**	**8.58**

IN-BED SAMPLING 3	Zone 1	Zone 2	Zone 3	Zone 4	Zone 5	Zone 6	Zone 7	Zone 8	Zone 9
mass empty vessel (kg)	77.41	86.98	85.03	76.1	80.24	78.4	63.32	78.35	73.7
mass ore added (kg)	20.83	20.6	20.4	20.8	20.79	20.59	20.62	20.94	20.63
mass after drying (kg)	95.83	105.56	103.07	94.17	97.04	96.91	81.37	97.02	92.01
mass difference (kg)	18.42	18.58	18.04	18.07	16.8	18.51	18.05	18.67	18.31
moisture content (%)	**11.57**	**9.81**	**11.57**	**13.13**	**19.19**	**10.10**	**12.46**	**10.84**	**11.25**

	Effluent copper concentration [mg/l]												
Leach Run Time [Days]	Port 1	Port 2	Port 3	Port 4	Port 5	Port 6	Port 7	Port 8	Port 9	Port 10	Port 11	Port 12	Port 13
0.00	0	0	0	0	0	0	0	0	0	0	0	0	0
2.04	536	393	811	138	484	316	234	259	228	430	483	371	557
2.90	1543	1726	1616	0	1366	801	948	798	757	1467	1638	1541	1670
3.90	1793	2112	1915	0	1771	1454	1452	1341	1448	1809	1846	1976	1861
4.98	1436	1601	1452	1586	1505	1663	1432	1630	1700	2695	1325	1904	1351
5.90	1308	1811	1223	0	1357	1782	1659	1762	0	1755	1120	1559	1084
6.97	1040	0	908	0	1173	1663	1733	1878	0	1106	943	0	768
9.92	619.1	1209.98	525	864.56	900.92	1453.39	1340.27	1457.43	0	687.3	546.1	692.6	613
11.91	194.2	198.6	164.6		198	486.7	1605.9	870.2		570.1	608.6	730.6	683.9
12.84	111.1	117.3	106.3		148.5	343.1		586.7				840.8	703.7
13.85	93.95		89.94	171.1	140.6	336.5		585.7				973.6	776.4
15.03	108.6	177.8	79.37	136.4	134.2			665.6				809	784.3
16.91	60.49	82.21	60.95	87.03	90.58	429.8		747.4	1953.34	1177.66		895.1	1027.17

Effluent copper concentration [mg/l]													
Leach Run Time [Days]	Port 1	Port 2	Port 3	Port 4	Port 5	Port 6	Port 7	Port 8	Port 9	Port 10	Port 11	Port 12	Port 13
17.86	58.61	72.92	58.97	85.44	88.51	329.6		1175.64					1237.25
20.01	56.11	77.73	58.04	137.7	83.49	393		1285.73		2026.06		3355.22	1315.02
20.82	56.34	71.16	57.23	83.53	154.8	439.8	2800.73	1419.05	2552.27				1246.34
21.99	53.64		56.86	65.32	88.06	133.1		666.7		1106.96			698.3
25.09	814.8	788.5	122.5	128.3	119	165.3		393.1				681.8	957.3
26.10	70.31	76.98	53.68	77.87	83.84	26.65		97.85				2125.04	1259.47
27.13	58.02	58.17	57.57	93.33	83.72				1563.48				1485.71
27.88	109.5	108.9	104.2	121.6	147.2			1191.8	912.2				1839.21
28.93	102.4	93.44	95.3	123.7	138.8			1264.52				2054.34	
30.05	70.03	73.67	65.24	99.6	110.7	408.8		1216.04				2031.11	
32.93	126.4	129.3	121.2	98.72	131.9	203				2366.43			
35.11	100.4	103.6	105.9	147.5	132.5			1292.8				1624.08	2559.34
38.83	84.08	90.38	95.2	105	123.4	191.2		989.7				1727.1	
39.85	76.78	84.48	80.23	82.29	120.1	192.9		791.9				1605.9	
41.88	84.16	85.5	99.1	100.6	133.6	183.9		570.1				715.9	
43.07	100.4	110.2	106.6	104.2	139.1	114.9		703.9					
45.09	106.7	109.1	108.2	110.5	135.8	201.7							
47.24													
50.02	102.2		100	98	124.8	204.2	417.3	831.6					
51.90		78.58	119.5	82.74	141.1	223.8		646.8				243.4	
52.92	103.3		99.7	106.1	130	239.2		890.9				183.1	
54.96	67.49		71.17	70.7	95.54	218.9		950.1				335	
59.04	109.1		108.3	121.2	129.4	290.6		868.4				200.7	
61.00	82.63		119.6	86.73	131.4	255.6		734.5				229.1	
64.13	61.94		64.39	63.34	95.03	267.1		669.8				201.8	

Effluent copper concentration [mg/l]													
Leach Run Time [Days]	Port 1	Port 2	Port 3	Port 4	Port 5	Port 6	Port 7	Port 8	Port 9	Port 10	Port 11	Port 12	Port 13
66.90	63.01		74.72	64.58	92.12	240.7		815.8		335.5		234.7	
67.87	70.35		71.46	73.88	109	260.8		1208.97				219.1	
68.82	58.23		56.6	56.61	84.79	233.8		1034.24					
69.85	52.77		53.9	54.44	83.23	151.6		467					
73.88	96.5	101.1	103.3	145.3	110.8	224.9		730.1	612.6	437.3		367.5	
79.88	124.8	165.2	125.6	179.9	158.4	513.6			695.8			397	
81.90	51.69		54.89	48.74	88.05	211.2			749.2				
84.44	54.79	53.34	47.56	41.42	107.1	186.3		972.1				200.1	
87.13	50.65		53.62	69.36	94.3	143.7		969		722.6		220.1	
89.92	73.41		69.83	64.51	111.4	166.5		1129.18				206.2	

Cumulative copper extracted [g]															Cumulative Cu extracted [g]
Leach Run Time [Days]	Port 1	Port 2	Port 3	Port 4	Port 5	Port 6	Port 7	Port 8	Port 9	Port 10	Port 11	Port 12	Port 13	Total Cu	
0.00	0.00	0.00	0.00	0.00	0.00	0.00	0.00	0.00	0.00	0.00	0.00	0.00	0.00	0.00	0.00
2.04	1.07	0.30	0.57	0.10	2.12	0.30	0.04	0.18	0.12	0.43	0.75	0.16	0.81	6.94	0.76
2.90	2.46	0.35	1.60	0.10	5.98	0.56	0.11	0.57	0.21	1.38	1.88	0.34	1.94	17.49	1.92
3.90	4.25	0.44	2.64	0.10	11.93	1.06	0.51	1.24	0.36	2.53	4.12	0.50	3.13	32.80	3.60
4.98	5.37	0.48	3.51	0.14	18.11	1.27	1.10	1.81	0.57	4.58	6.16	0.56	3.88	47.54	5.22
5.90	6.28	0.54	4.01	0.14	23.03	1.42	1.18	2.69	0.57	5.54	7.78	0.64	4.38	58.20	6.39
6.97	7.16	0.54	4.54	0.14	27.86	1.58	1.59	3.38	0.57	6.24	9.45	0.64	4.82	68.52	7.52
9.92	8.81	0.57	5.36	0.18	37.86	1.94	2.04	5.47	0.57	7.48	12.00	0.76	5.83	88.87	9.76

Leach Run Time [Days]	Cumulative copper extracted [g]														Cumulative Cu extracted [g]
	Port 1	Port 2	Port 3	Port 4	Port 5	Port 6	Port 7	Port 8	Port 9	Port 10	Port 11	Port 12	Port 13	Total Cu	
11.91	9.46	0.59	5.80	0.18	40.11	2.02	2.09	5.66	0.57	7.52	12.06	0.83	6.00	92.89	10.20
12.84	9.64	0.61	5.92	0.18	40.88	2.09	2.09	5.75	0.57	7.52	12.06	0.86	6.07	94.24	10.35
13.85	9.80	0.61	6.04	0.19	41.67	2.11	2.09	5.90	0.57	7.52	12.06	0.90	6.13	95.58	10.49
15.03	10.02	0.62	6.14	0.19	42.60	2.11	2.09	6.04	0.57	7.52	12.06	0.93	6.20	97.09	10.66
16.91	10.21	0.62	6.26	0.19	43.66	2.13	2.09	6.19	0.59	7.53	12.06	0.95	6.27	98.74	10.84
17.86	10.31	0.62	6.30	0.20	44.20	2.14	2.09	6.21	0.59	7.53	12.06	0.95	6.33	99.52	10.93
20.01	10.52	0.62	6.43	0.20	45.31	2.20	2.09	6.30	0.59	7.56	12.06	0.97	6.48	101.32	11.12
20.82	10.60	0.63	6.47	0.20	46.08	2.23	2.10	6.32	0.60	7.56	12.06	0.97	6.51	102.34	11.23
21.99	10.74	0.63	6.54	0.34	46.30	2.51	2.10	6.41	0.60	7.64	12.06	0.97	6.57	103.40	11.35
25.09	14.00	1.43	6.75	0.64	47.75	2.62	2.10	6.45	0.60	7.64	12.06	0.99	6.63	109.67	12.04
26.10	14.11	1.44	6.80	0.65	48.28	2.62	2.10	6.45	0.60	7.64	12.06	1.01	6.66	110.43	12.12
27.13	14.21	1.44	6.86	0.65	48.83	2.62	2.10	6.45	0.63	7.64	12.06	1.01	6.70	111.21	12.21
27.88	14.34	1.45	6.93	0.66	49.54	2.62	2.10	6.47	0.64	7.64	12.06	1.01	6.72	112.19	12.32
28.93	14.50	1.46	7.02	0.67	50.49	2.62	2.10	6.51	0.64	7.64	12.06	1.05	6.72	113.49	12.46
30.05	14.63	1.47	7.10	0.68	51.30	2.64	2.10	6.54	0.64	7.64	12.06	1.09	6.72	114.60	12.58
32.93	14.98	1.49	7.23	0.70	52.67	3.02	2.10	6.54	0.64	7.66	12.06	1.09	6.72	116.92	12.84
35.11	15.27	1.52	7.42	0.73	54.37	3.02	2.10	6.69	0.64	7.66	12.06	1.18	6.75	119.41	13.11
38.83	15.68	1.55	7.66	0.77	57.05	3.19	2.10	6.85	0.64	7.66	12.06	1.32	6.75	123.28	13.53
39.85	15.79	1.56	7.71	0.91	57.38	3.49	2.10	6.90	0.64	7.66	12.06	1.36	6.75	124.31	13.65
41.88	16.02	1.64	7.84	1.19	58.24	3.89	2.10	7.11	0.64	7.66	12.06	1.42	6.75	126.57	13.89
43.07	16.19	1.64	7.92	1.38	58.77	4.11	2.10	7.16	0.64	7.66	12.06	1.42	6.75	127.82	14.03
45.09	16.44	1.66	8.05	1.41	60.11	4.72	2.10	7.16	0.64	7.66	12.06	1.42	6.75	130.19	14.29
47.24	16.44	1.66	8.05	1.41	60.11	4.72	2.10	7.16	0.64	7.66	12.06	1.42	6.75	130.19	14.29
50.02	16.79	1.66	8.29	1.50	62.04	4.90	2.21	7.46	0.64	7.66	12.06	1.42	6.75	133.39	14.64
51.90	16.79	1.84	8.48	1.62	63.40	5.05	2.21	7.68	0.64	7.66	12.06	1.44	6.75	135.61	14.89

Leach Run Time [Days]	Cumulative copper extracted [g]														Cumulative Cu extracted [g]
	Port 1	Port 2	Port 3	Port 4	Port 5	Port 6	Port 7	Port 8	Port 9	Port 10	Port 11	Port 12	Port 13	Total Cu	
52.92	16.91	1.84	8.55	1.70	64.13	5.12	2.21	7.77	0.64	7.66	12.06	1.46	6.75	136.80	15.02
54.96	17.07	1.84	8.66	1.75	65.23	5.28	2.21	7.96	0.64	7.66	12.06	1.51	6.75	138.63	15.22
59.04	17.45	1.84	8.96	1.95	67.57	5.49	2.21	8.28	0.64	7.66	12.06	1.56	6.75	142.42	15.63
61.00	17.63	1.84	9.18	2.00	68.93	5.65	2.21	8.47	0.64	7.66	12.06	1.60	6.75	144.61	15.88
64.13	17.82	1.84	9.39	2.08	70.52	5.89	2.21	8.79	0.64	7.66	12.06	1.64	6.75	147.29	16.17
66.90	17.99	1.84	9.55	2.15	72.02	6.03	2.21	9.03	0.64	7.82	12.06	1.66	6.75	149.76	16.44
67.87	18.06	1.84	9.60	2.18	72.65	6.09	2.21	9.14	0.64	7.82	12.06	1.72	6.75	150.77	16.55
68.82	18.12	1.84	9.62	2.24	73.11	6.15	2.21	9.27	0.64	7.82	12.06	1.72	6.75	151.55	16.64
69.85	18.18	1.84	9.65	2.28	73.60	6.17	2.21	9.27	0.64	7.82	12.06	1.72	6.75	152.20	16.71
73.88	18.46	1.84	9.96	2.39	75.18	6.24	2.21	9.47	0.68	8.12	12.06	1.72	6.75	155.08	17.02
79.88	18.83	2.06	10.30	2.79	77.41	6.65	2.21	9.47	1.04	8.12	12.06	1.90	6.75	159.59	17.52
81.90	18.94	2.06	10.43	2.84	78.27	6.73	2.21	9.47	1.04	8.12	12.06	1.90	6.75	160.82	17.65
84.44	19.07	2.07	10.55	2.90	79.82	6.86	2.21	9.72	1.04	8.12	12.06	1.92	6.75	163.09	17.90
87.13	19.20	2.07	10.70	2.95	81.29	6.88	2.21	9.92	1.04	8.23	12.06	1.95	6.75	165.26	18.14
89.92	19.38	2.07	10.97	3.02	82.94	6.91	2.21	10.32	1.04	8.23	12.06	1.97	6.75	167.87	18.43

	Detachment on 20/08/2010								
		Zone 1	Zone 2	Zone 3	Zone 4	Zone 5	Zone 6	Zone 7	Zone 8	Zone 9
	Mass of Ore [g]	21.42	22.18	20.3	20.9	20.04	21.72	22	21.84	20.66
	Volume of Media added per wash [ml]	10	10	10	10	10	10	10	10	10
Media wash	Mass of centrifuge tube [g]	12.86	12.8	12.82	12.8	12.84	12.78	12.86	12.94	12.82
	Mass after sol + adjustment	23.06	22.46	22.32	23.18	22.8	22.8	23.28	22.58	22.78
	Mass Media added [g]	10.2	9.66	9.5	10.38	9.96	10.02	10.42	9.64	9.96
	Mass of centrifuge bottle after removal	15.72	15.34	14.66	15.7	15.38	15.8	15.4	15.06	15.25
	Mass of supernatant collected [g]	7.34	7.12	7.66	7.48	7.42	7	7.88	7.52	7.53
Media wash + vortex 1	Mass of centrifuge tube [g]	12.86	12.8	12.82	12.8	12.84	12.78	12.86	12.94	12.82
	Mass after sol + adjustment	26.84	26.16	25.24	26.26	25.9	26.66	25.22	25.48	25.5
	Mass Media added [g]	13.98	13.36	12.42	13.46	13.06	13.88	12.36	12.54	12.68
	Mass of centrifuge bottle after removal	16.38	16.54	15.42	16.18	16.22	16.24	15.66	15.62	15.9
	Mass of supernatant collected [g]	10.46	9.62	9.82	10.08	9.68	10.42	9.56	9.86	9.6
Media wash + vortex 2	Mass of centrifuge tube [g]	12.86	12.8	12.82	12.8	12.84	12.78	12.86	12.94	12.82
	Mass after sol + adjustment	25.98	26.74	25.15	25.84	26.5	26.16	26.52	25.72	25.74
	Mass Media added [g]	13.12	13.94	12.33	13.04	13.66	13.38	13.66	12.78	12.92
	Mass of centrifuge bottle after removal	16.62	17.12	15.75	16.29	16.32	16.35	15.8	15.92	16.03
	Mass of supernatant collected [g]	9.36	9.62	9.4	9.55	10.18	9.81	10.72	9.8	9.71

	Detachment on 20/08/2010	Zone 1	Zone 2	Zone 3	Zone 4	Zone 5	Zone 6	Zone 7	Zone 8	Zone 9
	Mass of Ore [g]	21.42	22.18	20.3	20.9	20.04	21.72	22	21.84	20.66
	Volume of Media added per wash [ml]	10	10	10	10	10	10	10	10	10
Media wash	Mass of centrifuge tube [g]	12.86	12.8	12.82	12.8	12.84	12.78	12.86	12.94	12.82
	Mass after sol + adjustment	23.06	22.46	22.32	23.18	22.8	22.8	23.28	22.58	22.78
	Mass Media added [g]	10.2	9.66	9.5	10.38	9.96	10.02	10.42	9.64	9.96
	Mass of centrifuge bottle after removal	15.72	15.34	14.66	15.7	15.38	15.8	15.4	15.06	15.25
	Mass of supernatant collected [g]	7.34	7.12	7.66	7.48	7.42	7	7.88	7.52	7.53
Media wash + vortex 1	Mass of centrifuge tube [g]	12.86	12.8	12.82	12.8	12.84	12.78	12.86	12.94	12.82
	Mass after sol + adjustment	26.84	26.16	25.24	26.26	25.9	26.66	25.22	25.48	25.5
	Mass Media added [g]	13.98	13.36	12.42	13.46	13.06	13.88	12.36	12.54	12.68
	Mass of centrifuge bottle after removal	16.38	16.54	15.42	16.18	16.22	16.24	15.66	15.62	15.9
	Mass of supernatant collected [g]	10.46	9.62	9.82	10.08	9.68	10.42	9.56	9.86	9.6
Media wash + vortex 2	Mass of centrifuge tube [g]	12.86	12.8	12.82	12.8	12.84	12.78	12.86	12.94	12.82
	Mass after sol + adjustment	25.98	26.74	25.15	25.84	26.5	26.16	26.52	25.72	25.74
	Mass Media added [g]	13.12	13.94	12.33	13.04	13.66	13.38	13.66	12.78	12.92
	Mass of centrifuge bottle after removal	16.62	17.12	15.75	16.29	16.32	16.35	15.8	15.92	16.03
	Mass of supernatant collected [g]	9.36	9.62	9.4	9.55	10.18	9.81	10.72	9.8	9.71
Media wash + vortex 3	Mass of centrifuge tube [g]	12.86	12.8	12.82	12.8	12.84	12.78	12.86	12.94	12.82
	Mass after sol + adjustment	26.42	27.31	26.14	25.8	26.05	26.57	25.59	26.28	25.81
	Mass Media added [g]	13.56	14.51	13.32	13	13.21	13.79	12.73	13.34	12.99
	Mass of centrifuge bottle after removal	16.64	17.13	16	16.47	16.38	16.45	16.21	16.01	16.34
	Mass of supernatant collected [g]	9.78	10.18	10.14	9.33	9.67	10.12	9.38	10.27	9.47
Tween wash + vortex 3	Mass of centrifuge tube [g]	12.86	12.8	12.82	12.8	12.84	12.78	12.86	12.94	12.82
	Mass after sol + adjustment	27.25	27.73	26.24	27.33	26.86	26.48	26.87	25.95	26.8
	Mass Media added [g]	14.39	14.93	13.42	14.53	14.02	13.7	14.01	13.01	13.98
	Mass of centrifuge bottle after removal	17.4	17.73	16.11	16.78	16.95	17.27	16.5	16.12	16.47
	Mass of supernatant collected [g]	9.85	10	10.13	10.55	9.91	9.21	10.37	9.83	10.33

	Detachment on 20/08/2010								
		Zone 1	Zone 2	Zone 3	Zone 4	Zone 5	Zone 6	Zone 7	Zone 8	Zone 9
Tween wash + vortex 3	Mass of centrifuge tube [g]	12.86	12.8	12.82	12.8	12.84	12.78	12.86	12.94	12.82
	Mass after sol + adjustment	27.56	27.49	24.22	26.27	27.06	27.61	26.47	26.62	26.38
	Mass Media added [g]	14.7	14.69	11.4	13.47	14.22	14.83	13.61	13.68	13.56
	Mass of centrifuge bottle after removal	17.59	17.92	16.85	17	17.32	17.2	16.42	16.22	16.58
	Mass of supernatant collected [g]	9.97	9.57	7.37	9.27	9.74	10.41	10.05	10.4	9.8

	Detachment on 03/09/2010								
		Zone 1	Zone 2	Zone 3	Zone 4	Zone 5	Zone 6	Zone 7	Zone 8	Zone 9
	Mass of Ore [g]	20.74	21.39	20.65	21.22	20.46	20.08	20.92	21.32	21.55
	Volume of Media added per wash [ml]	10	10	10	10	10	10	10	10	10
Media wash	Mass of centrifuge tube [g]	12.92	12.86	12.88	12.91	12.9	12.91	12.82	12.82	12.9
	Mass after sol + adjustment	23.64	22	22.04	23.29	23.56	22.58	22.84	23.4	23.01
	Mass Media added [g]	10.72	9.14	9.16	10.38	10.66	9.67	10.02	10.58	10.11
	Mass of centrifuge bottle after removal	15.84	15.08	15.42	15.85	16.28	15.3	15.33	15.3	15.59
	Mass of supernatant collected [g]	7.8	6.92	6.62	7.44	7.28	7.28	7.51	8.1	7.42
Media wash + vortex 1	Mass of centrifuge tube [g]	12.92	12.86	12.88	12.91	12.9	12.91	12.82	12.82	12.9
	Mass after sol + adjustment	25.7	26.15	26.5	25.96	26.95	26.05	25.49	21.19	24.95
	Mass Media added [g]	12.78	13.29	13.62	13.05	14.05	13.14	12.67	8.37	12.05
	Mass of centrifuge bottle after removal	16.83	16.44	16.45	16.86	16.99	16.42	16.11	16.19	16.24
	Mass of supernatant collected [g]	8.87	9.71	10.05	9.1	9.96	9.63	9.38	5	8.71
Media wash + vortex 2	Mass of centrifuge tube [g]	12.92	12.86	12.88	12.91	12.9	12.91	12.82	12.82	12.9
	Mass after sol + adjustment	27.26	26.66	26.89	27.42	26.68	26.54	26.31	26.24	26.66
	Mass Media added [g]	14.34	13.8	14.01	14.51	13.78	13.63	13.49	13.42	13.76
	Mass of centrifuge bottle after removal	17.27	16.62	16.98	17.34	17.27	16.72	16.71	16.51	16.53
	Mass of supernatant collected [g]	9.99	10.04	9.91	10.08	9.41	9.82	9.6	9.73	10.13

	Detachment on 03/09/2010								
		Zone 1	Zone 2	Zone 3	Zone 4	Zone 5	Zone 6	Zone 7	Zone 8	Zone 9
Media wash + vortex 3	Mass of centrifuge tube [g]	12.92	12.86	12.88	12.91	12.9	12.91	12.82	12.82	12.9
	Mass after sol + adjustment	27.32	26.99	27.12	27.09	27.71	26.36	26.48	26.99	26.57
	Mass Media added [g]	14.4	14.13	14.24	14.18	14.81	13.45	13.66	14.17	13.67
	Mass of centrifuge bottle after removal	17.67	16.93	17.38	17.65	17.31	17.02	16.88	16.8	16.77
	Mass of supernatant collected [g]	9.65	10.06	9.74	9.44	10.4	9.34	9.6	10.19	9.8
Tween wash + vortex 3	Mass of centrifuge tube [g]	12.92	12.86	12.88	12.91	12.9	12.91	12.82	12.82	12.9
	Mass after sol + adjustment	28.01	27.09	27.62	27	27.42	27.87	27.43	27.06	27.08
	Mass Media added [g]	15.09	14.23	14.74	14.09	14.52	14.96	14.61	14.24	14.18
	Mass of centrifuge bottle after removal	17.54	17.09	17.42	17.63	17.6	17.28	17.17	17.19	17
	Mass of supernatant collected [g]	10.47	10	10.2	9.37	9.82	10.59	10.26	9.87	10.08
Tween wash + vortex 3	Mass of centrifuge tube [g]	12.92	12.86	12.88	12.91	12.9	12.91	12.82	12.82	12.9
	Mass after sol + adjustment	27.51	26.69	27.98	27.61	27.84	27.41	26.97	27.16	26.07
	Mass Media added [g]	14.59	13.83	15.1	14.7	14.94	14.5	14.15	14.34	13.17
	Mass of centrifuge bottle after removal	17.45	17.14	17.79	17.84	17.78	17.36	17.04	17.08	16.88
	Mass of supernatant collected [g]	10.06	9.55	10.19	9.77	10.06	10.05	9.93	10.08	9.19

	Detachment on 23/09/2010								
		Zone 1	Zone 2	Zone 3	Zone 4	Zone 5	Zone 6	Zone 7	Zone 8	Zone 9
	Mass of Ore [g]	20.83	20.6	20.4	20.8	20.79	20.59	20.62	20.94	20.63
	Volume of Media added per wash [ml]	10	10	10	10	10	10	10	10	10
Media wash	Mass of centrifuge tube [g]	12.86	12.88	12.85	12.91	12.86	12.9	12.88	13.06	12.95
	Mass after sol + adjustment	23.05	22.97	22.66	23.56	24.38	23.14	22.91	23.1	23.39
	Mass Media added [g]	10.19	10.09	9.81	10.65	11.52	10.24	10.03	10.04	10.44
	Mass of centrifuge bottle after removal	15.71	15.81	15.53	16.1	16.24	15.83	15.42	15.48	15.71
	Mass of supernatant collected [g]	7.34	7.16	7.13	7.46	8.14	7.31	7.49	7.62	7.68

	Detachment on 23/09/2010									
		Zone 1	Zone 2	Zone 3	Zone 4	Zone 5	Zone 6	Zone 7	Zone 8	Zone 9
Media wash + vortex 1	Mass of centrifuge tube [g]	12.86	12.88	12.85	12.91	12.86	12.9	12.88	13.06	12.95
	Mass after sol + adjustment	26.36	26.44	26.26	26.28	26.81	26.14	25.36	26.08	25.71
	Mass Media added [g]	13.5	13.56	13.41	13.37	13.95	13.24	12.48	13.02	12.76
	Mass of centrifuge bottle after removal	16.42	16.76	16.18	16.61	16.84	16.28	15.84	16.09	16.39
	Mass of supernatant collected [g]	9.94	9.68	10.08	9.67	9.97	9.86	9.52	9.99	9.32
Media wash + vortex 2	Mass of centrifuge tube [g]	12.86	12.88	12.85	12.91	12.86	12.9	12.88	13.06	12.95
	Mass after sol + adjustment	26.55	27.33	26.38	26.69	27.33	26.31	25.64	26.2	26.24
	Mass Media added [g]	13.69	14.45	13.53	13.78	14.47	13.41	12.76	13.14	13.29
	Mass of centrifuge bottle after removal	16.84	17.23	16.76	16.91	17.45	16.82	16.32	16.77	16.75
	Mass of supernatant collected [g]	9.71	10.1	9.62	9.78	9.88	9.49	9.32	9.43	9.49
Media wash + vortex 3	Mass of centrifuge tube [g]	12.86	12.88	12.85	12.91	12.86	12.9	12.88	13.06	12.95
	Mass after sol + adjustment	27.19	27.63	26.58	26.79	27.26	25.87	26.61	26.86	26.47
	Mass Media added [g]	14.33	14.75	13.73	13.88	14.4	12.97	13.73	13.8	13.52
	Mass of centrifuge bottle after removal	17.01	17.37	16.83	17	17.54	16.97	16.4	17.05	16.99
	Mass of supernatant collected [g]	10.18	10.26	9.75	9.79	9.72	8.9	10.21	9.81	9.48
Tween wash + vortex 3	Mass of centrifuge tube [g]	12.86	12.88	12.85	12.91	12.86	12.9	12.88	13.06	12.95
	Mass after sol + adjustment	27.5	27.21	27.12	27.46	28.21	27.28	26.83	27.48	27.34
	Mass Media added [g]	14.64	14.33	14.27	14.55	15.35	14.38	13.95	14.42	14.39
	Mass of centrifuge bottle after removal	17.83	17.84	17.29	17.83	18.11	17.73	17.45	17.49	17.45
	Mass of supernatant collected [g]	9.67	9.37	9.83	9.63	10.1	9.55	9.38	9.99	9.89
Tween wash + vortex 3	Mass of centrifuge tube [g]	12.86	12.88	12.85	12.91	12.86	12.9	12.88	13.06	12.95
	Mass after sol + adjustment	27.08	27.82	27.27	27.74	27.74	27.62	27.53	27.32	27.1
	Mass Media added [g]	14.22	14.94	14.42	14.83	14.88	14.72	14.65	14.26	14.15
	Mass of centrifuge bottle after removal	17.69	17.56	17.19	17.81	17.98	17.42	17.49	17.44	17.4
	Mass of supernatant collected [g]	9.39	10.26	10.08	9.93	9.76	10.2	10.04	9.88	9.7

Detachment on 20/08/2010									
Cell counts	Zone 1	Zone 2	Zone 3	Zone 4	Zone 5	Zone 6	Zone 7	Zone 8	Zone 9
Media wash 1	63	3	0	82	4	0	58	4	1
Media wash 2	71	1	0	94	2	0	61	5	0
Media wash 3	60	1	0	87	4	0	53	2	0
Average cell count	**65**	**2**	**0**	**88**	**3**	**0**	**57**	**4**	**0**
Dilution factor	2	1	1	2	1	1	2	1	1
Average [cells/ml]	4.04E+07	5.21E+05	0.00E+00	5.48E+07	1.04E+06	0.00E+00	3.58E+07	1.15E+06	1.04E+05
Stdev	3.55E+06	3.61E+05	0.00E+00	3.77E+06	3.61E+05	0.00E+00	2.53E+06	4.77E+05	1.80E+05
Media wash & vortex 1	19	0	0	18	0	0	10	2	0
Media wash & vortex 2	16	0	0	19	0	0	13	1	0
Media wash & vortex 3	20	0	0	15	0	0	13	2	0
Average cell count	**18**	**0**	**0**	**17**	**0**	**0**	**12**	**2**	**0**
Dilution factor	1	1	1	1	1	1	1	1	1
Average [cells/ml]	5.73E+06	0.00E+00	0.00E+00	5.42E+06	0.00E+00	0.00E+00	3.75E+06	5.21E+05	0.00E+00
Stdev	6.51E+05	0.00E+00	0.00E+00	6.51E+05	0.00E+00	0.00E+00	5.41E+05	1.80E+05	0.00E+00
Tween wash & vortex 1	74	0	0	86	0	0	43	0	0
Tween wash & vortex 2	60	0	0	77	0	0	39	0	0
Tween wash & vortex 3	61	0	0	83	0	0	40	0	0
Average cell count	**65**	**0**	**0**	**82**	**0**	**0**	**41**	**0**	**0**
Dilution factor	1	1	1	1	1	1	1	1	1
Average [cells/ml]	2.03E+07	0.00E+00	0.00E+00	2.56E+07	0.00E+00	0.00E+00	1.27E+07	0.00E+00	0.00E+00
Stdev	2.44E+06	0.00E+00	0.00E+00	1.43E+06	0.00E+00	0.00E+00	6.51E+05	0.00E+00	0.00E+00

Detachment on 03/09/2010									
Cell counts	Zone 1	Zone 2	Zone 3	Zone 4	Zone 5	Zone 6	Zone 7	Zone 8	Zone 9
Media wash 1	31	1	0	28	23	0	43	14	3
Media wash 2	37	0	0	25	21	0	47	11	0
Media wash 3	29	1	0	30	29	0	41	13	2
Average cell count	**32**	**1**	**0**	**28**	**24**	**0**	**44**	**13**	**2**
Dilution factor	10	1	1	10	1	1	10	10	1
Average [cells/ml]	1.01E+08	2.08E+05	0.00E+00	8.65E+07	7.60E+06	0.00E+00	1.36E+08	3.96E+07	5.21E+05
Stdev	1.30E+07	1.80E+05	0.00E+00	7.86E+06	1.30E+06	0.00E+00	9.55E+06	4.77E+06	4.77E+05

Detachment on 03/09/2010 Cell counts	Zone 1	Zone 2	Zone 3	Zone 4	Zone 5	Zone 6	Zone 7	Zone 8	Zone 9
Media wash & vortex 1	10	0	0	15	2	0	7	19	0
Media wash & vortex 2	12	0	0	17	0	0	7	21	0
Media wash & vortex 3	9	0	0	16	3	0	9	18	0
Average cell count	**10**	**0**	**0**	**16**	**2**	**0**	**8**	**19**	**0**
Dilution factor	10	1	1	10	1	1	10	1	1
Average [cells/ml]	3.23E+07	0.00E+00	0.00E+00	5.00E+07	5.21E+05	0.00E+00	2.40E+07	6.04E+06	0.00E+00
Stdev	4.77E+06	0.00E+00	0.00E+00	3.13E+06	4.77E+05	0.00E+00	3.61E+06	4.77E+05	0.00E+00
Tween wash & vortex 1	79	0	0	57	7	0	80	14	0
Tween wash & vortex 2	81	0	0	60	5	0	79	20	0
Tween wash & vortex 3	70	0	0	61	4	0	85	23	0
Average cell count	**77**	**0**	**0**	**59**	**5**	**0**	**81**	**19**	**0**
Dilution factor	1	1	1	2	1	1	2	1	1
Average [cells/ml]	2.40E+07	0.00E+00	0.00E+00	3.71E+07	1.67E+06	0.00E+00	5.08E+07	5.94E+06	0.00E+00
Stdev	1.83E+06	0.00E+00	0.00E+00	1.30E+06	4.77E+05	0.00E+00	2.01E+06	1.43E+06	0.00E+00

Detachment on 23/09/2010									
Cell counts	Zone 1	Zone 2	Zone 3	Zone 4	Zone 5	Zone 6	Zone 7	Zone 8	Zone 9
Media wash 1	24	17	0	51	80	0	57	31	2
Media wash 2							63	28	
Media wash 3							66	35	
Average cell count	**24**	**17**	**0**	**51**	**80**	**0**	**62**	**31**	**2**
Dilution factor	10	1	1	10	2	1	10	1	1
Average [cells/ml]	7.50E+07	5.31E+06	0.00E+00	1.59E+08	5.00E+07	0.00E+00	1.94E+08	9.79E+06	6.25E+05
Stdev							1.43E+07	1.10E+06	
Media wash & vortex 1	10	7	0	22	24	0	8	39	0
Media wash & vortex 2	8			28			11		
Media wash & vortex 3	10			29			9		
Average cell count	**9**	**7**	**0**	**26**	**24**	**0**	**9**	**39**	**0**
Dilution factor	10	1	1	10	1	1	10	1	1
Average [cells/ml]	2.92E+07	2.19E+06	0.00E+00	8.23E+07	7.50E+06	0.00E+00	2.92E+07	1.22E+07	0.00E+00
Stdev				1.18E+07			4.77E+06		
Tween wash & vortex 1	68	1	0	86	30	0	66	37	0
Tween wash & vortex 2	73								
Tween wash & vortex 3	74								
Average cell count	**72**	**1**	**0**	**86**	**30**	**0**	**66**	**37**	**0**
Dilution factor	2	1	1	2	1	1	4	1	1
Average [cells/ml]	4.48E+07	3.13E+05	0.00E+00	5.38E+07	9.38E+06	0.00E+00	8.25E+07	1.16E+07	0.00E+00
Stdev	2.01E+06								